

## **INFORMATION TO USERS**

**This manuscript has been reproduced from the microfilm master. UMI films the text directly from the original or copy submitted. Thus, some thesis and dissertation copies are in typewriter face, while others may be from any type of computer printer.**

**The quality of this reproduction is dependent upon the quality of the copy submitted. Broken or indistinct print, colored or poor quality illustrations and photographs, print bleedthrough, substandard margins, and improper alignment can adversely affect reproduction.**

**In the unlikely event that the author did not send UMI a complete manuscript and there are missing pages, these will be noted. Also, if unauthorized copyright material had to be removed, a note will indicate the deletion.**

**Oversize materials (e.g., maps, drawings, charts) are reproduced by sectioning the original, beginning at the upper left-hand corner and continuing from left to right in equal sections with small overlaps.**

**Photographs included in the original manuscript have been reproduced xerographically in this copy. Higher quality 6" x 9" black and white photographic prints are available for any photographs or illustrations appearing in this copy for an additional charge. Contact UMI directly to order.**

**Bell & Howell Information and Learning  
300 North Zeeb Road, Ann Arbor, MI 48106-1346 USA  
800-521-0600**

**UMI<sup>®</sup>**



A

**TERTIARY TECTONICS OF THE HISPANIOLA FAULT ZONE  
IN THE NORTHWESTERN PIEDMONT OF THE  
CORDILLERA CENTRAL, DOMINICAN REPUBLIC**

by

**ANDREW JAY COLEMAN**

**A dissertation submitted to the Graduate Faculty in Earth and  
Environmental Sciences in partial fulfillment of the requirements for the  
degree of Doctor of Philosophy, The City University of New York**

**2000**

UMI Number: 9969684

Copyright 2000 by  
Coleman, Andrew Jay

All rights reserved.

UMI<sup>®</sup>

---

UMI Microform 9969684

Copyright 2000 by Bell & Howell Information and Learning Company.

All rights reserved. This microform edition is protected against  
unauthorized copying under Title 17, United States Code.

---

Bell & Howell Information and Learning Company  
300 North Zeeb Road  
P.O. Box 1346  
Ann Arbor, MI 48106-1346

© 2000

**ANDREW JAY COLEMAN**

**All Rights Reserved**

This manuscript has been read and accepted for the Graduate Faculty in Earth and Environmental Sciences in satisfaction of the dissertation requirement for the degree of Doctor of Philosophy.

4/7/2000  
Date

Margaret Anne Winslow  
Dr. Margaret Anne Winslow  
**Chair of Examining Committee**  
City College of New York

3/27/00  
Date

Frederick Shaw  
Dr. Frederick Shaw  
Member of Supervisory Committee  
Executive Officer - Earth and Environmental  
Sciences; Graduate School of the City University of  
New York

Dr. Allan Ludman  
Member of Supervisory Committee  
Queens College

Dr. Joseph W. Troester  
Member of Supervisory Committee  
U.S. Geological Survey  
Caribbean District

**THE CITY UNIVERSITY OF NEW YORK**

## Abstract

**TERTIARY TECTONICS OF THE HISPANIOLA FAULT ZONE  
IN THE NORTHWESTERN PIEDMONT OF THE  
CORDILLERA CENTRAL, DOMINICAN REPUBLIC**

by

**ANDREW JAY COLEMAN****Adviser: Professor Margaret Anne Winslow**

The Hispaniola Fault Zone (HFZ) separates the Cordillera Central from a piedmont in the west-central region of the Dominican Republic. The HFZ is part of a 250-km wide plate boundary zone known as the Northern Caribbean Plate Boundary Zone. This active zone of tectonic deformation separates the North American and Caribbean plates. New structural mapping within the piedmont zone, a dissected plateau that separates the Cordillera from the Cibao Valley, reveals strike-slip faulting began as early as the Oligocene and has continued until at least the late Miocene. Strike-slip faulting along the piedmont is responsible for creating a pull-apart basin. En echelon patterns of parallel and oblique faults cutting the piedmont have resulted in thick deposits of clastic rocks eroded from the Cordillera. In addition, carbonate reefs and reworked sediments can be found. Most of the sedimentary units have faulted boundaries with each other. Their complex geometries, including both dip-slip and strike-slip faulting as well as folding, can be explained by a Riedel model. The study area is bounded by the coordinates 70°45'W to 71°15'W and 19°30'N to 19°20'N within the San José de las Matas and Monción quadrangles of the piedmont. New road-cuts and a dam project within the study area

create a unique opportunity to produce a new, 1:50,000 scale geologic map. Folding and faulting within the pull-apart basin are consistent with regional deformation and the tectonic evolution of the North American/Caribbean plate boundary.

## ACKNOWLEDGMENTS

Foremost, the author gratefully acknowledges the guidance and encouragement given by Professor Margaret A. Winslow of the Department of Earth and Atmospheric Sciences at the City College of New York (CCNY). Professor Winslow assisted in the selection and refinement of the project and visited the writer in the field on numerous occasions. The writer's use of drafting equipment and other courtesies was graciously provided by Ing. Salvadore Brouwer, Superintendent of Mining at Falconbridge Dominicana, C. por A. and his exploration staff. Ing. Julio Espailat of Falconbridge visited the writer in the field and provided constructive criticism. The author acknowledges Professor Grenville Draper of Florida International University for several helpful discussions. Topographic maps and aerial photographs were supplied and purchased from the Instituto Cartográfico Militar, F.F.A.A. Republica Dominicana. Virgilio Miniño and undergraduates from CCNY provided some field assistance. Financial assistance was born, in part, by PSC-City University of New York (CUNY) Grant Nos. 6-62194 and 6-68242. Drafting associated with some of the production of figures were met by ENSR and its engineers, Michael Padula, Derek Tompka, and Scott Michalean. The author gratefully appreciates the superb guidance provided during the course of this dissertation by Professors Allan Ludman and Frederick Shaw of the CUNY's Graduate School and Dr. Joseph W. Troester of the U.S. Geological Survey-Caribbean District. I thank my parents, siblings, friends, and colleagues at ENSR and Public Service Electric and Gas Company for their moral support. And lastly, I dedicate this manuscript to Donna Sokolsky for her moral support during the final stages of this dissertation.

## TABLE OF CONTENTS

|  |    |
|--|----|
| ABSTRACT .....   | iv |
| ACKNOWLEDGMENTS .....                                    | vi |
| INTRODUCTION.....  | 1  |
| PREVIOUS WORK.....                                       | 4  |
| GEOTECTONIC SETTING OF THE CARIBBEAN.....                | 7  |
| <u>Regional Tectonic Setting</u>                         |    |
| <u>Origin of the Caribbean Plate</u>                     |    |
| Review of the Fixist vs. Mobilist Hypotheses             |    |
| Late Triassic to Jurassic-                               |    |
| Early Cretaceous-  |    |
| Late Cretaceous-   |    |
| Paleocene to Eocene-                                     |    |
| Oligocene-   |    |
| Miocene to Recent-                                       |    |
| Recent Motions-  |    |
| METHODS .....  | 19 |
| STRATIGRAPHY OF THE STUDY AREA .....                     | 22 |
| <u>Late Jurassic to Cretaceous Mafic Volcanics</u>       |    |
| Duarte Complex   |    |
| Amina Schist   |    |
| Hornblende Tonalite                                      |    |
| <u>Paleogene Rocks</u>                                   |    |
| Magua Formation  |    |
| Rodeo Basalt Member of the Magua Formation               |    |
| <u>Tavera Group of the Western Hispaniola Fault Zone</u> |    |
| Inoa Conglomerate  |    |
| Limestones   |    |
| <i>Pananao Limestone</i>                                 |    |
| <i>La Bruja Limestone</i>                                |    |
| <i>Monción Limestone</i>                                 |    |
| <u>Neogene Sedimentary Rocks</u>                         |    |
| Bulla Conglomerate                                       |    |
| Cercado Sandstone  |    |
| <u>Tectonic Breccias of Uncertain Age</u>                |    |
| Las Matas Breccia  |    |
| Pananao Abajo Breccia                                    |    |

**La Bruja Breccia**  
**Suí Breccia**  
**Higua Breccia**

**Rock Unit Contacts**

**Domain 1 - Northwest Corner**  
**Domain 2 - West**  
**Domain 3 - Central West**  
**Domain 4 - Southwest**  
**Domain 5 - Northwest**  
**Domain 6 - Central North**  
**Domain 7 - Left-Central Center**  
**Domain 8 - Right-Central Center**  
**Domain 9 and 10 - Central East**  
**Domain 11 - Northeast**  
**Domain 12 - Central East**  
**Domain 13 - East**  
**Domain 14 - East of Monción**

**MAJOR STRUCTURES OF THE STUDY AREA..... 48**

**Master Faults and their structure**

**Amina fault**  
**Inoa fault**

**Folds**

**Folds in the Inoa Conglomerate**  
**Folds in the Magua Formation**  
**Folds in the La Bruja Limestone**  
**Folds in the Monción Limestone**  
**Folds in the Pananao Limestone**  
**Folds in the Cercado Sandstone**  
**Foliation in the Amina Schist**

**Lineaments**

**Rose Diagrams**

**MINOR STRUCTURES OF THE STUDY AREA ..... 65**

**Shear Fractures**

**Monción Limestone**  
**Amina Schist**  
**Inoa Conglomerate**  
**Cercado Sandstone**  
**Duarte Greenschist facies rocks**

**DISCUSSION ..... 68**

**The Riedel Model vs. the Coulomb-Anderson Model**

**Structural Features of the San José de las Matas Pull-Apart Basin**

**Imposed Shear**  
**Conjugate Riedel (R') shears**  
**Conjugate Riedel (R) shears - Folds**  
**Conjugate Riedel (R) shears - Fractures**  
**Compression and Extension**  
**Fault Offsets**

**Pull-Apart Basin vs. Fault Wedge Basin**

**The Fault-Wedge Basin**  
**The Pull-Apart Basin**  
**Evidence Supporting Development of a Pull-Apart Basin Subsidence**

**Tectonic Relationship of the Pull-Apart Basin**

**Local Tectonics**

**Tectonic History of the Study Area**

**Late Cretaceous**  
**Paleocene to Eocene**  
**Neogene**  
**Quaternary**

**CONCLUSIONS ..... 83**

## LISTS OF FIGURES, MAPS, CROSS-SECTIONS AND DIAGRAMS

### FIGURES

|   |     |
|---|-----|
| Figure 1 - Map of Hispaniola and the study area .....                                 | 87  |
| Figure 2 - Simplified Geologic Map of the Hispaniola Fault Zone .....                 | 88  |
| Figure 3 - Tectonic Setting of the Caribbean .....                                    | 89  |
| Figure 4 - Map of the fault zones of the Dominican Republic .....                     | 90  |
| Figure 5 - Author Index Map .....   | 92  |
| Figure 6 - Tectonic Setting of the Northern Caribbean Plate<br>Boundary Zone.....     | 93  |
| Figure 7 - Tectonic Setting of the Caribbean during the Late Jurassic.....            | 94  |
| Figure 8 - Tectonic Setting of the Caribbean .....                                    | 95  |
| A. Early Cretaceous   |     |
| B. Late Cretaceous  |     |
| C. Paleogene to Eocene  |     |
| D. Present  |     |
| Figure 9 - Stratigraphic columns of Palmer, 1963 and Coleman, 2000.....               | 97  |
| Figure 10 - Paleotectonics of Hispaniola - Late Cretaceous.....                       | 99  |
| Figure 11 - Paleotectonics of Hispaniola - Paleogene .....                            | 100 |
| Figure 12 - Paleotectonics of Hispaniola - Neogene .....                              | 101 |
| Figure 13 - Paleotectonics of Hispaniola - Late Pliocene to Pleistocene.              | 102 |
| Figure 14 - Domain Map .....  | 103 |
| Figure 15 - Riedel Model.....   | 104 |
| Figure 16 - Anderson schematic model of strike-slip faults.....                       | 105 |
| Figure 17 - Block diagrams of a pull-apart and a fault wedge.....                     | 106 |
| Figure 18 - Plan view of a pull-apart and a fault wedge.....                          | 107 |
| Figure 19 - Formation of a Pull-Apart.....  | 108 |
| Figure 20 - Block diagram of a releasing and restraining bend .....                   | 109 |
| Figure 21 - Perspective diagram of the San José de las Matas<br>pull-apart basin..... | 110 |

### PLATES

|  |     |
|--|-----|
| Plate 1 - Geologic Map.....  | 111 |
| Plate 2 - Cross-sections A-A', B-B', C-C',<br>D-D', E-E', F-F', G-G', H-H' ..... | 112 |
| Plate 3 - Lineament Map.....   | 113 |

## PHOTOGRAPHS

|  |     |
|--|-----|
| Photograph 1 - Duarte subgreenschist facies rocks.....   | 114 |
| Photograph 2 - Duarte greenschist facies rocks.....  | 115 |
| Photograph 3 - Amina Schist.....   | 116 |
| Photograph 4 - Hornblende tonalite.....  | 117 |
| Photograph 5 - Magua Formation.....  | 118 |
| Photograph 6 - Rodeo Basalt.....   | 119 |
| Photograph 7 - Inoa Conglomerate.....  | 120 |
| Photograph 8 - Pananao Limestone.....  | 121 |
| Photograph 9 - La Bruja Limestone.....   | 122 |
| Photograph 10 - Monción Limestone.....   | 123 |
| Photograph 11 - Bulla Conglomerate.....  | 124 |
| Photograph 12 - Cercado Sandstone.....   | 125 |
| Photograph 13 - Las Matas Breccia.....   | 126 |
| Photograph 14 - Pananao Abajo breccia.....   | 127 |
| Photograph 15 - La Bruja Breccia.....  | 128 |
| Photograph 16 - Sui Breccia.....   | 129 |
| Photograph 17 - Higua Breccia.....   | 130 |
| Photograph 18 - Elongated clasts in Río Amina.....   | 131 |
| Photograph 19 - Left-lateral offsets of siltstone beds in Río Mao.....                                       | 132 |
| Photograph 20 - Pseudotachylite along Inoa fault.....  | 133 |
| Photograph 21 - Erosional unconformity between Inoa Conglomerate<br>and Duarte greenschist facies rocks..... | 134 |
| Photograph 22 - Elongated clasts in Río Honda.....   | 135 |
| Photograph 23 - Elongated clasts in Río Amina near El Corozo.....  | 136 |
| Photograph 24 - Brittle deformation of siltstone beds in Inoa Formation.....                                 | 137 |
| Photograph 25 - Flatirons of the Cordillera Central south of the<br>Inoa fault trace.....                    | 138 |

## EQUAL AREA LOWER HEMISPHERE PROJECTIONS

|  |     |
|--|-----|
| PLOT 1 - Domain No. 1 - Bedding in Monción Limestone.....                          | 139 |
| PLOT 2 - Domain No. 1 - Shear fractures in Monción Limestone.....                  | 140 |
| PLOT 3 - Domain No. 2 - Schistosity of Amina Schist.....                           | 141 |
| PLOT 4 - Domain No. 2 - Shear fractures in Amina Schist.....                       | 142 |
| PLOT 5 - Domain No. 2 - Fault planes and slickenlines in<br>Inoa Conglomerate..... | 143 |
| PLOT 6 - Domain No. 3 - Bedding in Inoa Conglomerate.....                          | 144 |
| PLOT 7 - Domain No. 3 - Shear fractures in Inoa Conglomerate.....                  | 145 |
| PLOT 8 - Domain No. 3 - Fault planes and Slickenlines in<br>Inoa Conglomerate..... | 146 |

|  |     |
|--|-----|
| <b>PLOT 9 - Domain No. 3 - Fault planes and Slickenlines in Inoa Conglomerate</b> .....                    | 147 |
| <b>PLOT 10 - Domain No. 4 - Shear fractures in Magua Formation</b> .....                                   | 148 |
| <b>PLOT 11 - Domain No. 4 - Bedding in Magua Formation</b> .....   | 149 |
| <b>PLOT 12 - Domain No. 5 - Bedding in Cercado Sandstone</b> .....   | 150 |
| <b>PLOT 13 - Domain No. 5 - Shear fractures in Cercado Sandstone</b> .....                                 | 151 |
| <b>PLOT 14 - Domains No. 5 and No. 6 - Shear fractures in Cercado Sandstone</b> .....                      | 152 |
| <b>PLOT 15 - Domain No. 6 - Shear fractures in Cercado Sandstone</b> .....                                 | 153 |
| <b>PLOT 16 - Domain No. 6 - Bedding in Cercado Sandstone</b> .....   | 154 |
| <b>PLOT 17 - Domain No. 7 - Schistosity of Amina Schist</b> .....  | 155 |
| <b>PLOT 18 - Domain No. 7 - Shear fractures in Amina Schist</b> .....                                      | 156 |
| <b>PLOT 19 - Domain No. 8 - Bedding in Inoa Conglomerate</b> .....   | 157 |
| <b>PLOT 20 - Domain No. 8 - Bedding in La Bruja Limestone</b> .....  | 158 |
| <b>PLOT 21 - Domain No. 8 - Shear fractures in Inoa Conglomerate</b> .....                                 | 159 |
| <b>PLOT 22 - Domain No. 8 - Elongated clasts - San José de las Matas</b> ....                              | 160 |
| <b>PLOT 23 - Domain No. 8 - Elongated clasts - Río Amina</b> .....   | 161 |
| <b>PLOT 24 - Domain No. 8 - Elongated clasts - El Corozo</b> .....   | 162 |
| <b>PLOT 25 - Domain No. 8 - Fault planes and Slickenlines in Inoa Conglomerate</b> .....                   | 163 |
| <b>PLOT 26 - Domain No. 9 - Schistosity of Amina Schist</b> .....  | 164 |
| <b>PLOT 27 - Domain No. 10 - Schistosity of Amina Schist</b> .....   | 165 |
| <b>PLOT 28 - Domain No. 10 - Shear fractures in Amina Schist</b> .....                                     | 166 |
| <b>PLOT 29 - Domain No. 10 - Bedding in Cercado Sandstone</b> .....  | 167 |
| <b>PLOT 30 - Domain No. 11 - Bedding in Cercado Sandstone</b> .....  | 168 |
| <b>PLOT 31 - Domain No. 11 - Shear fractures in Cercado Sandstone</b> .....                                | 169 |
| <b>PLOT 32 - Domain No. 12 - Schistosity of Amina Schist</b> .....   | 170 |
| <b>PLOT 33 - Domain No. 12 - Shear fractures in Amina Schist</b> .....                                     | 171 |
| <b>PLOT 34 - Domain No. 13 - Bedding in Inoa Conglomerate</b> .....  | 172 |
| <b>PLOT 35 - Domain No. 13 - Shear fractures in Inoa Conglomerate</b> .....                                | 173 |
| <b>PLOT 36 - Domain No. 13 - Fault planes and Slickenlines in Inoa Conglomerate</b> .....                  | 174 |
| <b>PLOT 37 - Domain No. 14 - Schistosity of Amina Schist</b> .....   | 175 |
| <b>PLOT 38 - Domain No. 15 - Shear fractures in Duarte greenschist facies rocks along Inoa fault</b> ..... | 176 |

## **ROSE DIAGRAMS**

|  |     |
|--|-----|
| <b>Rose Diagram No. 1 = Domain No. 1</b> ..... | 177 |
| <b>Rose Diagram No. 2 = Domain No. 2</b> ..... | 178 |
| <b>Rose Diagram No. 3 = Domain No. 3</b> ..... | 179 |
| <b>Rose Diagram No. 4 = Domain No. 4</b> ..... | 180 |

|  |            |
|--|------------|
| Rose Diagram No. 5 = Domain No. 5 .....            | 181        |
| Rose Diagram No. 6 = Domain No. 6 .....            | 182        |
| Rose Diagram No. 7 = Domain No. 7 and No. 14 ..... | 183        |
| Rose Diagram No. 8 = Domain No. 8 .....            | 184        |
| Rose Diagram No. 9 = Domain No. 9 .....            | 185        |
| Rose Diagram No. 10 = Domain No. 10 .....          | 186        |
| Rose Diagram No. 11 = Domain No. 11 .....          | 187        |
| Rose Diagram No. 12 = Domain No. 12 .....          | 188        |
| Rose Diagram No. 13 = Domain No. 13 .....          | 189        |
| <b>BIBLIOGRAPHY .....</b>                          | <b>190</b> |

## **INTRODUCTION**

This study presents an interpretation of the structural geology of the northwestern piedmont of the Cordillera Central on the island of Hispaniola (Figure 1). This study was conducted along the northwestern segment of the Hispaniola Fault Zone (HFZ) (Figures 1 and 2).

This study provides a description of existing and new stratigraphy of the rocks along the western part of the HFZ. The work focused on mapping the folded and faulted Tertiary rocks along the HFZ to aid in interpreting the timing of the motion of the opening of the San José de las Matas pull-apart basin. The San José de las Matas pull-apart basin is a structurally controlled basin that developed as a result of strike-slip movement in the HFZ. The duration of faulting in the pull-apart basin is based on existing paleontological studies of the formations in the study area.

An interpretation will be made between two types of basins, a fault wedge basin and a pull-apart basin to prove that the HFZ developed as the latter. The fault patterns in the study area are compared and contrasted to those predicted by a Riedel model for left-lateral movement (Tchalenko and Ambraseys, 1970; Wilcox and others, 1973, Biddle and Christie-Blick, 1985, Bartlett and others, 1981). Lastly, the local structures found in the study area will be compared to coeval deformation which has occurred along the North American/Caribbean (NOAM/CARIB) plate boundary. A relationship will be established between the HFZ and other fault zones to its north such as the Septentrional Fault Zone (SFZ) which is the on-shore NOAM/CARIB plate boundary (Figure 3).

Hispaniola is the second largest island of the Greater Antilles and is located west of

Puerto Rico partly on the NOAM/CARIB plate boundary (Figure 3). The plate boundary is on-shore in Hispaniola where strike-slip and compressional movements result in major fault zones (Figure 3). The NOAM/CARIB plate boundary is located along the SFZ north of the Cibao Valley (Figure 3). The SFZ is presently a transpressional left-lateral strike-slip fault (de Zoeten and Mann, 1991; Winslow and others, 1991). The WNW-trending Cibao Valley is a basin in northwestern Hispaniola and lies just south of the SFZ. The Cibao Basin developed in a forearc prior to Eocene time (Bowin, 1975; Lewis, 1982; Bowin and Nagle, 1982; Winslow and McCann, 1985; Guglielmo and Winslow, 1988). South of the Cibao Valley lies the HFZ. The HFZ is approximately 150-km long and 5- to 15- km wide (Figure 1). The HFZ is bounded to the south by the NW-trending Cordillera Central (Figure 1). The study area is located along the HFZ and is defined by the coordinates 70°45'W to 71°15'W and 19°30'N to 19°20'N within the San José de las Matas and Monción quadrangles (Figure 1). The Cordillera Central is the magmatic arc that formed from the mid-Cretaceous to Paleogene times.

The HFZ is comprised of two pull-apart basins, the San José de las Matas pull-apart basin and the Tavera pull-apart basin. The Tavera pull-apart basin extends to the southeast of the study area (Figure 2; Groetsch, 1983; Dolan and others, 1991). The San José de las Matas pull-apart basin is 60-km long by 3- to 7-km wide and is filled with a fault-bounded group of early Oligocene to late Miocene age sandstones, mudstones, and conglomerates. This group of sediments are known as the Tavera Group.

The San José de las Matas pull-apart basin is proposed to have evolved due to strike-slip movement along the HFZ in the early Oligocene. The San José de las Matas pull-

apart basin formed as a releasing bend along the HFZ due to a combination of compression and strike-slip movements (transpressional movements). The Tavera Group of Oligocene to late Miocene age is faulted, folded, pulled-apart, and regionally uplifted (cf. Vaughan and 5 others, 1921; Bowin, 1975; Palmer, 1963; Groetsch, 1983).

The Tavera Group is bounded to the north by two NW-trending steeply dipping master faults, the Inoa and Amina faults (Figure 2). The Amina fault is in contact with the Cretaceous Amina Schist and the Inoa fault is in contact with the Cretaceous Duarte Complex (Figure 2). Faulting occurs to the north of the Amina fault in a series of early to late Miocene shallow marine conglomerates and sandstones (Figure 2). The Inoa and Amina faults are WNW-trending, high-angle strike-slip faults (Figure 2).

This study will confirm that left-lateral strike-slip displacement occurred along the two master faults, i.e., the Inoa and Amina faults. Stepovers or en echelon segmentation (Aydin and Nur, 1982) of the strike-slip master faults in the HFZ have played a role in the further development of the San José de las Matas pull-apart basin to its present aperture. This study will prove the strike-slip nature of the master faults. The new formations found in the study area and added to the stratigraphic column assist in the timing of the faulting. The San José de las Matas pull-apart basin developed to its present aperture due also to the configuration of the Cretaceous rocks which bound the basin to the north and south of the master faults. The new structural and stratigraphic information used in this study helps to interpret the strike-slip nature and tectonic development of the San José de las Matas pull-apart basin relative to the regional tectonism. And lastly, this study will present a tectonic discussion of the relationship of the HFZ to the largely transcurrent contact

between the southeastern edge of the Bahama Platform with northeastern Hispaniola along the NOAM/CARIB plate boundary.

## **PREVIOUS WORK**

Vaughan and 5 others (1921) published the first geologic report of the Tertiary rocks as part of a generalized reconnaissance of the Dominican Republic. Their study was not confined to a specific area and is a basic source of lithostratigraphic and paleontological data of the study area. Bowin (1960; 1966; 1975) also conducted a reconnaissance of the northwestern piedmont of the Cordillera Central. Bowin focused his study south of the study area. The HFZ was first interpreted as a tectonic terrane by Bowin (1975) as a pre-middle Albian, possible Jurassic subduction zone which formed early in the development of the Hispaniola Arc and was later reactivated as a 'transcurrent fault' beginning in the Oligocene. Shortly thereafter, a 1:100,000 scale geologic map (produced by Standard Oil of New Jersey) and lithostratigraphic study were published by Palmer (1963; 1979; Figure 5).

Other investigations of the HFZ centered on lithostratigraphic studies (Figure 5; Palmer, 1963; 1979; Groetsch, 1983; Riemer, 1978) and geochemical and structural investigations of the Cretaceous basement rocks in the area (Figure 5; Draper and Lewis, 1982; Lapierre and others, 1997). Strata in the San José de las Matas pull-apart basin were assigned to the Tavera Group by previous workers (i.e., Vaughan and 5 others, 1921; Palmer, 1963).

Previous workers inferred a strike-slip history for the HFZ, but failed to present compelling evidence for their interpretation. Mann and Burke (1984) conducted the only

reconnaissance of the area and suggested that the sediments of the Tavera Group were deposited in a pull-apart formed by left-lateral strike-slip faults. They lacked the supporting structural data, however, to confirm their interpretation, Draper and Lewis (1982; 1989; 1991) studied the structure and petrology of the Amina Schist and Duarte Complex (Figure 5). The northern extension of the HFZ was proposed to contain a graben by Draper and Lewis (1982). Lithostratigraphic studies just east of the study area by Riemer (1978) and Groetsch (1983) lent an interpretation of the area's paleosetting as a setting of subaerial fans (Figure 5).

Previous investigators speculated about the strike-slip nature of the master faults along the HFZ (Palmer, 1963; 1979; Groetsch, 1983; Draper and Lewis, 1982; Dolan and others, 1991). Olivo (1985) created the first 1:50,000 scale structural map of the Tertiary rocks in the easternmost section of the study area (Figure 5). Left-lateral movement along the HFZ was proposed by Olivo (1985) to explain the contact between the Duarte Complex and the Amina Schist, but did not specifically discuss the structure along the Inoa and Amina faults. A paleontological study by Saunders and others (1986) clarified the age of some of the Tertiary rocks found in the study area (Figure 5). Lapierre and others (1997) completed geochemical studies on gabbros of the Duarte Complex suggesting that it represents the remnants of an oceanic plateau generated by a Galapagos-type hotspot. Their approximate field area is shown in Figure 5. Erikson and others (1998) studied the areas just north of the study area in the Cibao Valley (not depicted in Figure 5) and suggested that strata accumulated in a strike-slip basin formed near a "restraining bend" between right offset segments of a left-lateral strike-slip fault zone. Their age

estimates, suggest that subsidence of the northern part of the Cibao basin occurred as the Cordillera Septentrional was being uplifted in the early mid-Pliocene(?).

## **GEOTECTONIC SETTING OF THE CARIBBEAN**

### **Regional Tectonic Setting**

The Caribbean plate is bordered to the east by the Lesser Antilles and to the west by Central America (Figure 6). Hispaniola is a critical point of study for neotectonics because the crustal movements which occurred there during the Tertiary are well preserved in the central portion of the island. To the north, the boundary between the NOAM/CARIB plates is a 250-km-wide zone of tectonic deformation encompassing the northern and southern boundary of Puerto Rico and Hispaniola known as the Northern Caribbean Plate Boundary Zone (NCPBZ) (Figure 6; Dolan and others, 1998). The NCPBZ defines the north-central margin of the Caribbean Plate. The NOAM/CARIB plate boundary follows the southern margin of Cuba and continues eastward on-shore in northern Hispaniola (Figure 6; Mann and others, 1998).

To the north of Hispaniola lies the Hispaniola Basin and to the northeast is the Puerto Rico trench (Larue and Ryan, 1998; Figure 3). A south-dipping slab of oceanic crust extends from the Puerto Rico trench to 150 km depth (McCann and Sykes, 1969; Figure 3). On the south side of Hispaniola, the Muertos Trench is the zone of northward underthrusting where the north-dipping slab extends to a depth of 30 km (Byrne and others, 1985; Figure 3). The Septentrional Fault Zone (SFZ) is part of the on-shore NOAM/CARIB plate boundary (Figure 3). The SFZ trends westward offshore into the Windward Passage northwest of Hispaniola, toward the Cayman trough pull-apart basin (Mann and others, 1984; Rosencrantz and others 1988; Figure 6).

**Uplift of the Duarte Complex and strike-slip movement along the plate boundary**

caused transpressional movements along the HFZ's Inoa and Amina faults. This transpression is primarily responsible for the development the releasing bend or pull-apart along the HFZ. Subsidence of the pull-apart basin occurred from Oligocene through the late Miocene (Sykes and others, 1982; Mann and others, 1984; McCann and Sykes, 1984). During the Oligocene, the Amina Schist likely tilted to the NE, which further lowered the basin sediments (Draper and Lewis, 1982). Later phases of tectonic transpression into the early-late Miocene may be responsible for a late reactivation of the faults bounding the pull-apart basin. It has been suggested that the folding of the Tavera Group documents the last phases or secondary effects of transpression and resultant uplift of the Cordillera Central, which up until Recent time continues to provide subaerial detritus to the Cibao Valley (Bowin, 1975; Lewis, 1982, Bowin and Nagle, 1982; Burke and others, 1984; Saunders and others, 1982; Pindell and Barrett, 1990).

### **Origin of the Caribbean Plate**

#### **Review of the Fixist vs. Mobilist Hypotheses**

Two hypotheses, the *Fixist* and the *Mobilist*, explain the tectonic development of the Caribbean region (Pindell, 1990;1994). Both hypotheses explain the origin of the Caribbean Plate and the structural plate boundary features created in their wake (Molnar and Sykes, 1969). The *Fixist* hypothesis states that the present-day Gulf of Mexico and Caribbean region did not exist between North and South America during the Triassic, Jurassic, and early Cretaceous (Buffler and Sawyer, 1985; Klitgord and Schouten, 1986; Ladd, 1976; Pindell, 1985; Pindell and others, 1988; Rowley and Pindell, 1989). This hypothesis incorporates sea floor spreading to produce plate movement and island arc

development on the Caribbean Plate (Morris and others, 1990). Asthenosphere, rather than rigid plate tectonics, is responsible for the creation of the magmatic arcs (e.g., the Great Arc of the Caribbean).

The second and more accepted view, the *Mobilist* hypothesis, indicates that significant amounts of eastward Caribbean migration occur relative to the westward movement of the Americas. This hypothesis is further split into two models: 1) generation of Caribbean Plate lithosphere between the Americas (Anderson and Schmidt, 1983; Donnelly, 1989; James, 1990; Klitord and Schouten, 1986; Salvador and Green, 1982); and, 2) lithosphere originating in the Pacific (Dickenson and Coney, 1980; Duncan and Hargraves, 1984; Pindell and Barrett, 1990; Pindell and Dewey 1982).

In other words, the lithosphere of the Caribbean plate originated either due to sea floor spreading between Yucatan and South America (Pindell, 1985) creating the Proto-Caribbean Seaway (Fixist), or formed as an oceanic plateau in the Pacific which moved eastward relative to the Americas (Mobilist) (Figure 7). In both hypotheses, westward drift of the North and South American plates is mainly responsible for the present east-west trending faults on the northern and southern borders of the Caribbean Plate (Mann and others, 1995; Pindell and Barrett, 1990; Pindell, 1994). The motion of the Farallon Plate relative to the Proto-Caribbean seaway at the time North America separated from Gondwana suggests a Pacific origin of the Caribbean Plate (Maury and others, 1990; Pindell, 1994). Perfit and Heezen (1978) prove that approximately 1,100 km of displacement has occurred along the Cayman Trough.

Pindell (1990;1994) suggests that the Pacific origin argument is viable and can

generally be summarized in two phases. First, from the Triassic to early Cretaceous, NW-SE relative separation of North and South America opened the Proto-Caribbean Atlantic-type seaway (Figure 7; Pindell, 1994). The second phase involved an Albian to Recent subduction of the Proto-Caribbean lithosphere beneath the evolving island arcs along the eastern NOAM/CARIB plate boundary as the Americas drifted westward from Africa (Pindell, 1994).

Duncan and Hargraves (1984) suggest that the Caribbean Plate may have been born in the Jurassic to early Cretaceous in the Pacific as the Farallon Plate passed over the Galapagos hotspot. Oceanic fragments in island arc rocks of Hispaniola and central America have recently been proposed to have been derived from the Galapagos plume hot spot (Dupuis and others, 1998; Lapierre and others, 1997).

*Late Triassic to Jurassic* - In late Triassic to early Jurassic time, North America rifted from Gondwana, the late Paleozoic supercontinent of the Southern Hemisphere, (Figure 7; Pindell, 1990;1994). By the middle Jurassic, the North American continent was rifting from Africa (Pindell, 1994). The Pacific oceanic plate, which includes the Farallon Plate, began moving eastward and subducting beneath the western margin of the Proto Caribbean (Duncan and Hargraves, 1984). The Proto-Hispaniola Arc originated as part of a chain of islands called the Great Caribbean Arc (Burke, 1988).

By the middle Oxfordian, the Gulf of Mexico (Figure 7) began to open via intra-continental extension which subsequently accommodated the development of an evaporite basin (Pindell 1990; 1994). During the Latest Jurassic, a single triple junction is postulated to have been responsible for sea floor spreading in the Gulf of Mexico (Pindell,

1994).

The genesis of the Hispaniola Arc may be as old as Jurassic (middle Oxfordian to lower Tithonian), as radiolarian fragments were recognized in ribbon cherts from the Duarte Complex near the town of Janico, located east of the study area (Montgomery and others, 1994). The Proto Caribbean Plate formed as Jurassic oceanic crust was built up as a seamount (Lewis and Jiménez 1991; Donnelly and others, 1990; Draper and Lewis, 1991).

***Early Cretaceous*** - A continuous volcanic chain of Pacific-origin basement rocks between the Americas formed the Greater Antilles Arc as the Farallon crust plate subducted underneath the Proto-Caribbean seaway (Figure 8, Plate A; Malfait and Dinkelman, 1972; Pindell and Barrett, 1990; 1994). Along a triple junction, the South American continent began separating from the Jurassic oceanic crust to its north and west (Figure 8, Plate A). As these continents rifted apart, the Proto Caribbean seaway opened during the Late Cretaceous further widening the Gulf of Mexico (Figure 8, Plate A; Wilson, 1966; Malfait and Dinkelman, 1972; Dickinson and Coney, 1980; Pindell and Dewey, 1982; Burke and others, 1984; Pindell and Barrett, 1990).

An early Cretaceous, northward-dipping subduction zone started in the forming Hispaniola Arc which produced a suite of northwest-trending mafic rocks that were extruded on top of the Duarte Complex (Bowin, 1975). These basaltic seafloor rocks were metamorphosed to form the Amina Schist (Figure 2; Bowin, 1975; Draper and Lewis, 1982). Early island arc activity produced the Amina protolith which accumulated first on the flanks of, and later covered the Duarte seamount structure (Draper and

Lewis, 1991). The protolith of the Amina Schist, appears to be sedimentary, but is of volcanic provenance (Draper and Lewis, 1982; 1989; Lewis and Draper, 1991). The age of the Amina protolith is pre-Aptian to Albian (Draper and Lewis, 1991; Montgomery and others, 1994).

***Late Cretaceous*** - Farallon plate crust subducted beneath the Caribbean plate west of the proto-arc system (Figure 8, Plate B; Pindell, 1994). By the Maastrichtian to early Paleogene, the America plates began moving WSW relative to the ENE moving Caribbean plate. This ENE trending movement of the Caribbean plate created a 2,000 km long, NW-SE structurally derived proto-arc system of the Greater and Lesser Antilles (Figure 8, Plate B; Perfit and Heezan, 1978).

The genesis of the Greater Antilles Arc system suggests that prior to subduction of the Farallon Plate during the early Cretaceous, plume magmas from the Galapagos hotspot intruded into the Proto-Caribbean Arc during the late Cretaceous to form the Duarte Complex in Hispaniola (Pindell and Barrett, 1990; Mann and others, 1991; Storey and others, 1991; Lapierre and others, 1997; Dupuis and others, 1998). However, this has been refuted, in part, by Meschede (1998). He suggests that Caribbean oceanic crust formed in a “near-Americas” position rather than to the west of the current-day position of Latin America, at the Galapagos hotspot. This “hotspot” theory is supported by westward plate motion velocities of the American plates (Pindell, 1990; 1994). Whether the tectonic event which formed the Great Arc is at the hotspot or in a “near-Americas” position, this event probably represents the collision of the Proto-Caribbean Seaway crust subducting beneath the evolving Caribbean plate crust (Pindell and Barrett, 1990).

By the late Cretaceous, at the Hispaniola Arc, the Amina protolith, along with the underlying Duarte Complex, were metamorphosed and folded. This was due as a result of a polarity reversal which caused the south-facing arc to close the interarc basin as subduction resumed on the northern side of the arc (Figure 1; Draper and Lewis, 1991).

The Amina rocks were metamorphosed into mainly schistose rocks. The Amina Schist in northwestern Hispaniola is described as mainly well-foliated metasediments consisting of competent leucocratic, quartzo-feldspathic layers alternating with darker green, mafic layers (Draper and Lewis, 1982; 1989).

The oblique collision of the Hispaniola Arc with the Bahama Platform occurred during the late Cretaceous, choking the north-dipping subduction complex (Pindell and Barrett, 1990; Draper, and others, 1994a). A new southward-dipping subduction complex resumed along the north-northeastern side of the Hispaniola Arc (Figure 1; Mattson, 1979; Bourdon, 1985; Pindell and Barrett, 1990). The Bahama Platform attempted to subduct underneath northeastern Hispaniola. Draper and others (1994a) suggest that overprinting effects of the Cenozoic collision and strike-slip deformation obscure many of the manifestations of earlier north-dipping deformational events in the Duarte Complex and Amina Schist rocks.

***Paleocene to Eocene*** - During the Paleocene, the Greater Antilles Arc collided with the Bahama Platform (Figure 8, Plate C). This collision caused a change in subduction polarity and an end to the south-facing early Cretaceous proto-Caribbean Arc growth (Pindell and Barrett, 1990). This collision began near Cuba and decreased in intensity through Hispaniola and to the east toward the Lesser Antilles (Figure 8; Plate C).

The north-facing Greater Antilles Arc moved to the northeast edge of the Bahama Platform and the forearc region overrode first the carbonate-bank edge and then the bank itself (Figure 8; Plate C; Pindell and Barrett, 1990). An uplifted subduction complex exists in northern Hispaniola (Bowin and Nagle, 1982). This subduction complex caused uplift of the Duarte Complex and subsidence of the Cibao Basin (forearc basin) during the latest Eocene-earliest Oligocene (Joyce, 1991). Subduction continued into the Eocene, but failed to thrust the subduction complex of central Hispaniola onto the Bahama Platform (Bowin and Nagle, 1982; Pindell and Barrett, 1990). A southward-dipping subduction zone continued until middle Eocene time producing continued regional magmatism which includes the volcanic rocks (Rodeo Basalt) of the Magua Formation in the study area (Draper and Lewis, 1991). Subduction produced magmatism in the upper plate, but it is inferred that the Rodeo Basalt has arc affinities. By the middle to late Eocene, the Greater Antilles Arc-Bahama Platform collision terminated (Figure 8; Plate C; Pindell, 1994).

At the latest Eocene, left-lateral strike-slip movement along the NOAM/CARIB plate boundary developed as ENE migration of the Caribbean Plate continued relative to North America (Figure 8, Plate C; Pindell, 1994). Also at this time, the Cayman trough opened (Figure 8, Plate C; Donnelly, 1994). The Cayman Trough opened by sea floor spreading at the Mid-Cayman Spreading Center linked to left-lateral transcurrent movements, as evidenced by focal-mechanism solutions from earthquakes (Sykes and Ewing, 1965; Molnar and Sykes, 1969). Deformation continued along the NOAM/CARIB plate boundary and in the NCPBZ from the late Eocene into Oligocene time.

***Oligocene*** - Left-lateral relative motion between the North American and South American plates along the Cayman Trough began in the Oligocene (Figure 8, Plate D; Perfit and Heezen, 1978). Left-lateral strike-slip faulting started along the ancient Motagua-Polochic fault zone in Guatemala (Figure 8, Plate D; Perfit and Heezen, 1978). This left-lateral transcurrent faulting extended from Guatemala to the east through Hispaniola and north of Puerto Rico to the Lesser Antilles (Figure 8, Plate D; Larue, 1998). One compressional component in Hispaniola was likely caused by the effects of the Greater Antilles Arc-Bahama Platform collision as the Caribbean Plate moved eastward with respect to the Americas plates (Molnar and Sykes, 1969; Mann and others, 1983; Burke, 1988).

Left-lateral strike-slip fault movement continued along the HFZ during the early Oligocene this led to the opening of the San José de las Matas pull-apart basin (cf. Draper and Lewis, 1982; Groetsch, 1983; Dolan and others, 1991).

***Miocene to Recent*** - Eastward motion of the Caribbean plate along the NOAM/CARIB plate boundary continued relative to the North American plate (Figure 8, Plate D; Mann and Burke, 1984). Much of this deformation is complex and resulted in inboard island arc deformation associated with compressional strike-slip fault segments in Jamaica, Central America and Hispaniola (Figure 8, Plate D; Mann and Burke, 1984).

By the late Miocene, northeastern Hispaniola obliquely collided with and overrode the southeastern flank of the Bahama Platform culminating in a restraining bend (Figure 3; Sykes and others, 1982; Mann and others, 1984; McCann and Sykes, 1984).

Transpression at the NOAM/CARIB plate boundary attempted to force the Bahama

Platform beneath the Hispaniola Arc rocks. This failed subduction further uplifted the Duarte Complex where these Tavera Group rocks were earlier deposited and exposed in the Tavera and San José de las Matas pull-apart basins (Figure 2; Dolan and others, 1991; de Zoeten and Mann, 1991).

A restraining bend identified in the Puerto Rico Trench transform fault northeast of the Dominican Republic constricted the northeastward migration of the north-central Caribbean and became responsible for much transpression in Hispaniola from the Miocene to Present (Molnar and Sykes, 1969; Bracey and Vogt, 1970; Jordan, 1975; Minster and Jordan, 1978; Schell and Tarr, 1978; Mann and Burke, 1984; Mann and others 1984).

The island of Hispaniola became uplifted by the late Pliocene to late Pleistocene (Maurrasse, 1982; Erickson and others, 1998). Presently, the island of Hispaniola is rising along the west coast of the island in Haiti based on isotopic dating of raised late Quaternary coral reef terraces (Calais and Mercier de Lépinay, 1993; Mann and others, 1995). The high topography and large earthquakes around the SFZ support the contemporary deformation along Cordillera Septentrional (Winslow and McCann, 1985; Guglielmo, 1986). Other examples of left-stepping fault discontinuities in the region include restraining bends and pull-apart basins in northern Hispaniola.

**Present Motions** - Currently, the Caribbean plate is moving eastward relative to the North and South American plates at a rate of  $12 \pm 3$  mm/yr. according to DeMets and others (1990) NUVEL-1 global plate motion model. Slip and moment rates along the southern Cuban margin have been recalculated at 13-15 mm/yr by Calais and others (1998) using Global Positioning System (GPS) data. Dolan and others (1998)

suggest that the NOAM/CARIB plate boundary motion rate is ~20 to 25mm/yr based on earthquake focal mechanisms for the 1943 and 1946 mainshocks along the plate margin off northern Hispaniola (Calais and others, 1992; Calais and Mercier de Lépinay, 1995; Dillon and others, 1992; Dolan and Wald, 1998). Displacement continues along the two major strike-slip boundaries of the North American and South American plates. No active spreading centers exist along these boundaries except in the Cayman trough (Figure 8; Plate D).

To the north of Hispaniola, the southeastern margin of the Bahama Platform is actively colliding with the northern margin of Hispaniola (Bracey and Vogt, 1970; Mann and others, 1984; Dolan and Wald, 1998; Grindlay and others, 1999). Along the CARIB/NOAM plate boundary, seismicity data defines a south-dipping Atlantic oceanic slab (Dolan and others, 1998). An opposing, north-dipping slab of Caribbean lithosphere lies beneath the south side of Hispaniola, along the Los Muertos trough (Figure 3; Dolan and others, 1998). The Atlantic and Caribbean slabs may collide in the upper mantle at approximately 50 km depth between Hispaniola and the Puerto Rico (Dolan and others, 1998; Dolan and Wald, 1998).

Present-day motion along the NOAM/CARIB plate boundary is mostly left-lateral. Much of the left-lateral component of motion in northern Hispaniola occurs along the SFZ (Mann and others, 1984, 1991; Pindell and Barrett, 1990; Calais and others, 1992; Prentice and others, 1993; Winslow and others, 1991).

This combination of left-lateral strike-slip movement and subduction causes ongoing transpression of the Cordillera Septentrional and the eastern Cibao basin. Offset

of the HFZ is probably absorbed inboard of Hispaniola along with the SFZ to its north. Uplift and deformation of the Duarte Complex and the Tavera belt clastics of northwestern Hispaniola have resulted from this transpression (Mann and others, 1991).

In Hispaniola post-Pliocene deformation occurs just south of the Septentrional fault along the northeastern flank of the Cibao Valley (Winslow and others, 1991; Prentice and others, 1993). Fault traces of the Septentrional fault in the central Cibao Valley reveal evidence of displacement 730 years ago evidenced by paleoseismic data, along with stream and terrace offset data (Prentice and others, 1993; Mann and others 1998). Historical reports document movements, fracturing, land slides, liquefaction, and water spouts during the 1943, 1946, and 1953 earthquakes (Winslow and McCann, 1985). South of the Cibao Valley, Recent deformation has not been documented along the HFZ (Erikson and others, 1998) except for the destruction of nearby La Vega on November 2, 1564 which was caused by a large earthquake along an undocumented fault (McCann and Pennington, 1990).

## **METHODS**

Six months of field work were conducted over the past six years collecting structural data, lithostratigraphic descriptions, and observations of surface morphology to create a new 1:50,000 scale geologic map and cross-sections, and a stratigraphic column for the western HFZ. A recently available 1:1,000,000 scale satellite image (circa 1992) generated by Space Imaging-EOSAT™ and four 1:100,000 scale Space Imaging-EOSAT™ color satellite photos (circa 1988) aid in determining general structural trends in the study area.

Newly available topographic maps at 1:50,000 scale (circa 1988) and 1:40,000 scale (approximately) aerial photographs (circa 1984) generated by the United States Defense Mapping Agency and the Instituto Cartográfico Militar, F.F.A.A. Republica Dominicana form the base of the new 1:50,000 scale geologic map.

Aerial photographs were reviewed before, during, and after structural mapping. Structural data for this map were collected in outcrops along rivers and stream valleys, road-cuts (new and old), and from a dam construction project SE of the town of Monción. The outcrop exposures are numerous due to the amount of roadwork and dam construction occurring since 1994.

Field mapping reveals strong deformation in the Tertiary rocks of the Tavera Group which outcrops along the northwestern segment of the HFZ. Geologic information such as the attitudes of beds and fractures is predominantly in the Tertiary sedimentary rocks. All parts of this study area were not investigated in equal detail. The southwestern portion of the field area is not thoroughly mapped due to the limited access and exposure

of the Duarte rocks. In general, a lesser amount of structural data was collected in the Cretaceous rocks, as this study specifically concentrates on structural data from the Tertiary Tavera Group. The apparent thickness of each formation was compiled by measuring the widest transect perpendicular to strike using an average dip of the formation. If the formation was folded, an average dip was made based on the limb dips. Estimates are maximized.

A new geologic map at 1:50,000 scale is shown in Plate 1 and cross-sections are in Plate 2. A tectonic interpretation of the study area is possible by studying the local structures. The structures were separated into domains based on specific formations and specific trends established through study of the lineaments (Plate 3). Stereonets of the fold and fracture data along with rose diagrams of the lineaments compiled from trends found on satellite imagery, aerial photos, and the topographic maps help to support the conclusions drawn in this dissertation.

Stereonet plots are assembled for bedding, faults, fractures, schistosity, and trends of elongated clasts in the study area. An aerial photo study was conducted to plot the main lineaments in the study area. Lineaments were plotted from the aerial photographs using stereoglasses. The trends of lineaments are plotted on rose diagrams. The information is used in this study to help extend fault lengths. In a region of rapid weathering and widespread plant growth, scarps, and sharp linear trends found in areas along the HFZ are likely associated with Tertiary movements. The rose diagrams were constructed as frequency diagrams whose orientations are parallel to the average trends of the lineaments recognized in the air photos. Photographs are included in this dissertation which depict

the different formations, some formation contacts, the fault zone, and the elongated clasts in the study area.

## **STRATIGRAPHY OF THE STUDY AREA**

A stratigraphic column by Palmer is shown on Figure 9 (as modified by Groetsch, 1983) along with a new stratigraphic interpretation of the northwestern piedmont of the Cordillera Central based on this study. Interpretation and explanation of this stratigraphic column follows.

The stratigraphy of the northwestern flank of Cordillera Central may be categorized by three separate groups: 1) the Duarte Complex of late Jurassic to early Cretaceous and the Amina Schist of early Cretaceous age; 2) the Tavera Group's Inoa Conglomerate, Magua Formation, Monción Limestone, La Bruja Limestone, and the Pananao Limestone of early Tertiary age; and, 3) the Bulla Conglomerate and Cercado Sandstone of late Tertiary age.

### **Late Jurassic to Cretaceous Mafic Volcanics**

#### **Duarte Complex**

The oldest rocks in the field area are pre-Aptian-Albian (likely late Jurassic to early Cretaceous) metabasalts of the Duarte Complex (cf. Draper and Lewis, 1989; 1991; Montgomery and others, 1994; Lapiere and others, 1997). The Duarte Complex is comprised of a dominantly chlorite-grade metabasalts, amphibolites, greenschists, greenstones of the prehnite-pumpellyite facies, plus minor siliceous metasediments, and ultramafic rocks (Bowin, 1966, 1975; Palmer, 1963; Nagle, 1974; Draper and Lewis, 1989, 1991; Lewis and Jiménez, 1991; Donnelly and others, 1991). Gabbro has been identified in the south-central portion of the mapped area (Plate 1; Palmer, 1963).

**Rocks of the greenschist and subgreenschist facies outcrop south of the Inoa fault**

(Plate 1). The rocks of the subgreenschist facies are described as holocrystalline basic flows and flow breccias (Palmer, 1963). Typically these rocks are fine-grained and massive (Photograph 1). The lavas are foliated, as mapped south of San José de las Matas, near the Bomba de aqueducto on Río Honda (Plate 1). Elsewhere, the lavas also may be massive. Amygdules, or vesicles commonly formed during the cooling of basalt, constitute as much as 1/3 the volume of the rock (Palmer, 1963), and are more prevalent in the western half of the study area WSW of El Palmer. The fine-grained lavas weather reddish-brown to dark maroon to red, but fresh surfaces exposed in river cuts are dark grayish-green. The subgreenschist facies rocks of the Duarte Complex crop out at the distal ends of the field area south of the Inoa fault, as originally mapped by Palmer (1963). Petrographic studies by Palmer (1963) describe the subgreenschist facies rocks to contain varying proportions of albite, clinopyroxene, chlorite, and magnetite altered to hematite. Amygdules are filled with calcite, analcite, and sericite (Palmer, 1963).

The greenschist facies rocks outcrop centrally: east of Río Mao, west of Río Guanajuma, and south of the Magua Formation along an unnamed fault (Plate 1). The greenschist facies rocks outcrop as massive bodies with little to moderate schistosity (Photograph 2). The greenschist facies rocks are dark green to greenish-gray greenstones. Palmer's (1963) thin section analyses reveal varying proportions of actinolite, chlorite, albite, and epidote with amygdules, where present filled with either quartz, chlorite, epidote, and calcite.

### **Amina Schist**

The Amina Schist is a metamorphic rock which lies north of the Cordillera Central

and north of the Amina fault (Plate 1). This formation consists generally of grayish-green to greenish-gray schists with the following principal minerals: albite, quartz, chlorite, epidote, actinolite, and occasional white micas (Palmer, 1963). No isotopic age determinations have been made on the Amina Schist (Draper and Lewis, 1991). The Amina Schist is made of tuffs or immature epiclastic sediments consisting of competent leucocratic, quartzo-feldspathic layers (Photograph 3; Draper and Lewis, 1982;1989;1991 Pindell and Barrett, 1990; Mann and others, 1991; Draper, and others, 1994a).

The Amina Schist can be traced from the eastern end of the study area to the western end (Plate 1). The Amina Schist is the northwestern extension of the Amina-Maimon rocks which crop out from SE to NW in Hispaniola (Figure 3;Bowin, 1960). The Amina was mapped extensively by Palmer (1963; 1979) and Antonini (1968; 1979) and later studied by Draper and Lewis (1982;1991) and Draper and others (1994b).

At the widest point across the mapped area, the Amina Schist measures approximately 6.5 km of apparent thickness. The southern contact of the formation is the Amina fault which places the formation in contact with the Las Matas Breccia and the Inoa Conglomerate (Plate 1). The Amina Schist is unconformably overlain by the early Miocene Monción Limestone and the late Miocene Bulla Conglomerate, and Cercado Sandstone (Plate 1).

The protolith rocks of the Amina Schist were likely tuffs or immature epiclastic sediments and arc-derived graywackes mixed with carbonaceous shales, breccias, and conglomerates (Draper and Lewis, 1982). The age of the Amina Schist protolith is approximately Albian to Aptian (Draper and Lewis, 1991). The protolith rocks were

metamorphosed into the greenschist facies containing leucocratic quartzo-feldspathic layers alternating with green schistose layers (Draper and Lewis, 1991). The Amina Schist was likely metamorphosed from the Coniacian to the Campanian (Draper and Lewis, 1991).

Palmer (1963) describes a marble lens approximately 60 m thick exposed at two places in the Río Amina where the river makes a sharp V-shaped bend (Plate 1). In hand specimen the limestone was described generally as marble varying from white crystalline limestone to a mottled type with irregularly distributed carbonaceous (?) material (Palmer, 1963). The lens was described to have distinctive topographic expression from air photo interpretation. I searched extensively for this marble lens in Río Amina without success. Draper (per communication 1997) also could not find this outcrop in 1991.

### **Hornblende Tonalite**

A large intrusive body of hornblende tonalite crops out south of San José de las Matas and the Inoa fault, just south of Río Inoa (Plate 1; Photograph 4). The hornblende tonalites intruded during the post-Campanian, pre(?) -Late Maastrichtian (Bowin, 1960; Palmer, 1963). These tonalites contain hornblende, but little biotite (Palmer, 1963). Trace granules of epidote were evident in some samples. The hornblende tonalite from macroscopic inspection is made up of quartz, plagioclase feldspars, and hornblende. The presence of this hornblende tonalite is likely associated with the Loma de Cabrera Batholith which is an intrusive complex to the southwest of the study area (Cribb, 1986).

## **Paleogene Rocks**

### **Magua Formation**

The Magua Formation, as originally characterized by Palmer (1963), is a Paleocene to middle Eocene-age Conglomerate made up of poorly sorted, angular and subangular cobbles, and boulders of Duarte greenschist facies rocks, leucotonalites, sandstone, and sandy mudstones (Photograph 5; Figures 9 and 10). The cementing matrix of Magua Formation is composed predominately of a purplish-red siltstone. The Magua Formation was estimated to be 1,500 m thick (Palmer, 1963) and contains successive layers of pyroclastic flows, volcanic flow breccias, and angular conglomerates. These flows, flow breccias and angular conglomerates sometimes occur in a tuffaceous matrix. To determine the apparent thickness of the formation, a horizontal traverse line, perpendicular to strike, was measured across the ground surface. The Magua is approximately 300 to 500 m thick north of Rodeo Basalt extrusion (Plate 1). The Magua Formation is between 400 m and 800 m thick south of the Rodeo Basalt. The Magua is thicker to the west and thins to the east. Along the southernmost extension of the Magua Formation, an unnamed fault separates the Magua from the Duarte greenschist facies rocks (Plate 1). This unnamed fault is not well exposed in the field due to large boulder cover and thick vegetation, except for a noticeable sharp rise in relief along its inferred contact. The base of the Magua is discernible in only one locality south of the village of El Cacao (Plate 1). Here the Magua is in fault contact with the subgreenschist facies rocks of the Duarte Complex. To the north, the Magua is in fault contact with the Inoa Conglomerate along the Inoa fault and is exposed on the road from El Cacao northward

towards the village of Rodeo (Plate 1).

In cross-section, the Magua reveals several sequences of basaltic volcanics with alternating layers of pyroclastic flows and volcanic breccias ultimately overlain by conglomerates (Plate 2; Cross-sections A-A' through E-E'). The volcanic breccias are completely disordered and have angular clasts of Duarte greenschist facies rocks and tonalites which occur sometimes in a tuffaceous matrix.

Scant evidence of intraformational limestone clasts in the Magua Formation was found by Palmer (1963). These intraformational clasts include bioclastic limestone, and massive to thin-bedded recrystallized limestone, found along the Inoa fault. These limestone clasts contain rudistid fragments and other pelecypods, echinoid spines and a few foraminifera in a cryptocrystalline calcite matrix (Palmer, 1963). Rudistid fragments found by Palmer from three bioclastic limestone lenses within the formation were originally identified by A.G. Fischer (Cooke in Vaughan et al., 1921) as belonging to the family *Radiolitidae* and are suggested to be late Cretaceous in age. These bioclastic limestone clasts found in the Magua Formation are probably allochthonous. These limestone clasts may have been introduced into the Magua Formations through gravity sliding. There is little evidence to suggest that the fossiliferous clasts are intraformational if they are Cretaceous and the matrix is Eocene.

#### **Rodeo Basalt Member of the Magua Formation**

The middle of the Magua Formation from E to W is a single zone of amygdaloidal, aphanitic, basaltic lava. This Rodeo Basalt is a member of the Magua Formation (Figures 9 and 10; Palmer, 1963). According to Palmer (1963) the Rodeo Basalt is approximately

100 m thick. Calculations based on a horizontal ground surface traverse oblique to strike, approximates the thickness of the basalt to vary between 50 m and 850 m thick. The outcrop belt of the Rodeo Basalt has a wider traverse to the west due to the lower dips on the limbs of a plunging syncline. The Rodeo Basalt is made up of extrusions which are very fine grained and are characterized by a high density of amygdules (Photograph 6). Weathered, microlitic clasts of olivine, pyroxene, and augite predominate the holocrystalline rock and contain small occurrences of chlorite, and microlites of plagioclase (Palmer, 1963). Due to the deep weathering of the basalt's exposed surfaces, the amygdular lava is burnt red to reddish-gray in color rather than dark greenish-gray as would be expected in its fresh state. The amygdules are filled with clear, twinned albite, chlorite, and minor amounts of epidote (Palmer, 1963).

### **Tavera Group of the Western HFZ**

#### **Inoa Conglomerate**

The Inoa Conglomerate is predominantly a red boulder, cobble, and pebble conglomerate. Its clasts consist of metabasalts, amphibolites, greenschists, greenstones, ultramafic rocks, hornblende tonalite pebbles, and minor siliceous metasediments eroded from the Cordillera Central (Photograph 7; Palmer, 1963; 1979; Figures 9 and 10). This formation has a minimum thickness of 600 meters (Palmer, 1963). The Inoa is between 750 m and 2 km thick, based on an analysis of nonparallel layer boundaries along a traverse line, perpendicular to the strike of bedding. Palmer (1963) proposed that the Inoa Conglomerate has two members, a red fossiliferous-member and a gray non-fossiliferous-member (Figures 9 and 10). The writer confirms this and proposes this distinction as part

of the Inoa Conglomerate's stratigraphic classification (International Subcommission on Stratigraphic Classification, 1994; Figure 9).

The pervasive red color of the red member conglomeratic formation is due to its red siltstone or sandy-siltstone matrix. The pebbles of the Inoa vary in size from less than 10 cm up to cobbles at least 90 cm (Palmer, 1963; 1979). The clasts are mainly subrounded to well rounded in the red member and are coated with a hematitic desert-like varnish in unweathered strata (cf. Palmer, 1963). The thin, dark, shiny coating on the Inoa clasts is composed of iron oxide likely from exudation of mineralized solutions from long exposure (Dolan and others, 1991). Weathered and aurally exposed Inoa Conglomerate tends to be friable and the conglomerate pebbles can be easily removed from the siltstone or sandy-siltstone matrix. Palmer (1963) described the red conglomerate member as poorly sorted and poorly bedded. In most localities in the study area, however, the Inoa Conglomerate is well sorted with well developed beds of alternating siltstones, silty sandstones and conglomerates. Conglomeratic beds may be up to 10 m thick. The Inoa Conglomerate tends to be massively bedded in some places, but may still show rhythmic alternations between conglomerates and siltstones and sandstones on an even larger scale (tens of meters).

The clasts of the red conglomerates are almost entirely derived from the Duarte Complex. Amina Schist clasts are rarely found in the Inoa Conglomerate and have only been identified in close proximity to the Amina fault in the Las Matas Breccia (Plate 1).

The distribution of the gray member lies at the northern extent of the Inoa Conglomerate (Plate 1). The major difference between the red member and the gray

member is the color of the rock. The gray member has distinctive thinner, rhythmic beds of fossiliferous siltstone. The gray member contains conglomerate pebbles up to 100 cm. The transition from red beds to gray beds is usually abrupt. However, there are places where red beds alternate with gray beds (cf. Palmer, 1963).

The clasts of the gray member conglomerates are derived entirely from the Duarte Complex. Amina Schist clasts have not been identified in the gray member of the Inoa Conglomerate. Tonalites are common in the conglomerate, as well as chert clasts. Alternating beds of thin limestone bearing shells and rudistids are common only in the gray member conglomerates at the northern end of the Inoa Conglomerate. These limestones have been identified in the northernmost sections of Río Guanajuma, Río Amina and Río Pananao (Plate 1).

Anticlines and synclines with fold axes predominantly trending WNW of, and parallel to the Inoa fault occur in the Oligocene-age Inoa Conglomerate. The rocks of the Inoa Conglomerate are complexly deformed. The topography and river traces within the Inoa Conglomerate are fault controlled. The Inoa Conglomerate is in fault contact with the Amina Schist along the Amina fault (Plate 1). To the south, the Inoa Conglomerate is in fault contact with the Magua Formation in the western part of the study area and with the Duarte Complex in the eastern part of the study area (Plate 1).

### **Limestones**

Several formerly unnamed carbonate units crop-out in different locations of the study area in the Inoa and Amina fault zones (Plate 1). Limestones in the study area were reported by Palmer (1963) to occur as two main types: bioclastic limestone and massive to

thin-bedded aphanitic or recrystallized limestone. A summary of the different limestones found in the area follows:

### ***Pananao Limestone***

The Pananao Limestone outcrops along the Amina fault in Río Pananao northwest of the village of Pananao Abajo, southeast of Monción (Plate 1). The Pananao Limestone is a newly named formation. This limestone is a buff-white and yellowish-gray, hard, organic, bioclastic limestone. The Pananao Limestone remains undated. The Pananao Limestone remains undated because it has not been previously identified as a separate formation. This limestone may be associated with the distal progradation of limestone in the gray member of the Inoa Conglomerate as inferred from its position just north of the gray member (Plate 1). The Pananao Limestone is similar in texture, color, and thickness to the late Oligocene-age Monción Limestone which crops out beyond the western border of the study area (Photograph 8; Palmer, 1963; Saunders and others, 1986). It is hypothesized that these two formations may have a similar correlation; however more work is necessary to understand their relationship. The Pananao Limestone has thick, indurated beds. Mud cracks are visible on the underside of bedding surfaces. Algal mats are visible along exposed bedding surfaces. This limestone contains benthic fossils and exhibits evidence of much bioturbation. Large coral heads are strewn in the limestone and are interpreted as detrital matter in the matrix. It is significant that the coral heads are not in life positions, possibly suggesting an off-shore higher turbid environment. The thickness of the Pananao Limestone was measured in a section just east of Monción on the east side of Río Mao and is approximately 25 m.

### ***La Bruja Limestone Member of the Magua Formation***

This formerly unnamed limestone of the Magua Formation (cf. Palmer, 1963;1979) crops-out south of Monción between a thin sliver of the Inoa Conglomerate and the Magua Formation. It is newly named the La Bruja Limestone Member of the Magua Formation. This limestone outcrops near the village of La Bruja (Plate 1). The La Bruja is a limestone in most localities, but may crop out as a gray to white, aphanitic sheared marble in some localities (Photograph 9). This thin band of limestone is caught in the shear planes along the Inoa fault. The limestones to the west of La Bruja are less sheared and the degree of crystallization is less pervasive. Outcrops of La Bruja Limestone are sandwiched between the Magua Formation and the Inoa Conglomerate along the south side of Río Amina near the village of El Palmar. The thickness of the La Bruja Limestone is estimated to be less than 20 m. Massive limestone beds crop out just north of the Inoa fault along Río Amina (Plate 1). Limestone may be characterized in this locality as a thick-bedded, gray to black, recrystallized, aphanitic limestone.

West of La Bruja, the thin to massively bedded La Bruja Limestone is intensely sheared and crumpled. Algal mats, although not abundant, are in their growth position as found on the road from Rodeo leading to the village of El Cacao (Plate 1). The limestone is recrystallized to a grayish-white approaching the shear zone. The La Bruja Limestone along the Inoa fault, south of San José de las Matas, is characterized by several elongate lenses of recrystallized limestone. This limestone is consistently the same thickness, but is rarely exposed. The easternmost occurrence of the La Bruja Limestone crops out in Río Honda south of San José de las Matas (cf. Palmer, 1963; Olivo, 1985). At these few

localities in Río Honda, bedding cannot be measured. This recrystallized limestone is caught between the shear planes of the Inoa fault (Vaughan and 5 others, 1921; Olivo, 1985).

The La Bruja Limestone was likely deposited in narrow basins parallel to the paleo-coastline and later sheared (Saunders and others, 1982; Olivo, 1985). More work is necessary to determine the relative age of these carbonates with the formations bounding them. Limestones characterized as the La Bruja Limestone are the unnamed limestones discussed by Palmer (1963; 1979) may be the same age as the Paleocene to middle Eocene Magua Formation. Palmer collected paleontological evidence (samples) from two stations associated with this limestone formation. Planktonic foraminifera were examined by E.A. Pessagno (Palmer, 1963). Palmer proposed the age of the "La Bruja Limestone" to be middle Eocene from the samples. The age of the fossils in the La Bruja Limestone is the only tie to the Magua Formation.

### *Monción Limestone*

The Monción Limestone outcrops WNW of Monción (Plate 1). The contact between the Monción Limestone and the Amina Schist was not observed in the field. The Monción Limestone is a late Oligocene to earliest Miocene, hard, bioclastic, yellowish-gray to buff colored limestone (Photograph 10; Figures 9 and 10; Palmer, 1963; Saunders and others, 1986). The Monción Limestone has been previously reported to be 45 m thick (Palmer, 1963). Horizontal ground traverse lines oblique to strike were measured. The thickness of the bedding was calculated from the line. The true thickness of the limestone is calculated to be approximately 38 m thick. Algae and large orbitoidal foraminifera are

obvious in the rock (Photograph 10; Palmer, 1963). The composition of the Monción Limestone is similar to that of the Pananao Limestone. The Monción Limestone is well bedded with beds typically ranging from 1 to 3 m thick. Burrowing organisms produced a bioturbid, muddy limestone. This formation is well exposed in Río Gurabo and Arroyo Gurabito in the western portion of the study area (Plate 1).

### **Neogene Sedimentary Rocks**

The Cercado Sandstone and its basal member, the Bulla Conglomerate crops out in the northernmost parts of the field area (Plate 1). The late Miocene Cercado Sandstone (Maury, 1919; Saunders and others, 1986) and the conformably underlying Bulla Conglomerate (Cooke, in Vaughan and others, 1921) rest unconformably on top of both the Tavera Group and the Amina Schist, respectively (Figure 9; Palmer, 1979). Combined, the Cercado Sandstone and Bulla Conglomerate are between 275 m and 1000 m thick in the field area (Saunders and others, 1982; Butterlin and others, 1956).

### **Bulla Conglomerate**

The Bulla Conglomerate is characterized as a well-lithified boulder conglomerate (Photograph 11). The contact between the Bulla Conglomerate and the underlying Inoa Conglomerate is exposed in the eastern part of the study area. The well rounded to subrounded boulders of the Bulla Conglomerate are derived from island arc rocks of the Cordillera Central. Palmer (1963) estimates the Bulla Conglomerate to be 120 m thick. The Bulla Conglomerate, as calculated along a horizontal ground surface traverse line perpendicular to strike, is approximately 120 m thick in the vicinity of the town of Monción (Plate 1).

The matrix is a yellowish-tan, limey silty-sand. Tonalite boulders are the most abundant clasts in the formation followed by greenstones, felsic tuffs, and vein quartz (Palmer, 1979). The weathered outcrops of Bulla Conglomerate yield an unconsolidated, friable matrix. The Bulla Conglomerate tends to be semi-consolidated, and has a calcareous matrix. Macrofossils occur along the upper contacts with the Cercado Sandstone. Detrital shell matter and *Thalassia* (eel grass) are indicators of the transition zone into the Cercado Sandstone (Saunders and others, 1986).

### **Cercado Sandstone**

The late Miocene Cercado Sandstone is a poorly lithified fine- to medium-grained, limey, fossiliferous, cross-bedded sandstone containing fine-grained island arc mafic minerals (Photograph 12; Figure 9). Patch reef environments dominate its uppermost section in the study area. Island arc-derived boulders and cobbles sporadically occur in the Cercado Sandstone. The Cercado Sandstone conformably overlies the conglomerates of the Bulla Conglomerate. A horizontal ground surface traverse line perpendicular to strike calculates the Cercado Sandstone to be consistent with Palmer's (1963) estimate of approximately 580 m thick.

The Cercado is yellowish-orange to yellowish-tan colored. Cross-bedding is often identifiable between beds of rip-up clasts of mollusk shells which indicate high energy environments. Conversely, calmer, shallow water environments are prevalent in some upper sections of the Cercado Sandstone. *Callianassa* arthropods up to 20 cm long and gastropods as large as 30 cm in diameter are abundant. *Thalassia* is identifiable in the bedding of the Cercado Sandstone in the upper sections. According to Saunders (1982),

the top of the Cercado Sandstone is marked by coral-packed beds that are discordantly cut by the overlying conglomerate at the base of the early Pliocene Gurabo Sandstone. The Gurabo is stratigraphically above the Bulla Conglomerate and not depicted on the stratigraphic column. The Gurabo outcrops north of the study area.

### **Tectonic Breccias of Uncertain Age**

#### **Las Matas Breccia**

This breccia crops out along the Amina fault west of San José de las Matas in exposures along Arroyo Pinalitos in the vicinity of the village of Caobanico, and north and west of the village of El Rubio along Arroyo Quebrada del Oro (Photograph 13; Figures 9 and 10).

The Las Matas Breccia is predominantly a breccia of angular clasts of Amina Schist set in a finer-grained matrix of Inoa siltstones. Crushed angular clasts of greenstones and tonalites occur in the matrix, but rarely occur as intact pebbles or cobbles. The breccia is regularly cut by quartz veinlets. Palmer (1963) reports that these veinlets cutting the rock may also consist of albite, prehnite, and pumpellyite. The matrix is slightly metamorphosed and lithified. Rock color is a mixture of greenish-gray clasts in a reddish-brown matrix. The Las Matas Breccia is estimated by Palmer (1979) to be at least pre-early Oligocene. (Figure 9). Palmer estimates this only if these same types of rocks were found in the Magua Formation (Palmer, 1963). To date, no such occurrence has been established. This breccia incorporates tuffaceous siltstone clasts similar to those found in the Eocene Magua Formation but more work needs to be performed to establish this correlation.

The Las Matas Breccia takes on a pale greenish-white appearance on the road just east of El Rubio (Plate 1). This portion of the breccia is riddled with quartz veins in an almost entirely angular clastic matrix of Amina Schist with an intermixed finer matrix of siltstone beds of the Inoa Conglomerate. The brecciation of the rocks identified by Palmer (1963), named the Las Matas Breccia, is considered to be a tectonic feature related to movement on the Amina and possibly the Inoa faults (cf. Palmer, 1963). This study clearly identifies the Las Matas Breccia as tectonic because of the angularity of clasts and mixture of so many ages of rocks. The Las Matas Breccia only crops out along fault splays and fractures.

#### **Pananao Abajo Breccia**

The Pananao Abajo Breccia outcrops between the Amina Schist and the Pananao Limestone in one location northwest of Pananao Abajo in Río Pananao (Plate 1). The breccia is pale greenish-white with reefal limestone clasts (Photograph 14). The matrix is composed of crushed Amina Schist material. Subangular to subrounded reefal Pananao Limestone clasts are incorporated with highly angular, coarse fragments of the breccia. This breccia has not been dated. The Pananao Abajo Breccia is posited to be stratigraphically above the early Oligocene to middle Oligocene gray member of the Inoa Conglomerate (Figure 9). This position is relative to the increase in fossiliferous beds in the Inoa. Limestone breccia was produced by movement along the Amina fault after its deposition.

### **La Bruja Breccia**

The La Bruja Breccia outcrops between the subgreenschist facies rocks of the Duarte Complex and the Inoa Conglomerate in the vicinity of the village of La Bruja (Plate 1). The La Bruja Breccia crops out in steep ravine between two hills: Cerro de la Bruja and Loma de Piedra (Plate 1). The matrix is composed of very fine-grained subgreenschist facies rock clasts and grains along with finely ground siltstone of the Inoa Conglomerate (Photograph 15). Angular, elongate, La Bruja Limestone fragments occur in the dark gray, greenish-gray, or reddish gray matrix of weathered subgreenschist facies rocks, clays, and silt. Angular mafic volcanic rocks make up less than 10 percent of the clasts and are between 5 to 10 cm in length. This tectonic breccia occurs along the Inoa fault. The La Bruja Breccia is likely pre-middle Eocene in age based on structural evidence of the time of faulting along the Inoa fault (Figure 9).

### **Suí Breccia**

The Suí fault is a NW-striking fault north of San José de las Matas (Olivo, 1985). One outcrop of Suí Breccia was discovered along the Suí fault on a road north of the village of Vidal Pichardo (Plate 1). The Suí Breccia consists of predominantly angular, lithified Cercado Sandstone clasts in a finer matrix. Generally, there is no preferred orientation of the clasts (Photograph 16). Reefal limestone clasts, including pieces of *Callianassa* arthropods and mollusks, as well as rounded polymictic materials, are abundant in the breccia. Reefal limestones of a patch reef environment origin, along with conglomerates occur in the upper part of the Cercado Sandstone and are characteristic of the transition into the Pliocene Gurabo Sandstone (Saunders and others, 1986).

### **Higua Breccia**

The Higua Breccia is composed mostly of Inoa Conglomerate with large, angular clasts of tonalite intermixed in a finer grained matrix of reworked Inoa siltstone (Photograph 17). At the confluence of Río Higua and Río Inoa south of the town of Inoa is a tectonic breccia of Inoa Conglomerate and leucotonalite (Plate 1). The pebbles of the Inoa Conglomerate have been reworked and when identifiable are fractured. The matrix is composed of very fine-grained siltstone of the Inoa Conglomerate. Tonalite clasts make up approximately 10 to 15 percent of the breccia. The subangular to angular tonalite clasts are found up to boulder size and range from 5 mm up to over 275 mm.

### **Rock Unit Contacts**

The study area is divided into fifteen structural domains (Figure 14). Several of the domains have irregular shapes. The boundaries were chosen based on formations and separated by their contacts. They were further split intraformationally by fracture and fold trends established. For example, the domains relevant to the Inoa Conglomerate (Domains 3, 8 and 13) were split up based on the fact that the Inoa fault changed from an E-W trend to a WNW trend to NW trend, respectively. The domains also were shaped in their respective manner based on fracture trends. The Amina Schist was separated into four domains (i.e., Domains 2, 7, 10, and 12) based on a predominant schistosity found across the formation. The Cercado Sandstone was separated into Domains 4, 5, and 6; however, the fracture and folding patterns are almost identical. These domains were separated because there was sufficient data to support a consistent local analysis in the eastern, central, and western part of the study area. Fourteen of these domains are discussed in this section. Each domain contains consistent fracture, fault, and fold data for each rock unit (Plates 1 and 2). These structural domains assist the reader in the location and identification of formational contacts and specific structural trends. Each domain is defined by lithology and structural features. Data are segregated into specific formations, stratigraphic contacts, folds, faults, slickenlines, and fracture sets. Rock unit contacts for the fourteen domains are discussed below. The fifteenth domain lies south of the Inoa fault in the Duarte Complex. Structures within it will be discussed in the next section using the stereonet plots.

### **Domain 1 - NW Corner of Geologic Map**

Formations in Domain - upper Miocene Bulla Conglomerate and Cercado Sandstone  
middle to upper Oligocene Monción Limestone  
lower Cretaceous Amina Schist

The contact between the Monción Limestone and the Amina Schist was not observed in the field. The Monción Limestone overlies the Bulla Conglomerate. The Bulla Conglomerate is separated from the Monción Limestone by a subtle angular unconformity. The beds of Bulla Conglomerate tilt at a shallow angle of just 4° NE over the folded beds of the Monción Limestone. The bedding contact between the Monción Limestone and the Bulla Conglomerate is not parallel.

### **Domain 2 - West**

Formations in Domain - upper Miocene Bulla Conglomerate  
upper Miocene Cercado Sandstone  
lower to Middle Oligocene Inoa Conglomerate  
middle Eocene (?) La Bruja Limestone/Breccia  
Paleocene-middle Eocene Magua Formation  
lower Cretaceous Amina Schist

The Bulla Conglomerate and Cercado Sandstone are in fault contact with the Amina Schist southeast of Monción (Plates 1 and 2). The Inoa Conglomerate is in fault contact with the Amina Schist. The Inoa Conglomerate is in fault contact with the Magua Formation. The La Bruja Limestone is caught in a shear zone between the Magua Formation and the Inoa Conglomerate.

### **Domain 3 - Central West**

Formations in Domain - late Oligocene/early Miocene (?) Pananao Limestone/ Pananao Abajo Breccia  
lower to middle Oligocene Inoa Conglomerate  
middle Eocene (?) La Bruja Limestone/Breccia

**Paleocene-middle Eocene Magua Formation  
lower Cretaceous Amina Schist**

The Inoa Conglomerate is in fault contact with the Amina Schist. The Pananao Abajo Breccia is caught in the shear planes of the Amina fault along Río Pananao (Plates 1 and 2). Along the Inoa fault, the Inoa Conglomerate is in fault contact with the Magua Formation, divided by a thin band of crystalline La Bruja Limestone (Plates 1 and 2). The La Bruja Limestone crops-out north of the Inoa fault.

**Domain 4 - Southwest**

Formations in Domain -      lower to middle Oligocene Inoa Conglomerate  
   middle Eocene (?) La Bruja Limestone/Breccia  
   Paleocene-middle Eocene Magua Formation  
   Paleocene Rodeo Basalt  
   lower Cretaceous Duarte greenschist facies rocks

The Magua Formation trends E-W in the study area and contains volcanic breccias and volcanic agglomerates. The volcanic agglomerates consist of sandstones, sandy mudstones, tonalites, and Duarte rock clasts. The contact between the Rodeo Basalt and the Magua Formation appears to be transitional. The Rodeo Basalt occurs as higher topographic relief and forms steep slopes to the north and south. The Inoa fault marks the northern contact between the Magua Formation and the Inoa Conglomerate. The La Bruja Limestone outcrops in the shear zone between the Magua Formation and the Inoa Conglomerate (Plates 1 and 2). The Magua Formation is in fault contact with the Duarte greenschist facies rocks. This fault contact appears as a discrete fracture break with a white crystalline gouge formed along the steeply dipping, nearly vertical fault.

### **Domain 5- Northwest**

Formations in Domain -      Quaternary Alluvium  
    upper Miocene Bulla Conglomerate  
    upper Miocene Cercado Sandstone  
    lower Cretaceous Amina Schist

Quaternary Alluvium in the Río Mao area lies directly over the Bulla Conglomerate and Cercado Sandstone (Plates 1 and 2). The Bulla Conglomerate and Cercado Sandstone nonconformably overlie the Amina Schist in this domain area. The Bulla Conglomerate is likely in a fault contact along a normal fault with the Amina Schist in the south-central part of the domain area. The only evidence along this fault remains a steep change in relief of the topography of Bulla Conglomerate. In other localities where the contact between the Bulla Conglomerate and Amina Schist is exposed, the contact appears as a depositional surface.

### **Domain 6 - Central North**

Formations in Domain -      Quaternary Alluvium  
    upper Miocene Bulla Conglomerate  
    upper Miocene Cercado Sandstone  
    lower Cretaceous Amina Schist

The Alluvium overlies the Cercado Sandstone. The Bulla Conglomerate and Cercado Sandstone both nonconformably overlie the Amina Schist in this area. A fault contact between the Cercado Sandstone and the Amina Schist was not found in this part of the study area.

### **Domain 7 - Left-Central Center**

Formations in Domain -      upper Miocene Bulla Conglomerate  
    lower to middle Oligocene Inoa Conglomerate

### lower Cretaceous Amina Schist

The Bulla Conglomerate nonconformably overlies the Amina Schist. The Amina fault separates the Inoa Conglomerate and the Amina Schist to its north. The fault contact is distinguishable by the presence of a 50 to 75 m wide zone of Las Matas Breccia (Plates 1 and 2).

### **Domain 8 - Right-Central Center**

Formations in Domain -      lower to middle Oligocene Inoa Conglomerate  
    middle Eocene (?) La Bruja Limestone/Breccia  
    lower Cretaceous Amina Schist  
    lower Cretaceous Duarte subgreenschist facies rocks

The Inoa Conglomerate is in fault contact with the Amina Schist indicated by the Las Matas Breccia along the Amina fault (Plates 1 and 2). To the south of the Inoa Conglomerate are the subgreenschist facies rocks of the Duarte Complex along the Inoa fault. The fault contact is indicated by sheared La Bruja Limestone and the La Bruja Breccia (Plates 1 and 2).

### **Domain 9 and 10 - Central East**

Formations in Domain -      upper Miocene Bulla Conglomerate  
    upper Miocene Cercado Sandstone  
    lower to middle Oligocene Inoa Conglomerate  
    upper Eocene to lower Oligocene Las Matas Breccia  
    lower Cretaceous Amina Schist

The Bulla Conglomerate and Cercado Sandstone nonconformably overlie the Amina Schist. Evidence of a fault contact between the Cercado and the Amina was not found in this domain area. The Amina fault separates the Inoa Conglomerate from the Amina

Schist. The Amina fault is indicated, in part, by the presence of the Las Matas Breccia which occurs along the fault splays northwest of the town of San José de las Matas.

### **Domain 11 - Northeast**

Formations in Domain -      Quaternary Alluvium  
    upper Miocene Bulla Conglomerate  
    upper Miocene Sui Breccia  
    upper Miocene Cercado Sandstone  
    lower Cretaceous Amina Schist

The Quaternary Alluvium was deposited on top the Cercado Sandstone. The Bulla Conglomerate and Cercado Sandstone nonconformably overlie the Amina Schist. In the area around Arroyo Sui, the Cercado Sandstone is in fault contact with the Amina Schist (Plates 1 and 2). The sense of fault movement direction on the Sui fault is unknown due to the colluvium that covers the fault scarp. The Sui Breccia outcrops along the trend of the fault.

### **Domain 12 - Central East**

Formations in Domain -      upper Miocene Bulla Conglomerate  
    upper Miocene Cercado Sandstone  
    lower to middle Oligocene Inoa Conglomerate  
    lower Cretaceous Amina Schist

The Bulla Conglomerate and Cercado Sandstone nonconformably overlie the Amina Schist. A fault contact between the Cercado Sandstone and Amina Schist is not exposed in this domain. Along the southern boundary of this domain, the Amina fault separates the Amina Schist to the north from the Inoa Conglomerate (Plates 1 and 2). An abrupt change in topographic relief between the Amina Schist and the Inoa Conglomerate helps to demarcate the location of the Amina fault. To the south of the Amina fault, rivers have

eroded into the Amina Schist below the Inoa Conglomerate.

### **Domain 13 - East**

Formations in Domain -      upper Miocene Bulla Conglomerate  
    upper Miocene Cercado Sandstone  
    lower to middle Oligocene Inoa Conglomerate  
    middle Eocene (?) La Bruja Limestone/Breccia  
    lower Cretaceous Amina Schist  
    lower Cretaceous Duarte subgreenschist facies rocks

The Inoa Conglomerate is in fault contact with the Amina Schist as described above in Domain 12. The Inoa Conglomerate is in fault contact with the subgreenschist facies rocks of the Duarte Complex along the Inoa fault (Plates 1 and 2). In the vicinity of the aqueduct south of San José de las Matas, there is a fault contact where the Inoa Conglomerate overlies an erosional surface of the subgreenschist facies rocks of the Duarte Complex. This contact of the Inoa overlying the Amina is an erosional unconformity. The Duarte greenschist facies rocks are marked by load features and grooves. The Duarte greenschist facies rocks are very weathered at their contact with the Inoa Conglomerate. The base of the Inoa Conglomerate is a fault surface with polished surfaces. Slickenlines are not found at this locality. Along the south bank of Arroyo Hondo, south of San José de las Matas, is an outcrop of gray semi-crystalline limestone of the La Bruja Limestone occupies a shear zone contact between the Inoa Conglomerate and the Duarte subgreenschist facies rocks (Plates 1 and 2). A thin zone of approximately 5 cm of pseudotachylite is present along this fault to the south of San José de las Matas at a bend in the Inoa fault at the junction of Río Honda and Arroyo Capa Azul.

The La Bruja Limestone is caught in the shear planes of the Inoa fault west of the

village of La Bruja and brecciated (Plates 1 and 2). Near a waterfall located at the confluence of Arroyo Hondo and Río Inoa are elongated clasts in the Inoa Conglomerate (cf. Palmer, 1963; Olivo, 1985; Plate 1). The elongated clasts are separated from less deformed layers of the Inoa Conglomerate by fractured sandstones. The elongated clasts are intraformational.

#### **Domain 14 - East of Monción**

|                        |   |
|------------------------|---|
| Formations in Domain - | upper Miocene Bulla Conglomerate                    |
|                        | upper Miocene Cercado Sandstone                     |
|                        | lower to middle Oligocene Inoa Conglomerate         |
|                        | middle Eocene (?) La Bruja Limestone/Breccia        |
|                        | lower Cretaceous Amina Schist                       |
|                        | lower Cretaceous Duarte subgreenschist facies rocks |

The Bulla Conglomerate and Cercado Sandstone nonconformably overlie the Amina Schist. Along the southern boundary of this domain just southeast of Monción, the Inoa Conglomerate is in fault contact with the Amina Schist located along the Amina fault (Figures 10 and 12). The fault contact is evidenced by a steep change in topographic relief.

Just to the east of this area, the Amina Schist is in fault contact with the Pananao Limestone. Its contact is marked by the Pananao Abajo Breccia. A conformable depositional contact between the Pananao Limestone and the Inoa Conglomerate is exposed in Río Pananao. The contact is between the Pananao Limestone and the Inoa Conglomerate is slightly irregular to planar in form. The Pananao Limestone is folded along with the Inoa Conglomerate. Flexural slip folding occurs along the bedding planes of contact between the Pananao Limestone and the Inoa Conglomerate.

## **MAJOR STRUCTURES OF THE TERTIARY ROCKS**

### **Master Faults and their structure**

Faults along with slickenlines were measured from different localities along exposed sections of both the Amina and Inoa faults. Along the northern boundary of the San José de las Matas basin, the Amina fault trends WNW separating the Amina Schist and the Inoa Conglomerate. The Amina fault may be traced as a set of offset fault splays (Plates 1 and 2). The Inoa fault along the southern boundary of the San José de las Matas basin runs the entire length of the study area and strikes predominantly N75°W to N80°W and dips approximately 65°NE (Plate 1). The Amina fault zone is made up of several WNW-trending faults joined by NE-trending lineaments. The Amina fault strikes N65°W to N70°W and dips steeply. This study suggests that the Amina fault bounds the pull-apart basin, but is not the northernmost structural feature related to the formation of the basin.

### **Amina fault**

The Amina fault is separated into five NW-trending splays referred to as the Amina fault system. Air photo interpretation suggests that the Amina fault system is joined by five NE-trending lineaments within the study area (Plate 1). Most of the NE-trending lineaments reveal no structural data. However, field data suggest that these lineaments may likely be faults. The data are discussed below. The lineaments often follow the contacts between two formations which have great differences in topographic relief.

The Amina fault separates the Inoa Conglomerate from the Amina Schist along a series of NW-trending splays joined by NE-trending lineaments (Plate 1). The sharp

change in relief across the trace of the Amina fault and the great thickness of the Inoa Conglomerate suggests that some downward movement of the south side of the fault occurred. The width of the Amina fault zone is considerably smaller than the Inoa fault zone, at only tens of meters north and south of the trace of the fault.

Field mapping confirms that the Amina fault separates the Amina Schist from the Inoa Conglomerate. Starting from east to west, a NW-trending lineament is apparent through air photo interpretation. This lineament cuts through Arroyo Maquen, Arroyo Guajaca and Arroyo Iguamo (Plate 1). All three of these streams were traversed, and the contact between the Amina and Inoa was covered by colluvium. No evidence of faulting could be found along this lineament. The stream valleys south of this lineament cut through the Inoa Conglomerate and the Amina Schist (Plate 1). Here the contact is likely a fault.

Traveling westward, the first NE-trending lineament is located NE of the town of San José de las Matas and separates the Inoa Conglomerate from the Amina Schist (Plate 1). West of the first NE-trending lineament located due north of San José de las Matas is the first NW-trending splay of the Amina fault, (Plate 1). The first NW-trending splay of the Amina fault separates the Amina Schist to the north from the Inoa Conglomerate to the south. A steep scarp covered by colluvium separates the Inoa Conglomerate from the Amina Schist. Normal displacement is inferred; however, this displacement could not be confirmed due to the colluvium covering the scarp.

The second NE-trending lineament is west of San José de las Matas. Here there is a steep scarp covered by colluvium. The rocks on the southeast side of this lineament

likely dropped into the basin. A sense of normal displacement is inferred; however, it could not be confirmed due to the abundance of erosional debris covering the scarp.

The second NW-trending splay of the Amina fault trends NW through Arroyo Quebradilla and Río Amina. The Las Matas Breccia outcrops in the stream valley of Arroyo Quebradilla and can be identified by bush-covered topographic highs just north of the stream plateau (cf. Palmer, 1963). A fault scarp with a steep change in relief to the north separates the Las Matas Breccia from the Amina Schist. The second NW-trending fault is apparent in air photo interpretation; however, no structural data suggesting normal or oblique slip was collected. Left-lateral displacements of siltstone beds of the Inoa Conglomerate in Río Amina suggest left-lateral strike-slip movement occurred on this splay of the Amina fault. Up to one meter of maximum displacement of a siltstone bed was measured at one locality. The third NE-trending lineament is likely a right-handed normal slip fault.

Tonalite and greenstone clasts found near the fault zone appear “flattened” and “stretched”. The rakes of the elongated clasts trend an average of  $30^{\circ}\text{SE}$  and  $25^{\circ}\text{NW}$  in beds oriented  $\text{N}50^{\circ}\text{E}$ , dipping  $43^{\circ}\text{SE}$  (Plot 22; Photograph 18). Only the surfaces of the flattened, elongated clasts were accessible for measurement.

These possibly indicate a semi-ductile episode of strike-slip displacement along this fault (Plot 22). Elongated clasts measured in Río Amina possibly indicate right-lateral semi-ductile shearing of the Inoa Conglomerate (Plot 22). This incidence of right-lateral offset will be discussed further in the Discussion section.

The third NW-trending splay of the Amina fault runs along Arroyo Pinillo and

terminates in the village of Caobanico (Plate 1). The Las Matas Breccia outcrops in the stream valley of Arroyo Pinillo and can be identified just north of the stream (cf. Palmer, 1963). No sense of displacement could be measured on this lineament. Just south of Arroyo Pinillo there is a scarp, as observed in the field and evidenced by a sharp drop in relief. The Inoa Conglomerate represents the hanging wall block of a normal fault along this fault splay because, in part, the stratigraphy suggests that the overlying Inoa Conglomerate dropped relative to the Amina Schist. The slickenlines confirm that the Inoa Conglomerate dropped relative to the Amina Schist.

At the end of the third NW-trending splay is the fourth NE-trending lineament. It has been identified by aerial photograph interpretation. The village of El Corozo lies just southwest of the beginning of this lineament (Plate 1). Field inspection reveals only colluvium and little evidence of the lineament trace.

The fourth NW-trending splay of the Amina fault system trends NW along Arroyo Pinalitos and trends WNW, just north of the town of El Rubio (Plate 1). It continues through Arroyo Quebrada del Oro and through Arroyo Pananao terminating two km NW of the village of Pananao Abajo. There are elevated, bush-topped hills northeast of Arroyo Quebrada del Oro (cf. Palmer, 1963). The Las Matas Breccia outcrops along these bush-covered hills and in the stream valley of Arroyo Quebrada del Oro. The lineament splay is covered by colluvium. The Las Matas Breccia also crops out north of El Rubio. This splay is likely a fault.

The Pananao Limestone and Pananao Abajo Breccia outcrop parallel to the fault northwest of Pananao Abajo. The Pananao Abajo Breccia marks the northwestern extent

of the fourth splay of the Amina fault. Plot 8 shows NW-striking, SW-dipping faults with shallow SE-dipping slickenlines. This splay is confirmed to be a left lateral strike-slip fault (Plot 8). The low angle slickenlines are indicative of strike-slip movement along the fault plane. A scarp is evident along the northeast side of the river valley of Arroyo Pananao and Arroyo Quebrada del Oro (Plate 1). The rakes of slickenlines suggest a slight dip-slip component (Plate 1, Plot 8).

A fifth NE-trending lineament runs along Rio Mao along the contact between the Inoa Conglomerate and the Amina Schist. The faulted surface strikes N45°E and dips 60°SE with slickenlines at a rake of 85°NE. The faulted surface show that this is a normal fault. The fault lies east of Bomba Aqueducto on the eastern bank of Rio Mao, south of the Estrechuras de Negras where a new dam is under construction (Plate 1). Fault data gathered from the Inoa Conglomerate demonstrates on Plot 9 show that the normal fault strikes NNE and dips to the SE with slickenlines steeply dipping to the SE. There is an undetermined amount of normal slip on this fault.

The sixth NW-trending splay of the Amina fault system trends predominantly WNW along Rio Mao through Arroyo Boloncillo, south of the town of Monción. Left-lateral offsets of siltstone beds of the Inoa Conglomerate outcrop along the Río Mao north of the village of Magua. Two meters of offset were measured in some of the siltstone beds of the Inoa Conglomerate. (Photograph 19). These siltstone beds show evidence of brittle deformation.

The Amina fault is traceable through air photo interpretation further westward to the village of El Cruce. A continuation of the Amina fault is unknown west of El Cruce.

This area is overlain by the Bulla Conglomerate which does not show any lineament or abrupt topographic changes as do the preceding sections. This may be an indication that the depocenter of the Bulla is younger than reactivation of the Amina fault. However, more work is necessary to confirm this hypothesis.

### **Inoa fault**

Lower hemisphere equal area projections of many poles to faults and associated slickenlines from three separate domains (Domain Nos. 3, 8, and 13) show that the Inoa fault movements are predominantly strike-slip (Plots 5, 24, and 36). These low-angle WNW-striking slickenlines confirm that strike-slip fault movement occurred along the Inoa fault (Plots 5, 24, and 36). The Inoa fault is traceable through aerial photo interpretation, in the field, and in topographic map view along its entire length of the study area. The Inoa fault strikes approximately N85°W from south of San José de las Matas and changes in strike direction to N55°W south of Monción.

The fault begins east of San José de las Matas as a lineament evident in aerial photo interpretation. The fault contact between the greenschist facies rocks of the Duarte Complex and the Inoa Conglomerate outcrops in two locations south of San José de las Matas. The first location at the easternmost end of Arroyo Honda is a fault contact striking N55°W and dipping 45°NE. Pseudotachylite was found at this location (Photograph 20). Approximately 5 cm of dense, glassy siltstone matrix material of the Inoa Conglomerate is wedged between the Duarte subgreenschist facies rocks to the south and the Inoa Conglomerate to the north. A second location located west of Aqueducto de San José de las Matas reveals an erosional contact between the subgreenschist facies rocks

and the Inoa Conglomerate.

The subgreenschist facies rocks in this location contain chert nodules. This location represents both an erosional unconformity and a tectonic contact. Evidence for the erosional unconformity is marked by an undulating surface of the subgreenschist facies rocks containing erosional load features and grooves (Photograph 21). The undulating surfaces are inferred to be channels with loads and groove casts. Orientation of the schistosity in the subgreenschist facies rocks is  $N62^{\circ}W, 45^{\circ}NE$ . The Inoa Conglomerate beds on-top of the subgreenschist facies rocks trend  $N60^{\circ}W, 45^{\circ}NE$ . The basically parallel beds of greenschist facies rocks and conglomerate were likely refolded together during a later faulting event.

Tectonic evidence along the contact measured 50 m to the north of the fault includes elongated clasts (Photograph 22). The rakes of the elongated clasts trend an average of  $30^{\circ} NE$  and  $30^{\circ} SW$  in beds oriented  $N75^{\circ}W$ , dipping  $48^{\circ}NE$  (Plot 23; Photograph 22).

Progressing westward along the Inoa fault at the confluence of Río Higua and Río Hondo, south of the town of Inoa, is the Higua tectonic breccia (Photograph 17). This tectonic breccia lies along the Inoa fault between the tonalite intrusion to the south and the Inoa Conglomerate to the north. Río Hondo represents one of the best examples in the study area of an off set stream due to left-lateral strike-slip faulting.

The La Bruja Breccia crops out south of the village of La Bruja along Río Amina in the shear planes of the Inoa fault (Photograph 15; Plate 1). Just west of the village of El Palmar and south of El Corozo, an outcrop of the breccia suggests “flattening” and

“stretching” by cataclasis (Photograph 23; Plate 1). Rakes of the long axes of the elongated clasts in the bedding planes are plotted on a lower hemisphere equal area projection (Plot 24). The rakes of the elongated clasts trend an average of  $30^{\circ}\text{NE}$  and  $25^{\circ}\text{SW}$  in beds oriented  $\text{N}65^{\circ}\text{W}$ , dipping  $18^{\circ}\text{NE}$  (Plot 24; Photograph 23). This outcrop also shows the brittle deformation of the siltstone beds of the Inoa Conglomerate along the Inoa fault (Photograph 24). The strikes and dips of fault planes and respective slickenlines were measured in the vicinity of El Corozo (Plot 25). These attitudes show that the Inoa fault strikes NW and is nearly vertical with low to high angle SE-plunging slickenlines. Plot 25 shows that some oblique slip occurred along the Inoa fault. The different sets of slickenlines could be inferred as multiple fault episodes. However, more studies of local outcrop fault patterns would be necessary to confirm this hypothesis.

The Inoa fault continues to strike WNW through and parallel to Arroyo Los Corozos, Arroyo La Manacla and Arroyo Auyamas, south of the town of El Rubio (Plate 1). On the south side of the Inoa fault, steep scarps resembling flatirons rise up to the Duarte Complex (Photograph 25). These flatirons occur as a series of south facing, triangular spurs on the flanks of the mountainous Duarte Complex south of the Inoa fault trace. West of the confluence between Arroyo Pananao and Arroyo Auyamas the fault trace is covered by colluvium (Plate 1). Access to the fault is difficult due to the erosional debris and large car-size boulders in the stream valleys which makes access by foot nearly impossible.

The Inoa fault crosses through Río Magua and Río Mao (Plate 1). The fault is traceable through field observation and many zones of brittle deformation were measured

(Plot 21). The fault trace in Río Magua runs through a distinctive meander loop, as seen on map view (Plate 1), but it is too difficult to access at this part of the river valley.

Data sets of fault offsets from the vicinity east and west of Río Mao on Plot 36 show WNW-trending faults with low angle slickenlines plunging to the ESE. The fault here separates the Magua Formation from the Inoa Conglomerate. More fault data were gathered south of Monción along the road between the village of Rodeo and the village of El Cacao (Plate 1; Plot 5). Here the fault changes attitude and strikes NW and dips moderately to steeply SSW. Slickensides on the fault have shallow dips (Plot 5).

West of this road cut, the Inoa fault crosses through Arroyo La Abandonada where a vertical bed of limestone is mapped (Plate 1). Here, the Inoa fault cuts through Arroyo La Abandonada marked by a vertical 35-meter fault scarp and a vertical bed of Pananao(?) Limestone (Plate 1). Due to the heavy overgrowth and extremely large boulders, no measurements were obtained. The Pananao Limestone outcropping in Arroyo La Abandonada is partially recrystallized, which may indicate a shear zone. The fault is only traceable via aerial photo interpretation farther to the west, as this area is heavily covered by colluvium.

### **Folds**

Folds in the Magua Formation, Monción Limestone, and Cercado Sandstone are plotted on lower hemisphere equal area projections and in cross-sectional view. Folds are the most reliable evidence of ductile strain in the study area (Plots 1,6, 11, 12, 16, 19, 20, 29, 30, and 34). Cross-sections A-A' through H-H' (Plate 2) show trends of the fold axial planes and hinges throughout the study area.

The Amina Schist has been previously mapped and well interpreted by Palmer (1963;1979), Antonini (1968;1979) and Draper and Lewis (1982;1991). This study gathered only  $S_1$  schistosity measurements of these low-grade regionally metamorphosed rocks. The  $S_1$  schistosity is the first phase of folding of relict igneous layering. The schist has been folded into tight to isoclinal folds which have axes parallel to the regional trend of the belt (Draper and Lewis, 1989). There is a second phase of schistosity in the Amina Schist which has close to open chevron folds with NE-SW trending axes (Draper and Lewis, 1989). Few schistosity measurements were collected from the Duarte Complex.

### **Folds in the Inoa Conglomerate**

Both anticlines and synclines are mapped in the study area in the Inoa Conglomerate and systematically repeat north of the Inoa fault (Plate 1). The fold traces predominantly trend E-W across the study area and exhibit open to tight folding. The anticlines and synclines of the Inoa Conglomerate are not obvious parts of a continuous, repeated, sinusoidal waveform. The map-scale folds have spacing on the order of tens of meters up to one km between anticlines and synclines (Plate 1). Using a Riedel model for left-slip movement (Riedel, 1929), the folds should occur either parallel to or at  $45^\circ$  angles to the strike of the imposed shear. The folds are a result of compression along the imposed shear of a fault zone. A Riedel model can predict where the formation of folds will occur and this will be discussed in the Discussion section.

Domain No. 3 - This domain is comprised of multiple anticlines and synclines with fold axes striking  $N60^\circ E$  (Plate 1). Domain No. 3 is regional interpreted as a WSW, non plunging, asymmetric chevron fold with a narrow hinge zone (Plates 1 and 2; Plot 6).

Anticlines and synclines to the north of the Inoa fault strike N70°E. West of El Rubio, along Arroyo Pananao, the fold axes of the anticlines and synclines strike approximately N70°W (Plate 1). Folding is comprised of angular parallel folds with curved hinge zones (Plate 2; Cross-sections B-B' and C-C'). Cross-section C-C' shows that there is tighter, more non-parallel folding closer to the fourth NW-trending splay of the Amina fault.

Domain No. 8 - The fold axes of the anticlines and synclines are oblique to the WNW strike of the Inoa fault (Plates 1 and 2). Cross-section E-E', F-F' and G-G' show that the folding is comprised of parallel folds with curved hinge zones (Plate 2).

A WSW, gently plunging, upright, open fold with a narrow hinge strikes approximately N70°W in this domain (Plot 19; Plates 1 and 2). West of Caobanico and El Corozo, the fold axes of the anticlines and synclines strike approximately N70°E and are also oblique to the main strike of the Inoa fault (Plate 1).

Domain No. 13 - An interpretation of all of the compiled data from Domain No. 13 shows a WNW-striking, moderately plunging, open chevron fold (Plot 34). This chevron fold is interpreted from the data of multiple folds with similar strikes and dips (Plate 2; Cross-section H-H'), The anticline and syncline are open and parallel with angular hinge zones (Plates 1 and 2).

### **Folds in the Magua Formation**

A regional interpretation of Domain No. 4 shows a NW-plunging, asymmetric, open chevron fold (Plot 11; Figure 14). Plot 11 shows that the poles to bedding planes are tightly packed in opposite regions of the lower hemisphere equal area net. This is due to a predominant concentration of strikes and dips collected from multiple folds oriented

in the same direction. A few measurements of bedding occur perpendicular to the fold suggesting a separate fold within the domain offset possibly by a fault. On a local scale, the Magua has been folded into a tight syncline to the north of the Rodeo Basalt. On the south side of the Rodeo Basalt, there is a cylindrical anticline and a syncline (Plate 1). Fold axes strike approximately  $N60^{\circ}W$  and are roughly parallel to the Inoa fault (Plate 1). Cross-sections A-A' through E-E' show that the Magua Formation is made up of many parallel folds with curved hinge zones.

### **Folds in La Bruja Limestone**

Strikes and dips collected from the La Bruja Limestone in the vicinity of El Palmar on the south side of Río Amina suggest that there is a SW-plunging, upright, chevron fold of limestone (Plate 1 and 2; Plot 20). The plot of data suggests that the La Bruja Limestone has been highly folded. The La Bruja Limestone is south of the Inoa Conglomerate in a shear zone along the Inoa fault (Plate 1 and 2; Cross-section G-G').

### **Folds in the Monción Limestone**

Folds in the Monción Limestone outcrop in Río Gurabo and Arroyo Gurabito (Plate 1). In the study area, the Monción Limestone is folded into SW- to SE-striking, NW- and NE-dipping, upright, rounded, open folds (Plot 1). Domain Area No. 1 contains many strikes and dips of the curved bedding surfaces (Plate 2; Cross-section A-A').

The folded Monción Limestone rests unconformably atop the Amina Schist. The Bulla Conglomerate overlies the Monción Limestone. The Bulla Conglomerate is merely separated from the Monción Limestone by a subtle angular unconformity. The Monción Limestone was likely tilted with the overlying deposits of Bulla. The beds of Bulla

Conglomerate tilt at a shallow angle of just 4° NE over the folded beds of the Monción Limestone. A fault contact between the Bulla Conglomerate and the Monción Limestone was not observed. Loose boulders of the Bulla Conglomerate fill the river valley of Río Gurabo and obscure measurement of the underlying Monción Limestone.

#### **Folds in the Pananao Limestone**

Northwest of the village of Pananao Abajo one limb of an angular fold of limestone strikes N50°W and dips 47°NE. Too few measurements were obtainable from this river valley to determine the extent of the folding of the limestone. The Pananao Limestone outcrops again south and parallel to Arroyo Pananao along the slopes of a hillside facing the river valley. Due to the weathered condition of the outcrop in the hillside, no reliable structural data were gathered. This outcrop could represent the SW-dipping limb of a fold connecting the NE-dipping limb found in Arroyo Pananao (Plot 20). Plot 20 shows an upright, cylindrical fold plunging ESE.

#### **Folds in the Cercado Sandstone**

Folds in the Cercado Sandstone occur in the study area as upright, gentle folds. In Domain Area No. 5, the formation is broadly folded with a gentle plunge to the SW (Plates 1 and 2; Plot 12). In Domain Area No. 6, the folds are upright, broad, and predominantly strike E -W (Figures 10 and 12; Plot 16). In Domain Area No.10, the formation appears to gently arched into folds striking WNW-ESE (Plates 1 and 2; Plot 30). Domain Area No. 11 contains open, broad anticlines and synclines with a north-plunging limb (Plates 1 and 2). The fold axes of the anticlines and synclines are spaced approximately 0.5 to 1 km apart (Plate 1). Some isolated steeply dipping beds of Cercado

Sandstone outcrop along the Sui fault. This may have been a result of dip-slip faulting in the Cercado Sandstone. Some beds along the Sui fault strike N40°W and dip steeply 55°NE.

### **Foliation in the Amina Schist**

Draper and Lewis (1982) describe three distinct groups of folds. The Amina Schist rocks were folded more than once (Draper and Lewis, 1991). The folds occur as tight to isoclinal sinusoidal folds, chevron folds, and low amplitude kink bands, which occur only in those schists which have a well developed planar fabric (Plate 2; Draper and Lewis, 1982; 1991).

The Amina Schist is tightly folded with axial surfaces of tens of meters apart (Plates 1 and 2; Cross-sections A-A' through H-H'). The deformation history of the Amina Schist proposed by Draper and Lewis (1982; 1991) suggests three separate folding episodes to form the schistose fabric. The first deformation stage formed the schistose fabric in a NW-SE trending sinusoidal fold due to NE-SW compression (Draper and Lewis, 1982; 1991). The second deformation event caused further folding on the NW-SE axes, and the third deformation caused NE-SW trending open chevron folds and kink bands (Draper and Lewis, 1982; 1991). This could be explained by continuous transpression and rotation of earlier axes by shear. The sequence of these deformation events is currently under reinterpretation according to Draper (personal communication, 1998 and 1999).

Tight folding of the schistosity in Río Amina and Río Guanajuma becomes less pervasive westward toward the town of Monción (Plates 1 and 2) where a more planar

schistose fabric dominates. The strike of the schistosity also changes several times from across the study area (Plate 1). The strikes and dips of foliations are shown in Domains 2, 7, 9, 10, 12, and 14 (Plates 1 and 2). The Amina Schist generally has a NW-striking foliation which dips to the southwest (Plots 3, 17, 26, 27, 32, and 37). Domain No. 2 shows that foliation predominantly dips to the southwest (Plates 1 and 2; Plot 3). Domain No. 7 shows an tight fold with a WNW vertical axis and horizontal crest (Plates 1 and 2; Plot 17). The foliations in Domain Nos. 9, 10, 12, and 14 are generally similar (Figures 10 and 12; Plots 26, 27, 32, and 37, respectively) to the foliations in Domain No. 2 (Plot 3). The foliations in the Amina Schist in Domain Nos. 9 and 12 strike NW-SE and have low to medium dips to the SW (Plots 26 and 27, respectively). The foliations in Domain Nos. 10 and 14 strike WNW-ESE, but have a moderate to steep dip to the SW (Plots 32 and 37, respectively).

Consistent with previous investigations, the axial planes of these folds dip consistently SW, as does the schistosity that cuts the hinge zones of the folds (cf. Draper and Lewis, 1991). Deformation of the Amina Schist is most intense to the east and decreases to the west. This may be directly related to the imposed left-lateral shear on the Amina Schist during its movement in the Cretaceous.

### **Lineaments**

Aerial photographs were analyzed before, during, and after structural mapping. Geological interpretation of the photographs is based on comparing features in the mapped study area with faults, fractures, contacts, and foliations identified on the ground during field mapping (Plate 3). The lineament map captures patterns of linear features that

truncate or offset rock or physiographic patterns.

### **Rose Diagrams**

The lengths and orientations of each lineament were measured in meters and plotted on rose diagrams (Rose diagrams 1 through 14). The rose diagrams plot the density of oriented lineament lengths. The density of lineaments trending in the same direction is calculated by taking the cumulative length of all lineaments per 5° class interval of an inventory half-circle. The rose diagrams present a lineament density of percentage per class interval for Domain Area Nos. 1 through 14. Domain Area Nos. 7 and No. 14 were combined into one domain, which joins the exposures of the Amina Schist.

An analysis of the lineament data shows that there is a concentration of lineaments trending E-W to WNW in Domain Nos. 2, 3, 4, 8, and 13 adjacent to the Inoa fault (Rose diagrams 2, 3, 4, 8, and 13). There is a concentration of lineaments trending NE in the Amina Schist in Domain Nos. 7, 9, 10, 12, and 14 (Rose diagrams 7, 9, 10, and 12). Lineaments trend to the NW and NE in Domain Nos. 1, 5, 6, and 11 in both the Monción Limestone (Domain Area No. 1) and the Cercado Sandstone (Rose diagrams 5, 6, and 11).

The lineaments trending E-W to WNW in Domains Nos. 2, 3, 4, 8, and 13 represent the Inoa fault. The predominant lineaments in the Cercado Sandstone show the expected shearing pattern of imposed left-lateral shear along a strike-slip fault. These 45° lineament patterns can be predicted by a Riedel model for left-slip movement. This relationship will be described in the Discussions section. The predominant lineament trend

in the Amina Schist to the NE may represent the traces of the NE-SW fold axes zones related to the second phase of regional deformation (Draper and Lewis, 1989).

## MINOR STRUCTURES OF THE STUDY AREA

### Shear Fractures

Shear fractures measured in the siltstone beds of the Inoa Conglomerate and Cercado Sandstone indicate the presence of brittle deformation. Shear fractures are reported for each domain and formation of the field area and plotted on lower hemisphere equal area projections (see table below). The relationship of the fractures to the faulting will be covered in the Discussion section.

| Domain Area Number           | Geologic Formation              | Lower Hemisphere Equal Area Plot Number |
|------------------------------|---------------------------------|---|
| Domain Area 1                | Monción Limestone               | Plot 2                                  |
| Domain Area 2                | Amina Schist                    | Plot 4                                  |
| Domain Area 3                | Inoa Conglomerate               | Plot 7                                  |
| Domain Area 4                | Magua Formation                 | Plot 10                                 |
| Domain Area 5                | Cercado Sandstone               | Plot 13                                 |
| Domain Area 5 and 6 combined | Cercado Sandstone               | Plot 14                                 |
| Domain Area 6                | Cercado Sandstone               | Plot 15                                 |
| Domain Area 7 and 14         | Amina Schist                    | Plot 18                                 |
| Domain Area 8                | Inoa Conglomerate               | Plot 21                                 |
| Domain Area 10               | Amina Schist                    | Plot 28                                 |
| Domain Area 11               | Cercado Sandstone               | Plot 31                                 |
| Domain Area 12               | Amina Schist                    | Plot 33                                 |
| Domain Area 13               | Inoa Conglomerate               | Plot 35                                 |
| Domain Area 15               | Duarte greenschist facies rocks | Plot 38                                 |

### **Monción Limestone**

The Monción Limestone outcrops in Domain Area No. 1 and as shown on Plot No. 2, shear fractures strike north and moderately dip to the west (Plates 1 and 2).

### **Amina Schist**

Shear fracture data were collected in a few outcrops of the Amina Schist. The Amina Schist outcrops in Domain Area Nos. 2, 7, 10, and 12 (Plates 1 and 2). Plot No. 4

from Domain Area No. 2 shows the shear fractures trending E-W and dipping to the SE. Vertical shear fractures from Plot No. 18 from Domain Area No. 7 strike E-W and N-S. Plot No. 28 from Domain Area No. 10 shows that shear fractures strike to the NNE and dip moderately to the NW. Plot No. 33 from Domain Area No. 12 shows NW- and NE-striking vertical fractures.

### **Inoa Conglomerate**

The Inoa Conglomerate is separated into Domain Area Nos. 3, 8, and 13 (Plates 1 and 2). The shear fractures in the Inoa Conglomerate appear to be conjugate to the strike of the Inoa fault. Plot No. 7 is compiled from data in Domain Area No. 3 and shows fractures that strike NNE and dip steeply to the west. The fractures also strike NE and dip steeply to the NW and SE. Plot No. 21 from data in Domain Area No. 8 shows a conjugate set of shear fractures. Plot No. 21 contains NNE-striking vertical fractures and NNE-striking vertical to steeply NE- and SW-dipping fractures and N-S striking vertical fractures. Plot No. 35 from data collected in Domain Area No. 13 shows NE-striking, moderately to steeply SE-dipping fractures and NW-striking, moderately SW-dipping fractures, and E-W-striking vertical fractures.

### **Cercado Sandstone**

The Cercado Sandstone fractures are mapped in Domain Area Nos. 5, 6, and 11 and compiled on Plot Nos. 13, 15, and 31, respectively (Plates 1 and 2). Plot Nos. 13 and 15 each show NW-striking moderately SW-dipping fractures and NNE striking, steeply NW-dipping fractures. Plot No. 14 is a combined plot of both Domain Nos. 5 and 6 and shows the consistency of the conjugate sets of fractures between the two domains. Plot

No. 31 compiled from data in Domain Area No. 11 also shows two discrete shear fracture sets. The fractures in Plot No. 31 are NW-striking, steeply NW-dipping fractures and NE-striking, moderately to steeply SE-dipping fractures. The shear fractures in Plot No. 31 are consistent with Plot Nos. 13, 14, and 15 except that the fractures in the eastern half of the study area dip to the NE and SE rather than to NW, and dip SW in the western half of the study area.

#### **Duarte greenschist facies rocks**

Shear fractures within the Duarte greenschist facies rocks south of the Inoa fault are plotted from Domain No. 15 (Plates 1 and 2). Plot No. 38 shows NW-striking, steeply NE-dipping fractures and N-S-striking, steeply E-W-dipping fractures. This plot indicates that shear fractures located close to the Inoa fault occur in conjugate sets.

## DISCUSSION

### **The Riedel Model vs. the Coulomb-Anderson Model**

The Riedel model for left-lateral shear explains the formation of this fault zone. The faults measured in the field closely match the geometry of the shear arrays for a left-handed Riedel model. Not all of the expected features which are created by a Riedel model are found in the study area. This may be due to the specific tectonic setting of regional transpression in the Caribbean or due to the poor preservation of structures in the tropical environment. The dominant features found in this study area support why a Riedel model was chosen to explain the area's structural development rather than another model, such as the Anderson model which incorporates Coulomb's Law of Failure (Figure 15; Coulomb, 1773; Anderson, 1951). I will refer to this as a 'Coulomb-Anderson' model for the sake of simplicity.

The Coulomb-Anderson model predicts "pure shear" with equal sets of conjugate strike-slip faults resulting in areas having a few kilometers of displacement, most typically found as tear faults in fold and thrust belts. The Coulomb-Anderson model does not adequately explain the tensional and compressional effects due to "simple shear", where crustal strain is the direct result of pervasive horizontal shear in a consistent sense and direction (Figure 16; Aydin and Page, 1984). Stress would have to change from horizontal ( $\sigma_1$ ) to vertical ( $\sigma_2$ ) for normal faulting to occur (Figure 16). The Coulomb-Anderson model therefore cannot explain the features observed in the study area.

The Riedel model better explains the observed and mapped patterns of faulting and associated structures within the pull-apart basin. The Riedel model can predict left-lateral

strike-slip faulting and the simultaneous formation of sets of conjugate shears, folds and normal faults (Figure 15-B; Ramsay, 1967). Not all left-lateral strike slip zones contain every feature shown on a Riedel model (Figure 15-B). However, folds can form en echelon to the imposed shear. Extension fractures or oblique normal slip faults can typically form perpendicular to the axis of shortening as a basin is opened (Figure 15-B). As deformation continues, the fold axes and fault splays alike will rotate according to the amount of shearing (Figure 15-B; Ramsay, 1967). During the Riedel shearing, the development of a fault zone is typically difficult to unravel sequentially, especially if the fault zone has had a long history of movement (Sylvester, 1988). As a fault zone develops, resulting faults and folds are often rotated into orientations parallel to the principal displacement zone (Sylvester, 1988).

Figure 15-A and B shows the left-lateral strike-slip kinematics of a Riedel model for left-slip movement. Riedel shears (R-shears) form acute angles to the master fault. Their arrangement is often en echelon. Conjugate Riedel shears (R'-shears) form at angles of about  $75^\circ$  to the main line of faulting (Figure 15-A). Additional sets of acute shears known as P-shears develop at small acute angles of about  $10^\circ$  to the main line of imposed shear (Figure 15-A). Left-lateral strike-slip faulting can produce compressional structures, like folds, perpendicular to the local greatest compressive stress (Figure 15-B).

In a Riedel model along an imposed left-lateral shear, R and R' are conjugate Riedel shears (Figure 15-A). R is synthetic whereas R' is antithetic to the main movement. P shears form "a little later" (Davis, 1996) in the process of the development of the shear arrays for left-lateral movement and are often difficult to identify in an actual

basin (Figure 15-A; Davis, 1996). As strike-slip faulting proceeds, R-shears achieve a closer angle with the main line of faulting, and R' shears may be rotated to a higher angle (Davis, 1996).

### **Structural Features of the San José de las Matas Pull-Apart Basin**

#### **Imposed Shear**

Many structural features in the San José de las Matas pull-apart basin were identified in the Inoa Conglomerate and in the Cercado Sandstone (Plate 1 and Figure 15-B). Imposed shear along the master faults, i.e., the Inoa and Amina faults, has deformed the Cercado Sandstone. Although the Cercado Sandstone is not part of the pull-apart basin, the structural features found in this formation may be considered part of its evolution (Plate 1).

#### **Conjugate Riedel (R') Shears**

Antithetic NE-trending lineaments joining the WNW and NW-striking splays of the Amina fault system occur in the study area. The Riedel model predicts that these NE-trending lineaments are Riedel (R') shears (Figure 15-A). Elongated clasts along the third NE-trending lineament joining the Amina fault system confirm that strike-slip movement (along a possible R' shear) occurred conjugate to the Amina fault (Plate 1 and Figure 15-A).

### **Conjugate Riedel (R) Shears - Folds**

The spacing of anticlinal and synclinal fold axes in the Inoa Conglomerate decreases from east to west. The fold axes are oblique (synthetic) to the Inoa fault and trend to the WNW in the eastern segment of the study area (Plates 1 and 2; Domain No. 13). Fold axes then change trend to ENE in the central portion of the study area and then back to WNW at the western end (Domain 3; Domain 8) of the pull-apart basin (Plates 1 and 2). Rotation of fold axes may be due to block rotation of the Inoa Conglomerate (Christie-Blick and Biddle, 1985). The folding arrangement is en echelon. The folds are parallel to one another along a common line of bearing (Figure 15-B).

Strike of the axial planes of folds within the Inoa Conglomerate and Cercado Sandstone occur oblique to the main strike of the Inoa fault, and results in an en echelon pattern. The axial planes of the folds in the Magua Formation occur parallel to the Inoa fault and may be unrelated to the Late Paleogene to Neogene strike-slip deformation. The folding in the Magua Formation may be related to deformation caused by the extrusion of the Rodeo Basalt Member of the Magua Formation. The folds in the Magua Formation could also be the result of subtle vertical components of movement along the Inoa fault (Harding and others, 1985).

### **Conjugate Riedel (R) Shears - Fractures**

The structural domains show that shear fractures occur as conjugate pairs relative to the strike of the master faults. The conjugate sets of shear fractures suggest a close likeness to the expected conjugate (i.e., R-shears) arrangement of shear fractures in a Riedel model (Figure 15B; Plate 1).

### **Compression and Extension**

Other features of the pull-apart basin include local alternating zones of compression and extension that have caused the formation of shear lenses along the Inoa fault. For example, limestones like the La Bruja Limestone and Pananao Limestone outcrop only in shear lenses along the Inoa fault.

### **Fault Offsets**

The amount of slip along the master faults cannot be calculated due to a lack of traceable marker beds in the Inoa Formation (Plates 1 and 2; Plots 5, 24, 25, and 36). Siltstone beds occur infrequently in the Inoa Conglomerate. Cretaceous rocks of the Duarte Complex bound the pull-apart basin. Five km offset of Arroyo Hondo conjoining Rio Inoa along the Inoa fault is evident on map scale (Plate 1). Other offset rivers including Arroyo Las Auyamas, Rio Magua and Rio Mao all have left-stepping jogs between 0.5 km to 2 km in length (Plate 1). Measurements of off set streams valleys are not reliable as datable stratified units.

The movement along the master faults leaves trace evidence of their left-lateral nature in the lateral facies clast trends in the basin (Christie-Blick and Biddle, 1985). Tonalite clasts are evident in the Inoa Conglomerate at the western distal end of the pull-apart basin. This likely occurred from the time of the tonalite's unroofing in the Eocene through the Oligocene when the Inoa Conglomerate was deposited. The closest source of tonalites occurs in the southeastern segment of the study area. These conglomerate clasts were likely laterally transported from the source. Source sediment may have been moved

episodically from the east end of the study area to the west end along the displacement of the Inoa fault. This means that the Inoa fault may have slipped 5 to 10 km laterally.

### **Pull-Apart Basin vs. Fault Wedge Basin**

Data from this study confirm that this sedimentary basin should be classified as a pull-apart basin (Figures 17-A and 18A), rather than a fault wedge basin (Figures 17-B and 18A) as has been suggested by Erikson and others (1998). Differentiating between the two types of basins is made by comparing the expected arrangement of faulting in a pull-apart basin vs. the expected arrangement of faulting in a fault-wedge basin.

### **The Fault-Wedge Basin**

Basins which form at a left-lateral common bifurcating fault are called fault wedge basins (Figures 17-B and 18-B; Freund, 1982). In a fault wedge basin, the wedge between the faults is said to drop down between the two diverging master faults (Figure 17-B and 18-B; Mann, 1983). Various depressions or sag ponds may occur along the fault divergence. Usually, there is a normal component on the main master fault. The deepest part of a fault wedge basin occurs at the tip of divergence (Figure 18-B; Freund, 1982). Although the San José de las Matas may look like a fault wedge basin from map view (Plate 1; Figure 18-B), the amount of separation between the Amina and Inoa faults does not originate from a single bifurcating fault.

### **The Pull-Apart Basin**

Pull-apart basins form when two long segments of strike-slip faults are offset such that they create a local region of extension, also called a releasing bend (Freund, 1982; Figure 17-A). Normal faults usually occur on the remaining two sides not bounded by

strike-slip faults (Figure 19 A and B). Pull-apart basins can form important depocenters. Continued offset and movement along the master faults, however, usually closes the basin which can fold, thrust, and uplift the sediments (Sylvester, 1988). Pull-apart basins formed by left-lateral strike-slip faults may also develop normal faults when the length of the basin exceeds the displacement (Figure 17-A and 18-A; Freund, 1982). The normal faults connecting the master faults are normally  $45^\circ$  from the main strike-slip master fault (Figure 17-A and 18-A; Freund, 1982).

### **Evidence Supporting Development of a Pull-Apart**

The study area is categorized as a pull-apart basin because it is a subsided area, a depocenter bounded by two generally parallel strike-slip faults (Figures 19-A and 19-B; Burchfiel and Stewart, 1966; Crowell, 1974; Rodgers, 1980; Mann and others, 1983; Biddle and Christie-Blick, 1985). Stepovers were formed between the left-stepping, left-lateral WNW-trending Amina fault system (Plate 1; Aydin and Nur, 1985). Along the Amina fault alone, the splays of the WNW-trending faults and lineaments are close enough so that they form an en echelon geometry (Plate 1; Aydin and Nur, 1985).

The arrangement of the fault bounded crustal blocks within the faulted zone is considered the principal control on the formation of the pull-apart. The bounding blocks (i.e., the Duarte metabasalts and the Amina Schist) are torsionally rigid and deform only slightly at their edges. Subsidence of the basin is due to extension along a releasing bend (Figure 20) in a direction parallel to the regional strike of the faults (Figure 20; Crowell, 1974). Figure 21 is a perspective diagram showing the down-thrown basin between the relatively parallel left-lateral strike-slip master faults.

## **Basin Subsidence**

The overall strike-parallel view of the Inoa Conglomerate in the pull-apart basin shows a series of NW-plunging anticlines and synclines bounded by the Inoa and Amina faults (Plate 2; Cross-sections B-B' through H-H'). The slightly warped Cercado Sandstone rests nonconformably and in fault contact with the Amina Schist. Anticlines and synclines formed in the Cercado Sandstone also trend in a NW direction, oblique to the imposed shear of the master fault. Topographic elevations are generally lower for the Inoa Conglomerate between the Inoa and Amina faults. Lower hemisphere equal area projections (Plots 9 and 25) show a component of dip-slip which suggests that the Inoa Conglomerate and limestone formation units (i.e., the La Bruja and Pananao) dropped into the pull-apart basin due to local extension (Plate 2; Cross-sections C-C' through G-G').

## **Tectonic Relationship of the Pull-Apart Basin**

### **Local Tectonics**

The present site of the San José de las Matas pull-apart basin was part of a forearc basin during the Neogene. The Magua Formation and the Tavera Group's Inoa Conglomerate, Monción Limestone, La Bruja Limestone, and Pananao Limestone were deposited up until the early Miocene. The late Tertiary Cercado Sandstone and Bulla Conglomerate were deposited up until the late Miocene. Deposition of these sediments was associated with a combination of uplift of the Duarte Complex during the Eocene [due to the south-dipping subduction complex in northern Hispaniola and the initiation of strike-slip movement during the Oligocene along the NOAM/CARIB plate boundary (Draper and Lewis, 1982)].

In the central portion of the pull-apart basin, the Cordillera Central produced sediment sources that generated subaerial fans of the Magua Formation and Inoa Conglomerate from the Eocene to Oligocene time. Conglomeratic sediments were deposited in the pull-apart basin from the Eocene (Magua time) through the Oligocene (Inoa time) into the early Miocene. As these fans were emplaced they were deformed by movement along the Amina and Inoa faults. A local unconformity from the early Miocene until the late Miocene occurred (Figure 9). This may be related to the major angular unconformity recorded in the Cibao region during the same period of time (Edgar, 1991). Erikson and others (1998) report that the Cibao Basin began to subside in the late early Miocene, as indicated by the subsidence of the upper lower Miocene - lower middle Miocene Baitoa Formation, which rests on a subaerial unconformity above the Tavera Group, east of the study area. The deposition of the late Miocene Bulla Conglomerate and the Cercado Sandstone may indicate the last stages of distal source movements of sediments from Cordillera Central into the forming pull-apart basin due to tectonism. The Bulla Conglomerate contains large boulders of Duarte Complex source rocks which were eroded into a very shallow marine sea. Open shallow to moderately deep marine conditions prevailed into the late Miocene just north of the Inoa Conglomerate towards the Cibao Valley (Cercado time).

Based on an evaluation of stratigraphy and structures, several observations can be made about the deformational phase or phases which occurred from Inoa to Cercado time to produce the San José de las Matas pull-apart basin. Deformation of the basin likely began in the Eocene to early Oligocene based on foraminifera data from the La Bruja

Limestone collected along the Inoa fault (Palmer, 1963; 1979). This suggests that the opening of the basin started in the Eocene but mainly occurred in Oligocene time, according to data from the eastern segment of the Tavera belt (Riemer, 1978; Groetsch, 1983).

The Inoa Conglomerate was deformed when the pull-apart was sheared during the Oligocene. The rocks of the pull-apart basin have characteristics intermediate between those of brittle and ductile shear zones. Ductile deformation is recorded in the elongated clasts which outcrop along both the Inoa and Amina faults (Plate 1). En echelon fold patterns are quite evident in map scale in the Inoa Conglomerate.

Along both the Inoa and Amina faults, brittle deformation of the Inoa Conglomerate is recorded in conjugate sets of shear fractures (Plates 1 and 2; Plots 7, 21, and 34). Tectonic breccias, bedding offsets, and shear fractures along the master faults are key indicators of a brittle shear zone. Upon closer observation on an outcrop level, the rocks look like they have deformed in a brittle fashion. Brittle features such as shear fractures and sharp off-sets of bedding are more widespread and predominant throughout the study area.

Unconformities between the Oligocene Inoa Conglomerate and the late Miocene clastic formations (i.e., the Bulla Conglomerate and Cercado Sandstone) suggest that continued subsidence and deformation of the basin occurred post Inoa time. The presence of tectonic breccias (La Bruja and Pananao Abajo Breccias) record deformation events between Magua and Inoa time and between Inoa and Cercado time, respectively.

Another major faulting event is recorded by the Sui Breccia in the Cercado

Sandstone. The Suí Breccia contains reefal limestone clasts which are characteristic of the upper portion of the Cercado Sandstone's transition into the Pliocene Gurabo Sandstone. The contact between the Cercado Sandstone and Gurabo Sandstone outcrop just north of the study area (Saunders and others, 1986). This faulting occurred in the late Miocene and possibly in the early Pliocene. Deformation in the Cercado Sandstone post-dates its deposition.

### **Tectonic History of the Study Area**

#### **Late Cretaceous**

Between the Cretaceous and Eocene, the Hispaniola Arc is thought to have developed behind the leading edge of the Caribbean plate as it moved northeastward from the Pacific region along a SW-facing subduction zone (Pindell and Dewey, 1982; Burke, 1988; Pindell and Barrett, 1990; Dolan and others, 1998). During the Paleocene Hispaniola smashed up against the Bahama Platform. A NE-facing subduction zone developed which was responsible for a major shift in motion of the Caribbean plate and for NE-SW compression of the island arc (Pindell and Barrett, 1990; Mann and others, 1995). Due to this collision the Hispaniola Arc began a shift eastward from the Eocene to present along the NOAM/CARIB plate boundary as the Caribbean Plate twisted in a more easterly direction (Pindell and Dewey, 1982; Burke, 1988; Pindell and Barrett, 1990; Dolan and others, 1998).

#### **Paleocene to Eocene**

Northward thrusting produced northeast-verging isoclinal folds and regional metamorphism in the Amina Schist rocks (Draper and others, 1994A). By Maastrichtian

time, large granitoids, which include hornblende tonalites intruded into northwestern Cordillera Central partially due to the thrusting events (Bowin, 1960; Palmer, 1963; Draper and Lewis, 1991).

The north-northeastward thrusting caused folding and regional metamorphism, followed by arc volcanism and hornblende tonalite plutonism (Draper and Lewis, 1989). Extrusion of the Rodeo Basalt and deposition of the conglomerates of the Magua Formation (Draper and Lewis, 1991) occurred at this time. In the middle Eocene, the Hispaniola Arc-Bahama Platform collision terminated (Pindell, 1994).

During the late Eocene, calc-alkaline magmatism terminated. Subsequent volcanism produced scattered alkalic and calc-alkalic volcanic flows and plugs that are related to movement along strike-slip faults. These strike-slip faults along the northwestern segment of the HFZ produced a narrow fault-bounded belt where conglomerates, sandstones, mudstones, limestones, and volcanoclastic rocks accumulated (Bowin, 1966; Palmer, 1963, 1979; Lewis and Draper, 1990).

The conglomerates of the Magua Formation contain boulders of the hornblende tonalite indicating that it was deposited as early as Latest Maastrichtian through late Eocene (Palmer, 1963; 1979).

The earliest evidence of the Hispaniola Arc's eastward mobilization along the NOAM/CARIB plate boundary is the opening of the Tavera pull-apart basin during the Oligocene (Figure 2; Dolan and others, 1991; 1998). Dolan and others (1998) suggest that since the onset of this eastward motion of Hispaniola, initiation of the left-handed strike-slip faulting along the HFZ, Septentrional, and Camu fault zones must have

occurred before ~25 Ma. Evidence of the study area's tectonic evolution with respect to the NOAM/CARIB plate boundary is preserved in the structures of the San José de las Matas pull-apart basin. The San José de las Matas pull-apart basin, therefore, is a valuable indicator of the inboard deformation caused by the NOAM/CARIB plate boundary fault zone.

Left-lateral strike-slip faulting along the Inoa fault controlled the development of the sedimentary basin. As faulting occurred along the Inoa fault, subsidence began occurring to the north in the Cibao basin (Erikson and others, 1998). As a result of regional subsidence, conglomerates were deposited subaerially in the San José de las Matas pull-apart basin. Conglomerates were deposited with minor marine sequences of calciferous mudstones, e.g. the gray beds of the Inoa Conglomerate (Palmer, 1963).

The HFZ was likely the northernmost tectonically active region during the Oligocene through the early Miocene and could represent the location of the former plate boundary (Palmer, 1979; Groetsch, 1982; Draper and Lewis, 1982; Dolan and others, 1991). Left-lateral offset occurred along the SFZ since early Miocene time (Erikson and others, 1998). Left-lateral movements in Hispaniola switched to a combination of compression along a restraining bend in northeastern Hispaniola from the late Miocene to present due to the collision of the Bahama Platform (Grindlay and others, 1999). The Cercado Sandstone underwent folding during the late Miocene. There was presumably less folding in the Cercado Sandstone than in older units of the pull-apart basin.

After the collision of the Bahama Platform with northeastern Hispaniola there was an increase in the transpressional component in the inboard forearc basin. Deformation of

northern Hispaniola likely slowed the left-lateral movements along the HFZ. The left-lateral movements may have transferred northward. Continued oblique collision between Hispaniola and the southeasternmost Bahamas banks during the late Miocene likely contributed to deformation of the northernmost reaches of the San José de las Matas pull-apart basin.

### **Neogene**

The island arc continued uplifting as the Bahama Platform and Hispaniola collided with one another. During uplift of the Cordillera Central, the San José de las Matas pull-apart basin likely tilted to the NE and limestones, such as the Monción Limestone and Pananao Limestone were deposited along the northern reaches of the basin. Strike-slip faulting continued into the early Miocene. In post-early Miocene time, oblique collision between the Caribbean plate and southeastern Bahama Platform produced transpression (Pindell and Barrett, 1990; Mann and others, 1995). By late Miocene time, Bulla Conglomerate and the Cercado Sandstone were deposited in the San José de las Matas pull-apart basin (Vaughan and others, 1921; Palmer, 1963; Saunders and others, 1986).

The Cercado Sandstone was deposited unconformably on the Amina Schist in the field area. Farther to the north of the study area, mudstones of the Gurabo Sandstone and Mao Formation blanketed the deeper water closer to the Cibao basin (Palmer, 1963). The Mao Formation is stratigraphically above the Gurabo Sandstone and located north of the study area (Saunders and others, 1986). These Miocene rocks are faulted in the study area. The Cercado Sandstone and Bulla Conglomerate were gently warped up to at least the latest Miocene. In some isolated locations, steeply dipping beds reveal faults in the

Cercado Sandstone. Fault breccias crop out along one major fault in the Cercado Sandstone.

Faulting and slight warping in the northernmost reaches of the San José de las Matas pull-apart basin (of the Cercado Sandstone) may have continued into the early Pliocene. Little tectonic deformation has been identified in the Late Neogene rocks located north of the study area (Erikson, 1999, personal communication). A thorough structural analysis has not been conducted north of the study area.

### **Quaternary**

By the Quaternary, the San José de las Matas basin was uplifted to form a piedmont north of the Cordillera Central. Alluvial deposits overlie fluvial drainage systems running northward from the Cordillera Central and across the piedmont. These deposits contain only clasts of Oligocene conglomerates, which were derived from Cretaceous source rocks in the Duarte Complex. Distal alluvial deposits at the northern reaches of the study area are composed of fine-grained sand, mud and carbonate rocks from the Bulla and Cercado Formations. Neither liquefaction sites or faulting of the Alluvium was found in these unconsolidated deposits in the study area.

## CONCLUSIONS

The HFZ in the northwestern Dominican Republic developed in a former forearc region from the Oligocene until at least the late Miocene. Sediments derived from the Duarte Complex formed the Tertiary age Magua Formation, Inoa Conglomerate, Bulla Conglomerate, and Cercado Sandstone which filled the basin. The Monción Limestone, La Bruja Limestone, Pananao Limestone formed along a paleocoastline. The structural development and movement along the Inoa and Amina faults, bounding the pull-apart basin, are related to the predominant trend of motion along the on-shore NOAM/CARIB plate boundary, which combines transform slip with a minor component of convergence (Molnar and Sykes, 1969; Sykes and others, 1982; Pindell and Barrett, 1990; Mann and others, 1991). The descriptive term "graben" should no longer be applied to this area because this term implies that only normal faulting occurred to form the basin. This area should be called the "San José de las Matas pull-apart basin" (cf. Lewis and Draper, 1990), because this basin has developed by strike-slip faulting associated with dip-slip motion.

The San José de las Matas pull-apart basin is cut by high-angle, WNW-trending, left-lateral strike-slip faults. Limestones of middle Eocene age are caught in slivers of the shear zones of both the Inoa and Amina faults. The southern boundary of the basin is defined by a left-lateral strike-slip oblique fault bounded by a high strength buttress of tonalite plutons, serpentinite bodies, and mafic schist of the Duarte Complex. The northern boundary of the pull-apart basin is defined by the Amina fault. Numerous NE and NW-striking lineaments and faults continue northward into the Cercado Sandstone.

An unconformity and faulting separates the Oligocene Inoa Conglomerate from the late Miocene shallow marine clastics Bulla Conglomerate and Cercado Sandstone. The La Bruja Breccia suggests faulting occurred along the Inoa fault from at least the Eocene through the Oligocene. The Pananao Abajo Breccia provides evidence of faulting along the Amina fault from the Oligocene into the early Miocene. The Sui Breccia suggests faulting in the pull-apart basin continued into the late Miocene, possibly into the early Pliocene.

Strike-slip movement along the Amina and Inoa faults is proven by low-angle slickenlines on fault surfaces. Fault types and orientations measured in the study area can be compared to a Riedel model for left-slip movement. N-, NE-, and NW-trending shear fractures best fit a Riedel model for development of a pull-apart basin along a WNW left-lateral shear. In addition, the measurement of elongated clasts found along the Inoa and Amina faults shows that the long axes of elongated clasts in the Inoa Conglomerate are oriented in a WNW elongation, which is consistent with the Riedel model.

Structural orientations of faults of the San José de las Matas pull-apart basin are consistent with those predicted by a Riedel model for left-slip movement. Faulting occurs on both sides of the basin. Shear fractures can be antithetic and synthetic to the main left-lateral shear on the master fault. Folds occur en echelon to the Inoa fault and are considered compressional features which are also predicted by a Riedel model. Faults such as the Inoa fault have shallow dipping slickenlines suggesting the movement to be strike-slip in nature. The San José de las Matas pull-apart basin is bounded on the western end by a normal dip slip fault. The lineaments which have been mapped in the field area are

consistent with those predicted by a Riedel model for the conjugate Riedel shears. Strong NE-trending lineations suggest an tensional component was partly responsible for the opening of the pull-apart basin.

The major fracture sets and fold patterns suggest that the San José de las Matas pull apart basin opened along a line of weakness along the Inoa fault. E-W strike-slip movement is primarily responsible for the tight en echelon folding found in the Inoa Conglomerate and Monción Limestone. Deposition of the Inoa Conglomerate was likely associated with uplift of the Cordillera Central during the Oligocene. This left-lateral movement appears to have stopped and started several times through the late Miocene along the HFZ. Left-lateral movement along the NOAM/CARIB plate boundary continued into the early Pliocene time, rapidly uplifting Cordillera Septentrional. Sediments were deposited in the Cibao basin to the north of the study area. This continued plate boundary movement may well have reactivated the HFZ to some degree.

Further work is necessary to refine the ages of the Pananao and La Bruja Limestones with respect to the Pananao Abajo Breccia and the La Bruja Breccia. This will help constrain the time of faulting in the study area. Locating faults just north of the study area will be necessary to confirm a transitional tectonic model of left-lateral movements of the HFZ transferring northward toward the present NOAM/CARIB plate boundary.

The WNW-trending left-lateral shear movement along the HFZ may have transferred northward from the HFZ to the next zone of regional weakness (i.e., the SFZ) during the Pliocene. This paradigm of a transcurrent movement shifting northward may be

consistent with changes in the regional slip direction for the NOAM/CARIB plate boundary (Molnar and Sykes, 1969; Sykes and others, 1982; Pindell and Barrett, 1990; Mann and others, 1991; Dolan and others, 1998; Erickson and others, 1998). The slip direction from the Oligocene to the middle Eocene may have evolved from left-lateral shear to one of transpression consistent in the post-early Miocene time when the Bahama Platform obliquely collided with the Caribbean plate. This post-early Miocene event produced tectonic transpression and uplift in Hispaniola.

Tectonic evidence in the study area leads me to conclude that the last re-activation of the HFZ was in the late Miocene, and continued into the early Pliocene (~5.3 Ma). As long as the HFZ remains a zone of weakness, there could be future reactivations of this fault zone due to continued slip along the NOAM/CARIB plate boundary. This reactivation could also occur along other Tertiary faults such as the SFZ which has had major earthquakes as recent as 1946. With this understanding, a potential geohazard exists along the Amina and Inoa faults. A new dam and bridge constructed along Río Mao could potentially be at risk to earthquake damage if the HFZ is reactivated. Earthquake management should be taken into consideration as new roads and additional bridges continue to be built to support population growth in this economic center for the production of tobacco.

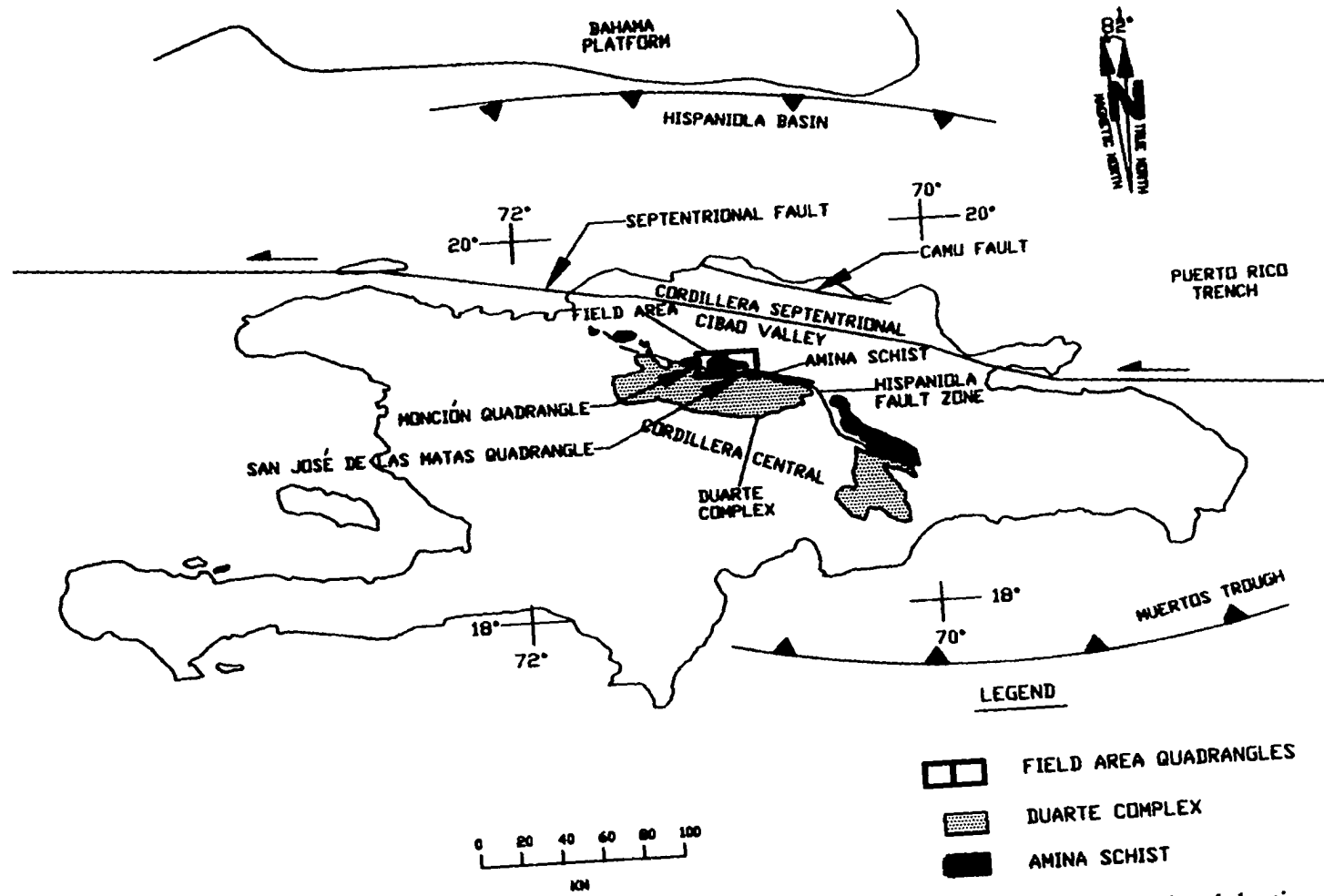


Figure 1. Map of Hispaniola and the study area. Puerto Rico trench subduction zone lies north of Hispaniola. The Muertos trough lies to the south of Hispaniola.

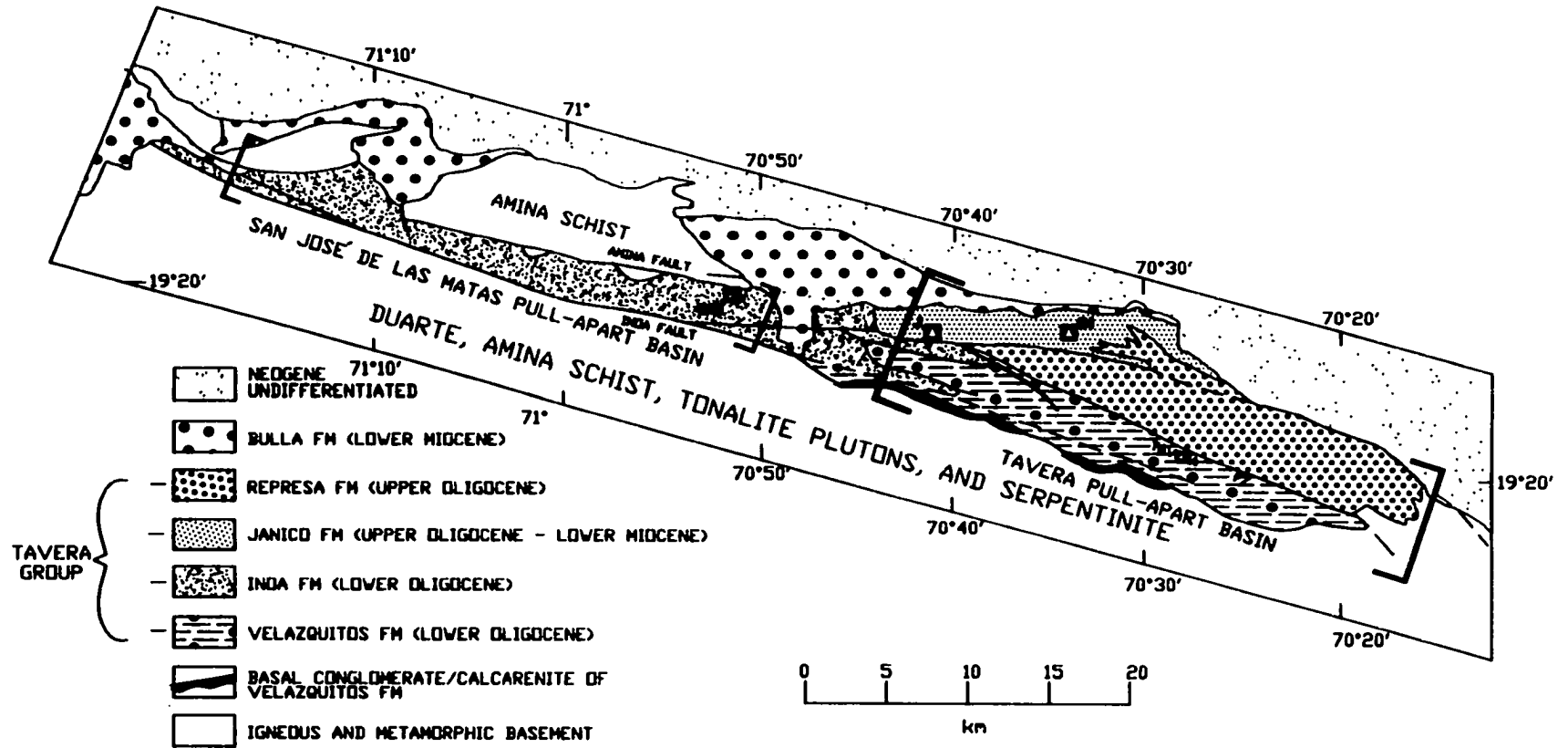


Figure 2. Simplified Geologic Map of the Hispaniola Fault Zone. SI=Sabana Iglesia; J=Janico; SM=San José de las Matas. Modified after Dolan and others (1991).

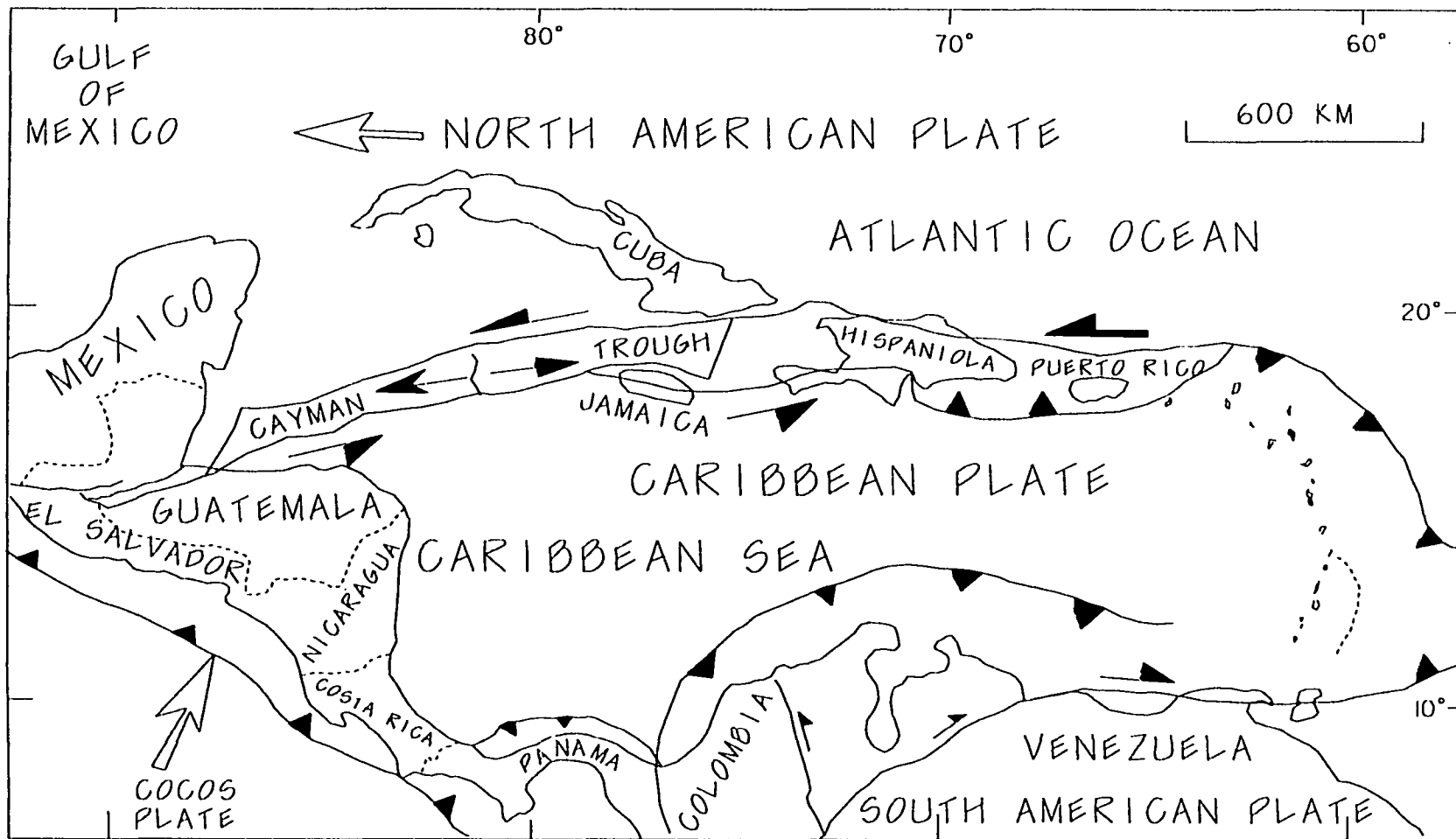
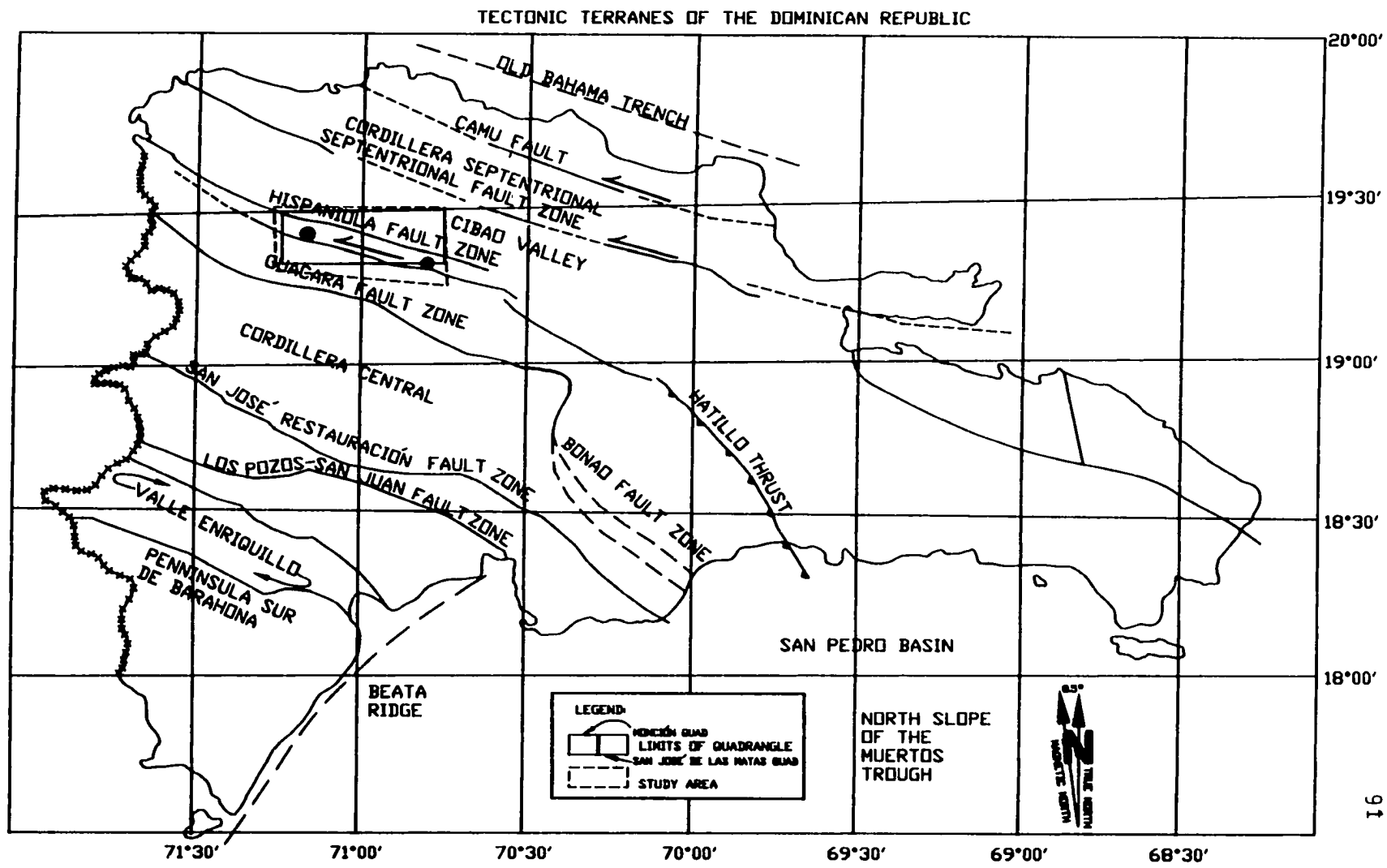
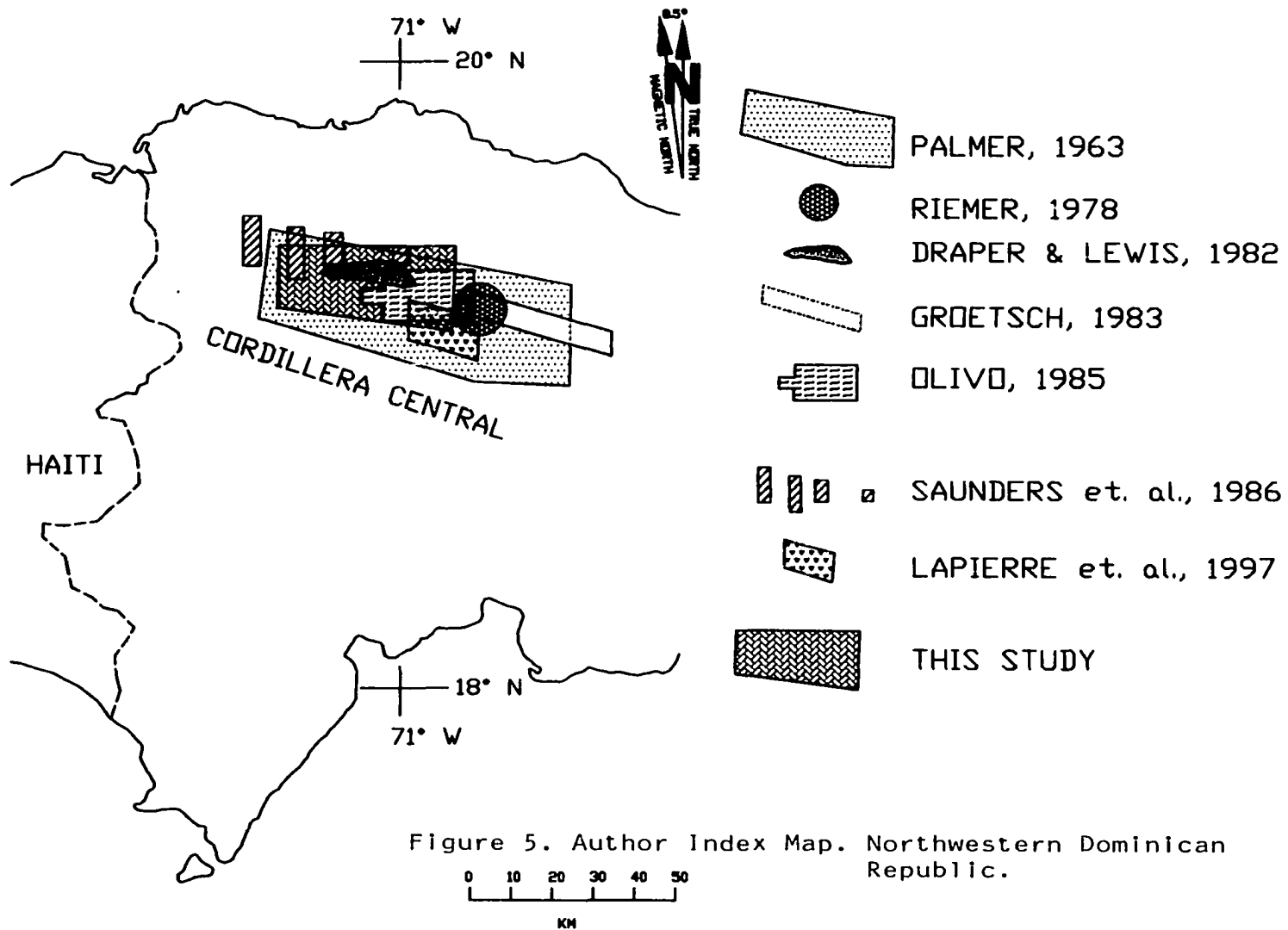


Figure 3. Location and tectonic map of the Caribbean region. Modified from Mann and others (1990; 1991) and Dolan and the others (1998). Large arrows represent plate motion directions from Mann and others (1984).

**Figure 4. Tectonic terranes of Hispaniola. After Mann and others (1991). Study area includes both the Monción and San José de las Matas quadrangles.**





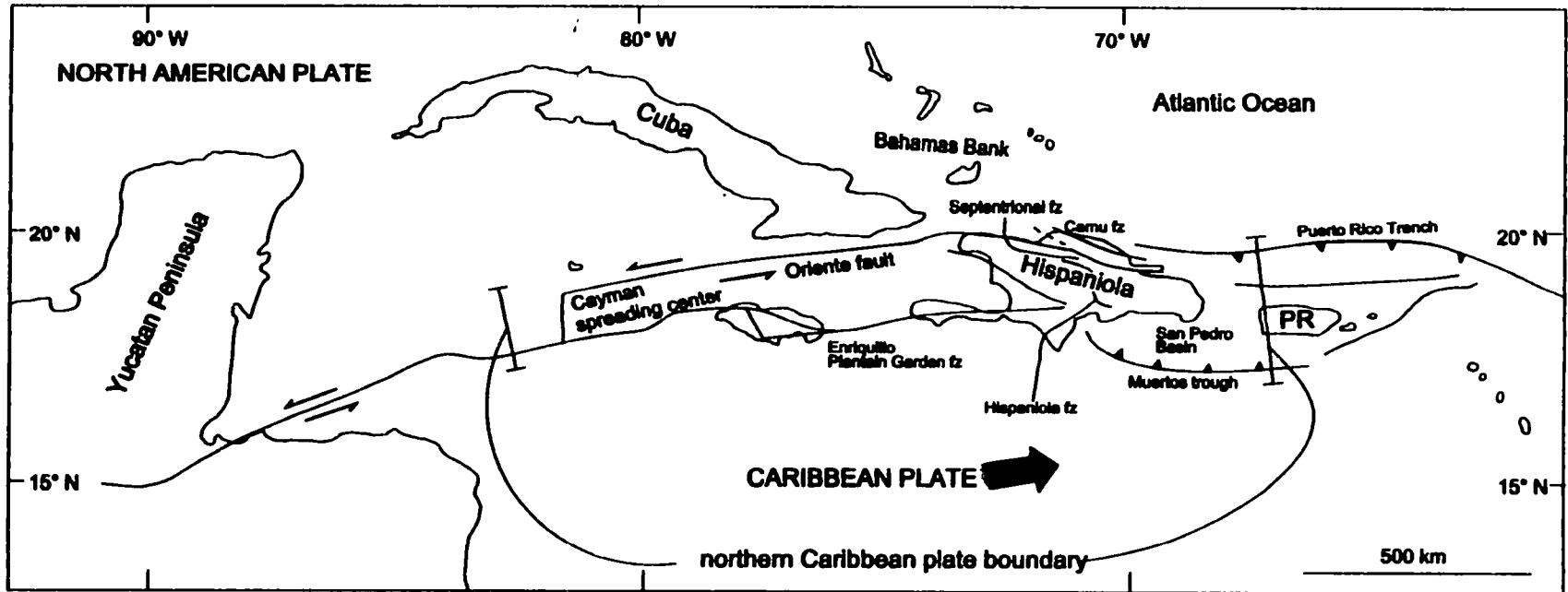


Figure 6. Tectonic Setting of the Northern Caribbean Plate Boundary Zone. Modified after Erikson (1998). Since the Eocene, there has been approximately 1100 km of relative E-NE movement of the Caribbean plate with respect to the North American plate according to Rosencrantz and others (1988). PR = Puerto Rico; fz = fault zone.

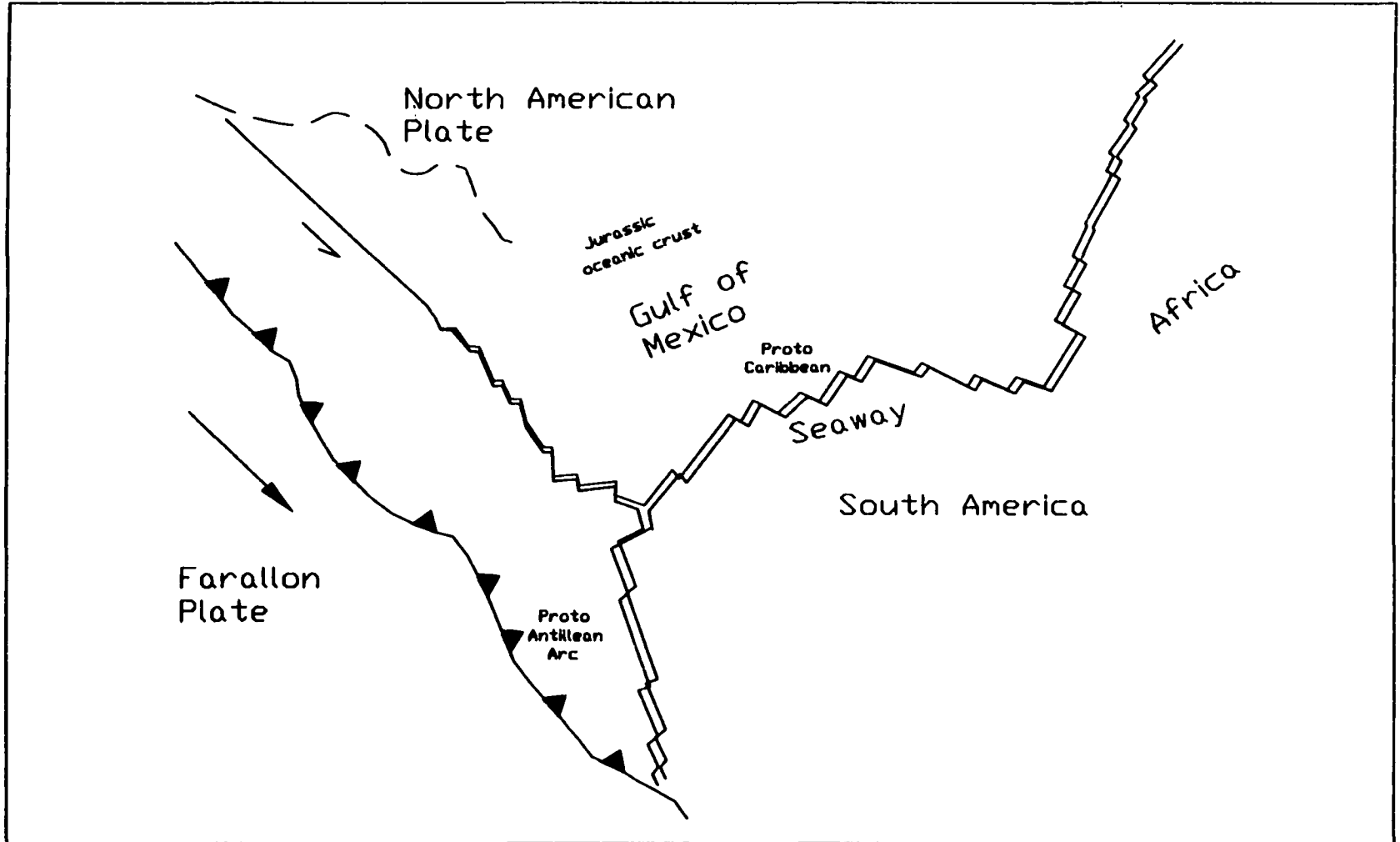
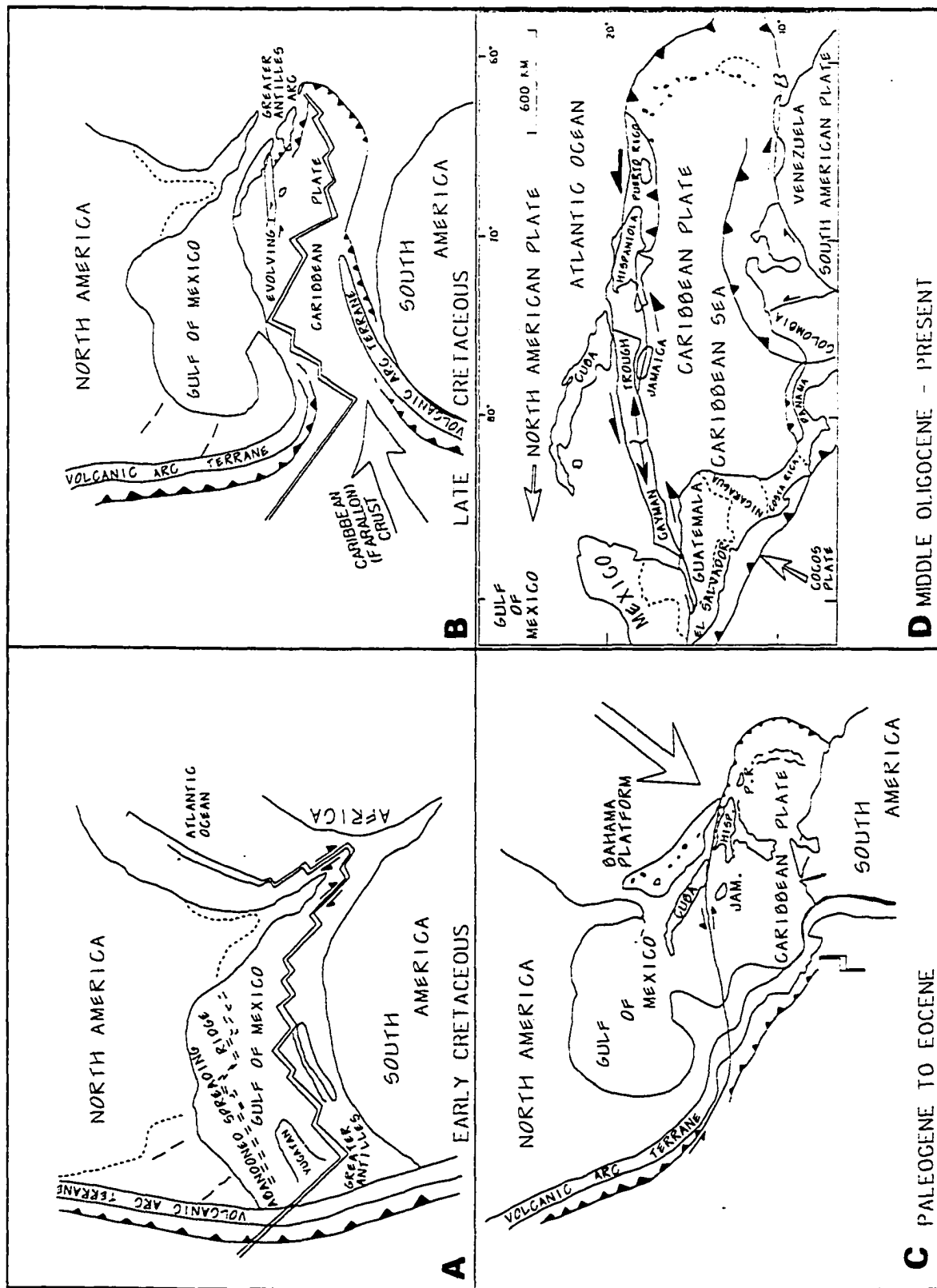


Figure 7. Tectonic Setting of the Caribbean during the Late Jurassic. Modified after Pindell (1994).

**Figure 8. Tectonic reconstruction of the Caribbean Plate. Plates A through C are after Walper, 1982. Plate D is after Pindell, 1994.**



**Figure 9. Stratigraphic column of Palmer (1963) after modifications by Groetsch (1983) on the right. To the left is the new stratigraphic column for the northwestern piedmont of Cordillera Central as it relates to this study.**



# PALEOTECTONICS OF HISPANIOLA

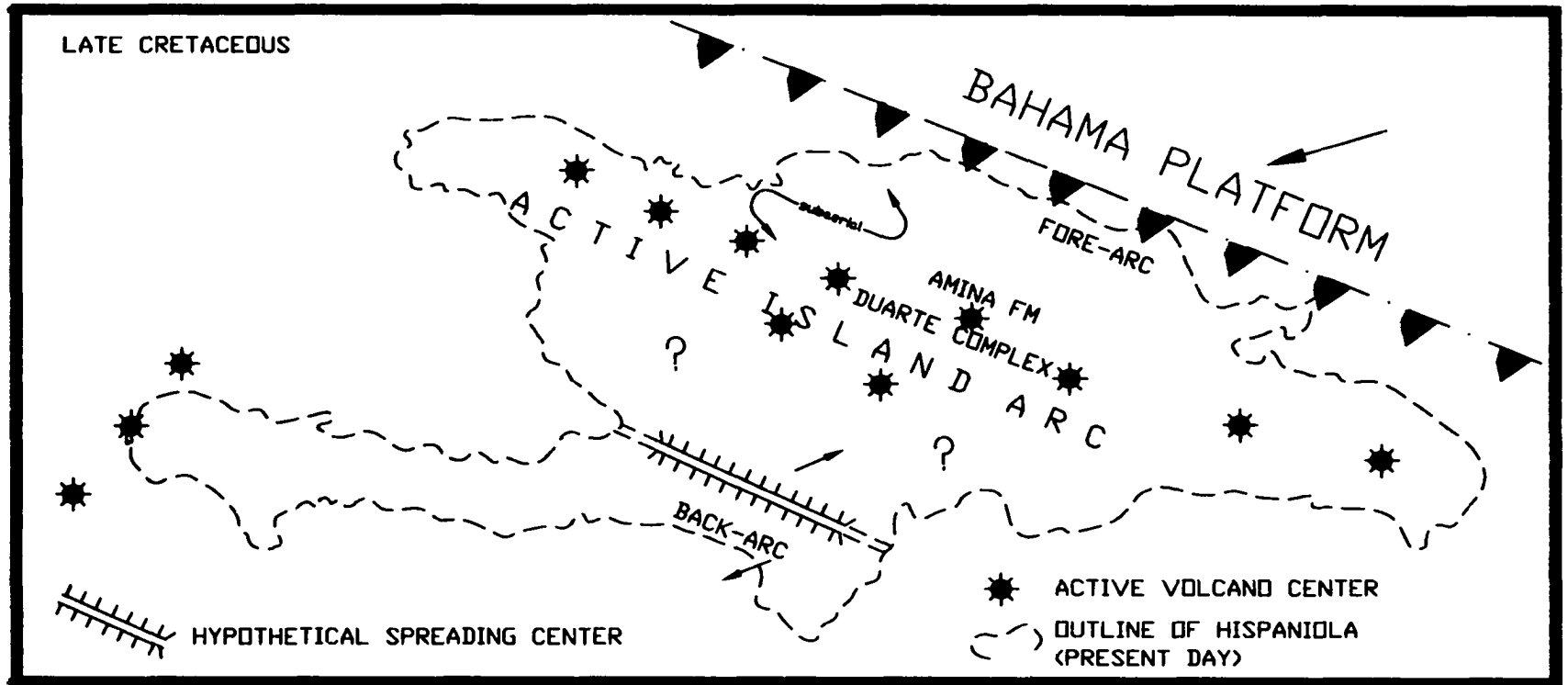


Figure 10. Tectonic setting of Hispaniola during the late Cretaceous.

AFTER MAURRASSE, 1982

# PALEOTECTONICS OF HISPANIOLA

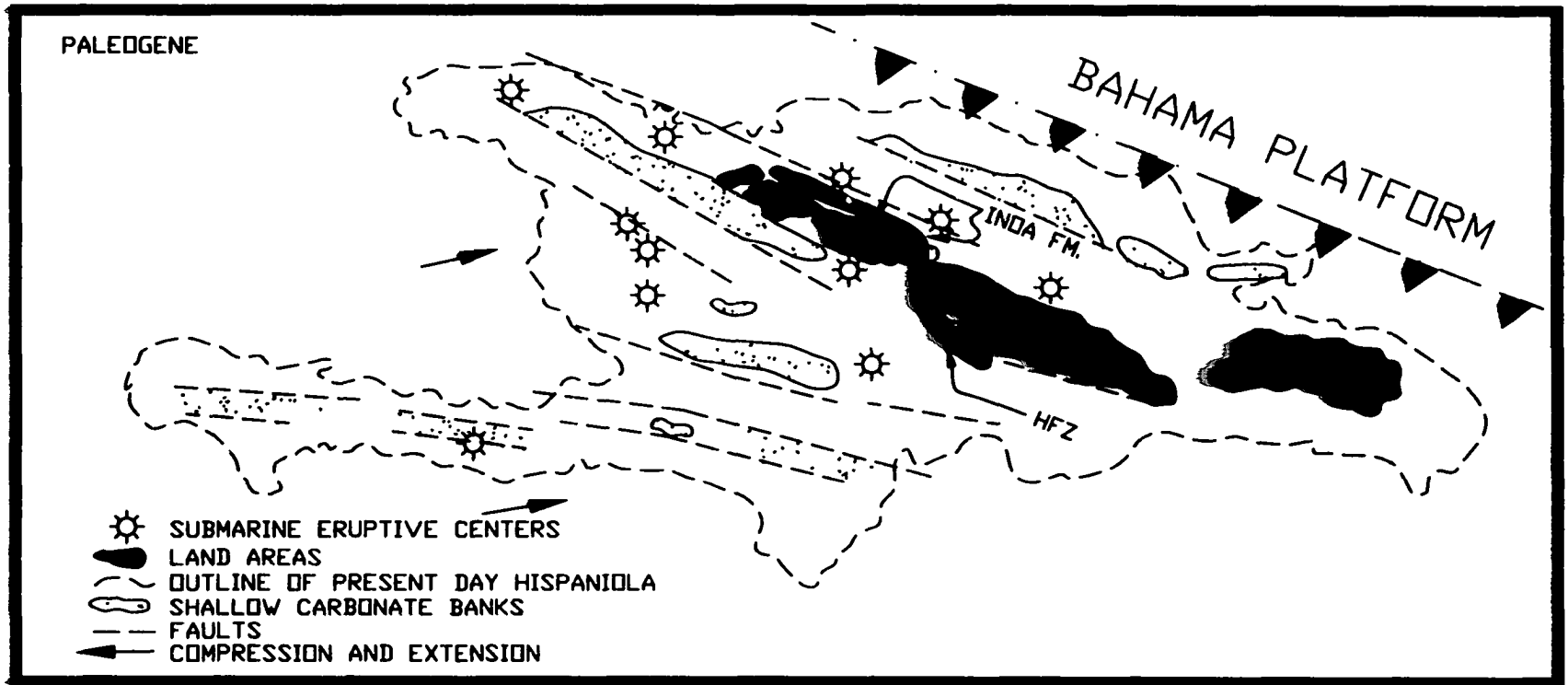


Figure 11. Tectonic setting of Hispaniola during the Paleogene.

AFTER MAURRASSE, 1982

# PALEOTECTONICS OF HISPANIOLA

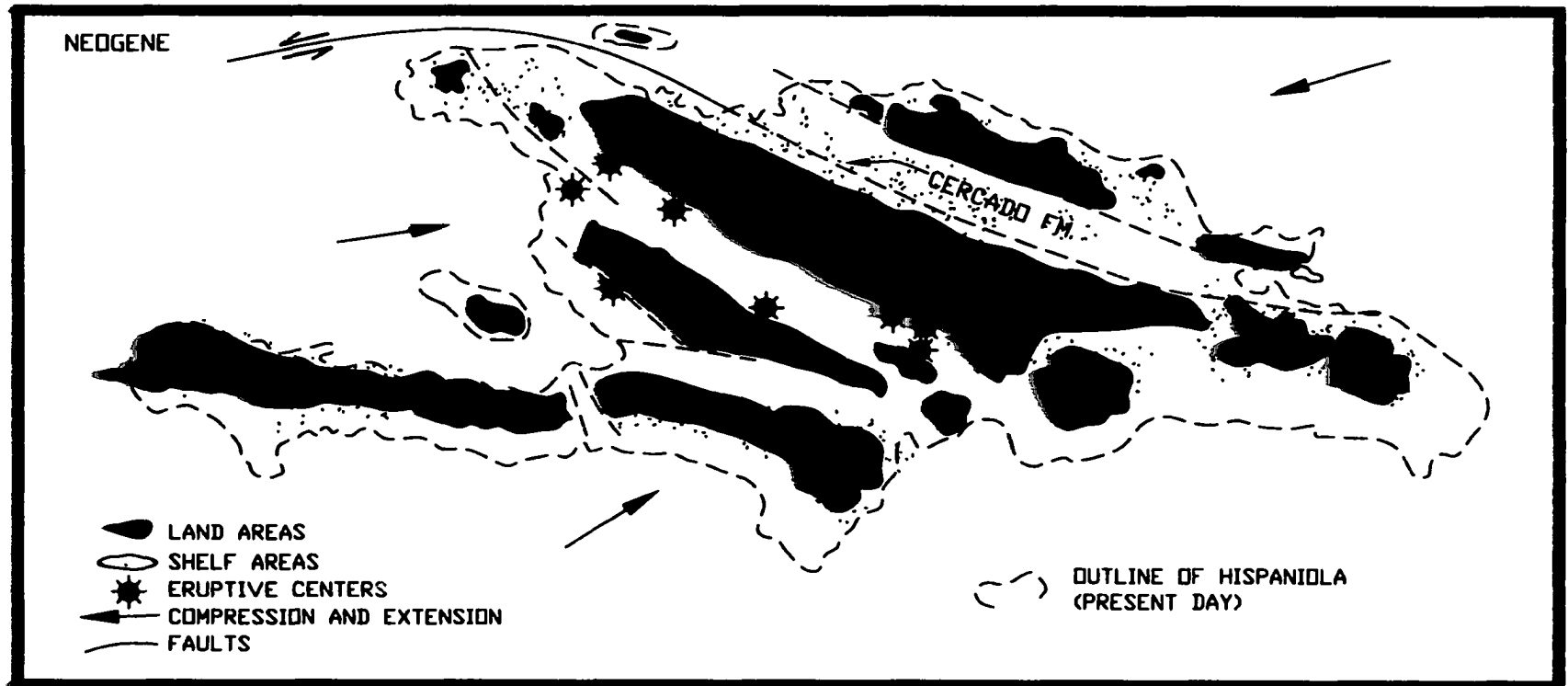


Figure 12. Tectonic setting of Hispaniola during the Neogene.

AFTER MAURRASSE, 1982

# PALEOTECTONICS OF HISPANIOLA

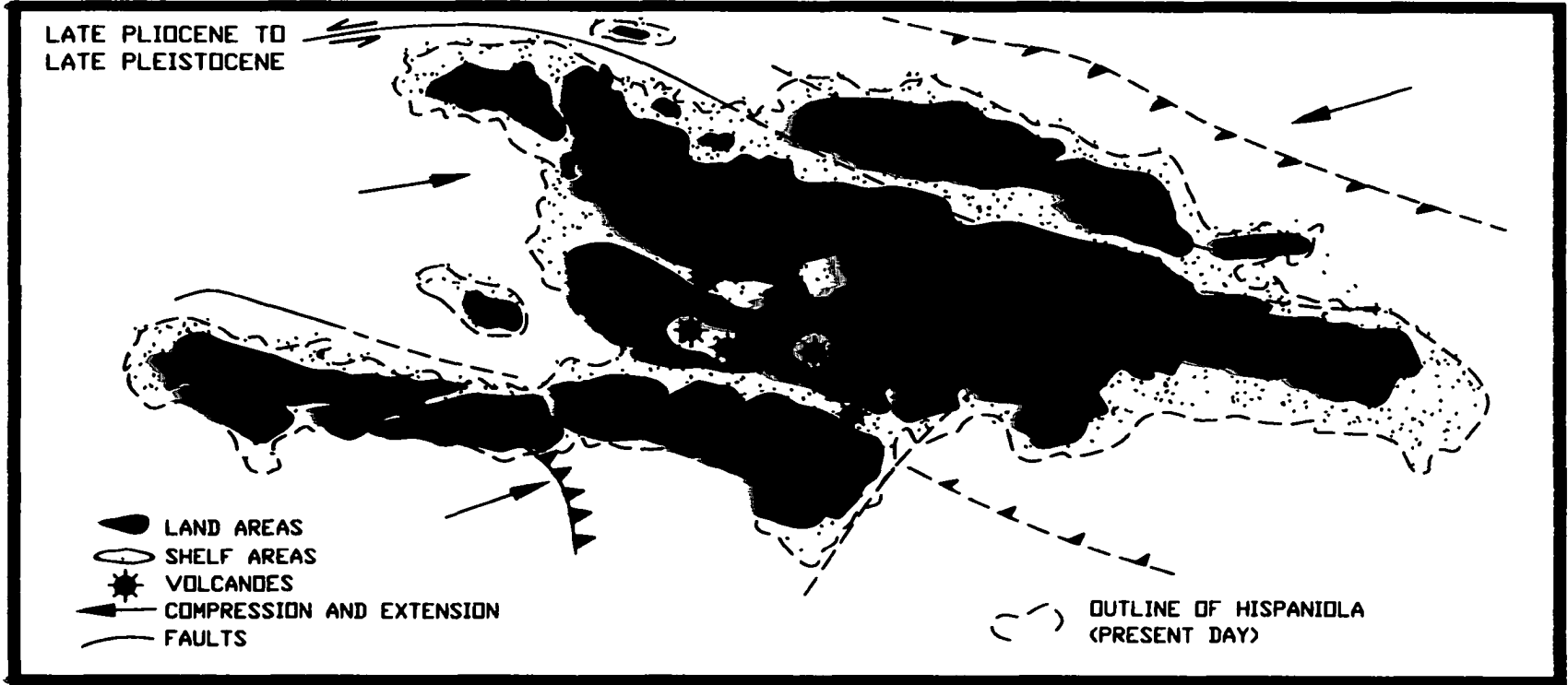
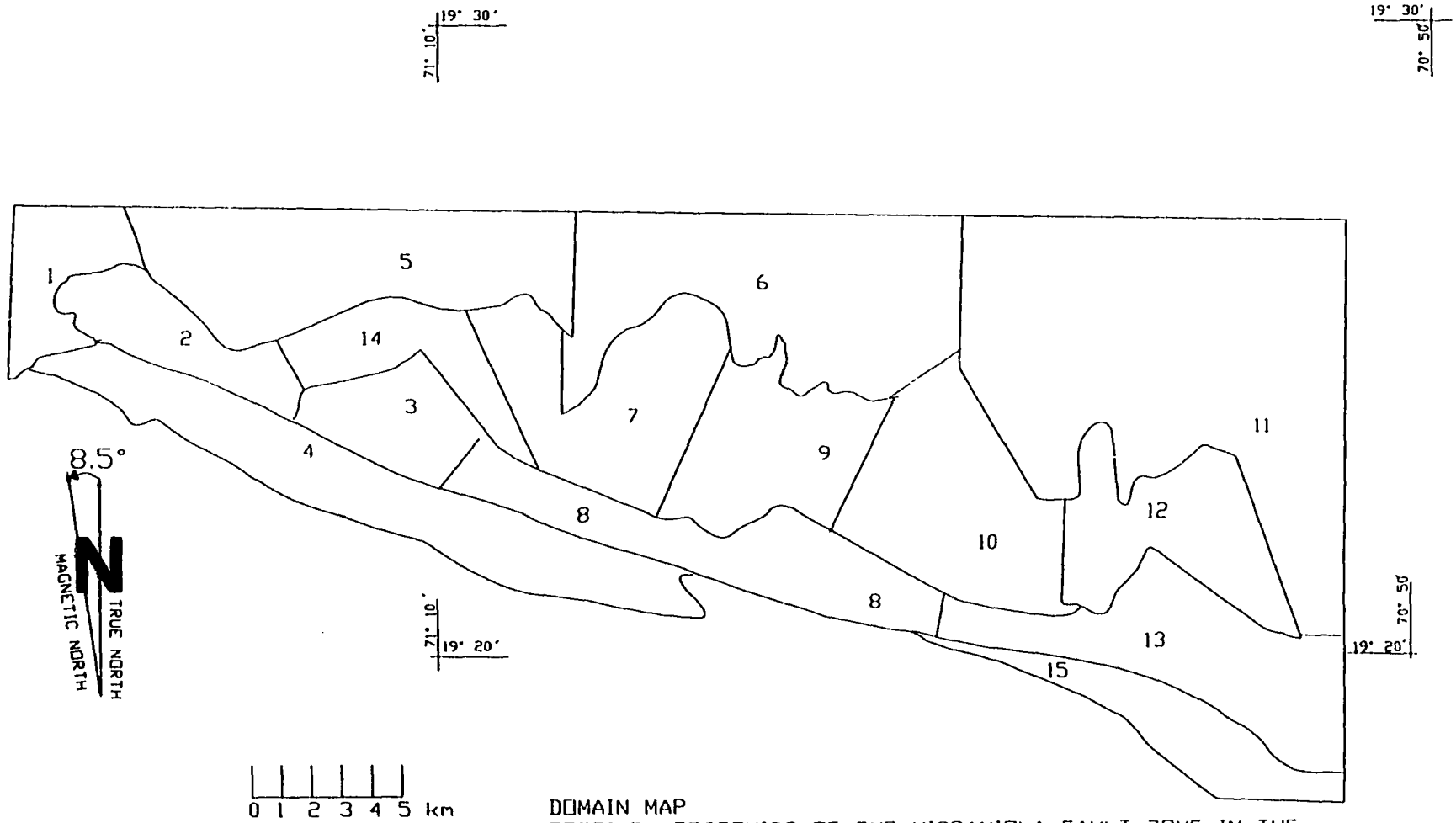


Figure 13. Tectonic setting of Hispaniola during the late Pliocene to late Pleistocene.

AFTER MAURRASSE, 1982



DOMAIN MAP  
TERTIARY TECTONICS OF THE HISPANIOLA FAULT ZONE IN THE  
NORTHWESTERN PIEDMONT OF THE CORDILLERA CENTRAL,  
DOMINICAN REPUBLIC  
GEOLOGY: ANDREW JAY COLEMAN 2000

Figure 14. Domain Map of the northwestern piedmont of Cordillera Central.

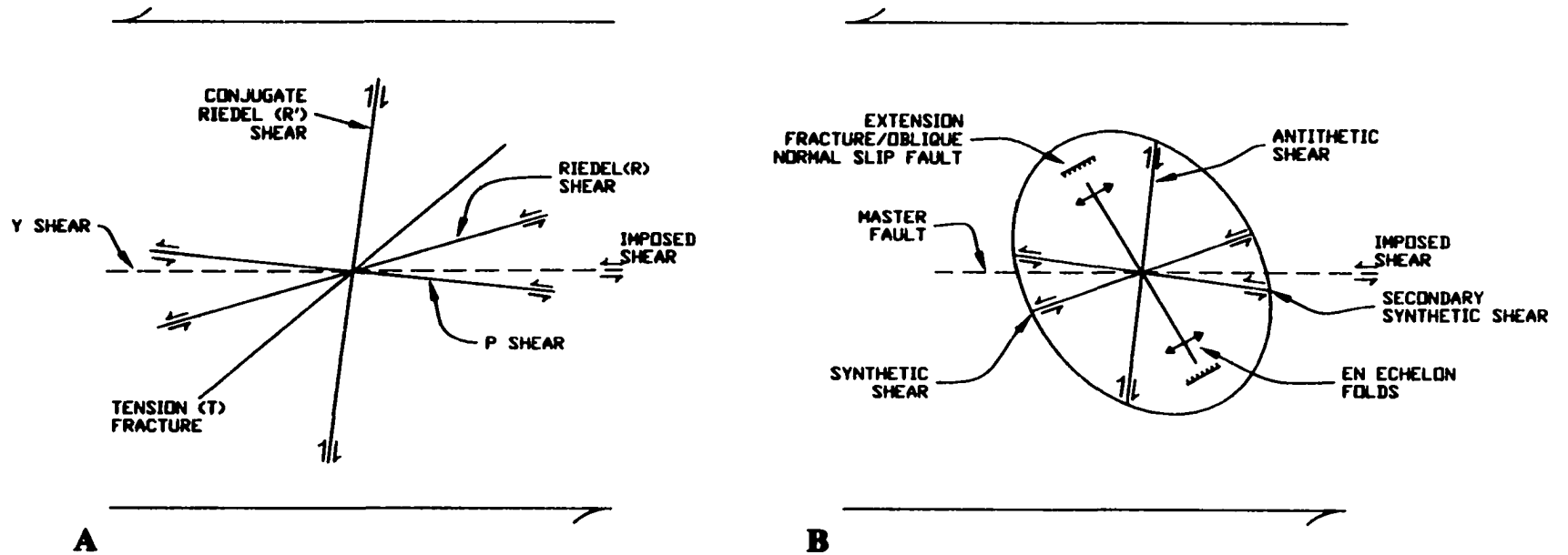


**Figure 15.** The angular relations between structures that form in left-lateral simple shear under ideal conditions, compiled from clay-cake models and from geological examples. A) Riedel shear terminology, modified from Tchalenko and Ambraseys (1970) and Bartlett and others (1981). B) Terminology from Wilcox and others (1973) superimposed on a strain ellipse for the overall deformation. Modified after Biddle and Christie-Blick and Biddle (1985).

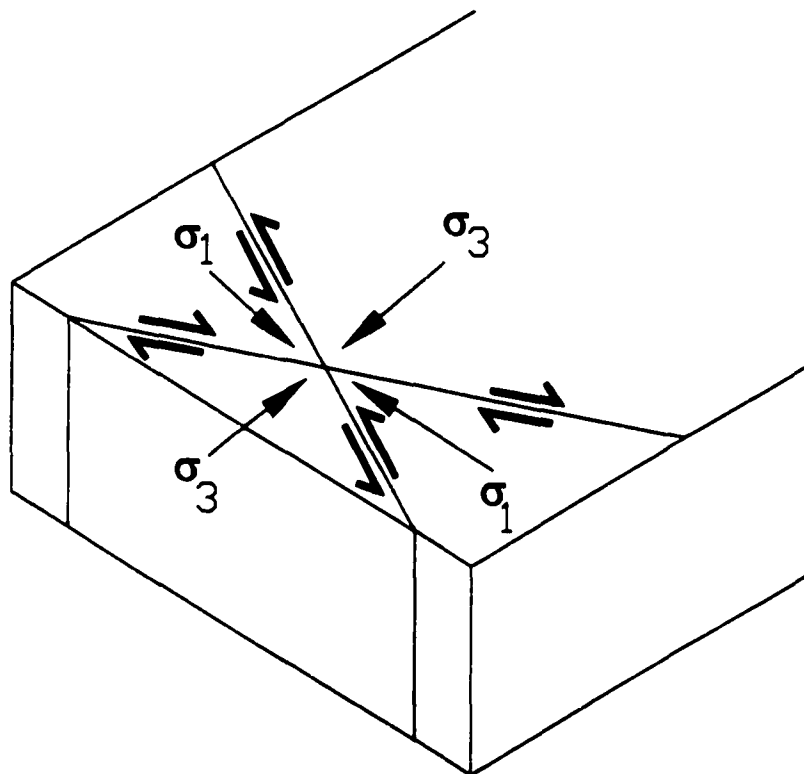


**Figure 16. Strike-slip faults at or near the surface of the Earth. Likely orientations of the principal stress directions at or near the surface of the Earth is either horizontal or vertical. A Coulomb-type model such as this after Anderson (1951) allows for the development of strike-slip faulting, but always produces conjugate sets of  $30^\circ$  angles. Normal slip faults usually only develop when  $\sigma_1$  is vertical. After Suppe (1996).**

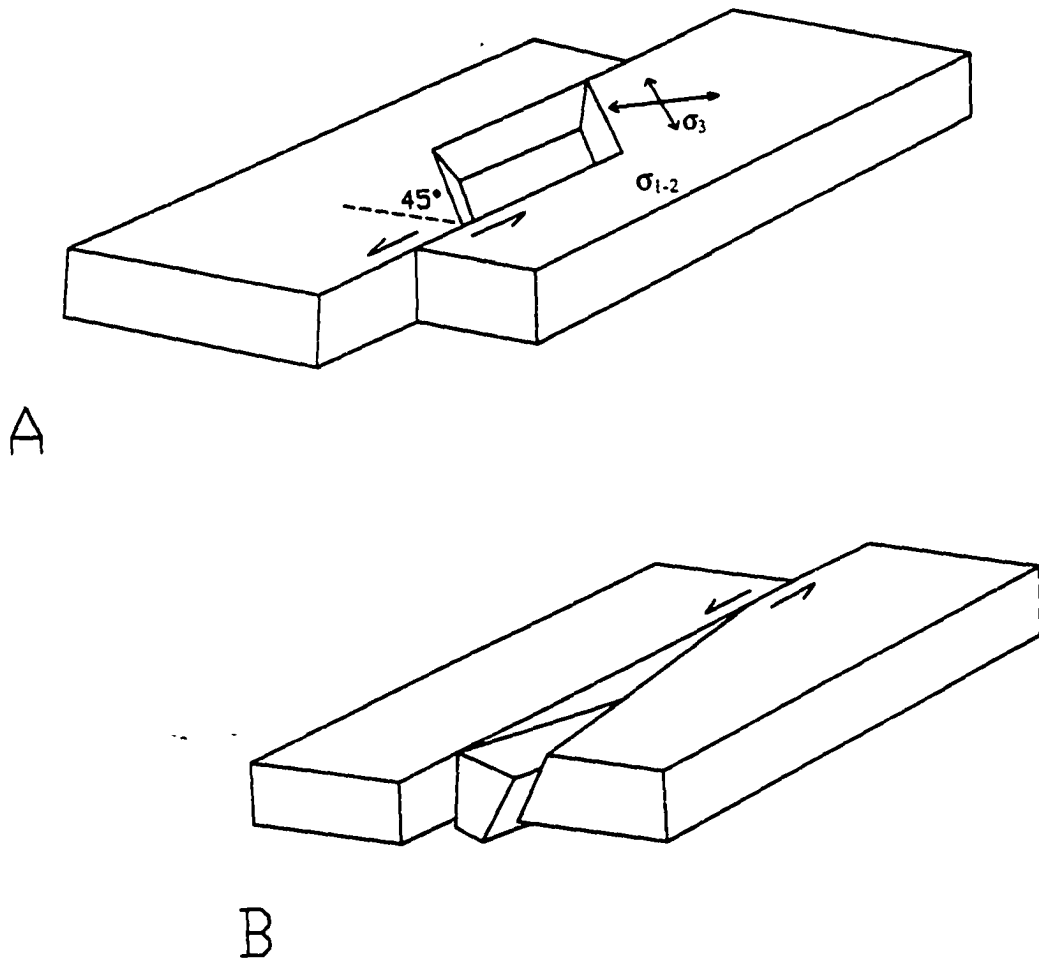


Figure 17. A) Schematic model of a left-lateral pull-apart. The vertical strike-slip fault becomes an inclined normal fault along the basin whose length exceeds the displacement, and the connecting faults are normal and their strike deviates by  $45^\circ$  from the main strike-slip fault, normal to the least principal stress coaxial with the shear stress. B) A schematic model of a fault wedge basin which occurs between a strike-slip fault and a branch fault which deviates from the main fault by an acute angle against the direction of shear. The branch fault is normal, but the dip of the main fault remains unaltered. The deepest part occurs at the tip. A and B are after Freund (1982).

AFTER CROWELL (1974)

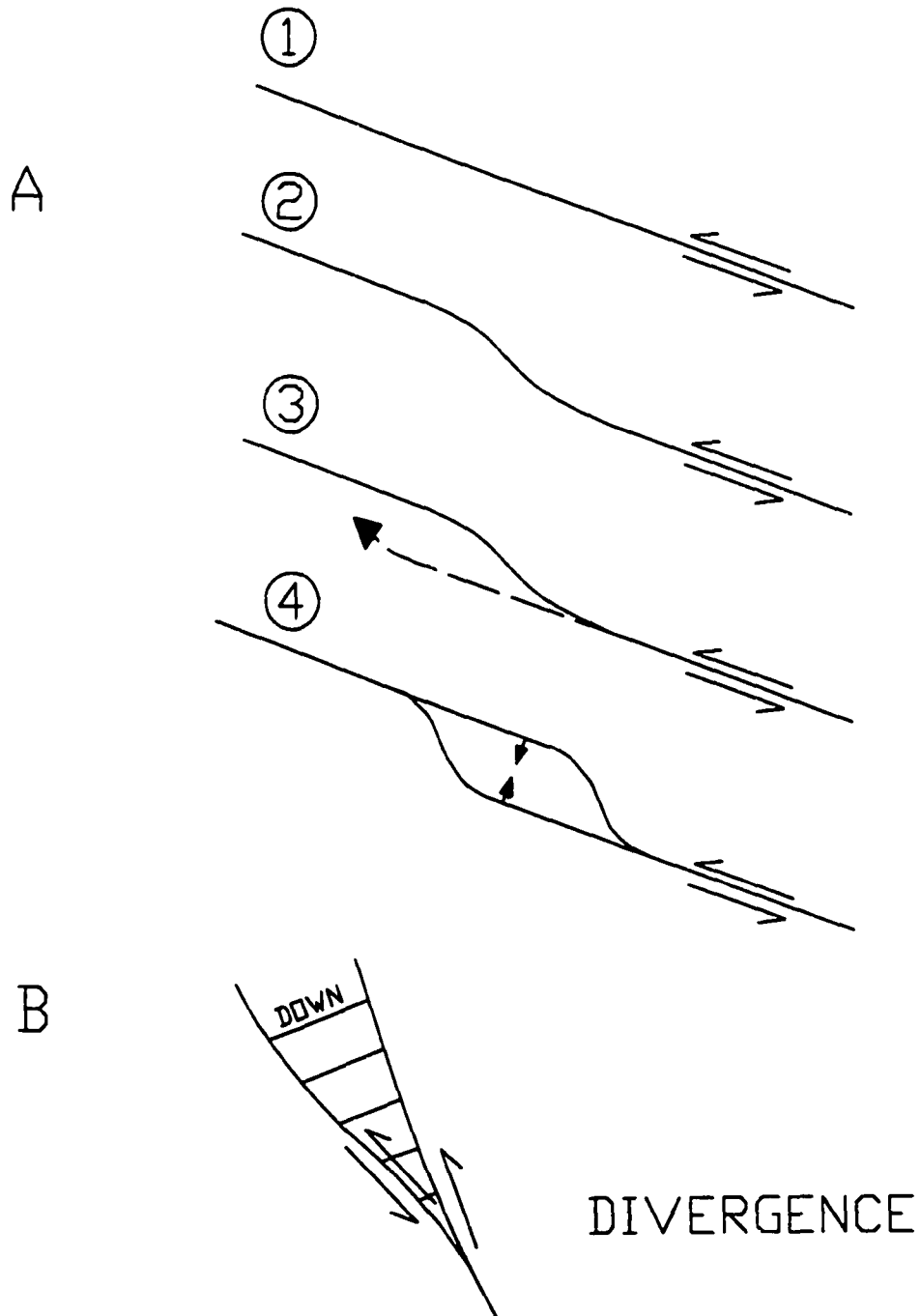


Figure 18. A) Diagrammatic map showing progressive development of fault splays and wedges on a left slip fault. Straight fault (1) gradually develops a bend through time (2 and 3) and eventually forms a typical pull-art (4). Modified after Crowell (1974). B) Diagrammatic map showing subsidence of tip with divergence. Modified after Crowell (1974).

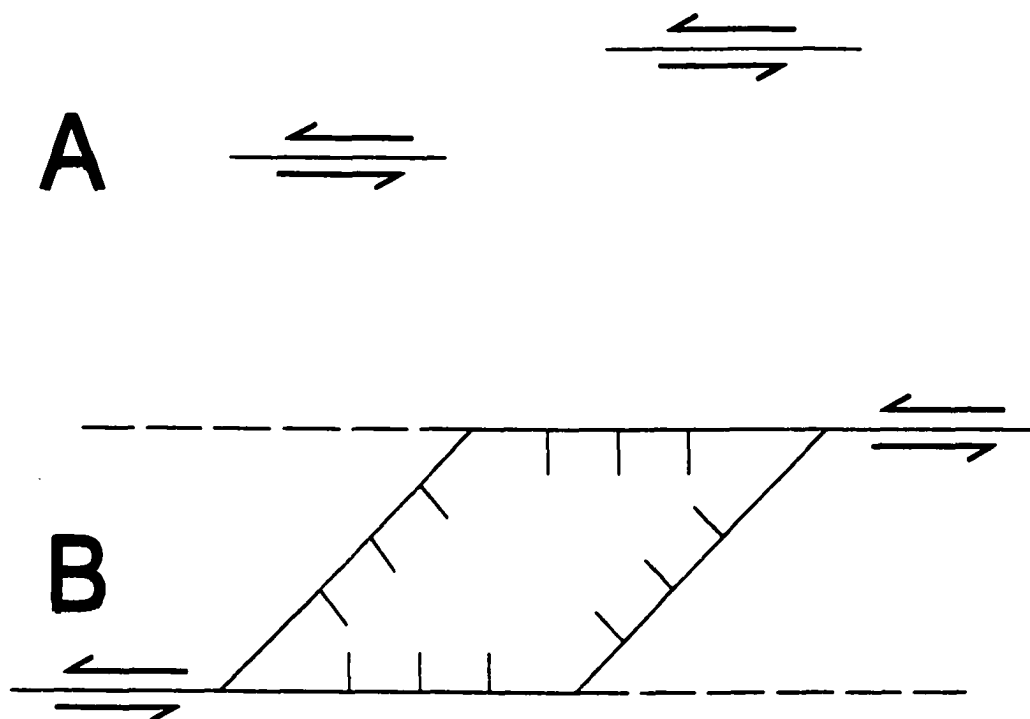


Figure 19. Mechanisms of strike-slip faulting and possible implications for geometry of stepover configurations and the geometry of pull-apart basins. A) Lateral propagation of non-colinear shear faults. B) Formation of stepovers and pull-apart basin. After Aydin and Nur (1985).

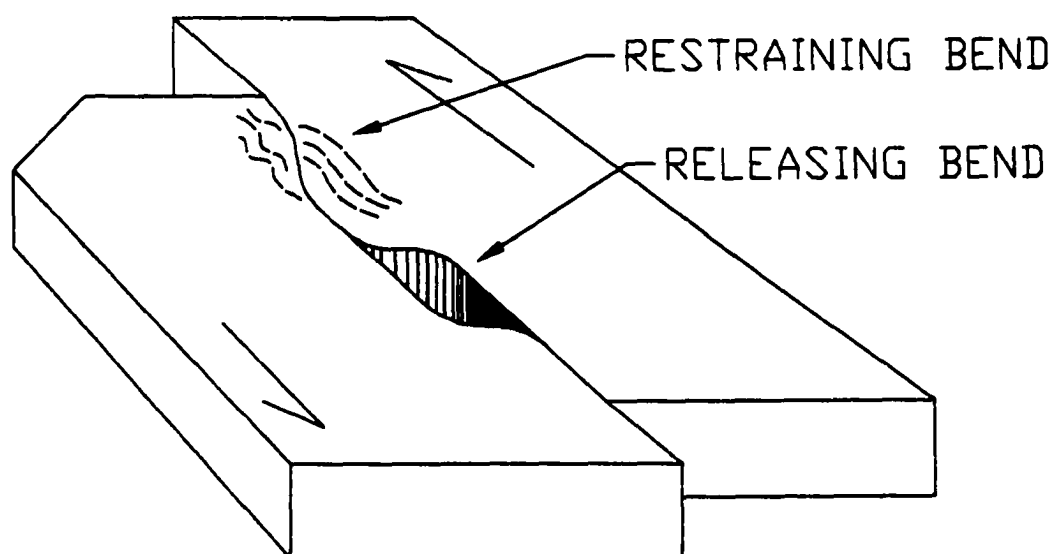


Figure 20. Left slip on a fault with marked double bends resulting in a pull-apart at a releasing bend and deformation and uplift at a restraining bend. After Crowell (1974).

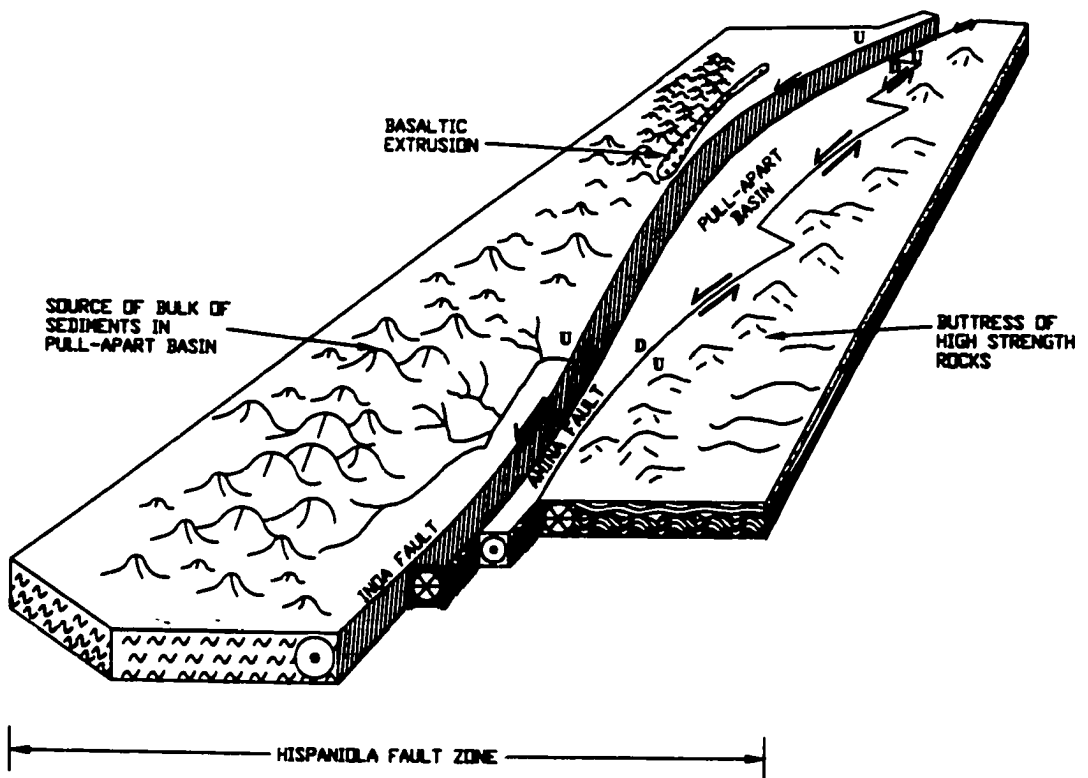


Figure 21. Perspective diagram of the San José de las Matas pull-apart basin. This pull-apart basin has developed along two NW-trending left-lateral strike-slip faults.

**Plate 1. Geologic map of the northwestern piedmont of Cordillera Central, Dominican Republic. Scale is at 1:50,000. Map in back cover pocket.**

**Plate 2. Cross-sections A-A', B-B', V-C', D-D', E-E', F-F', G-G', H-H'. Cross-sections are drawn perpendicular to strike at 1:50,000 scale. No vertical exaggeration. Map in back cover pocket.**

**Plate 3. Lineament map of the northwestern piedmont of the Cordillera Central. Lineaments originally were compiled from approximately 1:40,000 scale aerial photographs. A composite of the lineaments from the aerial photographs were reduced-down to 1:50,000 scale. Map in back cover pocket.**



**Photograph 1.** Duarte Subgreenschist facies rocks are fine-grained and massive. This photograph was shot in a Arroyo Hondo just south of San José de las Matas. Hammer is 30 cm long.



**Photograph 2.** Duarte Greenschist facies rocks are very dark green to greenish-gray greenstones. The greenstones outcrop as massive bodies with little to moderate schistosity. Hammer is 30 cm long.



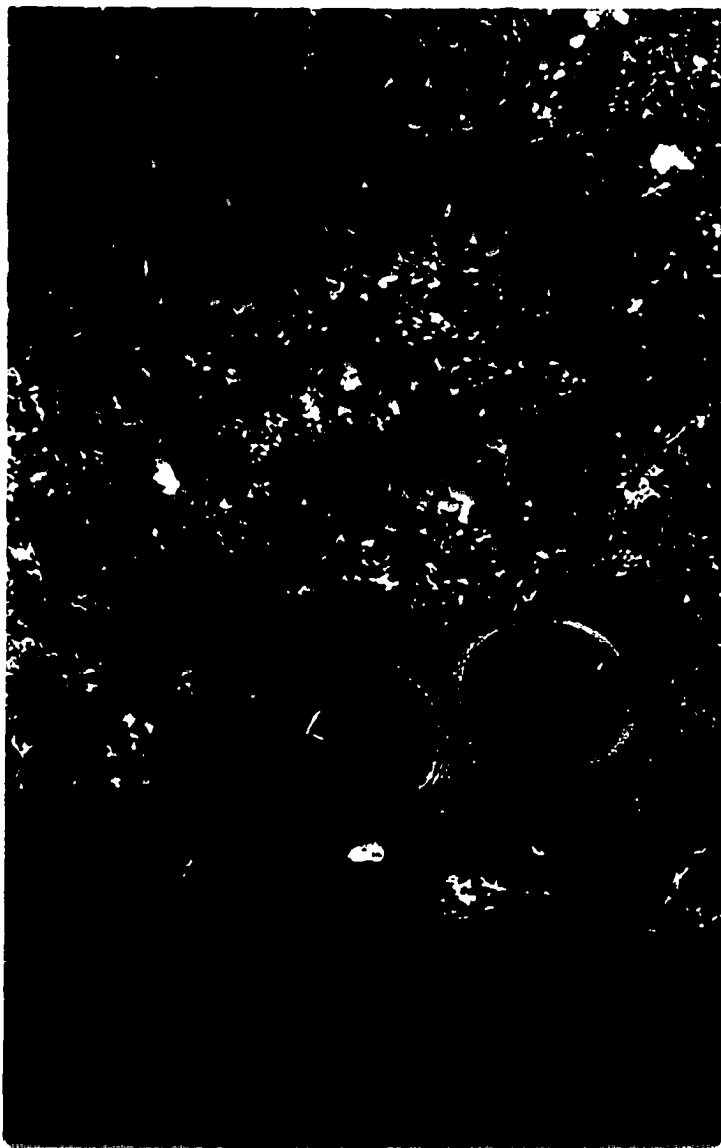
**Photograph 3.** The Amina Schist is a metamorphosed rock which outcrops across the study area. The Amina has a rhythmically bedded multilayer lithology in the eastern part of the study area and becomes more massive towards the west. This photograph taken in the Amina River.



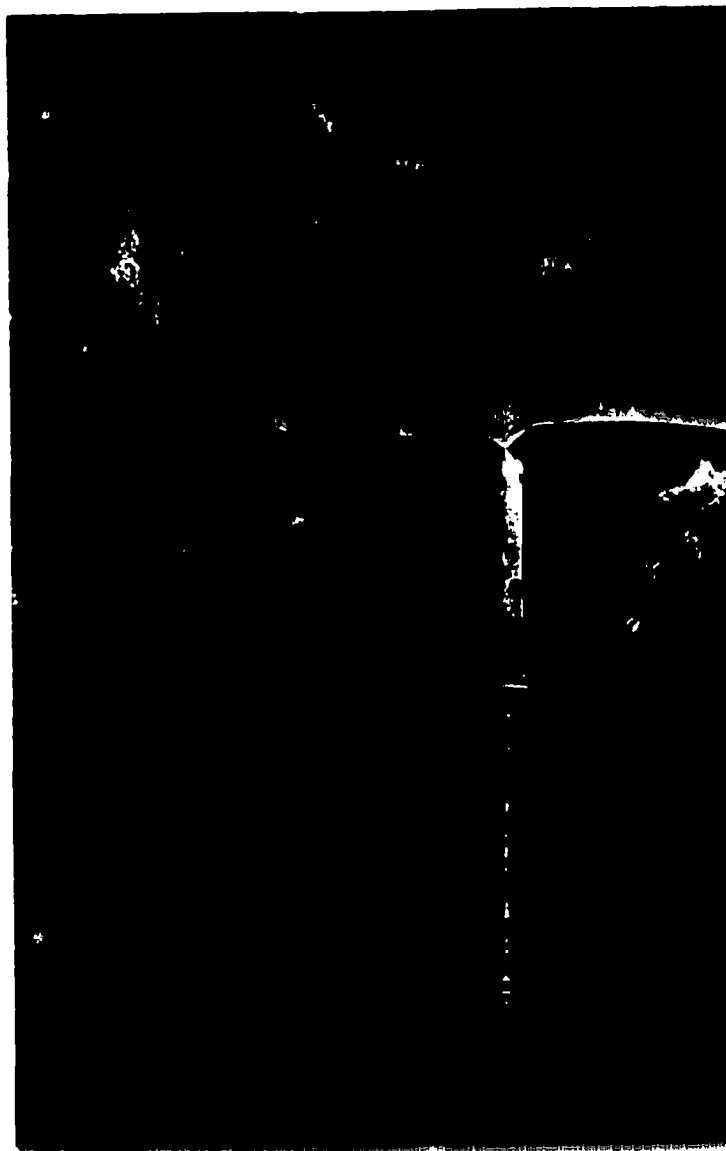
**Photograph 4.** Hornblende Tonalite outcrops south of San José de las Matas and Rio Inoa. The hornblende tonalite intruded into the Duarte Complex south of the Inoa fault. Hammer is 30 cm long.



**Photograph 5.** The Magua Formation contains Eocene volcanic and sedimentary rocks. Shown above is a fault contact where shallow dipping slickenlines are being measured.



**Photograph 6.** Very fine grained amygdaloidal basalt typical of the Rodeo Basalt member of the Magua Formation. Brunton™ compass measures approximately 20 cm.



**Photograph 7.** The Inoa Conglomerate is a red boulder, cobble and pebble conglomerate lithified in a silty matrix. The Inoa Conglomerate contains interbedded siltstone and sandy-siltstone beds. Hammer is 30 cm long.



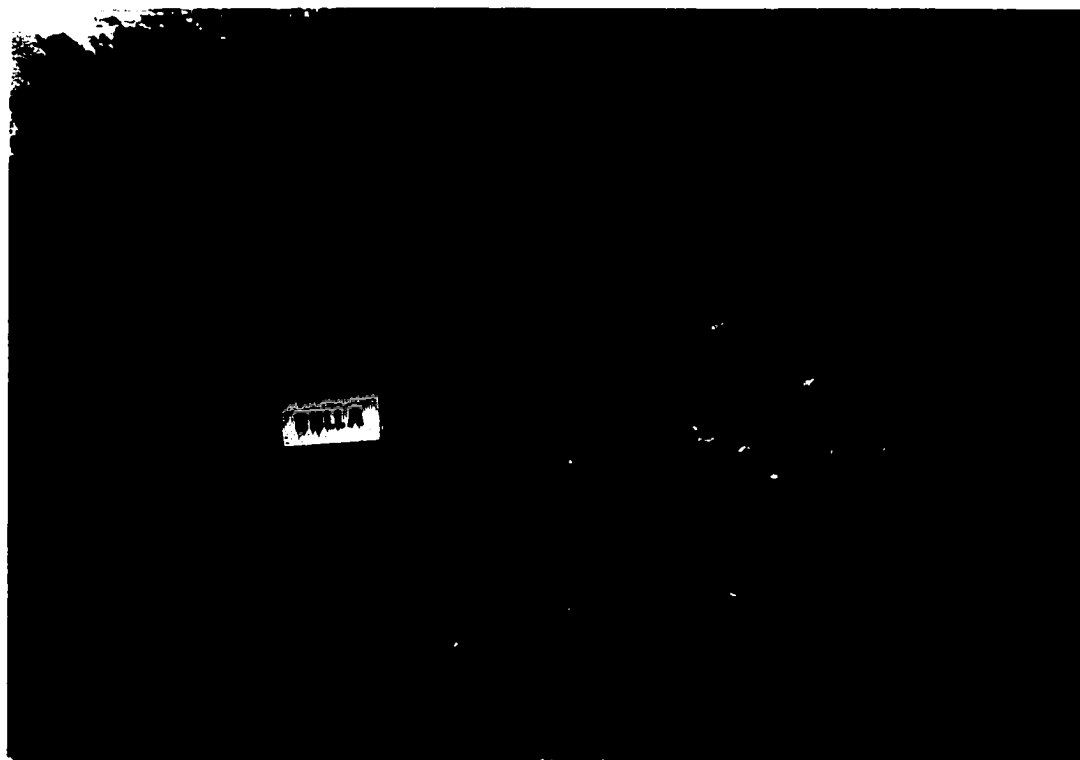
**Photograph 8.** The Pananao Limestone crops out in Rio Pananao. The Pananao Limestone is a buff-white and yellowish-gray, hard, organic, bioclastic limestone. Knapsack in lower left for scale.



**Photograph 9.** The La Bruja Limestone crops out along the Inoa fault in a shear zone between the Duarte Greenschist facies rocks and the Inoa Conglomerate. East of the La Bruja, the limestone is recrystallized as shown here. Hammer is 30 cm long.



**Photograph 10.** The Monción Limestone is a yellowish gray, hard, organic limestone with thick, ill-defined beds. Limestone outcrop in Rio Gurabo.



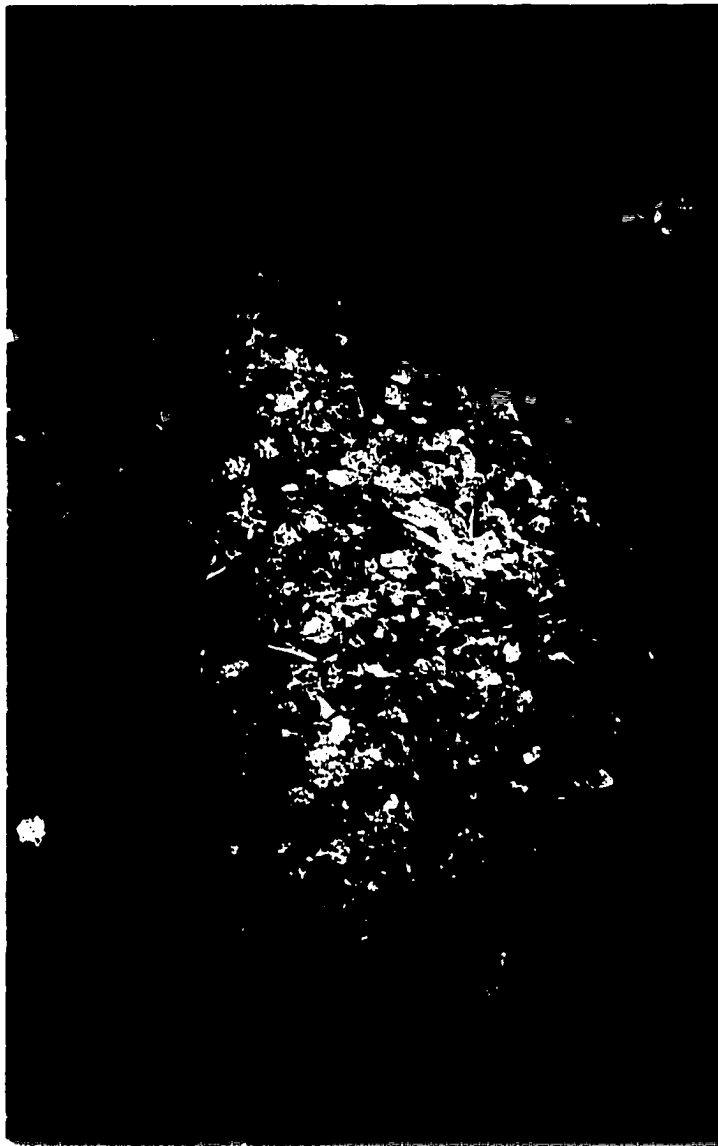
**Photograph 11.** The Bulla Conglomerate is a well-lithified boulder conglomerate composed of well rounded and subrounded boulders in a semi-calcareous, sandy matrix.



**Photograph 12.** The Cercado Sandstone is a poorly lithified fine- to medium-grained, calcareous sandstone. Cross-beds, as shown above are common in the formation and alternate with conglomerate beds. Hammer is 30 cm long.



**Photograph 13.** The Las Matas Breccia contains a fine-grained matrix of Inoa siltstone containing very angular fragments of Amina Schist. The Las Matas Breccia is a tectonic breccia which outcrops along the Amina fault, specifically north, east, and west of the town of El Rubio. Hammer is 30 cm long.



**Photograph 14.** Pananao Breccia showing angular fragments of reefal limestone and Amina Schist porphyroclasts in a limey matrix. Hammer is 30 cm long.



**Photograph 15.** The La Bruja Breccia is made up of finely ground greenschist facies rock material with occasional pieces of Inoa siltstone and angular clasts of La Bruja Limestone. This tectonic breccia is found between the Duarte Complex and the Inoa conglomerate along the Inoa fault. Hammer is 30 cm long.



**Photograph 16.** The Sui Breccia is a tectonic breccia made up of angular clasts of lithified Cercado Sandstone in a finer matrix of sandstone mixed with very angular reefal limestone clasts. The Sui Breccia crops-out along the Sui fault north of San José de las Matas. Hammer is 30 cm long.



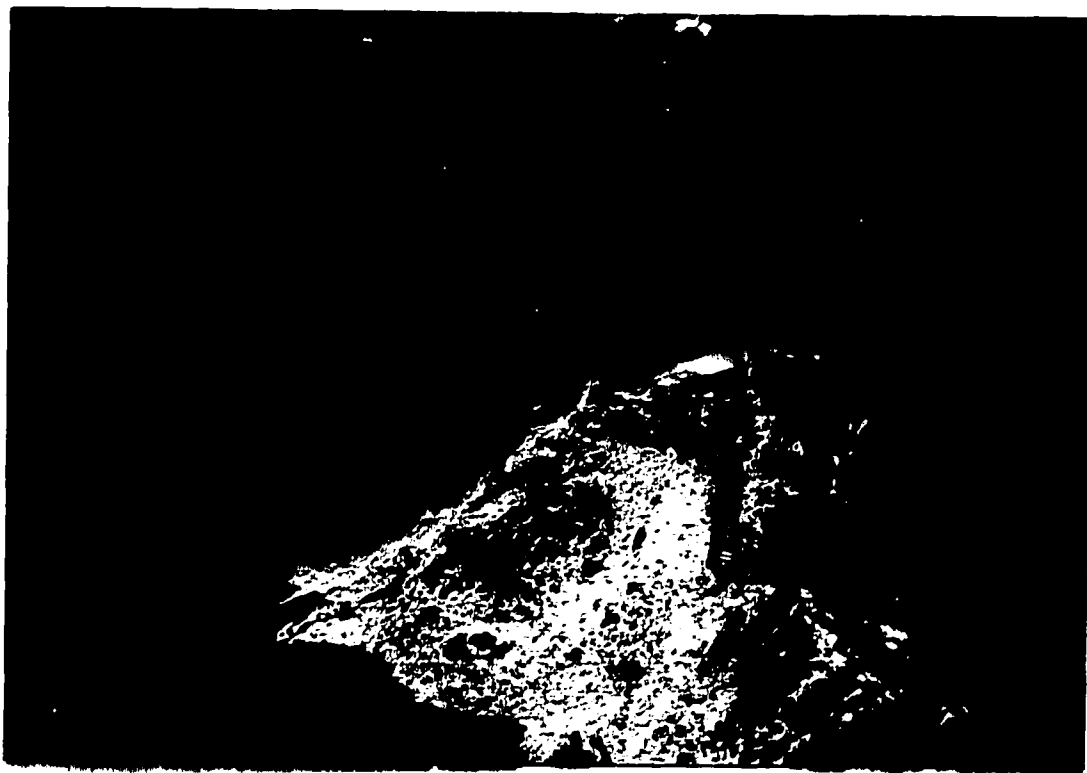
**Photograph 17.** The Higua Breccia is made up of a groundmass of finely ground Inoa siltstone with massive angular boulders of hornblende tonalite. The conglomerates of the Inoa Formation are fractured and sheared. This tectonic breccia outcrops at the confluence of Rio Higua and Rio Inoa along the Inoa fault. Hammer is 30 cm long.



**Photograph 18.** Elongated tonalite and greenstone clasts.  
Elongated clasts trend NE in Rio Amina. Field book is 18 cm long.



**Photograph 19.** Left-lateral strike-slip faults off-set a siltstone bed of the Inoa Formation. Left-lateral offset shown in this photograph is approximately 40 cm. Hammer head is approximately 20 cm long.



**Photograph 20.** Shown here is the Inoa fault contact south of San José de las Matas between the Inoa Conglomerate and the subgreenschist facies rocks of the Duarte Complex. This photograph shows a very thin pseudotachylite between the two formations.



**Photograph 21.** Shown here is the fault contact between the subgreenschist facies rocks of the Duarte Complex and the Inoa Conglomerate. This contact also represents an erosional unconformity because the contact is marked by an undulating subgreenschist facies rock surface with erosional load features and grooves as well as slickensides in some localities. Tape measure in foreground for scale.



**Photograph 22.** Elongated greenstone and tonalite clasts are found in several locations along the Inoa fault in Rio Hondo. Hammer is 30 cm long.



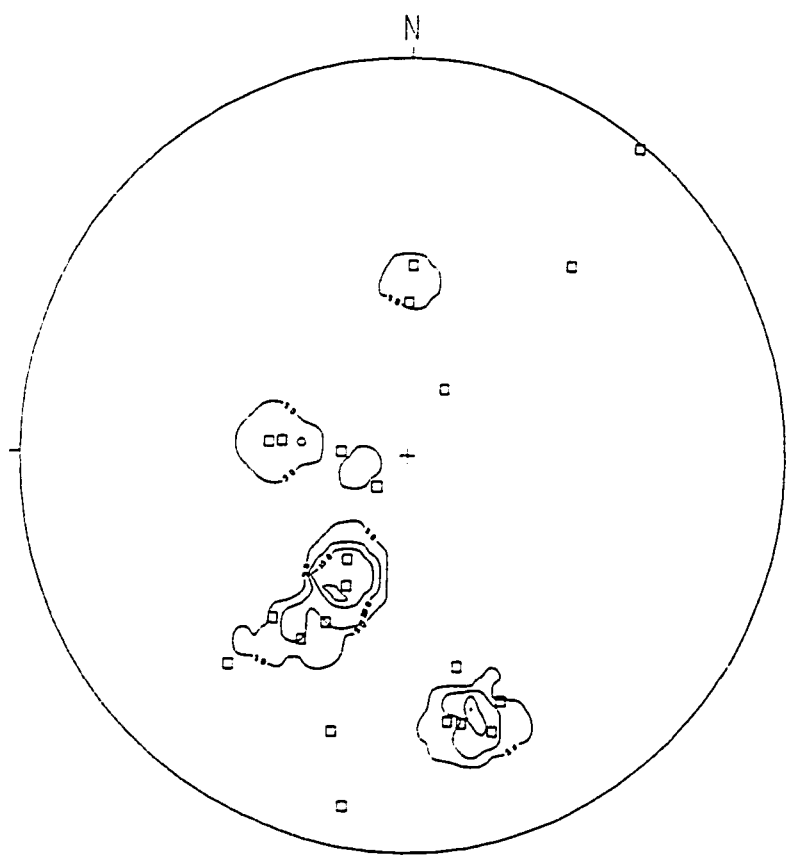
**Photograph 23.** Elongated greenstone and tonalite clasts in Rio Amina near the town of El Corozo occur along the Inoa fault. Deformation of the clasts occur in thin zones of up to two meters. Hammer is 30 cm long.



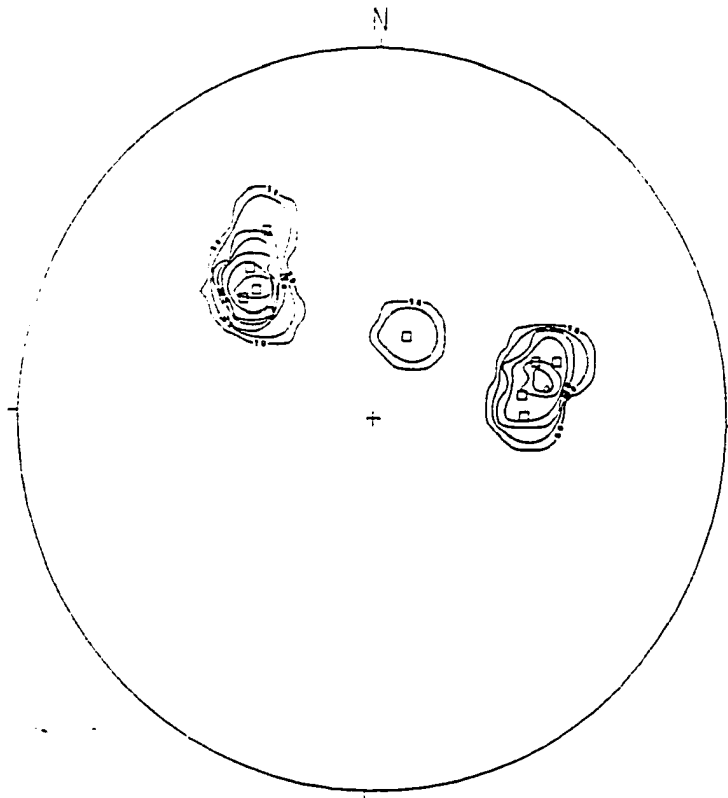
**Photograph 24.** Shown here is evidence of brittle deformation in the siltstone beds of the Inoa Conglomerate. Brittle deformed siltstone in the vicinity of the town of El Corozo shows shear fractures approximately  $45^\circ$  apart from one another. Shaft of rock hammer shown is approximately 20 cm. long.



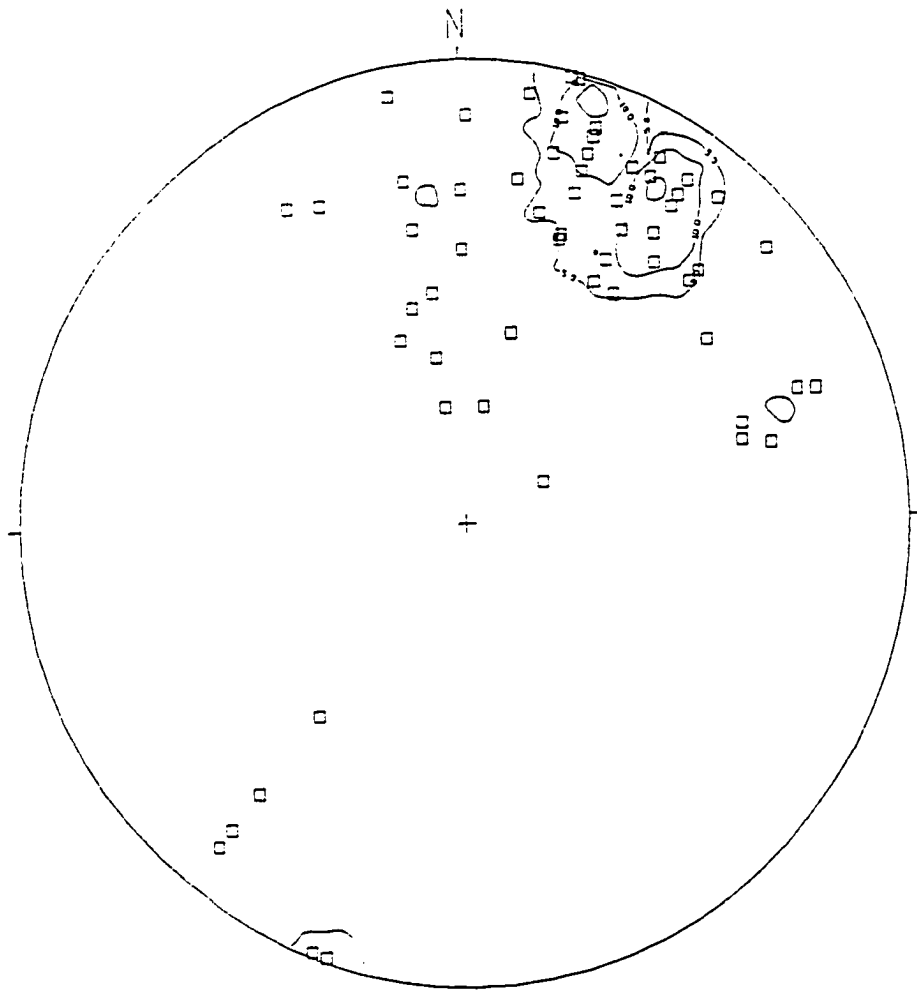
**Photograph 25.** Looking westward along the Inoa fault just west of the town of Inoa are the flatirons of the Cordillera Central. These flatirons clearly mark the location of the Inoa fault trace. The flatiron mountains are part of the Duarte Complex, whereas the rocks to the north (i.e., to the right of the flatirons in this photograph) are part of the Tertiary sedimentary rocks of the San José de las Matas pull-apart basin.



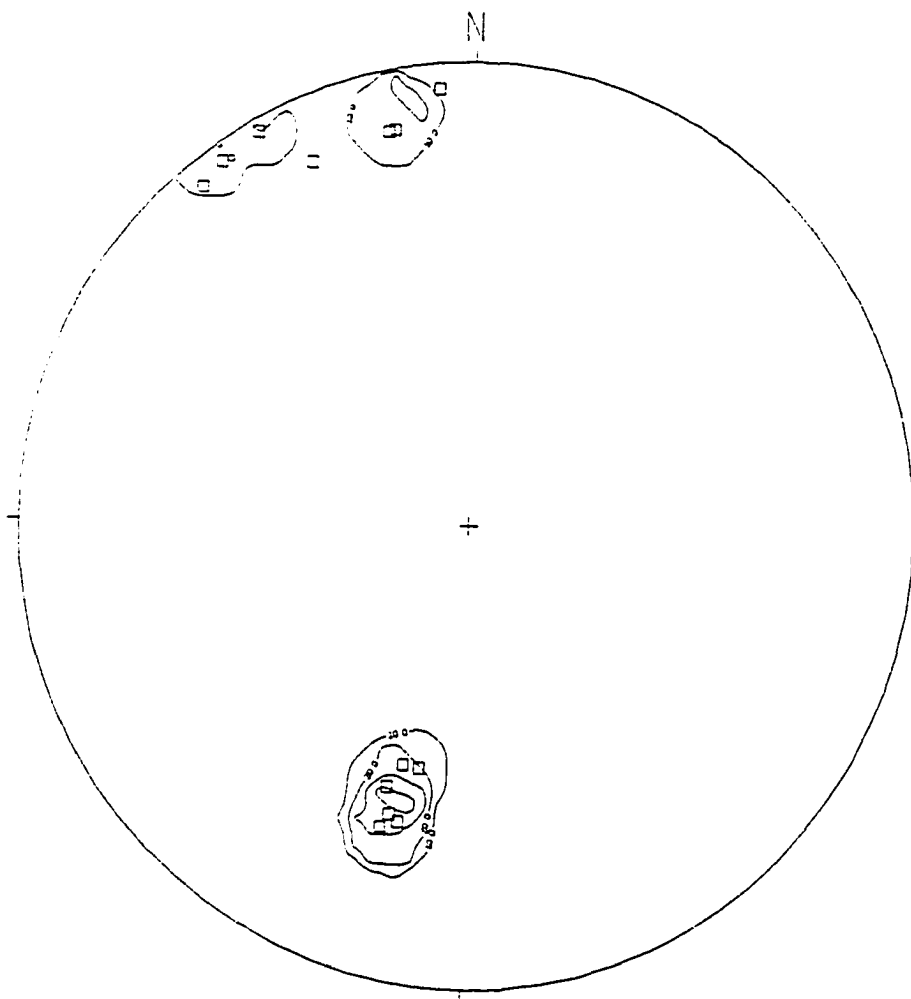
**PLOT 1 - Domain Area 1, Bedding in Monción Limestone.**  
□ Bedding n=24



**PLOT 2 - Domain Area 1, Shear Fractures in Monción Limestone**  
□ Shear Fractures n=10

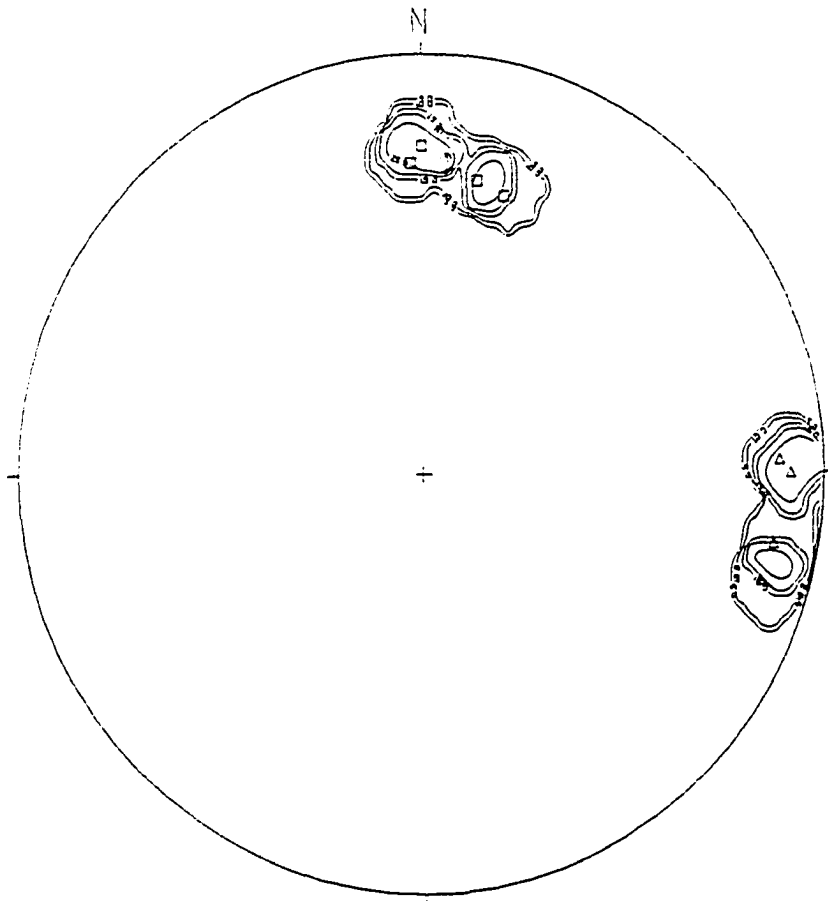


**PLOT 3 - Domain Area 2, Amina Schist**  
□ Schistosity n=110



**PLOT 4 - Domain Area 2, Amina Schist**

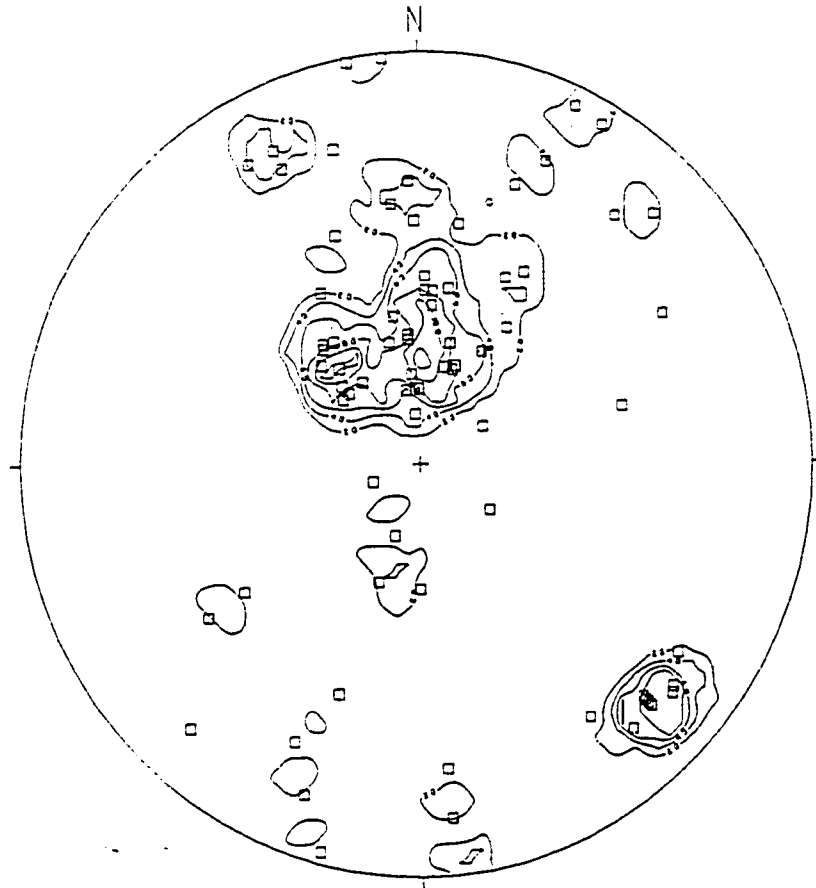
□ Shear Fractures n=1



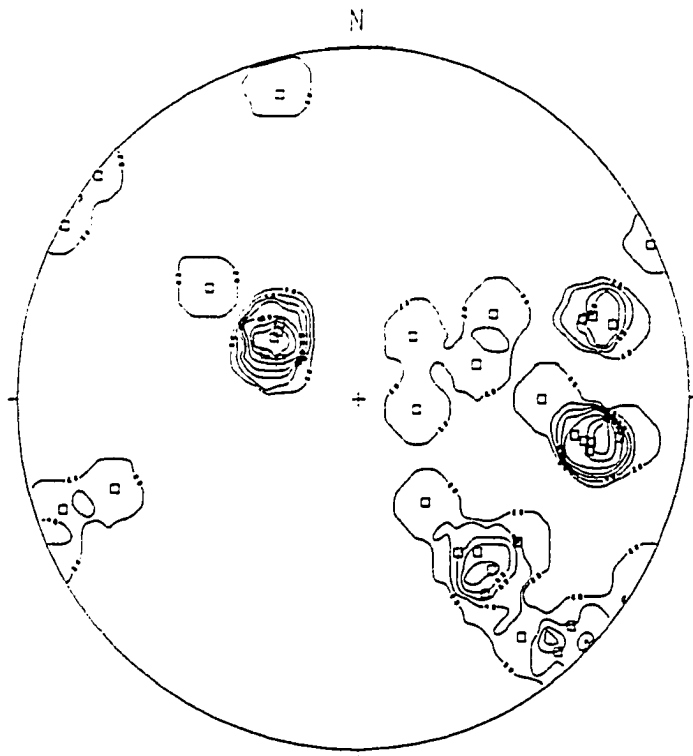
**PLOT 5 - Domain Area 2, West of Monción - Inoa Fault**

□ Fault Planes n=4

▲ Slickenlines n=4

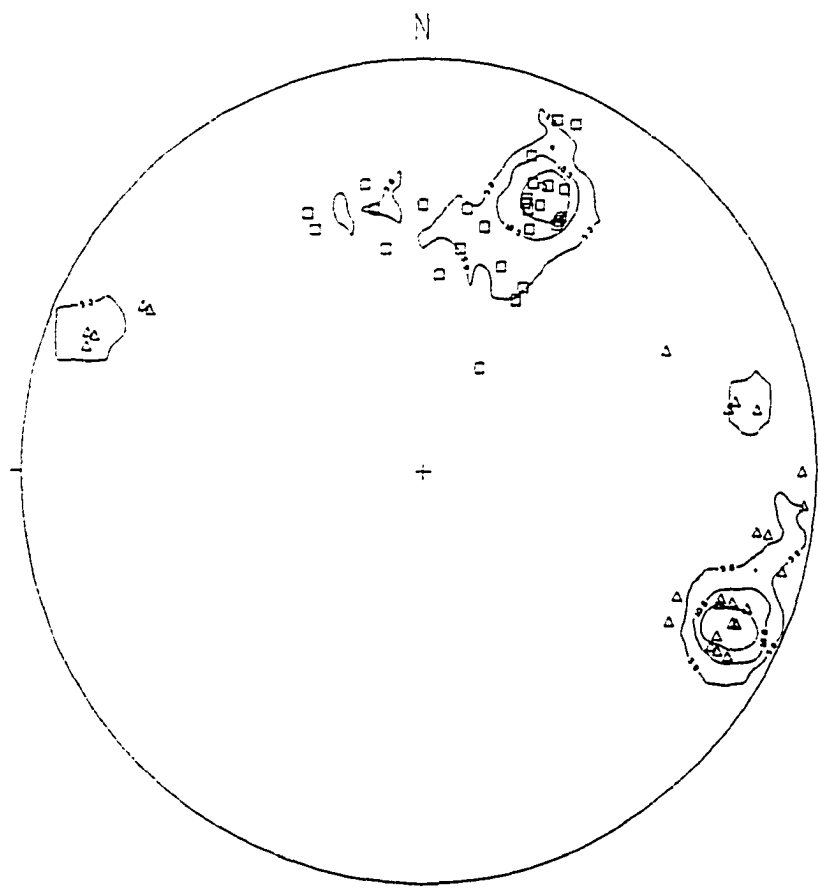


**PLOT 6 - Domain Area 3, Arroyo Pananao, Inoa Conglomerate**  
□ Bedding n=65



**PLOT 7 - Domain Area 3, Arroyo Pananao, Shear Fractures in Inoa Conglomerate**

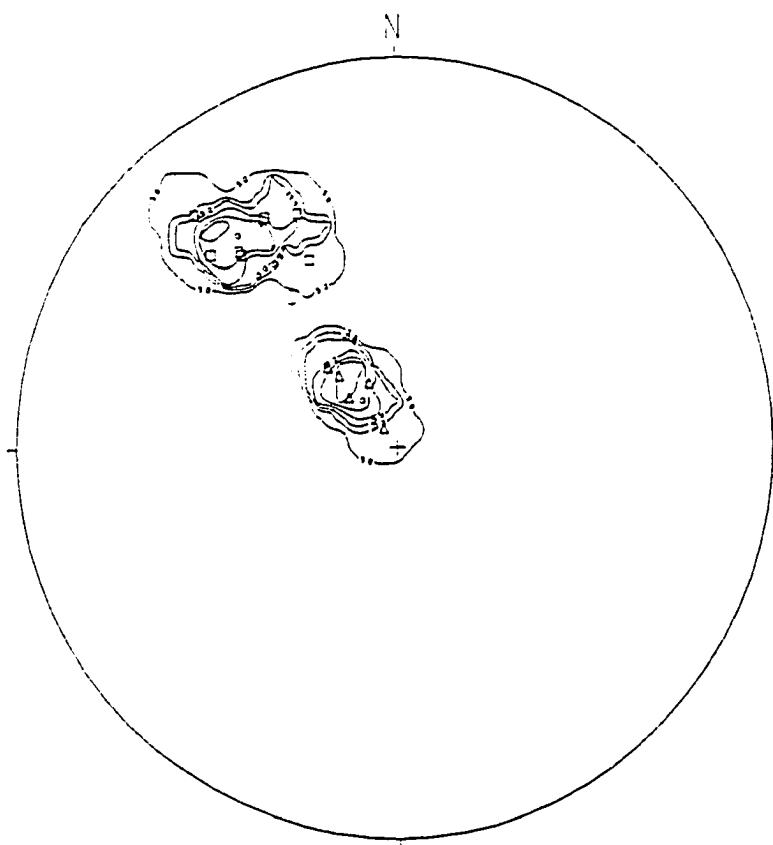
□ Shear Fractures n=34



**PLOT 8 - Domain Area 3, Arroyo Pananao, Inoa Conglomerate**

□ Poles to Fault Planes n=28

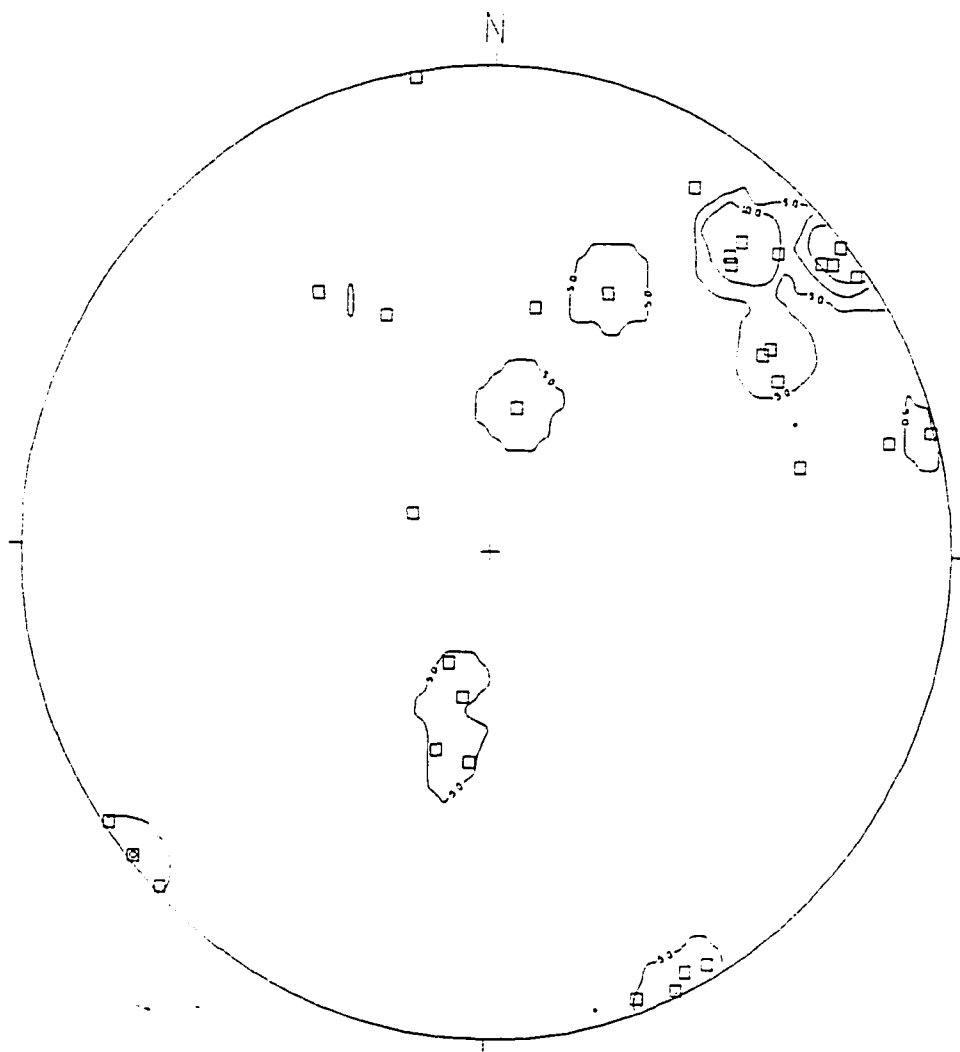
▲ Slickenlines n=28



**PLOT 9 - Domain Area 3, Rio Mao, Inoa Conglomerate, Amina Fault**

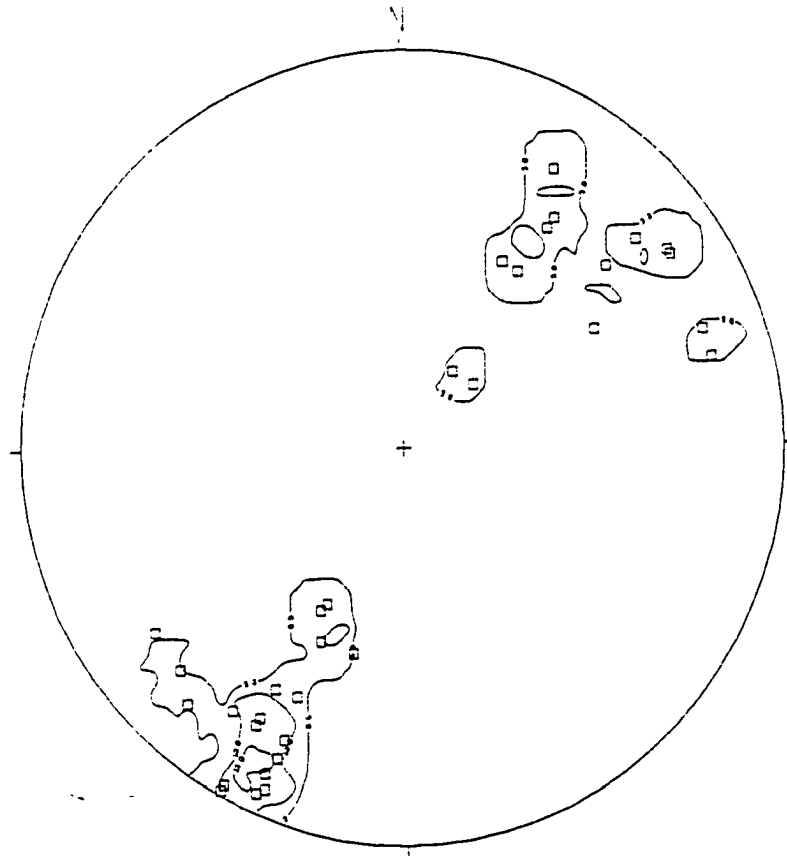
□ Poles to Fault Planes n=7

▲ Slickenlines n=5

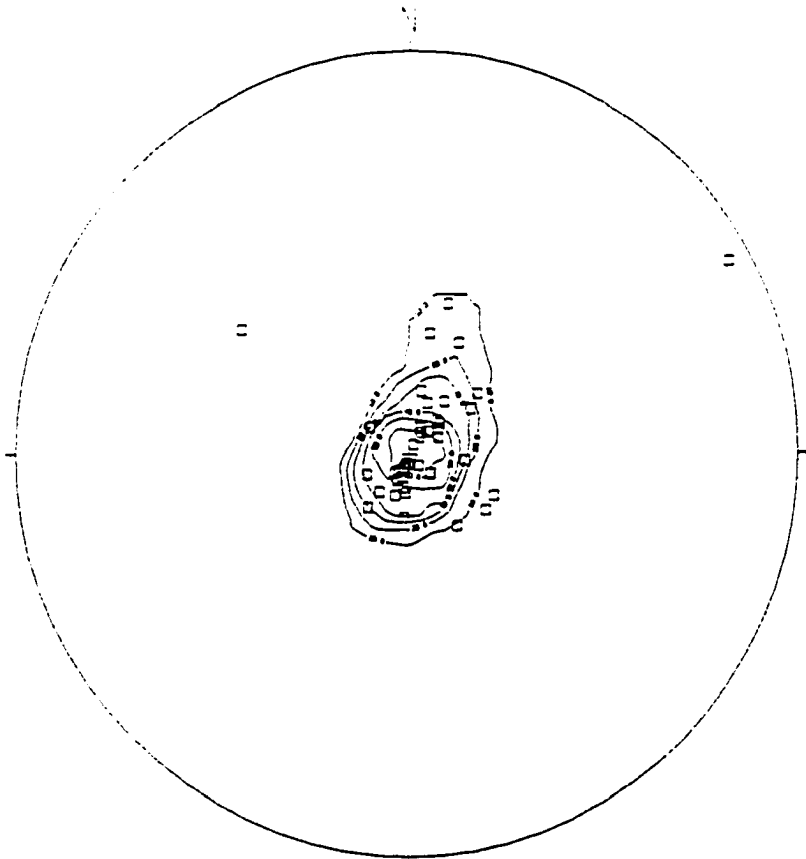


**PLOT 10 - Domain Area 4, South of El Rubio, Shear Fractures in Magua Formation**

□ Shear Fractures n=36

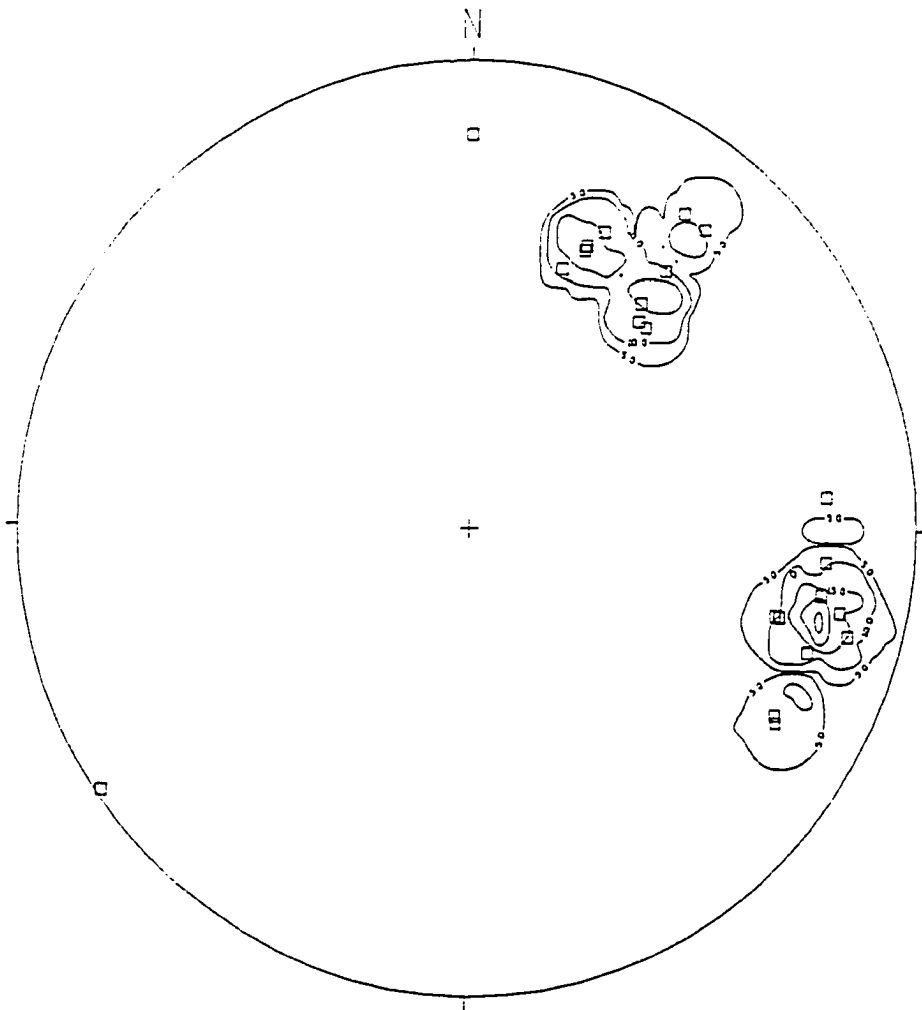


**PLOT 11 - Domain Area 4, South of El Rubio, Magua Formation**  
□ Bedding n=35



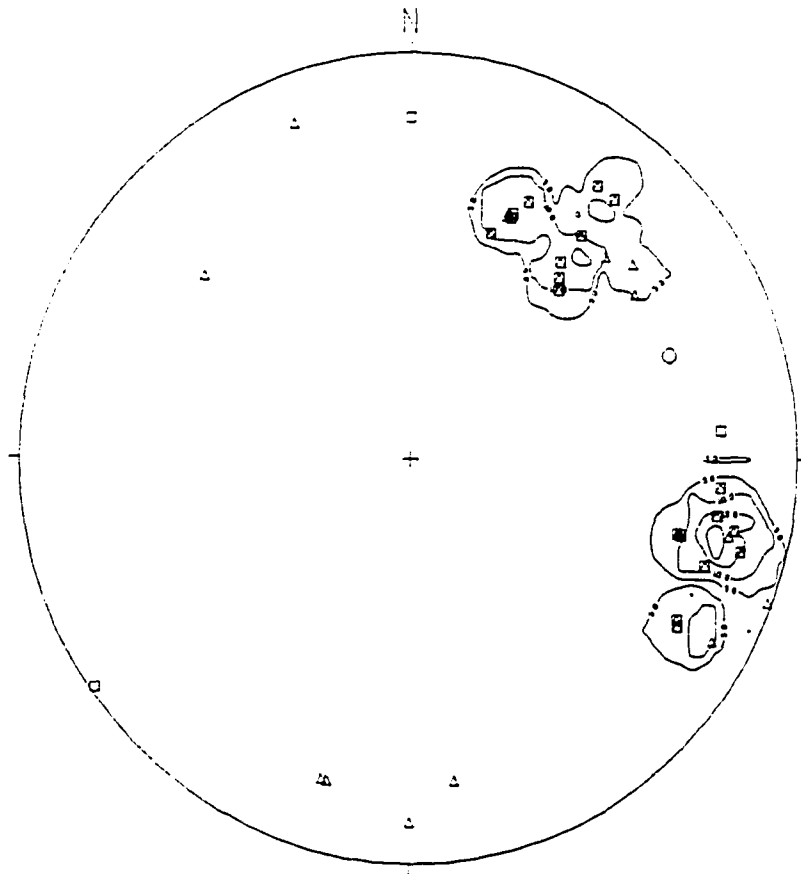
**PLOT 12 - Domain Area 5, Cercado Sandstone**

□ Bedding n=49



**PLOT 13 - Domain Area 5, Cercado Sandstone**

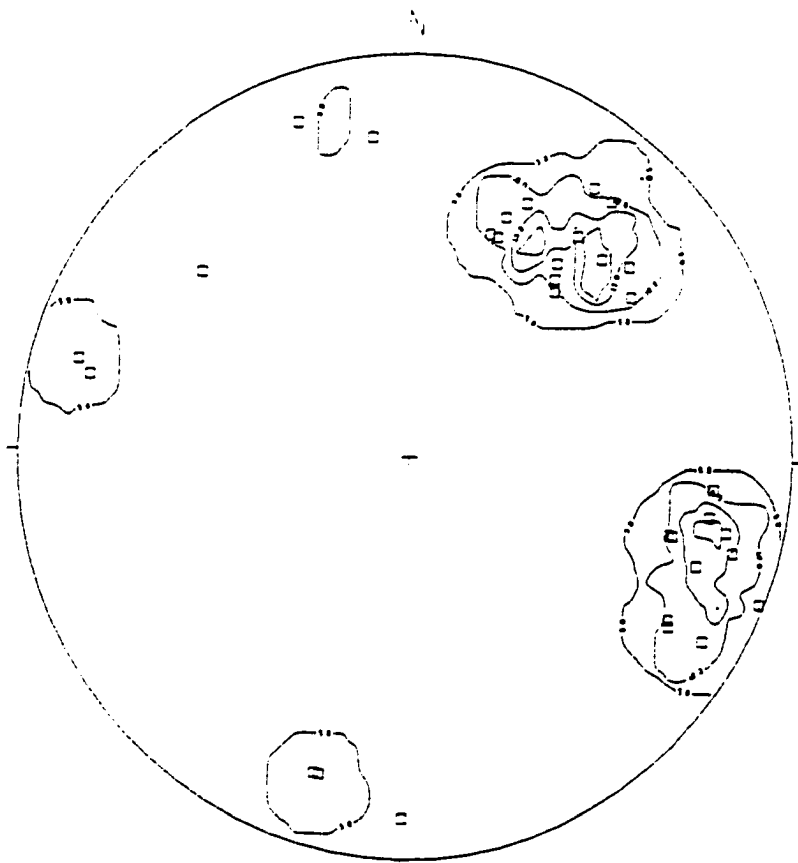
□ Shear Fractures n=22



**PLOT 14 - Domain Areas 5 & 6, Cercado Sandstone**

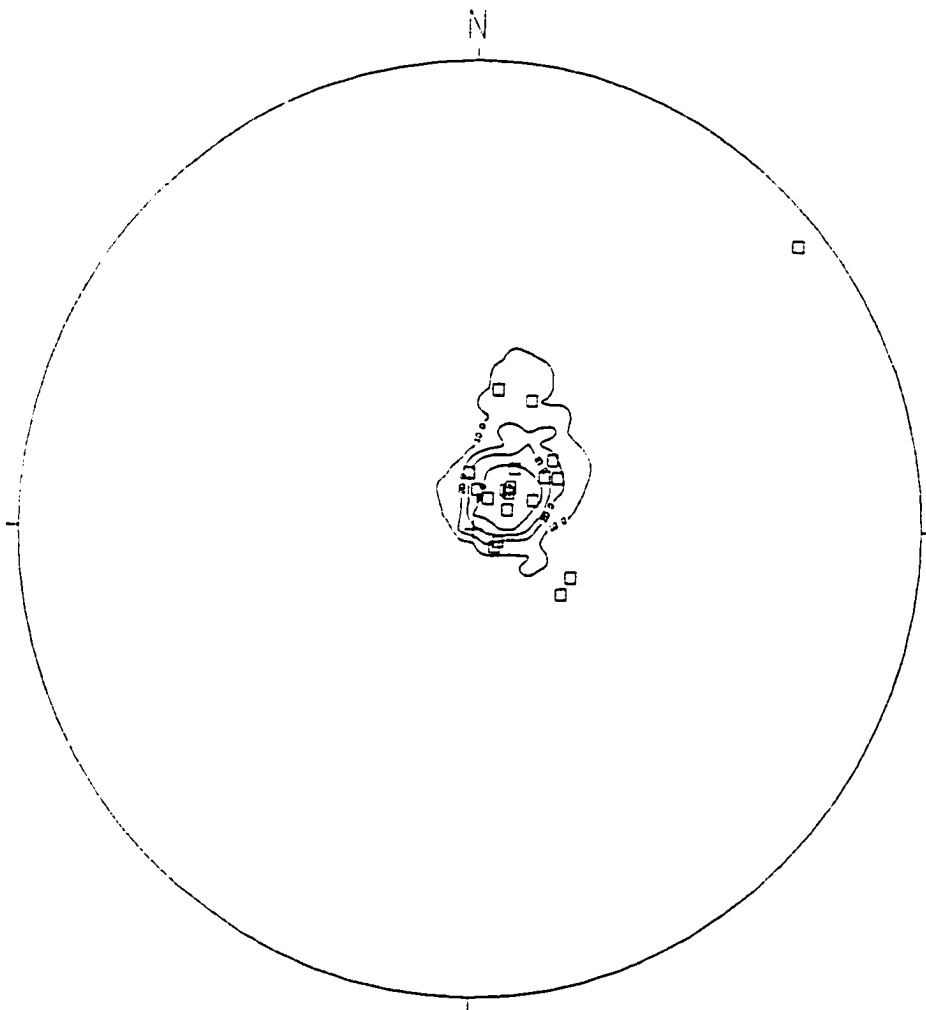
□ Poles to Shear Fractures n= 22, Area 5

▲ Poles to Shear Fractures n=34, Area 6

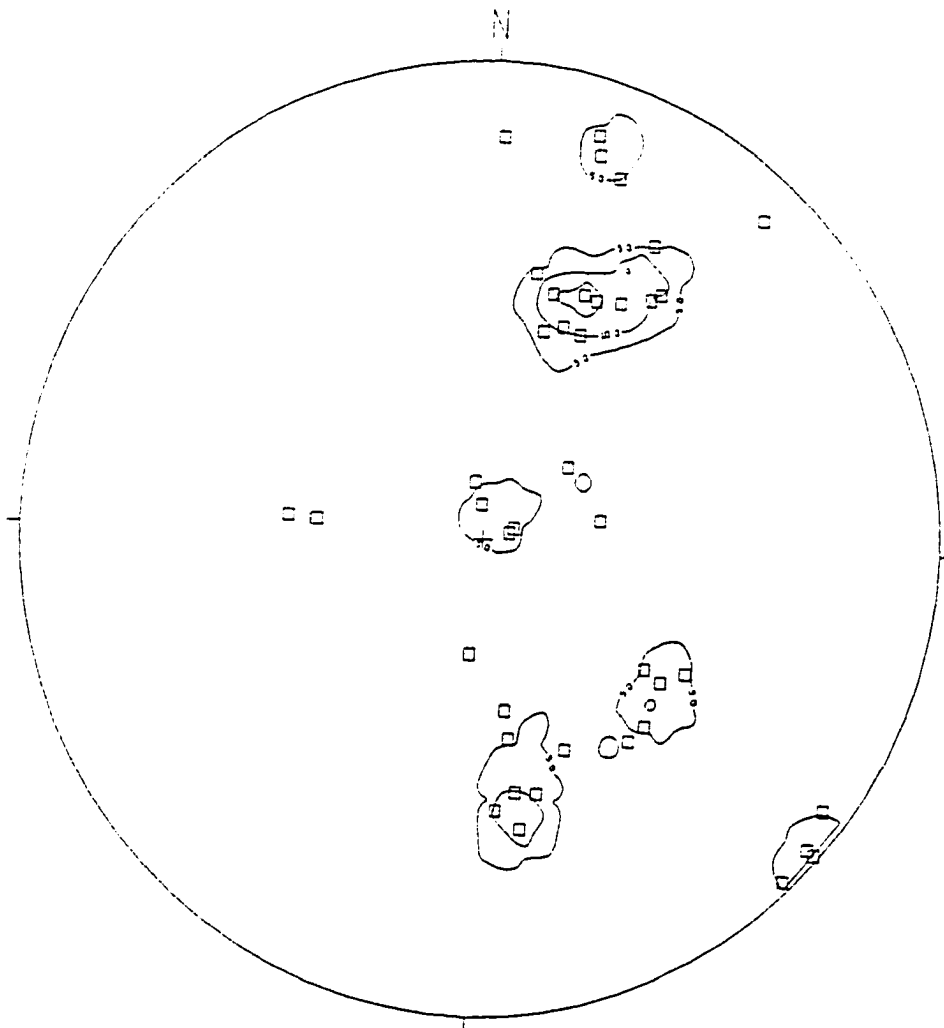


**PLOT 15 - Domain Area 6, Cercado Sandstone**

□ Shear Fractures n=34

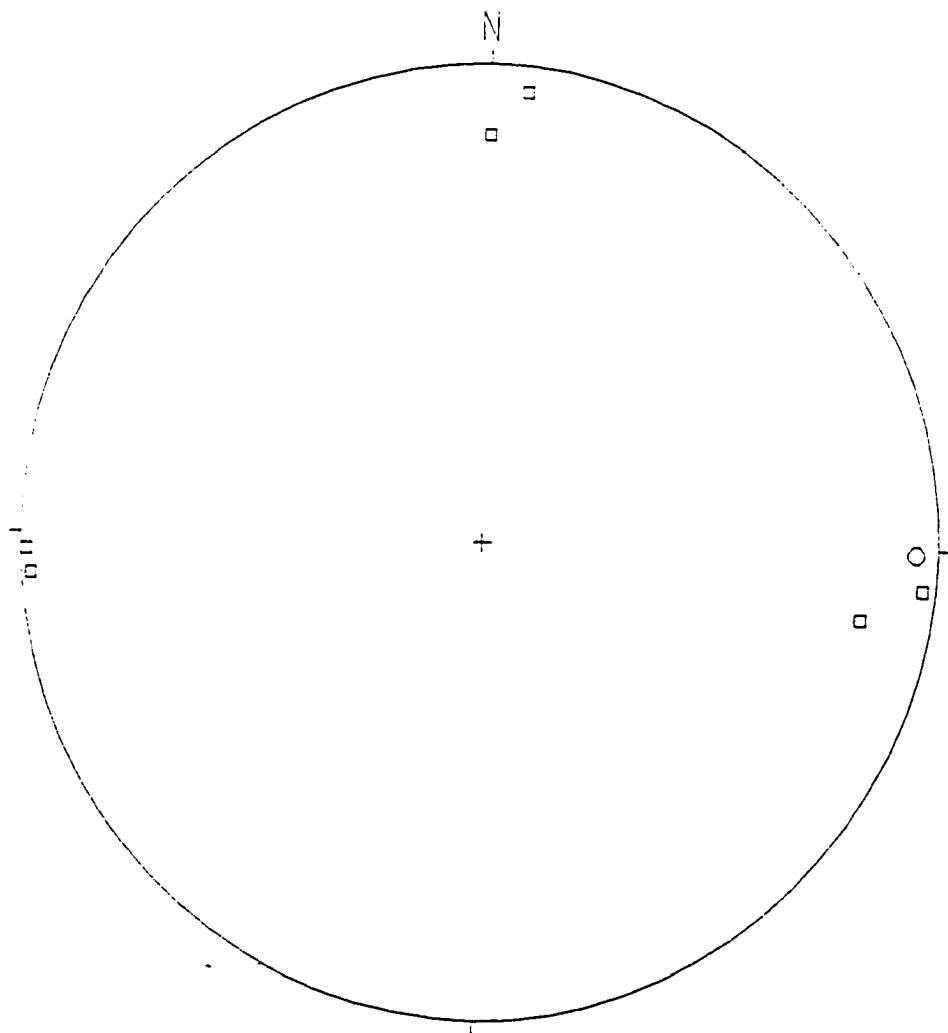


**PLOT 16 - Domain Area 6, Cercado Sandstone**  
□ Bedding n=22



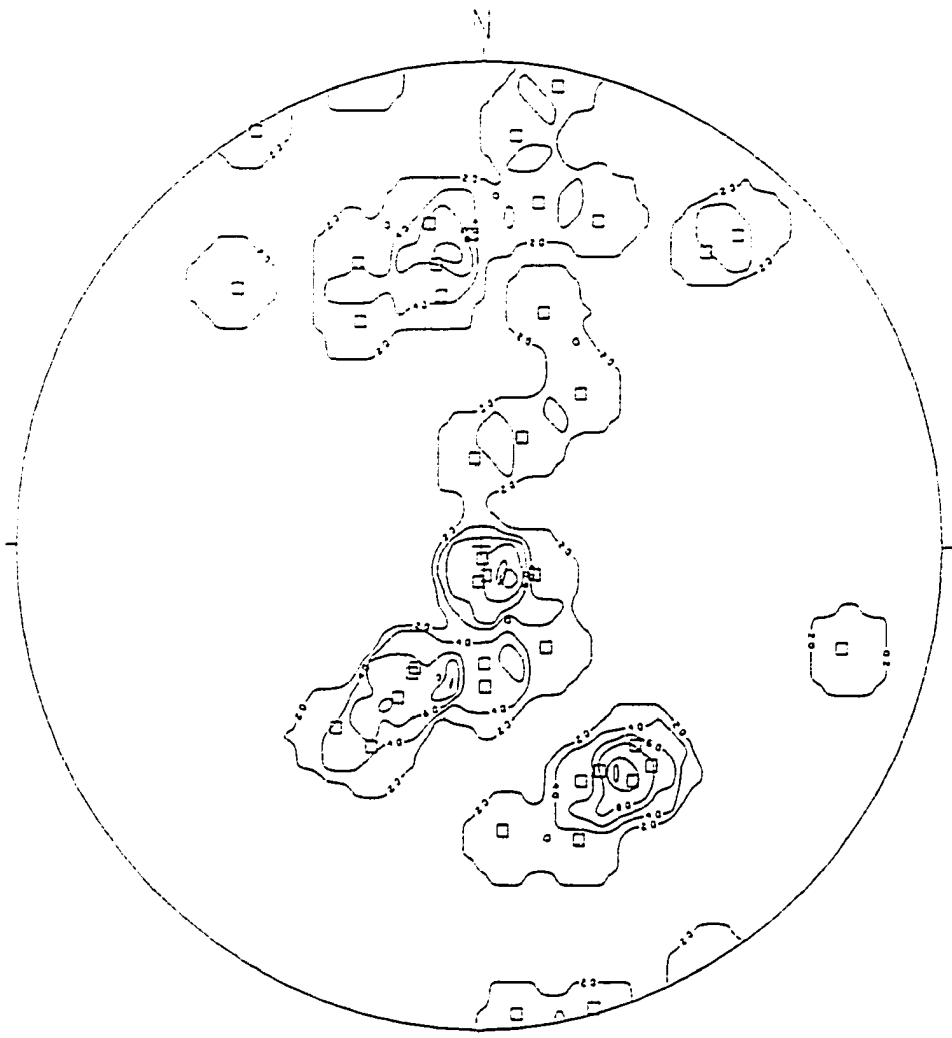
**PLOT 17 - Domain Area 7, Amina Schist**

□ Schistosity n=43



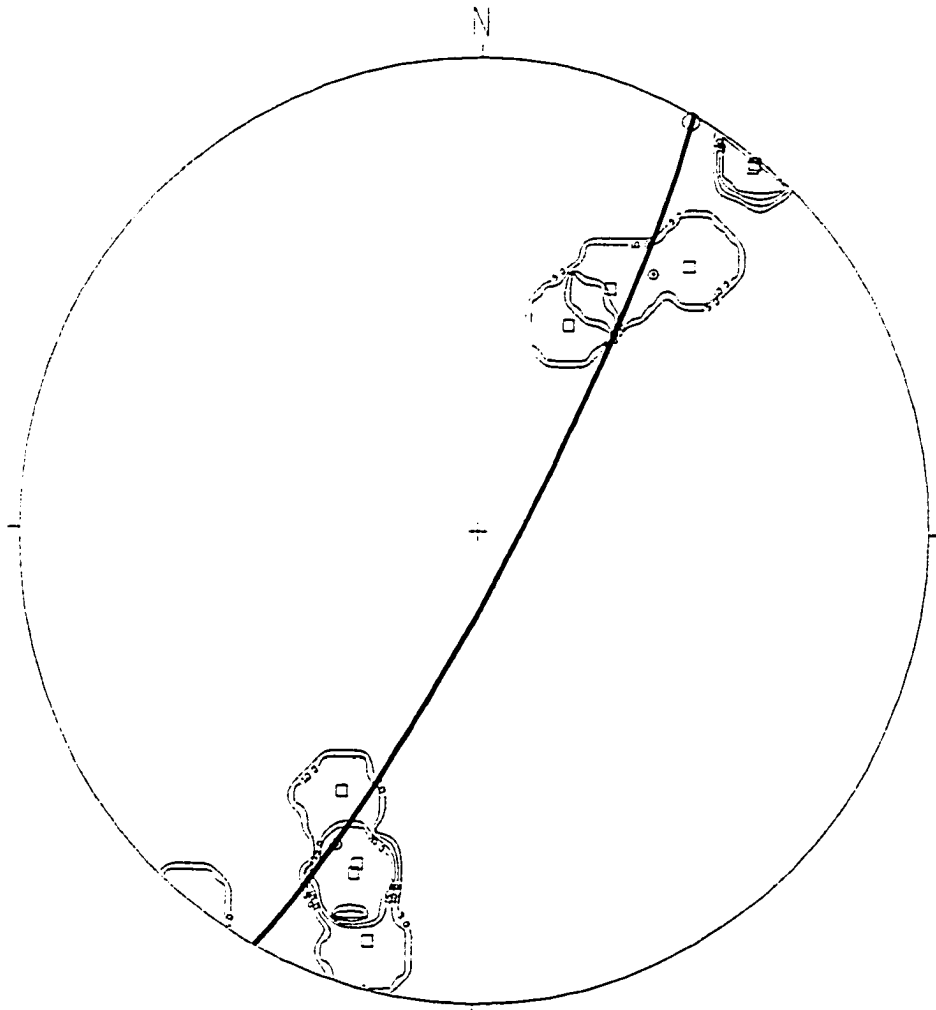
**PLOT 18 - Domain Area 7, Amina Schist**

□ Shear Fractures n=6



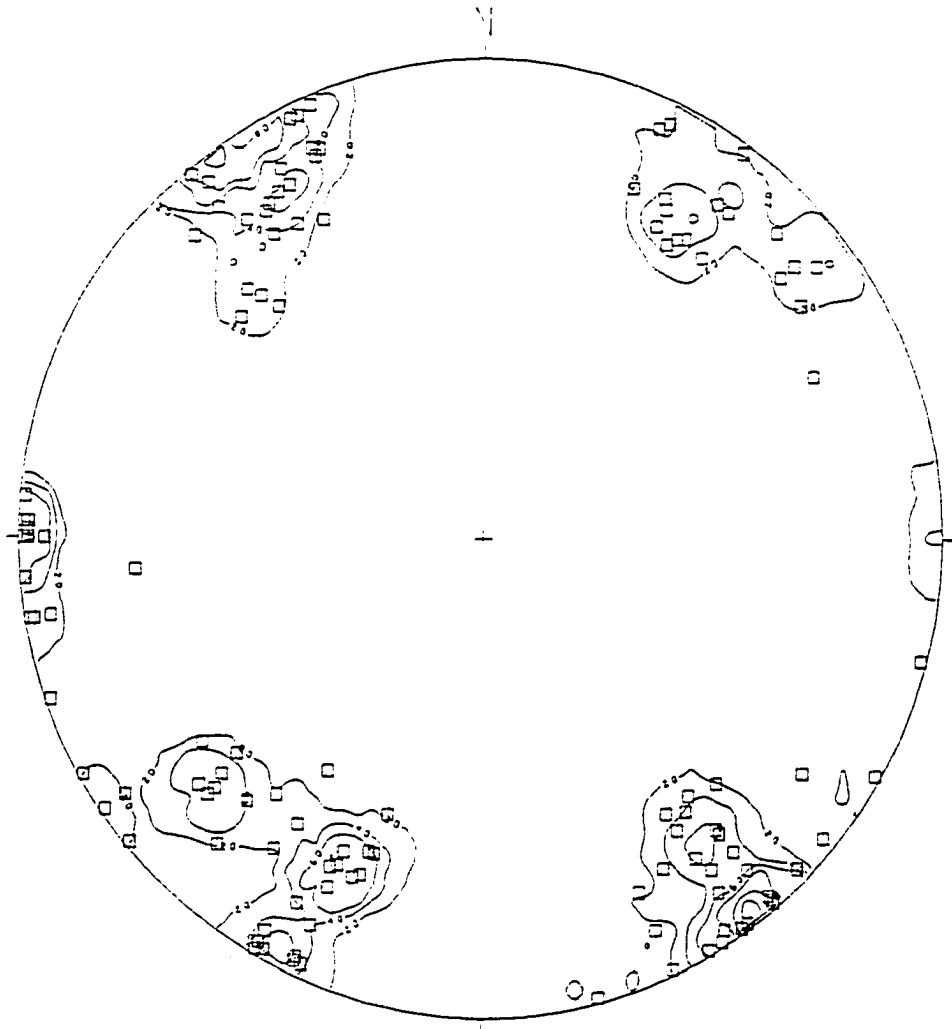
**PLOT 19 - Domain Area 8, Inoa Conglomerate**

□ Bedding n=40



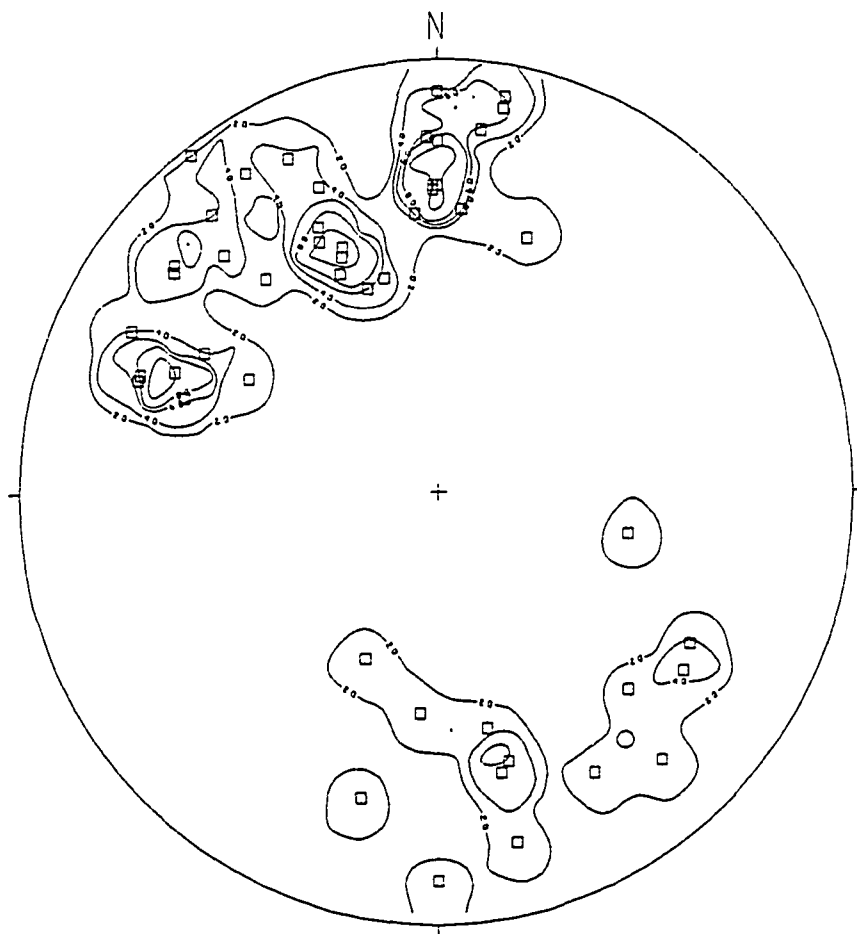
**PLOT 20 - Domain Area 8, Limestones**

□ Bedding n=9

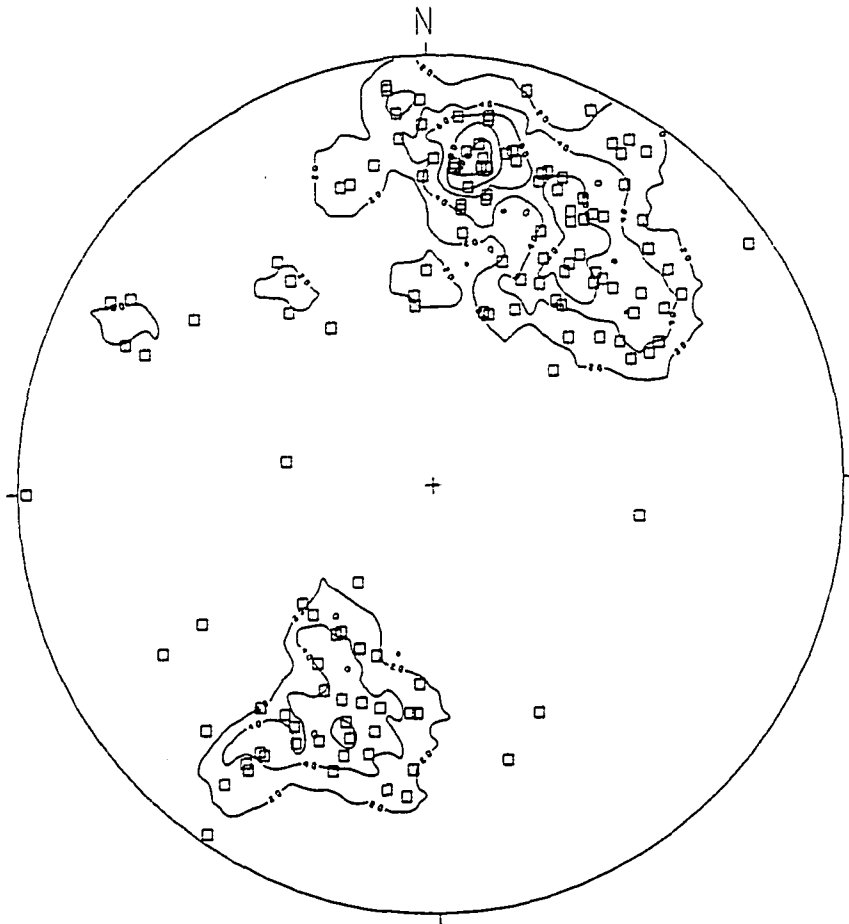


**PLOT 21 - Domain Area 8, Inoa Conglomerate**

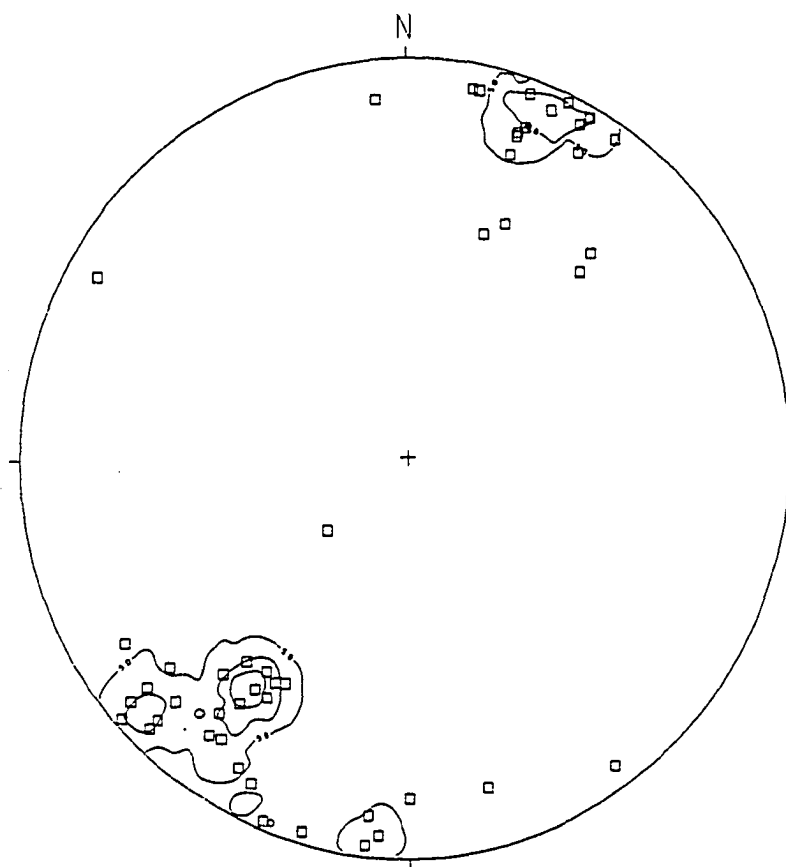
□ Shear Fractures n=134



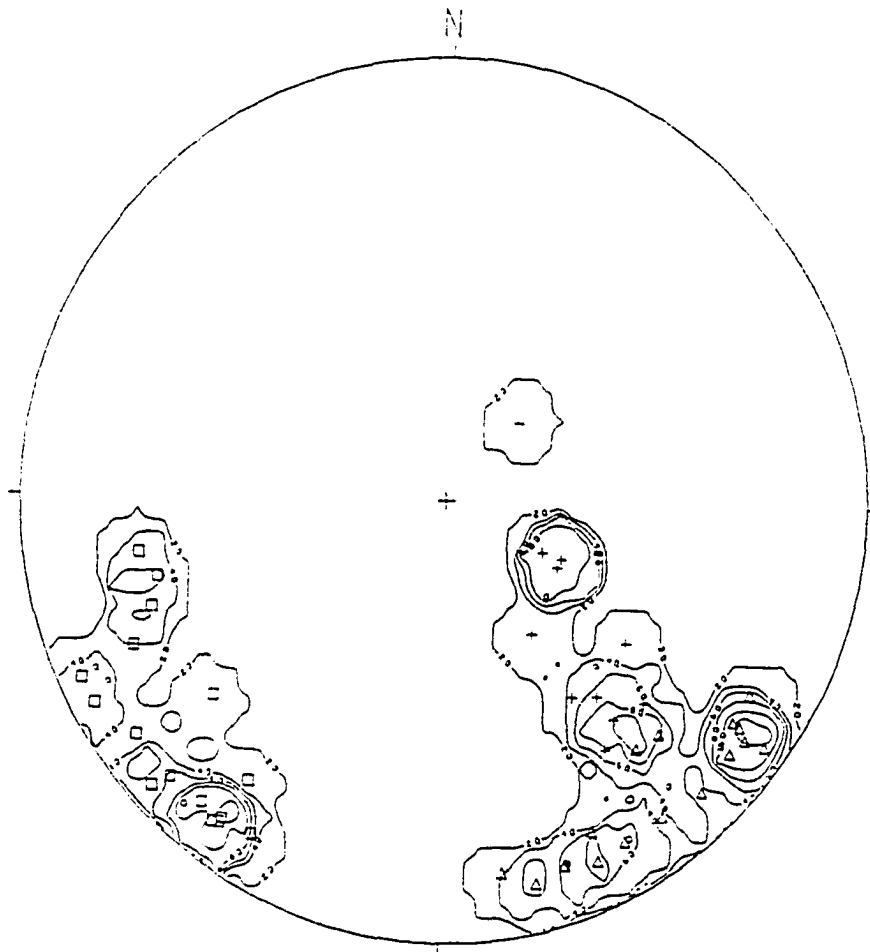
**PLOT 22 - Domain Area 8, Inoa Conglomerate**  
□ Rakes of the long axes of the elongated clasts  
measured in the bedding planes n=50



**PLOT 23 - Domain Area 8, Inoa Conglomerate, Rio Amina**  
□ Rakes of the long axes of the elongated clasts  
measured in the bedding planes n =139



**PLOT 24 - Domain Area 8, Inoa Conglomerate, Rio Amina (El Corozo)**  
□ Rakes of the long axes of the elongated clasts measured in the bedding planes n=50

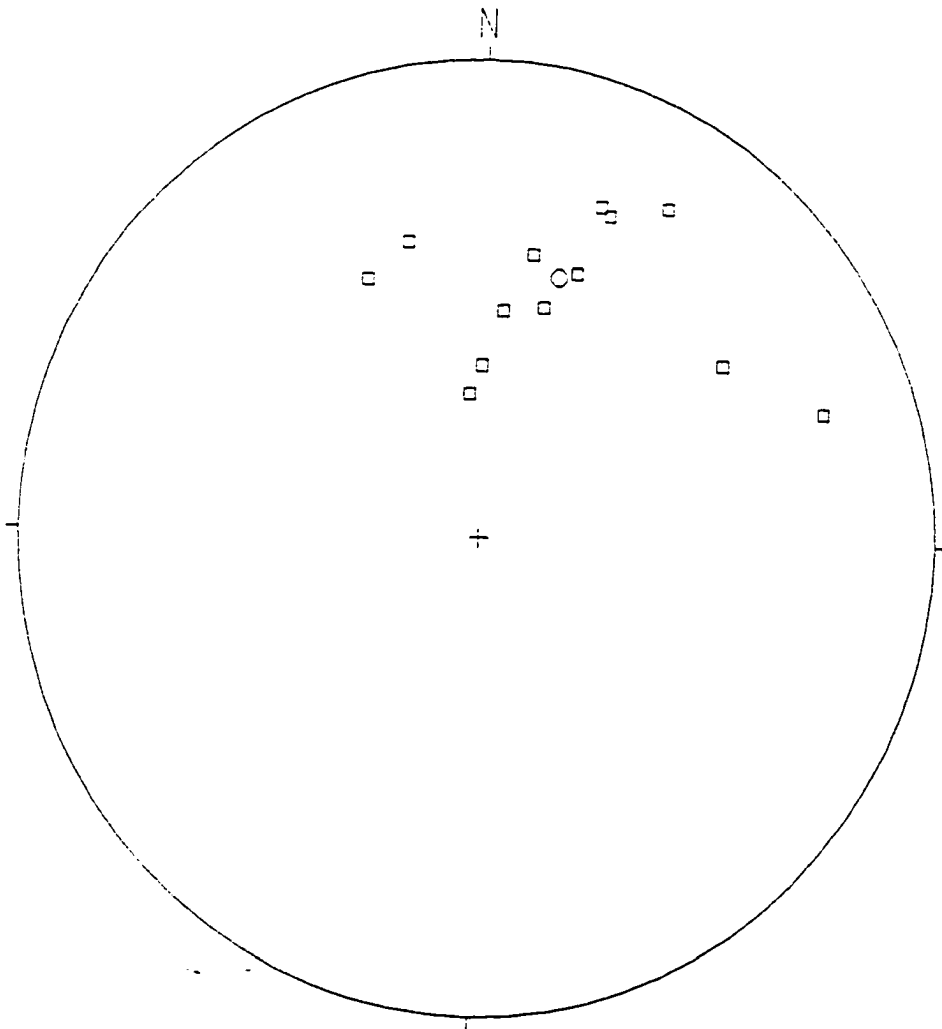


**PLOT 25 - Domain Area 8, Inoa Conglomerate**

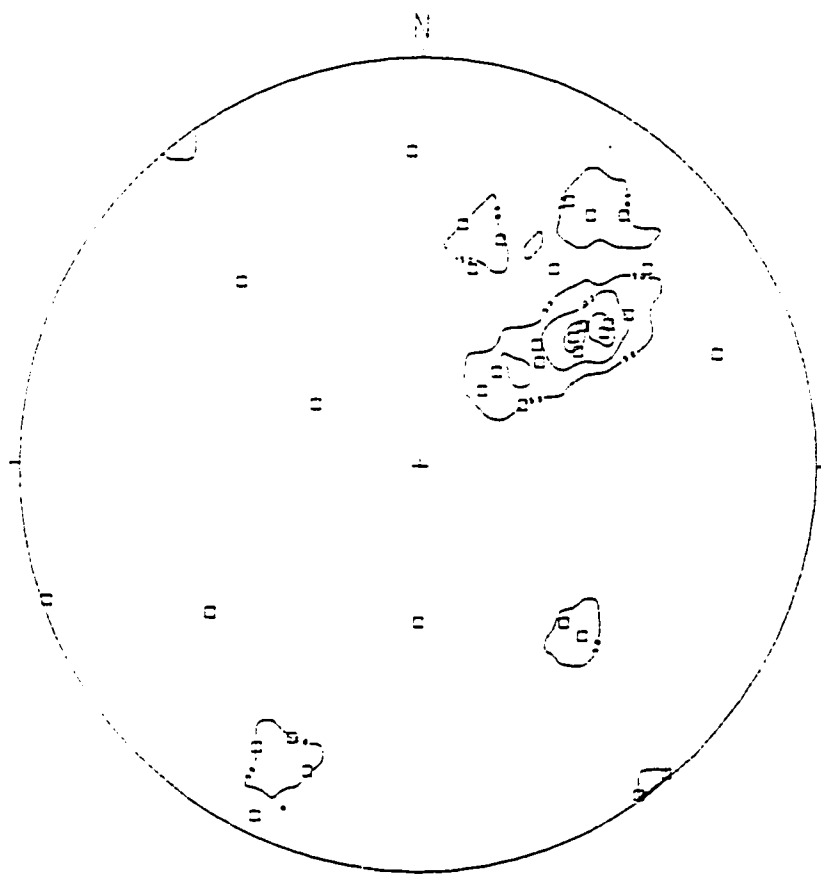
□ Poles to Fault Planes n=16

▲ Slickenlines (Strike-slip) n=16

+ Slickenlines (Dip Slip) n=12

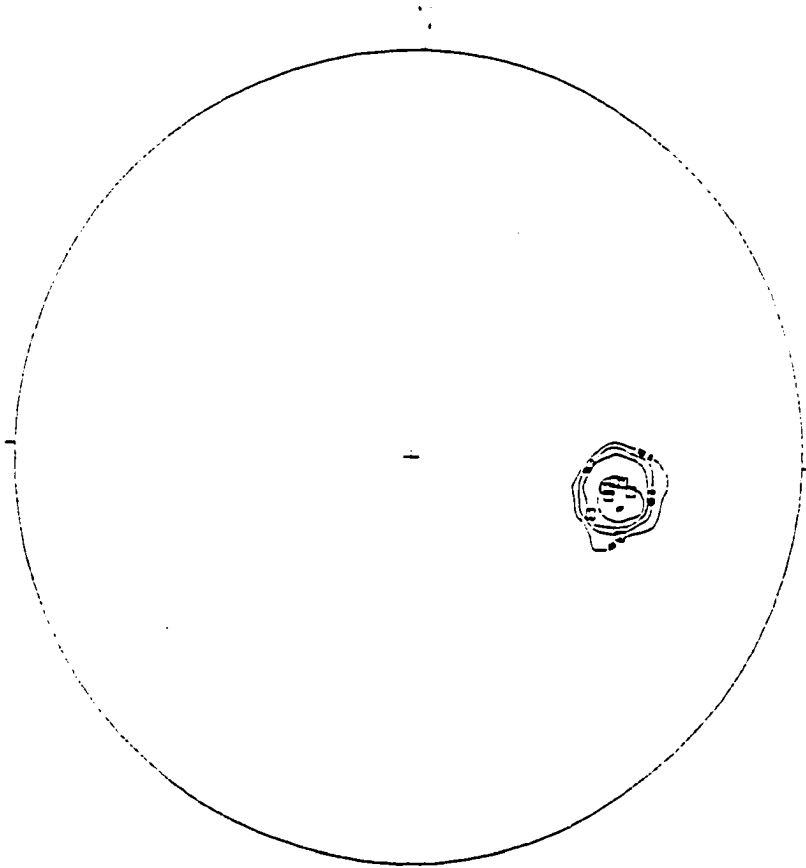


**PLOT 26 - Domain Area 9, Amina Schist**  
□ Schistosity n=13



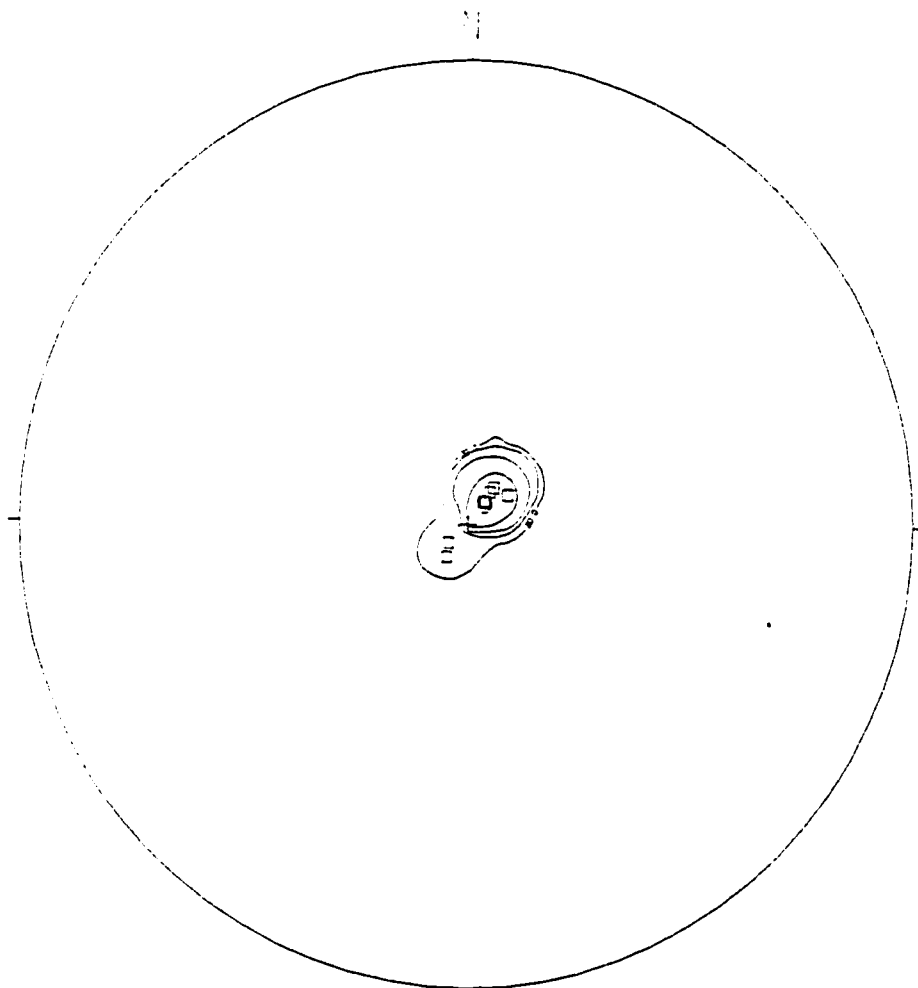
**PLOT 27 - Domain Area 10, Amina Schist**

□ Schistosity n=34

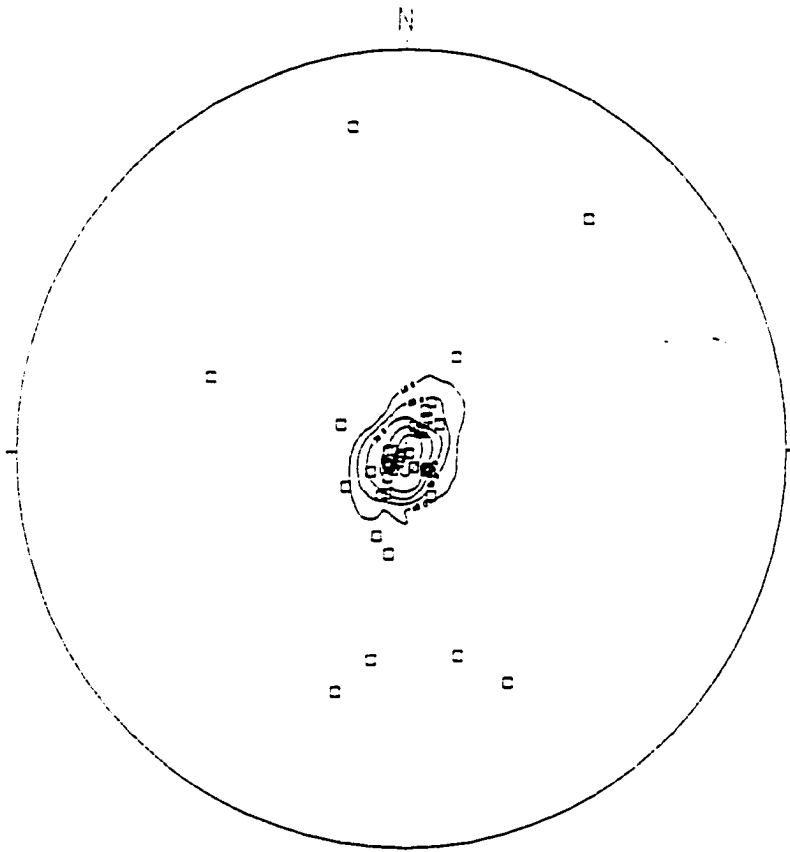


**PLOT 28 - Domain Area 10, Amina Schist**

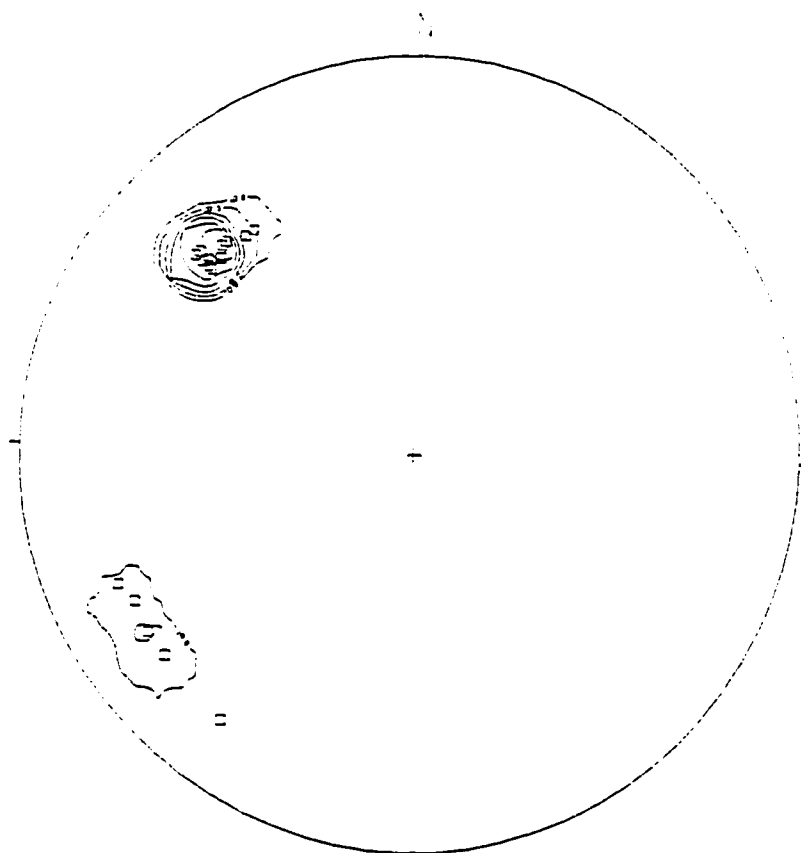
□ Shear Fractures n=9



**PLOT 29 - Domain Area 10, Cercado Sandstone**  
□ Bedding n=10

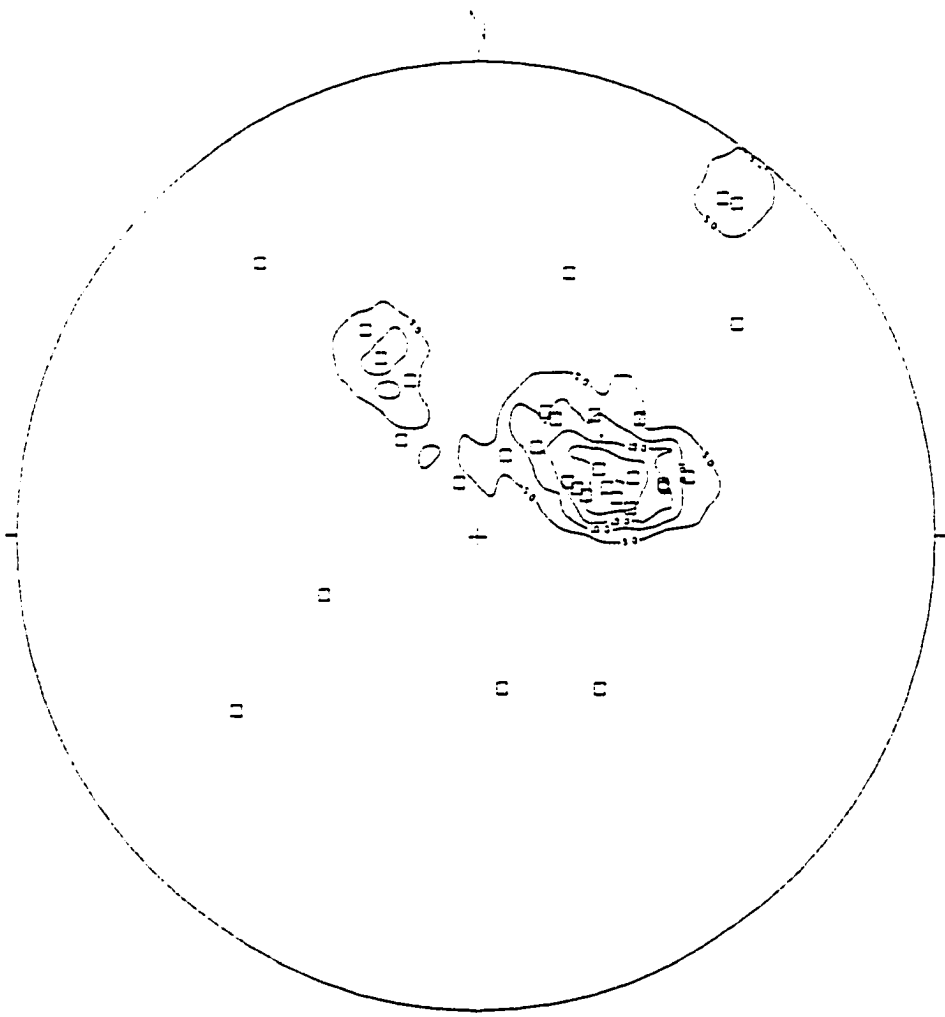


**PLOT 30 - Domain Area 11, Cercado Sandstone**  
□ Bedding n=43



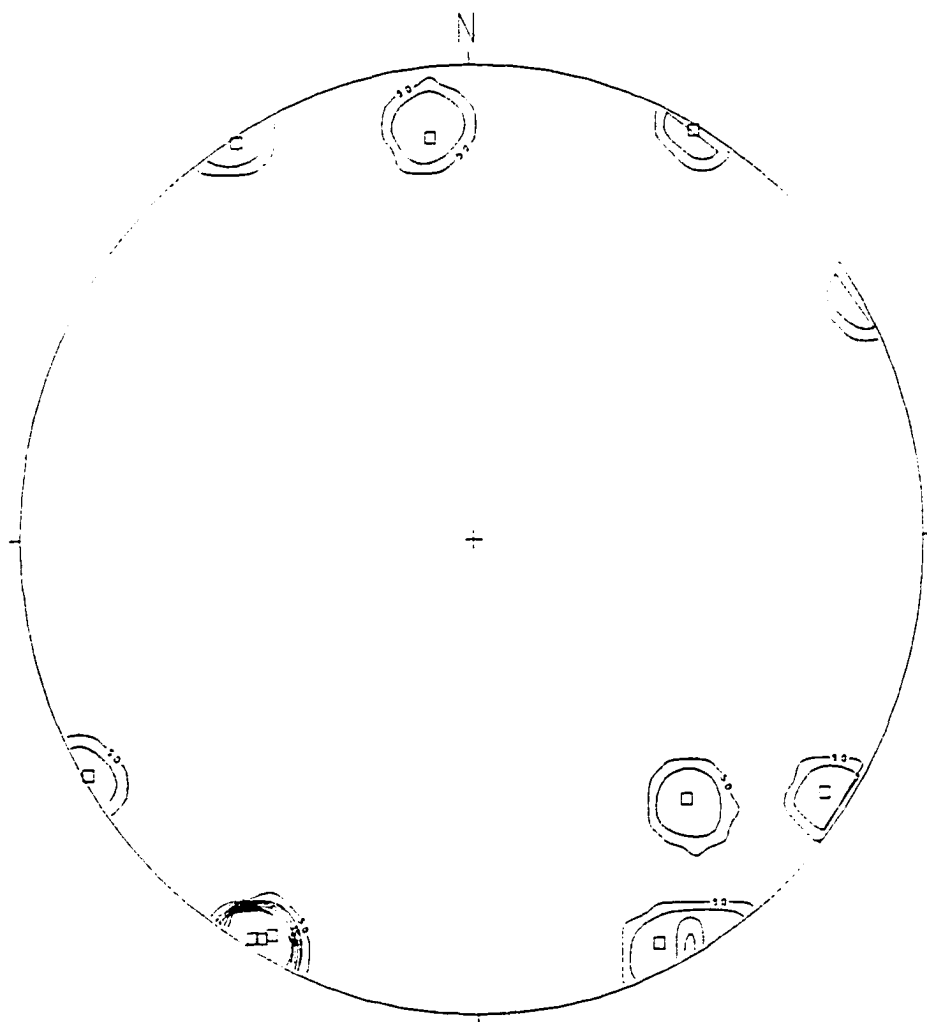
**PLOT 31 - Domain Area 11, Cercado Sandstone**

□ Shear Fractures n=17



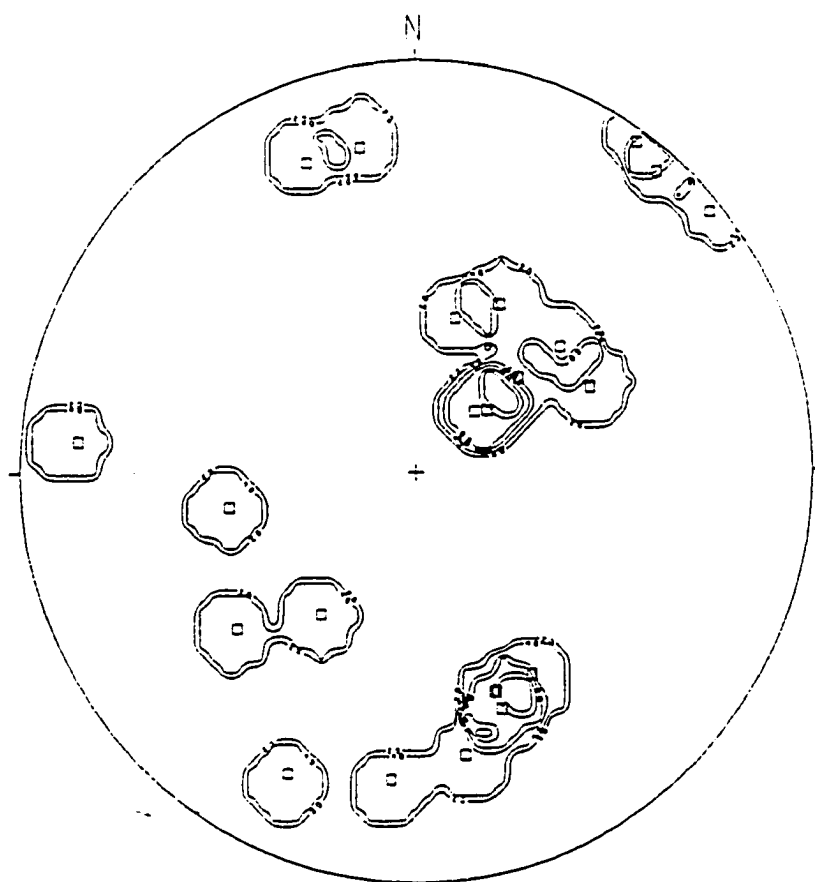
**PLOT 32 - Domain Area 12, Amina Schist**

□ Schistosity n=32



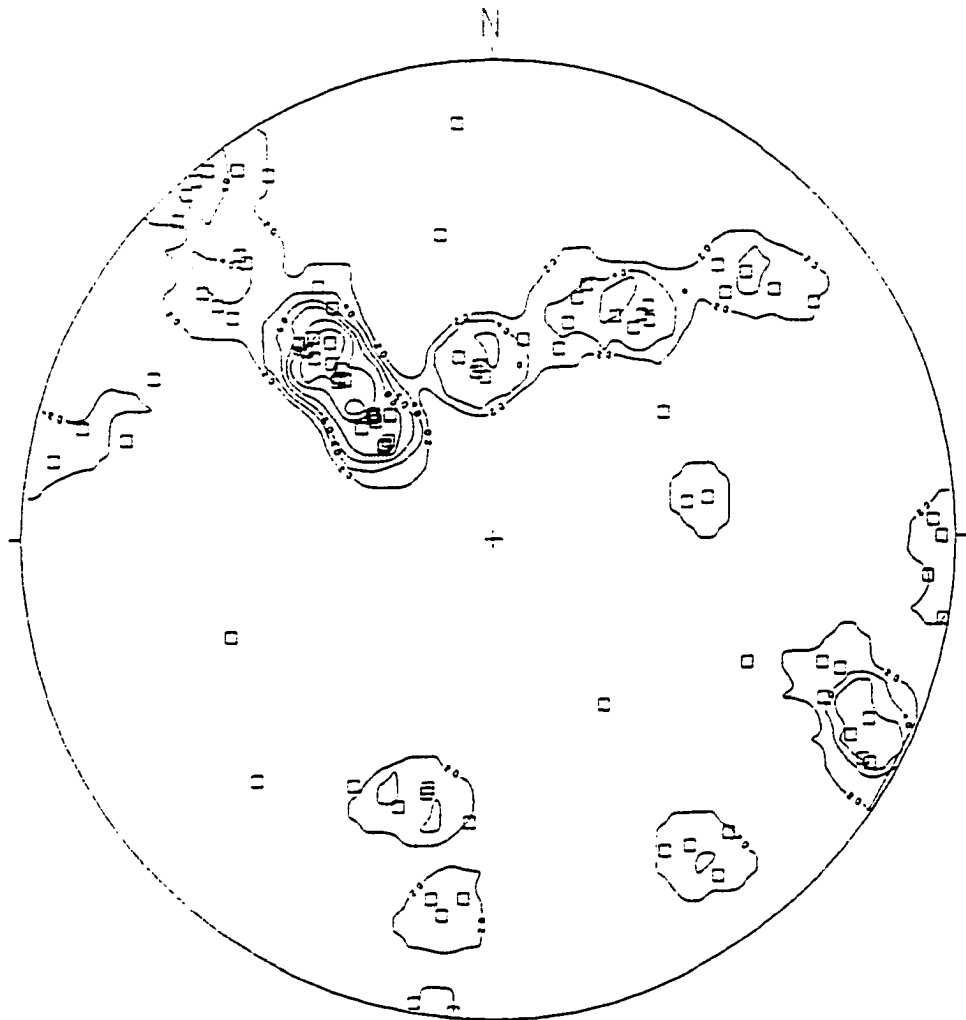
**PLOT 33 - Domain Area 12, Amina Schist**

□ Shear Fractures n=12



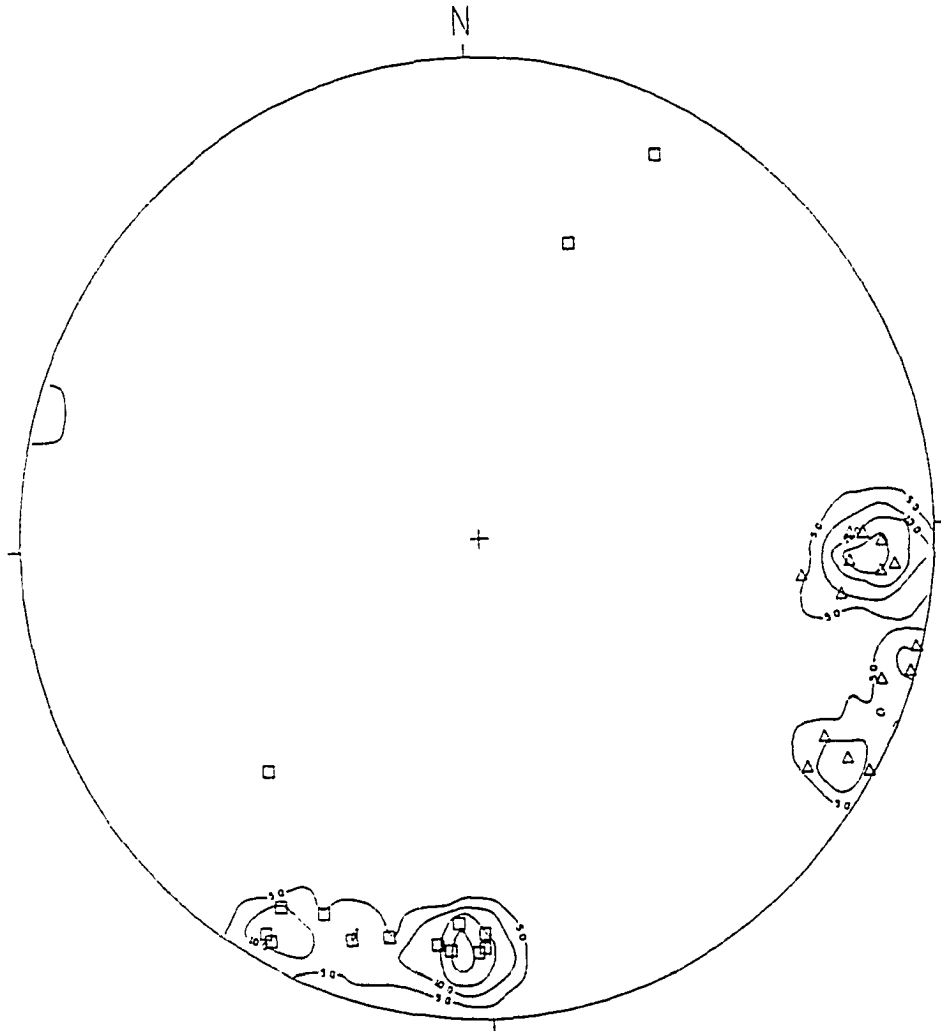
**PLOT 34 - Domain Area 13, Inoa Conglomerate**

□ Bedding n=22



**PLOT 35 - Domain Area 13, Inoa Conglomerate**

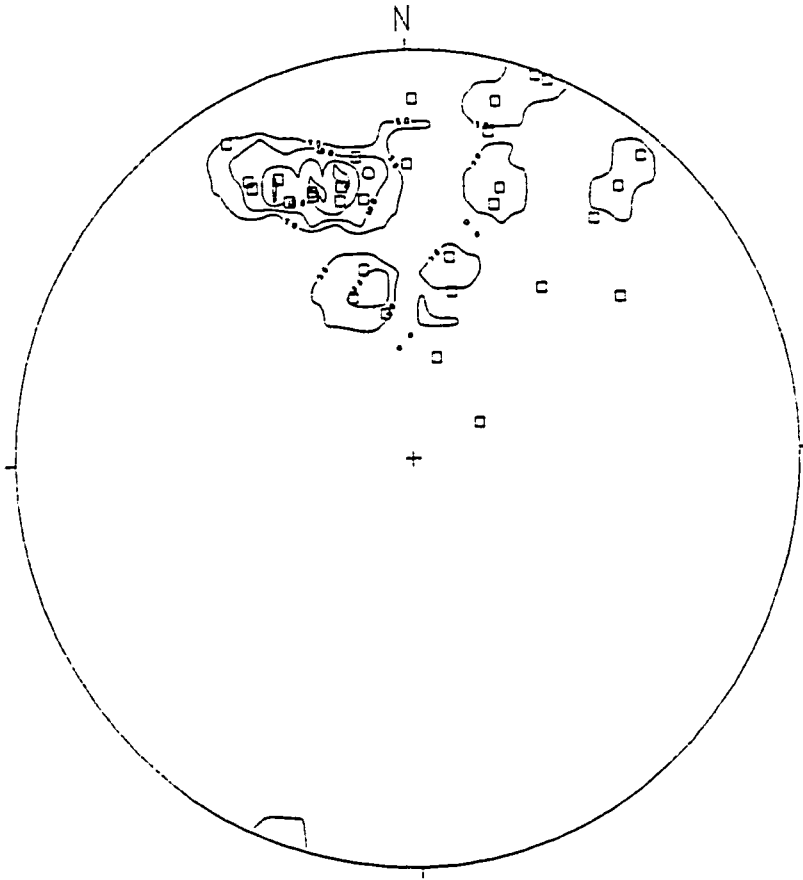
□ Shear Fractures n=93



**PLOT 36 - Domain Area 13, Inoa Conglomerate**

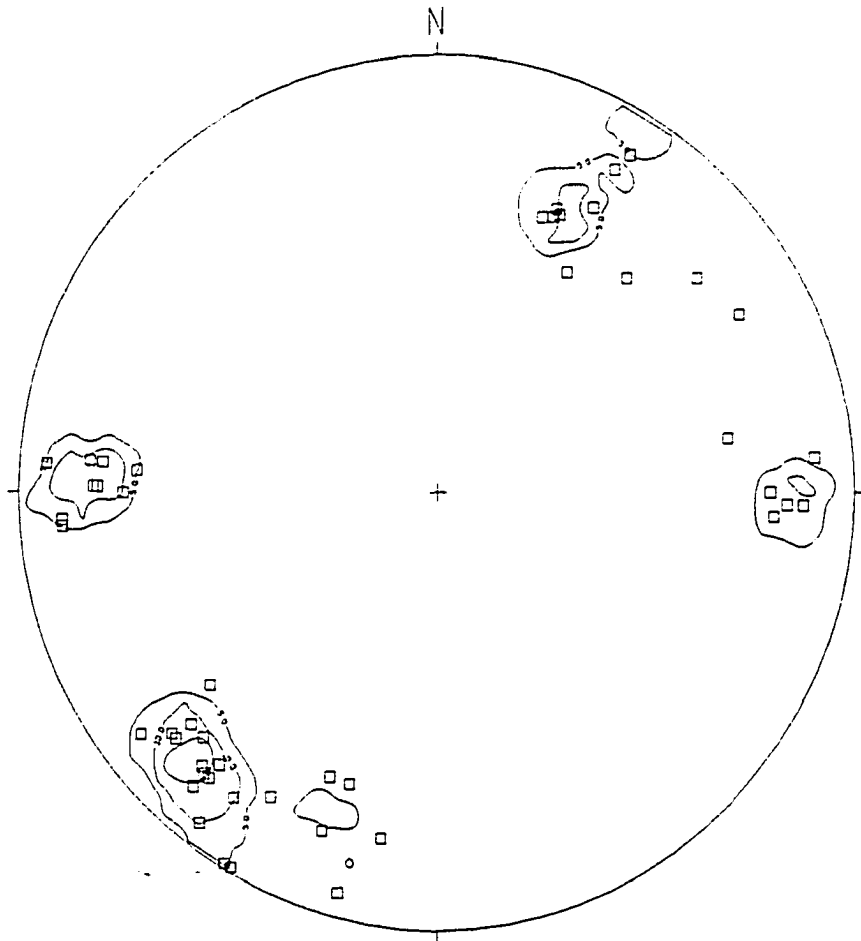
□ Poles to Fault Planes n=15

▲ Slickenlines n=15

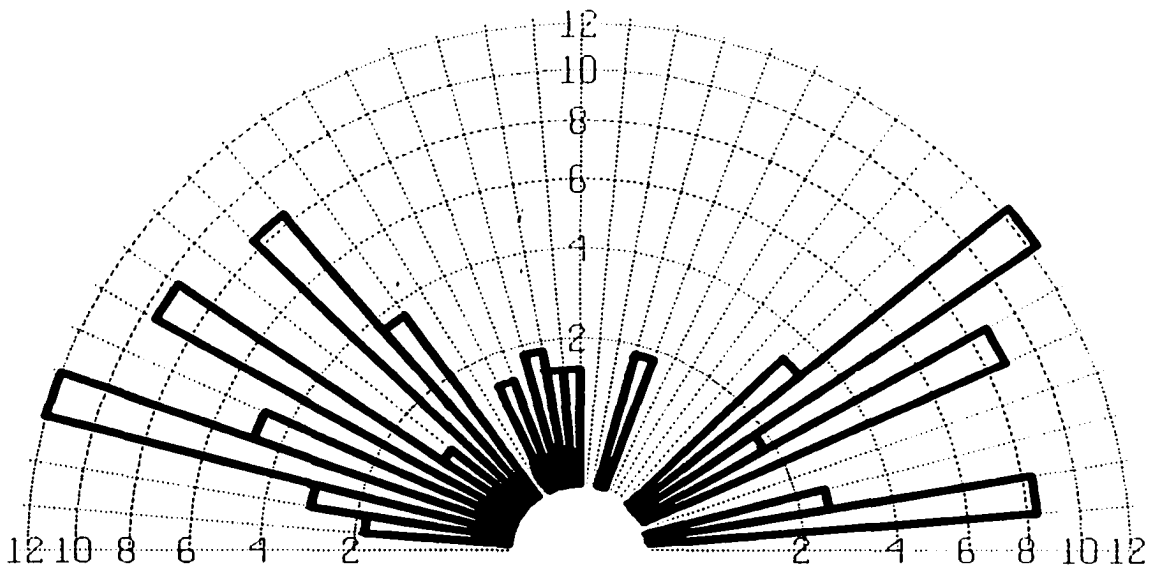


**PLOT 37 - Domain Area 14, Amina Schist**

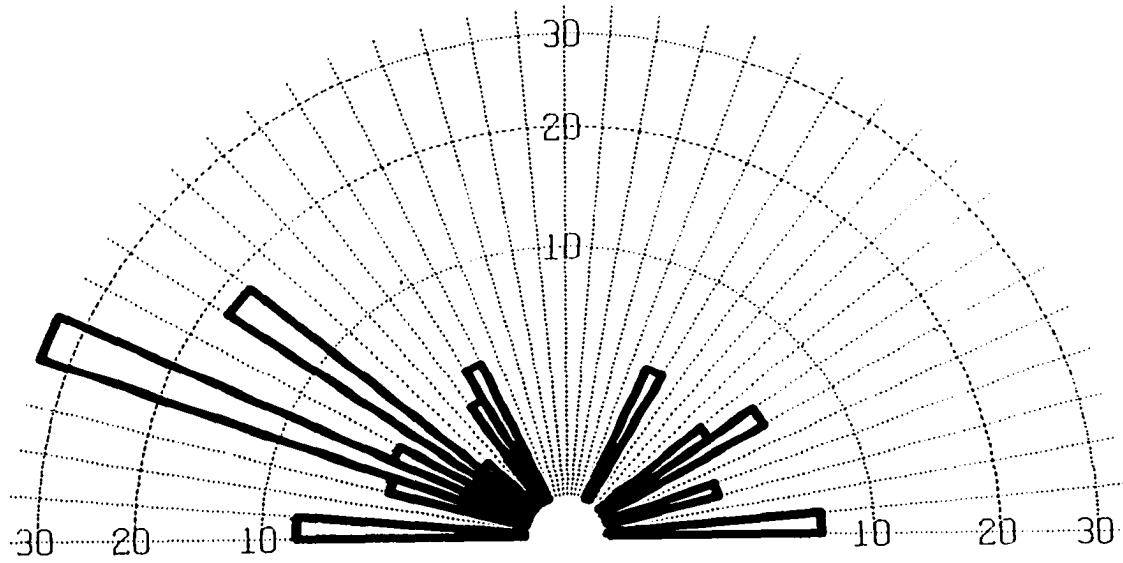
□ Schistosity n=34



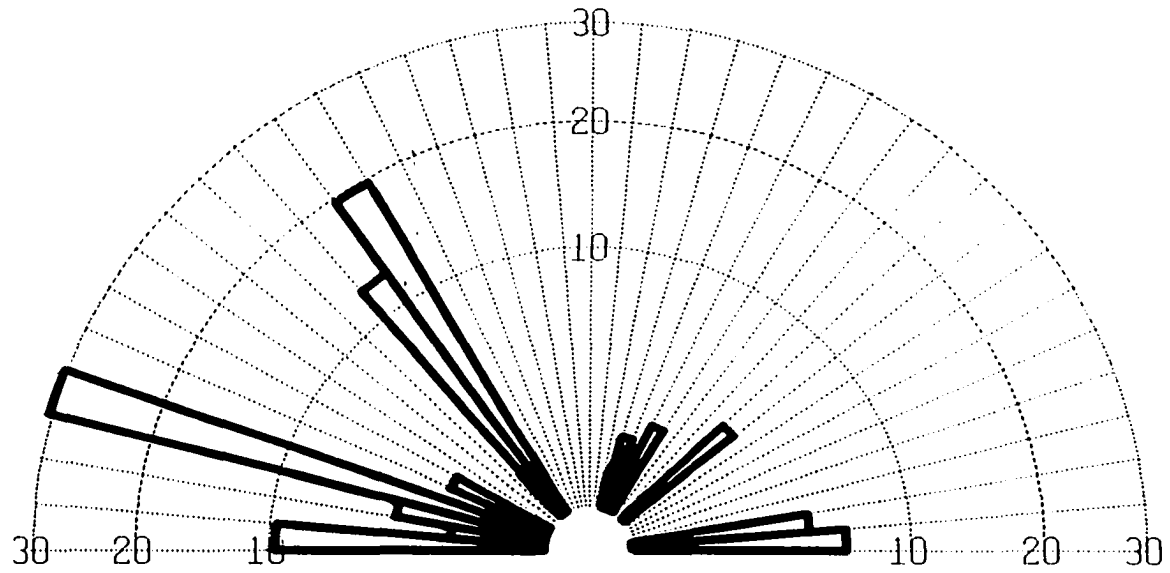
**PLOT 38 - Domain Area 15, Duarte Greenschist Facies Rocks**  
□ Shear Fractures n=47



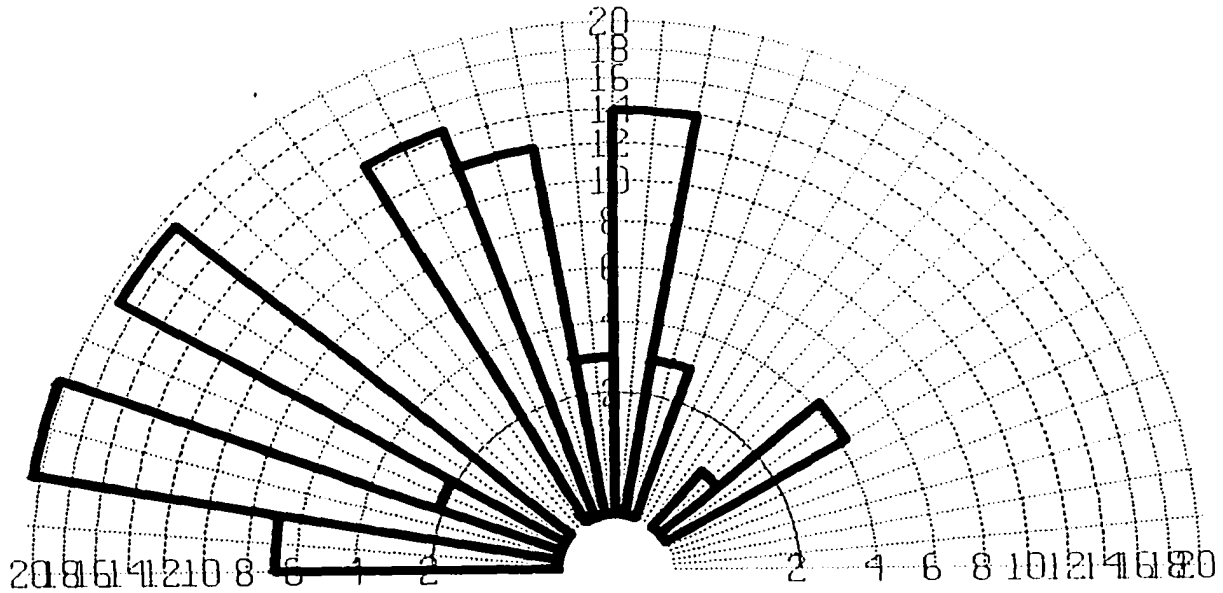
**Rose Diagram 1 - Rose diagram of orientation of lineaments measured on aerial photographs from domain no. 1. Cumulative lineament length is 55.5 cm. 1 reading per 0.1 cm Trace Length. Fracture density shown in percent.**



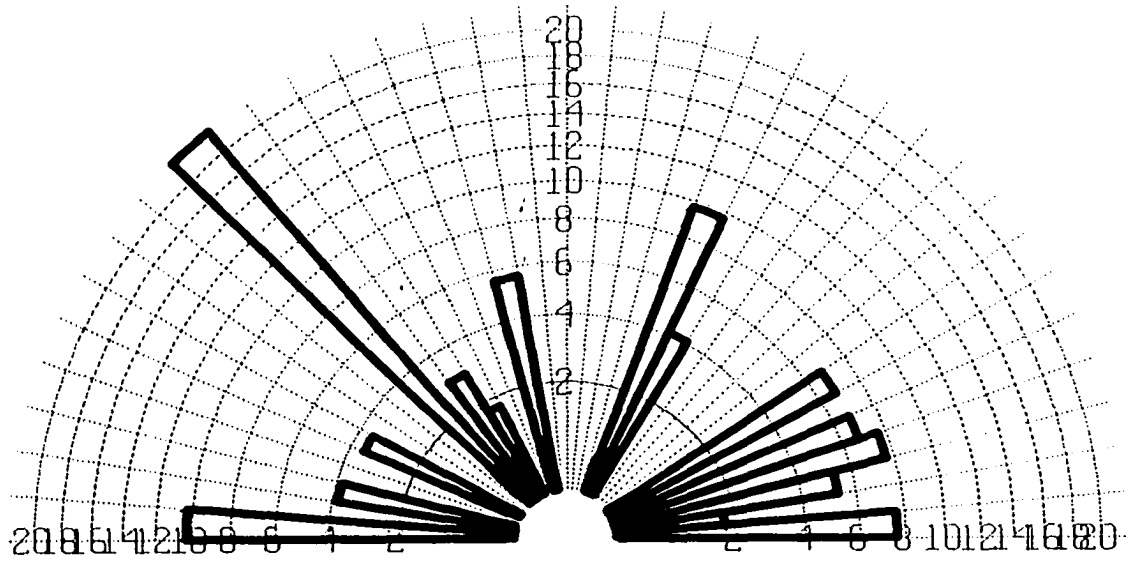
**Rose Diagram 2 - Rose diagram of orientation of lineaments measured on aerial photographs from domain no. 2. Cumulative lineament length is 31.9 cm. 1 reading per 0.1 cm Trace Length. Fracture density shown in percent.**



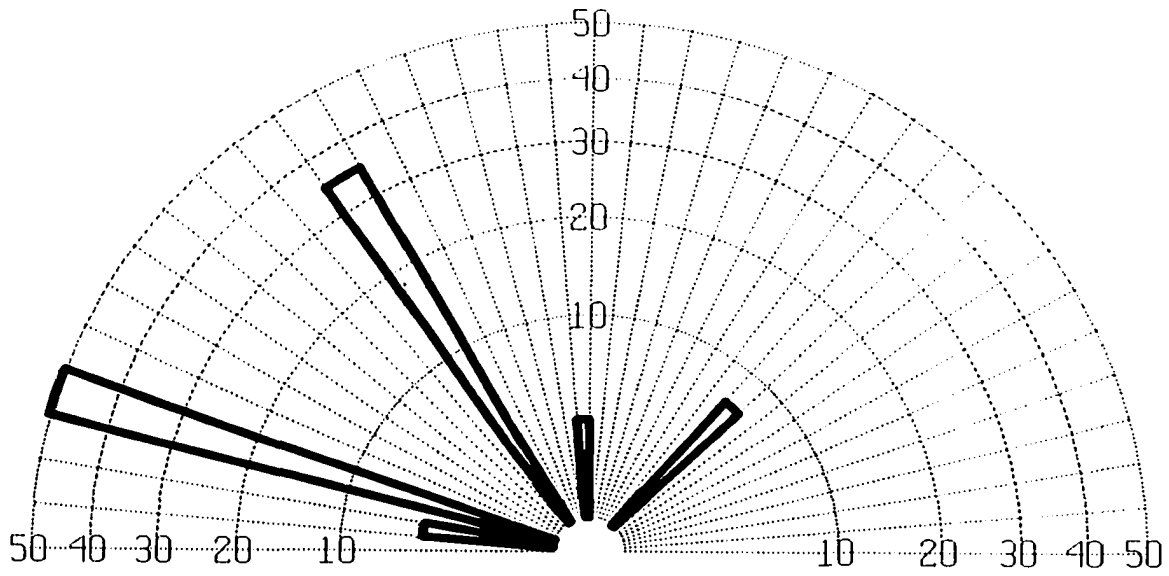
**Rose Diagram 3 - Rose diagram of orientation of lineaments measured on aerial photographs from domain no. 3. Cumulative lineament length is 52 cm. 1 reading per 0.1 cm Trace Length. Fracture density shown in percent.**



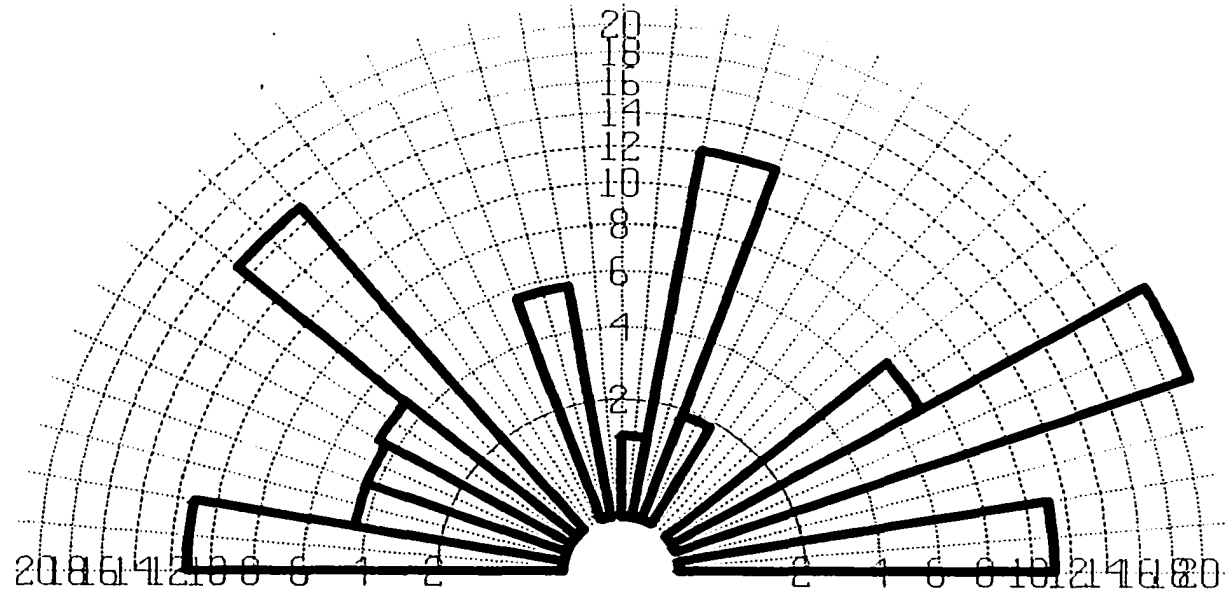
**Rose Diagram 4 - Rose diagram of orientation of lineaments measured on aerial photographs from domain no. 4. Cumulative lineament length is 9.3 cm. 1 reading per 0.1 cm Trace Length. Fracture density shown in percent.**



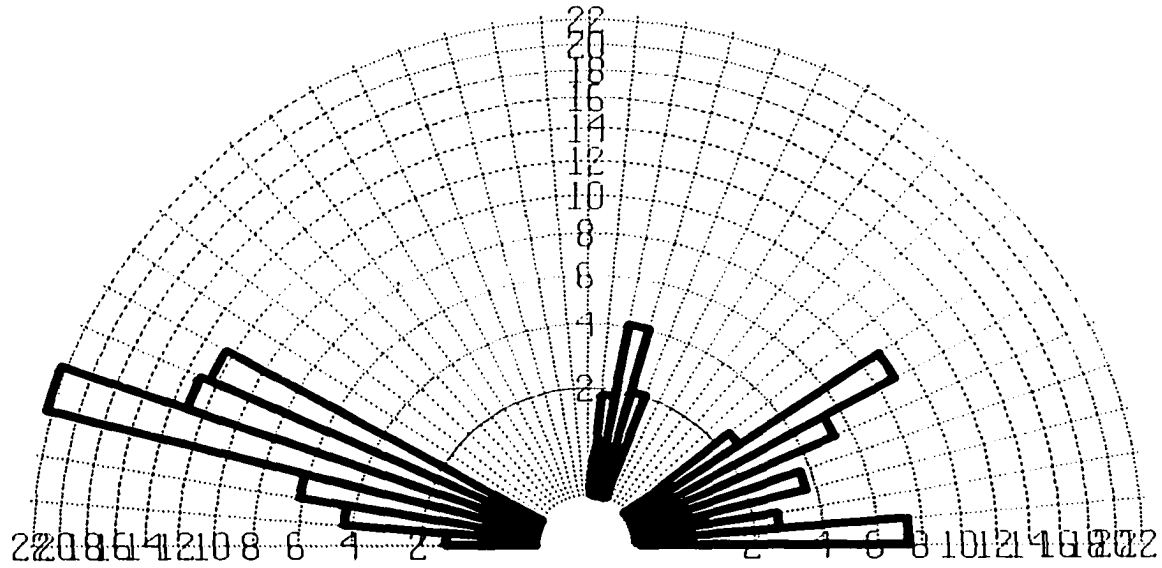
**Rose Diagram 5 - Rose diagram of orientation of lineaments measured on aerial photographs from domain no. 5. Cumulative lineament length is 29.67 cm. 1 reading per 0.1 cm Trace Length. Fracture density shown in percent.**



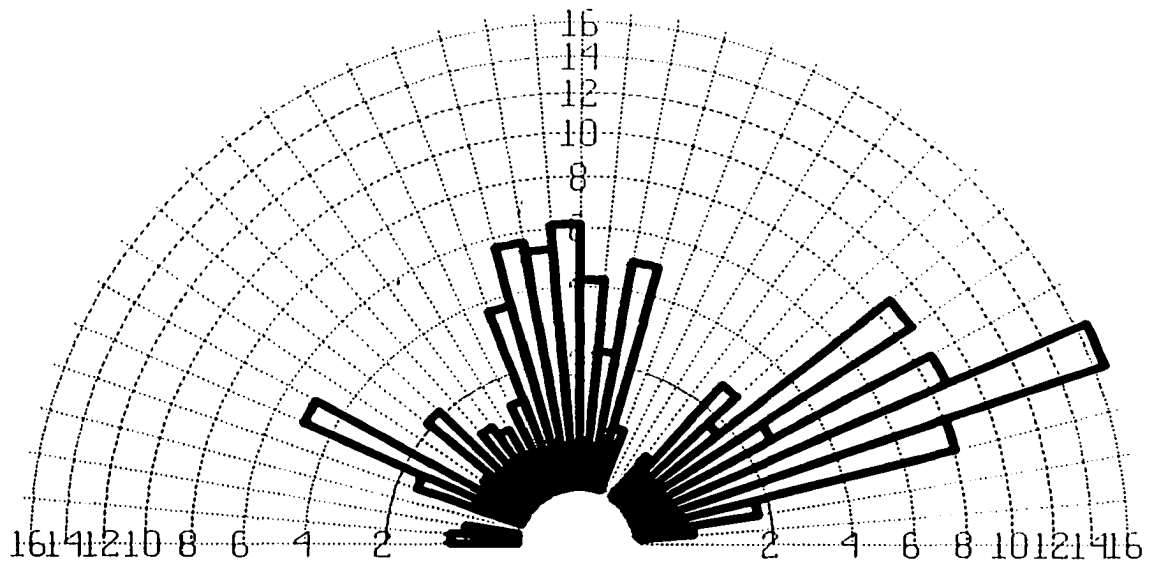
**Rose Diagram 6 - Rose diagram of orientation of lineaments measured on aerial photographs from domain no. 6. Cumulative lineament length is 15.5 cm. 1 reading per 0.1 cm Trace Length. Fracture density shown in percent.**



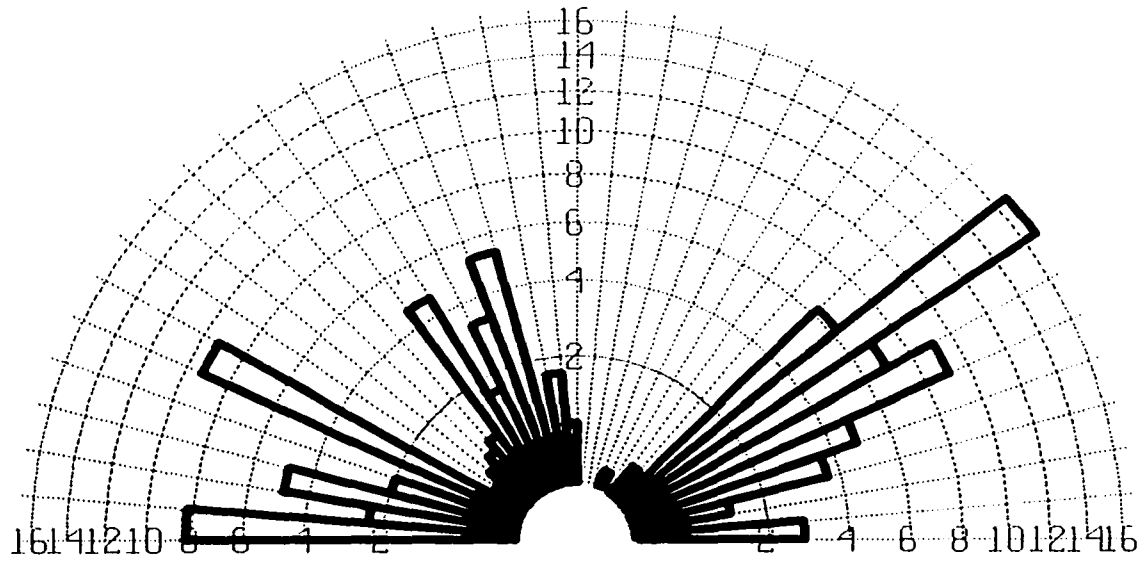
**Rose Diagram 7 - Rose diagram of orientation of lineaments measured on aerial photographs from domain nos. 7 and 14. Cumulative lineament length is 161.5 cm. 1 reading per 0.1 cm Trace Length. Fracture density shown in percent.**



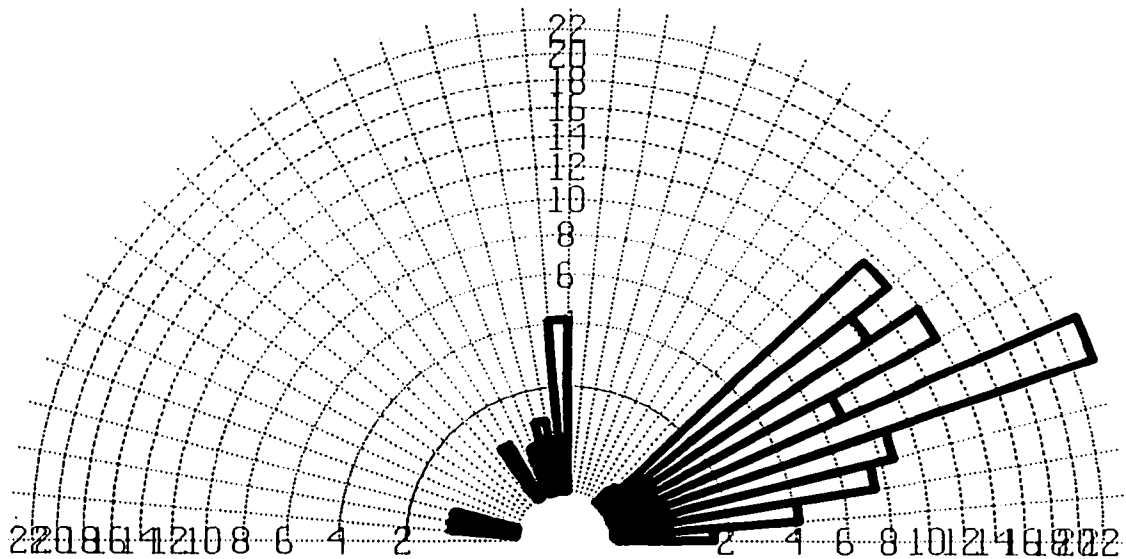
**Rose Diagram 8 - Rose diagram of orientation of lineaments measured on aerial photographs from domain no. 8. Cumulative lineament length is 55.75 cm. 1 reading per 0.1 cm Trace Length. Fracture density shown in percent.**



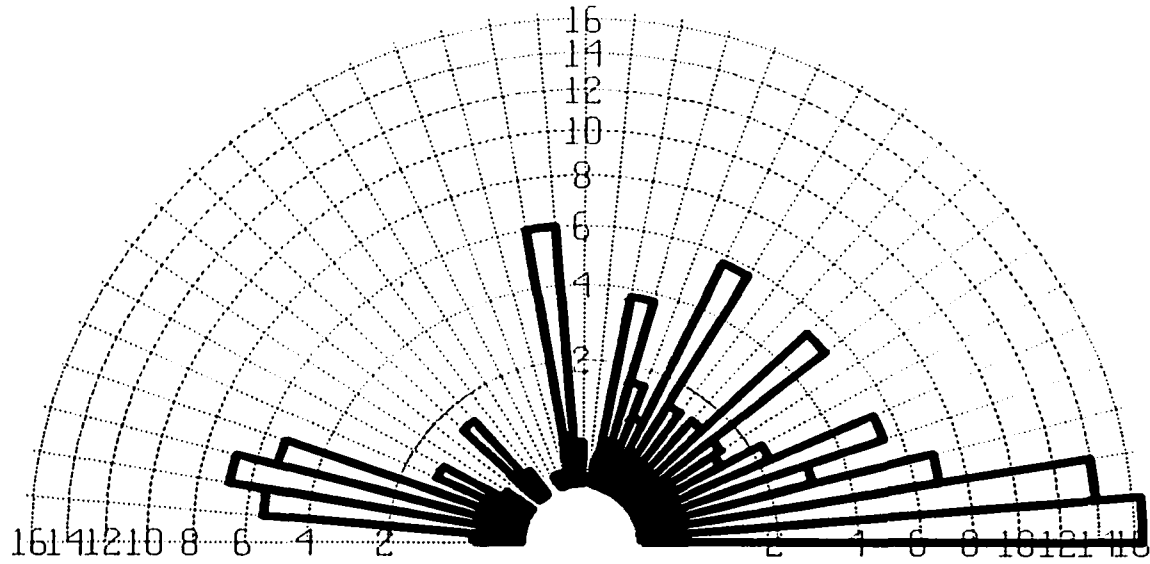
**Rose Diagram 9 - Rose diagram of orientation of lineaments measured on aerial photographs from domain no. 9. Cumulative lineament length is 60.5 cm. 1 reading per 0.1 cm Trace Length. Fracture density shown in percent.**



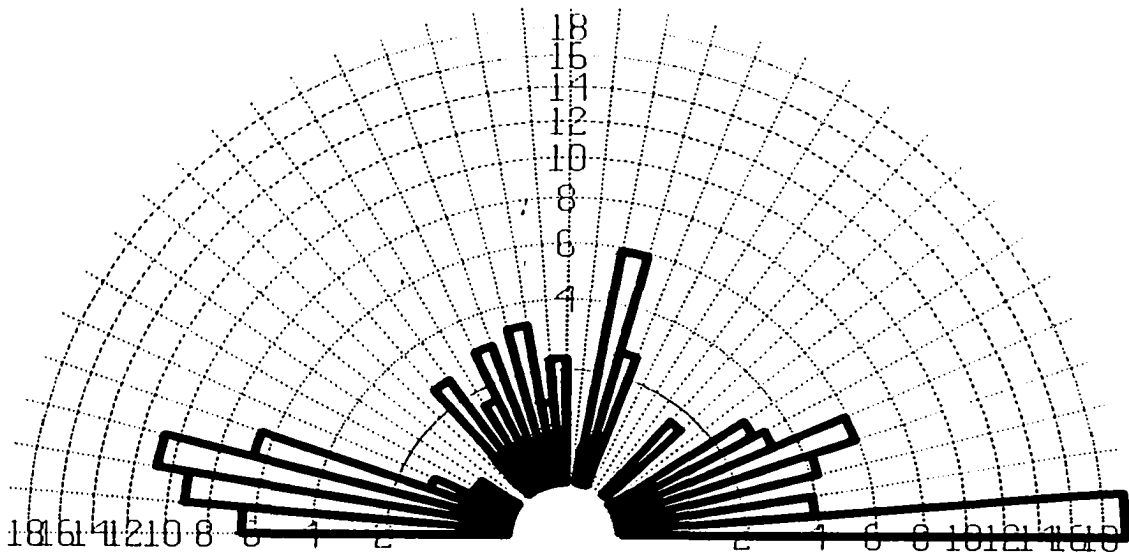
**Rose Diagram 10 - Rose diagram of orientation of lineaments measured on aerial photographs from domain no. 10. Cumulative lineament length is 58.7 cm. 1 reading per 0.1 cm Trace Length. Fracture density shown in percent.**



**Rose Diagram 11 - Rose diagram of orientation of lineaments measured on aerial photographs from domain no. 11. Cumulative lineament length is 24.7 cm. 1 reading per 0.1 cm Trace Length. Fracture density shown in percent.**



**Rose Diagram 12-** Rose diagram of orientation of lineaments measured on aerial photographs from domain no. 12. Cumulative lineament length is 32.5 cm. 1 reading per 0.1 cm Trace Length. Fracture density shown in percent.



**Rose Diagram 13-** Rose diagram of orientation of lineaments measured on aerial photographs from domain no. 13. Cumulative lineament length is 16 cm. 1 reading per 0.1 cm Trace Length. Fracture density shown in percent.

## BIBLIOGRAPHY

- Anderson, E.M, 1951. The dynamics of faulting and dyke formation with applications to Britain: Oliver and Boyd, Edinburgh, 206 p.
- Anderson, T.H. and Schmidt, V.A., 1983. The evolution of Middle America and the Gulf of Mexico-Caribbean Sea region during Mesozoic time, *Geological Society of America Bulletin*, 94, 941-966.
- Antonini, G. A., 1968. Process and patterns of landscape change in the Linea Nordeste, Dominican Republic [Ph.D. Thesis]: New York, Columbia University, 196.
- Antonini, G. A., 1979. Physical Geography of Northwest Dominican Republic: in Lidz, B., and Nagle, F., (eds), Hispaniola; Tectonic focal point of the northern Caribbean; Three geological studies in the Dominican Republic, *Miami Geological Society*, 29-68.
- Aydin A. and Nur, A. 1982. Evolution of pull-apart basins and their scale independence, *Tectonics*, 1, 91-105.
- Aydin, A. and Page, B.M., 1984. Diverse Pliocene-Quaternary tectonics in a transform environment, San Francisco Bay region, California, *Geological Society of America Bulletin*, 95. 1303-1317.
- Bartlett, W.L., Friedman, M., and Logan, J.M., 1981. Experimental folding and faulting of rocks under confining pressure. Part IX. Wrench faults in Limestone layers, *Tectonophysics*, 79, 225-277.
- Biddle, K.T. and Christie-Blick, N., 1985. Glossary-Strike-Slip Deformation, Basin Formation, and Sedimentation, *The Society of Economic Paleontologists and Mineralogists*, Special Publication No. 37, 375-386.
- Bonini, W.E., Hargraves, R.B., Shagam, R., eds. 1984. The Caribbean South American Plate Boundary and Regional Tectonics, *Geological Society of America Memoirs*, 162, 421 p.
- Bourdon, L., 1985. La Cordillere Orientale Dominicaine, Hispaniola, Grandes Antilles; Un Arc insulaire cretace polystructure [Ph.D. thesis]: Paris, France, Universite Pierre et Marie Curie, 203 p.
- Bowin, C.O. 1960. Geology of central Dominican Republic [Ph.D. thesis]: Princeton University. 211 p.

- Bowin, C.O. 1966. Geology of the central Dominican Republic--A case history of part of an island Arc, in Hess, H.H., (ed), Caribbean geological investigations, *Geological Society of America Memoir*, 98, 11-84.
- Bowin, C.O. 1975. The Geology of Hispaniola, in Nairn, A.E.M. and F. G. Stehli, (eds), *The Ocean Basins and Margins. 3. The Gulf of Mexico and Caribbean*, 500-552.
- Bowin, C.O., and Nagle, F., 1982. Igneous and metamorphic rocks of northern Dominican Republic; An uplifted subduction zone complex: Transactions of the 9<sup>th</sup> *Caribbean Geological Conference*, Santo Domingo, Dominican Republic, Amigo del Hogar Publishers, 16<sup>th</sup>-20<sup>th</sup> August, 1980, 39-50.
- Bracey, D.R. and Vogt, P.R., 1970. Plate tectonics in the Hispaniola area, *Geological Society of America Bulletin*, 81, 2855-2860.
- Buffler, R.T., and Sawyer, D.S., 1985. Distribution of crust and early history, Gulf of Mexico Basin, *Transactions of the Gulf Coast Association of Geological Societies*, 35, 333-344.
- Burke, K. 1988. Tectonic evolution of the Caribbean: *Annual Review of Earth and Planetary Sciences*, 16, 201-230.
- Burke, K., Cooper, C., Dewey, P., Mann, P., and Pindell, J.L., 1984. Caribbean Tectonics and Relative Plate Motions, *Geological Society of America Memoir*, 162, 31-63.
- Burchfiel, B.C., and Stewart, J.H., 1966. "Pull-apart" origin of the central segment of Death Valley, California: *Geological Society of America Bulletin*, 77, 439-443.
- Butterlin, J., Ramirez, R., and Hoffstetter, R., 1956. Ile d'Haiti = Hispaniola et îles adjacentes: République Dominicana. Pp. 351-414 in *Lexique Stratigraphique International. Amérique Latin. Fascicule 2b: Antilles. Centre National de la Recherche Scientifique Paris*.
- Byrne, D.B., Suarez, G., and McCann, W.R., 1985, Muertos trench subduction; Microplate tectonics in the northern Caribbean?: *Nature*, 317, 420-421.
- Calais, E., Bethoux, N., and Mercier de Lépinay, B., 1992, From transcurrent faulting to frontal subduction: A seismotectonic study of the northern Caribbean plate boundary from Cuba to Puerto Rico, *Tectonics*, 11, 114-123.

Calais, E., and Mercier de Lépinay, B., 1993. Semi-quantitative modeling of strain and kinematics along the Caribbean/North America strike-slip plate boundary zone. *Journal of Geophysical Research*, 98, 8293-8308.

Calais, E. and Mercier de Lépinay, B., 1995. Strike-slip tectonic processes in the northern Caribbean between Cuba and Hispaniola (Windward Passage), *Marine Geophysical Research Letters*, 17, 63-95.

Calais, E., Perrot, J., and Mercier de Lépinay, B., 1998. Strike-slip tectonics and seismicity along the northern Caribbean plate boundary from Cuba to Hispaniola, in Dolan, J.F., and Mann, P., eds., *Active Strike-Slip and Collisional Tectonics of the Northern Caribbean Plate Boundary Zone: Boulder, Colorado*, *Geological Society of America Special Paper 326*, 125-142.

Christie-Blick, N., and Biddle, K.T., 1985. Deformation and basin formation along strike-slip faults, in Biddle, K.T., and Christie-Blick, N., eds., *Strike-Slip Deformation, Basin Formation, and Sedimentation: Society of Economic Paleontologists and Mineralogists Special Publication 37*. 1-34.

Coulomb, C.A., 1773, Sur une applicaton des regles de maximus et minimis a quelques problemes de statique relatifs a l'architecture: Academie Royale des Sciences, Memoires de Mathematique et de Physique par divers Savants, 7, 343-382.

Cribb, Joshua Warner, 1986. The Petrology and Geochemistry of Eastern Loma de Cabrera Batholith, [M.S. Thesis]: George Washington University, 122 p.

Crowell, J.C. 1974. Origin of late Cenozoic basins in southern California, in Dickinson, W.R., ed., *Tectonics and Sedimentation: Society of Economic Paleontologists and Mineralogists*, Special Publication No. 22, 190-204.

Davis, G.H., 1996. *Structural geology of rocks and regions - 2<sup>nd</sup> ed.* John Wiley and Sons, Inc., 776 p.

de Zoeten, R. and Mann, P., 1991. Structural geology and Cenozoic tectonic history of the central Cordillera Septentrional, Dominican Republic: in P. Mann, G. Draper, and J.F., Lewis (eds) *Geologic and Tectonic Development of the North American-Caribbean Plate Boundary in Hispaniola. Geological Society of America, Special Paper 262*, 265-279.

DeMets, C., Gordon, R.G., Argus, D.F., and Stein, S., 1990. Current plate motions, *Geophysical Journal of the Royal Astronomical Society*, 101, 425-478.

- Dickinson, W.R. and Coney, P.J., 1980. Plate tectonics constraints on the origin of the Gulf of Mexico: *in* Pilger, R.H. (ed.), *The Origin of the Gulf of Mexico and the Early Opening of the Central Atlantic*, Louisiana State University, Baton Rouge, 27-36.
- Dillon, W., Austin, J.A., Scanlon, K.M., Edgar, N.T., and Parson, L.M., 1992, Structure and development of the insular margin north of western Hispaniola: A tectonic accretionary wedge on the Caribbean plate boundary, *Marine and Petroleum Geology*, 9, 70-88.
- Dolan, J., Mann, P., de Zoeten, R., Heubeck, C., and Shiroma, J., 1991. Sedimentologic, stratigraphic, and tectonic synthesis of Eocene-Miocene sedimentary basins, Hispaniola and Puerto Rico, *in* Mann, P., Draper, G., and Lewis, J.F., eds., *Geologic and tectonic development of the North American-Caribbean plate boundary in Hispaniola*, *Geological Society of America*, Special Paper 262, 217-263
- Dolan, J.F., Mullins, H.T., and Wald, D.J., 1998. Active tectonics of the north-central Caribbean: Oblique collision, strain partitioning, and opposing subducted slabs, *in* Dolan, J.F., and Mann, P., eds., *Active Strike-Slip and Collisional Tectonics of the Northern Caribbean Plate Boundary Zone*, *Geological Society of America*, Special Paper 326, 1-61.
- Dolan, J.F., and Wald, D.J., 1998. The 1943-1953 north-central Caribbean earthquakes: Active tectonic setting, seismic hazards, and implications for Caribbean-North America plate motions, *in* Dolan, J.F., and Mann, P., eds., *Active Strike-Slip and Collisional Tectonics of the Northern Caribbean Plate Boundary Zone*: Boulder, Colorado, *Geological Society of America* Special Paper 326, 143-169.
- Donnelly, T.W., 1989, Geologic history of the Caribbean and Central America: *in* Bally, A.W. and Palmer, A.R. (eds), *The Geology of North America-An Overview*, *Geological Society of America*, 299-321.
- Donnelly, T.W., Beets, D.; Carr, M., Jackson, T., Klaver, G., Lewis, J., Maury, R., Schellenkens, H., Smith, A., Wadge, G., and Westercamp, D., 1990. History and tectonic setting of Caribbean magmatism, *in* Dengo, G., and Case, J.E., eds., *The Caribbean Region*, *Geological Society of America*, H, 339-374.
- Donnelly, T.W. 1994. The Caribbean Sea Floor: *in* Donovan, S., and Jackson, T.A., (eds), *Caribbean Geology: An Introduction*. *University of the West Indies Publishers Association*, Kingston, Jamaica, 41-65.

- Draper, G., and Lewis, J.F. 1982. Petrology, deformation, and tectonic significance of Amina Schist, northern Dominican Republic: *in Transactions of the 9th Caribbean Geological Conference*, Santo Domingo, Dominican Republic, Amigo del Hogar Publishers, 16<sup>th</sup>-20<sup>th</sup> August, 1980, 53-64.
- Draper, G., and Lewis, J.F. 1989. Petrology and structural development of the Duarte Complex, central Dominican Republic; A preliminary account and some tectonic implications: *in* Duque-Caro, H., (ed), *Transactions of the 10<sup>th</sup> Caribbean Geological Conference*, Cartagena, Colombia, 14<sup>th</sup>-20<sup>th</sup> August, 1983: Bogota, Colombia, Ingeominas, 103-112.
- Draper, G., and Lewis, J.F. 1991. Metamorphic belts in central Hispaniola: *in* Mann, P., G. Draper, and J.F., Lewis (eds) *Geologic and Tectonic Development of the North America-Caribbean Plate Boundary in Hispaniola*, *Geological Society of America*, Special Paper 262, 29-45.
- Draper, G., Jackson, T.A., and S.K. Donovan. 1994a. Geologic Provinces of the Caribbean Region: *in* Donovan, S.K., and Jackson, T.A.(eds), *Caribbean Geology: An Introduction*, *University of the West Indies Publishers Association*, Kingston, Jamaica, 3-12.
- Draper, G., Mann, P., and Lewis, J.F. 1994b. Hispaniola: *in* Donovan, S.K., and Jackson, T.A. (eds), *Caribbean Geology: An Introduction*, *University of the West Indies Publishers Association*, Kingston, Jamaica, 129-150.
- Duncan, R.A. and Hargraves, R.B. 1984. Plate tectonic evolution of the Caribbean region in the mantle reference frame, *Geological Society of America*, *Memoir* 162, 81-84.
- Dupuis, V., Lapirre, H., Hernandez, J., Mercier De Lépinay, R.M., and Tardy, M., 1998. The Duarte Complex and Siete Cabezas Formation (Dominican Republic): Remnants of the CCOP, *Transactions of the Fifteenth Caribbean Geological Conference: (Abs.)*, University of the West Indies Mona, Kingston, Jamaica, June 29-July 2.
- Edgar, N.T., 1991. Structure and geologic development of the Cibao Valley, northern Hispaniola, *in* Mann, P.; Draper, G.; and Lewis, J.F., eds., *Geologic and tectonic development of the North America-Caribbean plate boundary in Hispaniola: Geological Society of America Special Paper 262*, 281-299.
- Erikson, J. P., Pindell, J.L., Karner, G.D., Sonder, L.J., Fuller, E. and Dent, L., 1998. Neogene Sedimentation and Tectonics in the Cibao Basin and Northern Hispaniola: An Example of Basin Evolution near a Strike-Slip-Dominated Plate Boundary. *The Journal of Geology*, 106, 473-494.

- Freund, R., 1982. The role of shear in rifting, *in* Pálmason, G. ed., Continental and Oceanic Rifts, *American Geophysical Union Geodynamics Series*, 8, 33-39.
- Grindlay, N.R., Mann, P., and Dolan, J. 1999. Oblique collision of the Bahama Platform in the Hispaniola-Puerto Rico area, northeastern Caribbean, *Subduction to Strike-Slip Transitions on Plate Boundaries, Geological Society of America Penrose Conference*, Jan. 18-24, p.36 Abstract Volume.
- Groetsch, G. I., 1980. Resedimented Conglomerates and Turbidites of the Upper Tavera Group, Dominican Republic: *Transactions of the 9th Caribbean Geological Conference*, Santo Domingo, Dominican Republic, Amigo del Hogar Publishers, 16<sup>th</sup>-20<sup>th</sup> August, 1980, 191-198.
- Groetsch, G. I. 1983. Resedimented Conglomerates and turbidites of the Represa and Janico Formations, north-central Dominican Republic [M.S. Thesis]: Washington, D.C., George Washington University. 118 p.
- Goreau, P., 1981. The tectonic evolution of the north central Caribbean plate margin [Ph.D. thesis]: Boston/Woods Hole Oceanographic Institution Joint Program in Oceanography, 245 p.
- Guglielmo, G., and Winslow, M. A., 1988. Geology of the eastern San Francisco push-up; Northeastern Hispaniola, *in* Barker, L., ed., *Transactions of the 11th Caribbean Geological Conference*, Dover Beach, Barbados: St. Michael, Barbados, Energy and Natural Resources Division, 18-1 - 18-21.
- Guglielmo, G., 1986, Push-Up Structure in a Transpressional Environment: Northeastern Hispaniola. [M.A. thesis]: City College of New York, 52 p.
- Harding, T.P., Virbuchen, R.C. and Christie-Blick, N. 1985. Structural Styles, Plate Tectonic Settings, and Hydrocarbon Traps of Divergent (Transensional) Wrench Faults, *The Society of Economic Paleontologists and Mineralogists Special Publication No. 37*, 51-77.
- International Subcommittee on Stratigraphic Classification (ISSC). 1994. International Stratigraphic Guide: *in* H.D. Hedberg (ed), A guide to stratigraphic classification, terminology, and procedure, *Geological Society of America*, 214 p.
- Iturralde-Vinent, Manuel A., 1996, Introduction to Cuban Geology and Geophysics in Ofiolitas y Arcos Volcanicos de Cuba, Project 364 Caribbean Ophiolites and Volcanic Arcs, International Geological Correlation Program, Special Contribution No. 1, eds. Iturralde-Vinent, Manuel A., 3-35.

James, K., 1990. The Venezuelan Hydro habitat: in Brooks, J. (ed.), *Classic Petroleum Provinces*, *Geological Society of London*, Special Publication 50, 9-36.

Jordan, T. H., 1975. The Present - Day Motions of the Caribbean Plate, *Journal of Geophysical Research*, 80, (32), 4433-4499.

Joyce, J., 1991. Blueschist metamorphism and deformation on the Samaná Peninsula-A record of subduction and collision in the Greater Antilles, in Mann, P., Draper, G., and Lewis, J.F., eds., *Geologic and tectonic development of the North America-Caribbean plate boundary in Hispaniola*, *Geological Society of America*, Special Paper 262, 47-76.

Klitgord, K and Schouten, H., 1986, Plate kinematics of the central Atlantic: in Tucholke, B.E. and Vogt, P.R. (eds), *The Geology of North America, The Western Atlantic Region*, *Geological Society of America*, M, 351-378.

Ladd, J.W., 1976. Relative motion of South America with respect to North America and Caribbean tectonics, *Geological Society of America Bulletin*, 87, 969-976.

Lapierre, Henriette, Dupuis, V., Mercier de Lépinay, B., Tardy, M., Ruiz, J., Maury, R., Hernandez, J., and Loubet, M. 1997. Is the Lower Duarte Igneous Complex [Hispaniola] a Remnant of the Caribbean Plume-Generated Oceanic Plateau?, *Journal of Geology*, 105, 111-120.

Larue, D.K., and Ryan, H.F. 1998. Seismic reflection profiles of the Puerto Rico Trench: Shortening between the North American and Caribbean plates: in Lidiak, E.G., and Larue, D.K., (eds), *Tectonics and Geochemistry of the Northeastern Caribbean*. *Geological Society of America*, Special Paper 322, 193-210.

Lebron, M.C., 1989. Petrochemistry and tectonic significance of Late Cretaceous, calc-alkaline volcanic rocks, Cordillera Oriental, Dominican Republic, [M.S. Thesis]: Gainesville, University of Florida, 153 p.

Lewis, J.F., and Draper, G. 1990. Geology and tectonic evolution of the northern Caribbean margin: in Dengo, G., and Case, J.E., (eds), *The Caribbean region*. *Geological Society of America*, H, 77-140.

Lewis, J.F., and Jiménez, J.G. 1991. Duarte Complex in the La Vega-Jarabacoa-Janico area, central Hispaniola: Geologic and geochemical features of the sea floor during the early stages of Arc evolution: in Mann, P.; Draper, G.; and Lewis, J.F., (eds), *Geologic and tectonic development of the North American-Caribbean plateau boundary in Hispaniola*, *Geological Society of America*, Special Paper 262, 115-141.

- Lewis, J.F., 1982. Cenozoic Tectonic Evolution and Sedimentation in Hispaniola: *Transactions of the 9th Caribbean Geological Conference*, Santo Domingo, Dominican Republic, Santo Domingo, Dominican Republic, Amigo del Hogar Publishers, 16<sup>th</sup>-20<sup>th</sup> August, 1980, 65-74.
- Malfait, B.T. and Dinkelman, M.G., 1972. Circum-Caribbean tectonic and igneous activity and the evolution of the Caribbean plate, *Geological Society of America Bulletin*, 83, 250-272.
- Mann, P., Hempton, M.R., Bradley, D.C., and Burke, K. 1983. Development of Pull-Apart Basins, *Journal of Geology*, 91, 529-554.
- Mann, P., and Burke, K., 1984. Neotectonics of the Caribbean, *Reviews of Geophysics and Space Physics*, 22, (4), 309-362.
- Mann, P., Burke, K., and Matumoto, T., 1984, Neotectonics of Hispaniola; Plate motion, sedimentation, seismicity at a retraining bend: *Earth and Planetary Science Letters*, 70, 311-324
- Mann, P., Schubert, C., and Burke, K., 1990. Review of Caribbean neotectonics, in Dengo, G., and Case, J.E., eds., *The Caribbean region*, *Geological Society of America*, H, 307-338.
- Mann, P., Draper, G., and Lewis, J.F. 1991. An overview of the Geologic and Tectonic Development of Hispaniola, in Mann, P., Draper, G., and Lewis, J.F., (eds), *Geologic and Tectonic Development of the North America - Caribbean Plate Boundary in Hispaniola*, *Geological Society of America*, Special Paper 262, 1-28.
- Mann, P., Taylor, F., Edwards, R.L., and Ku, T., 1995. Actively evolving microplate formation by oblique collision and sideways motion along strike-slip faults. An example from the northeast margin of the Caribbean plate, *Tectonophysics*, 246, 1-69.
- Mann, P., Prentice, C.S., Burr, G., Peña, L.R., and Taylor, F.W., 1998. Tectonic geomorphology and paleoseismology of the Septentrional fault system, Dominican Republic, in Dolan, J.F., and Mann, P., eds., *Active Strike-Slip and Collisional Tectonics of the Northern Caribbean Plate Boundary Zone*, *Geological Society of America*, Special Paper 326, 63-124.
- Masclé, A., ed. 1985. *Géodynamique des Caraïbes*, Paris: *Ed. Technip.*, 566 pp.
- Mattson, P.H., 1979. Subduction, buoyant breaking, flipping, and strike-slip faulting in the northern Caribbean, *Journal of Geology*, 87, 293-304.

- Mattson, P.H., 1984. Caribbean Structural Breaks and Plate Movements, *Geological Society of America*, Memoir 162, 131-153.
- Maury, R.C., Westbrook, G.K., Baker, P.E., Bouysse, Ph., and Westercamp, D., 1990. Geology of the Lesser Antilles, in Dengo, G., and Case, J.E., eds., *The Caribbean region: The Geology of North America*, *Geological Society of America*, H, 141-175.
- McCann, W.R., and Pennington, W.D., 1990, Seismicity, large earthquakes, and the margin of the Caribbean Plate, in Dengo, G., and Case, J.E., eds., *The Geology of North America*, H, 291-306.
- Meschede, M., 1998. Geometric Constraints for a near-American origin of the Caribbean Plate, *Fifteenth Caribbean Geological Conference (Abs.)*, Monday June 29-Thursday July 2, University of the West Indies Mona, Kingston 7, Jamaica, 79 p.
- Molnar, P. and Sykes, L.R. 1969. Tectonics of the Caribbean and Middle America Regions from Focal Mechanisms and Seismicity, *Geological Society of America Bulletin*, 80, 1639-1684.
- Montgomery, H., Pessagno, Jr., E.A., Lewis, J.F., and Schellekens, J., 1994. Paleogeography of Jurassic fragments in the Caribbean, *Tectonics*, 13, (2), 725-732.
- Morris, A.E.L., Taner, I., Meyerhoff, H.A., and Meyerhoff, A.A., 1990. Tectonic evolution of the Caribbean region; Alternative hypothesis, in Dengo, G. and Case, J.E., eds., *The Caribbean Region*, *Geological Society of America*, H, 483-510.
- Mullins, H.T., Breen, N., Dolan, J., Wellner, R.W., Petruccione, J.L., Gaylord, M., Andersen, B., Melillo, A.J., Jurgens, A.D., and Orange, D., 1992. Carbonate platforms along the southeast Bahamas-Hispaniola collision zone, *Marine Geology*, 105, 169-209.
- Olivo, Ramon A. 1985. Structural Study of the Hispaniola fault zone [M.A.Thesis]: The City College, New York, New York, 29 p.
- Palmer, H.C. 1963. Geology of the Monción-Jarabacoa Area, Dominican Republic [Ph.D. Thesis]: Princeton University, 256 p.
- Palmer, H.C., 1979. Geology of the Monción-Jarabacoa area, Dominican Republic: in Lidz, B., and Nagle, F., (eds), *Hispaniola; Tectonic focal point of the northern Caribbean; Three geological studies in the Dominican Republic*, *Miami Geological Society*, 29-68.
- Perfit, M.R., and Heezen, B.C. 1978. The geology and evolution of the Cayman Trench, *Geological Society of America Bulletin*, 89, 1155-1174.

- Pindell, J.L. and Dewey, J.F. 1982. Permo-Triassic reconstruction of western Pangea and the evolution of the Gulf of Mexico/Caribbean region. *Tectonics*, 1, 179-212.
- Pindell, J.L., 1985. Alleghenian reconstruction and the subsequent evolution of the Gulf of Mexico, Bahamas and Proto-Caribbean Sea, *Tectonics*, 4, 1-39.
- Pindell, J.L., Cande, S.C., Pitman, W.C., Rowley, D.B., Dewey, J.F., LaBrecque, J. and Haxby, W., 1988. A plate-kinematic framework for models of Caribbean evolution., *Tectonophysics*, 155, 121-138.
- Pindell, J.L., and Barrett, S.F., 1990. Geological evolution of the Caribbean region; A plate tectonic perspective, in Dengo, G., and Case, J.E., eds, *The Caribbean region, Geological Society of America, The Geology of North America*, H, 405-432.
- Pindell, J.L. 1990. Arguments for a Pacific origin of the Caribbean Plate: in Larue, D.K. and Draper, G. (eds), *Transactions of the 12<sup>th</sup> Caribbean Geological Conference*, St. Croix, U.S. Virgin Islands, 7<sup>th</sup>-11<sup>th</sup> August 1989, Miami Geological Society, Florida, 1-4.
- Pindell, J.L. 1994. Evolution of the Gulf of Mexico and the Caribbean, in Donovan, S., and Jackson, T.A., (eds), *Caribbean Geology: An Introduction. University of the West Indies Publishers Association*, Kingston, Jamaica, 13-39.
- Prentice, C., Mann, P., Taylor, F.W., Burr, G., and Valastro, S., Jr., 1993. Paleoseismicity of the North America-Caribbean plate boundary (Septentrional fault), Dominican Republic, *Geology*, 21, 49-52.
- Ramsay, J.G., 1967. *Folding and fracturing of rocks*: New York, McGraw-Hill, 568 p.
- Ramsay, J.G., 1980. Shear zone geometry: a review, *Journal of Structural Geology*, 2, 83-99.
- Riedel, W. 1929. Zur Mechanik geologischer Brucherscheidungen. Ein Beitrag zum Problem der "Fiederspalten": *Centralblatt für Mineralogie, Geologie, und Paleontologie*, Part B. 354-368.
- Riemer, V.W. 1978. Results of geological investigations in the northwestern part of the Dominican Republic. *Neues Jahrbuch Geologisches Paleontologisches Monatsheft*, 35, 162-172.
- Rodgers, D.A. 1980. Analysis of pull-apart basin development produced by *en echelon* strike slip faults: in Ballance, P.F., and Reading, H.G. (eds). *Sedimentation in oblique-slip mobile zones, International Association of Sedimentology, Special Publication 4*, 27-41.

Rosencrantz, E., Ross, M., and Sclater, J.G., 1988. Age and spreading history of the Cayman Trough as determined from depth, heat flow, and magnetic anomalies: *Journal of Geophysical Research*, 93, 2141-2157.

Rowley, D.B. and Pindell, J.L., 1989. End Paleozoic-early Mesozoic western Pangean reconstruction and its implications for the distribution of Precambrian and Paleozoic rocks around Meso-America, *Precambrian Research*, 42, 411-444.

Salvadore, A. and Green, A.G., 1982. Opening of the Caribbean Tethys, geology of the Alpine chain born of the Tethys, Memoir of the 26<sup>th</sup> International Geological Congress, *Bureau de Recherches Geological et Minerologie*, 115, 224-229.

Saunders, J.B.; Jung, P.; Geister, J. and Biju-Duval, B., 1982. The Neogene of the South Flank of the Cibao Valley, Dominican Republic: A stratigraphic Study, *Transactions of the 9<sup>th</sup> Caribbean Geological Conference*, Santo Domingo, Amigo del Hogar Publishers, 16<sup>th</sup>-20<sup>th</sup> August, 1980, 151-160.

Saunders, J., Jung, P., and Biju-Duval, B. 1986. Neogene paleontology in the northern Dominican Republic; 1, Field surveys, lithology, environment, and age, *Bulletins of American Paleontology*, 89, (323), 79 p.

Schell, B.A., and Tarr, A.C., 1978. Plate tectonics of the northeastern Caribbean Sea region, *Geologie En Mijnbouw*, 57, 319-324.

Smith, A.L., Schellekens, J.H., and Muriel Díaz, A.-L., 1998. Batholiths as markers of tectonic change in the northeastern Caribbean, in Lidiak, E.G., and Larue, D.K., eds., *Tectonics and Geochemistry of the Northeastern Caribbean*, *Geological Society of America*, Special Paper 322, 99-122.

Sykes, L.R., and Ewing, M. 1965. The seismicity of the Caribbean region. *Journal of Geophysical Research*, 70, 5065-5074.

Sykes, L.R., McCann, W.R., and Kafka, A.L. 1982. Motion of Caribbean plate during the last 7 million years and implications for earlier Cenozoic movements, *Journal of Geophysical Research*, 87, 10656-10676.

Sylvester, A.G., 1988. Strike-slip faults, *Geological Society of America Bulletin*, 100, 1666-1703.

Theyer, P., 1983. An Obducted Ophiolite Complex in the Cordillera Central of the Dominican Republic, *Geological Society of America Bulletin*, 94, 1438-1441.

- Tchalenko, J.S., and Ambraseys, N.N., 1970. Structural analysis of the Dasht-e Bayaz (Iran) earthquake fractures, *Geological Society of America Bulletin*, 81, 41-60.
- Vaughan, T.W., and 5 others. 1921. A geological reconnaissance of the Dominican Republic. *Geological Survey of the Dominican Republic Memoir*, 1, 268 p.
- Vespucchi, P., 1989. Summary of trace element and isotope data, late Cretaceous volcanics, Hispaniola: in Duque-Caro, H. (ed.), *Transactions of the Tenth Caribbean Geological Conference*, Cartagena, Colombia, 14<sup>th</sup>-20<sup>th</sup> August, 1983, 467-472.
- Vogt, P.R., Anderson, C.N. and Bracey, D.R., 1971. Mesozoic magnetic anomalies, seafloor spreading, and geomagnetic reversals in the southwestern north Atlantic, *Journal of Geophysical Research*, 76, 4796-4823.
- Walper, J.L. 1982. Geologic Evolution of the Greater Antilles: in Duque-Caro, H., (ed), *Transactions of the 9<sup>th</sup> Caribbean Geological Conference*, Santo Domingo, Dominican Republic, Amigo del Hogar Publishers, 16<sup>th</sup>-20<sup>th</sup> August, 1980, 13-22.
- Wilcox, R.E., Harding, T.P., and Seely, D.R., 1973. Basic wrench tectonics: *American Association of Petroleum Geologists Bulletin*, 57, 74-96.
- Wilson, J.T., 1966. Did the Atlantic close and then reopen?, *Nature*, 211, 676-680.
- Winslow, M.A., and McCann, W.R., 1985. Neotectonics of a subduction/strike-slip transition zone; The northeastern Dominican Republic, *Geological Society of America, Abstracts with Programs*, 17, 753.
- Winslow, M.A., Guglielmo, G., Jr., Nadai, A.C., Vega, L.A., and McCann, W.R. 1991. Tectonic Evolution of the San Francisco Ridge of the Eastern Cibao Basin, Northeastern Hispaniola: in Mann, P., G. Draper, and J.F., Lewis. (eds), Geologic and tectonic development of the North America-Caribbean plate boundary in Hispaniola. *Geological Society of America, Special Paper* 262, 301-313.

## **NOTE TO USERS**

**Oversize maps and charts are microfilmed in sections in the following manner:**

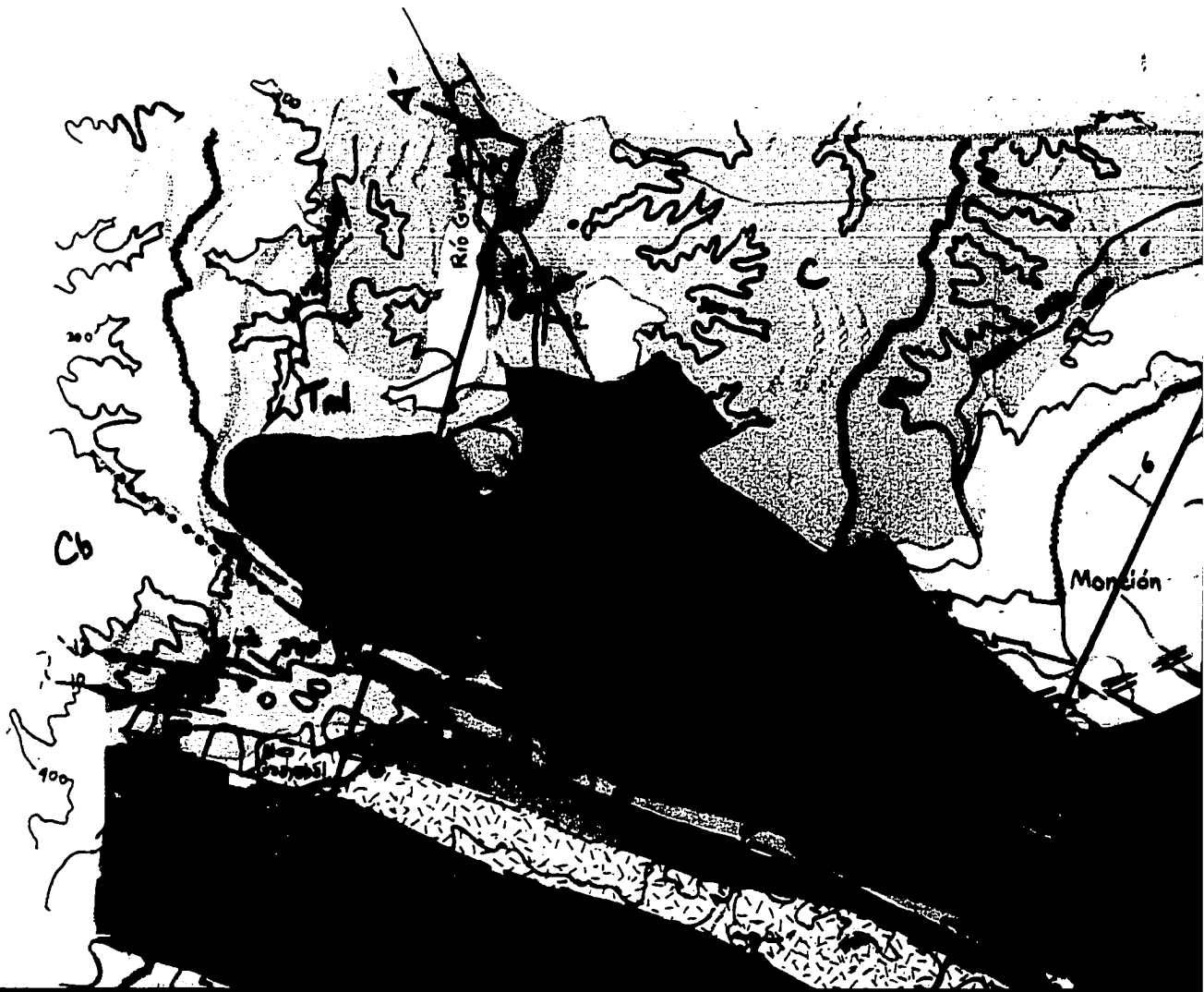
**LEFT TO RIGHT, TOP TO BOTTOM, WITH  
SMALL OVERLAPS**

**UMI**



71°10'

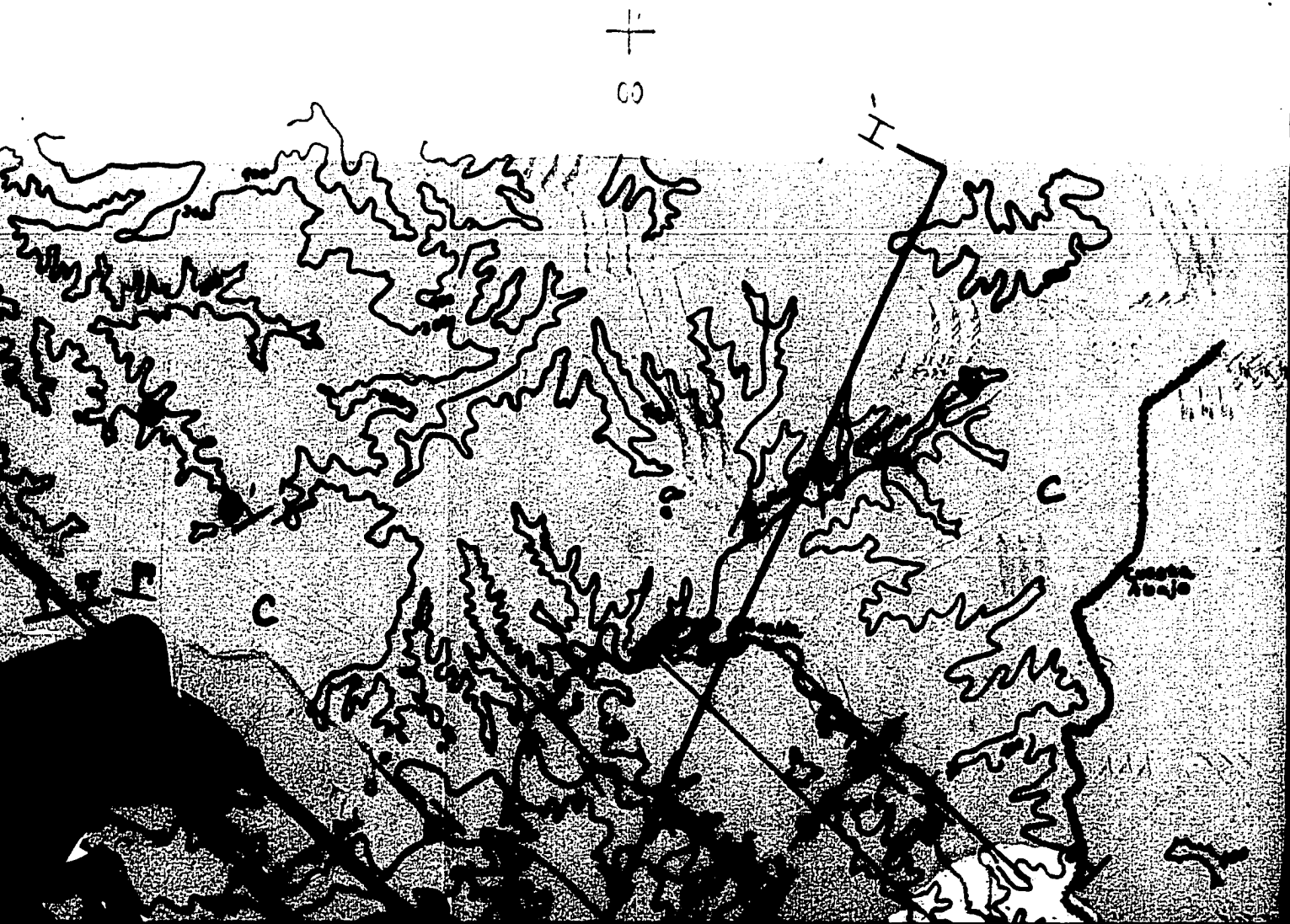
19°30'





71° 00'  
19° 30'





+

03

H

C

C

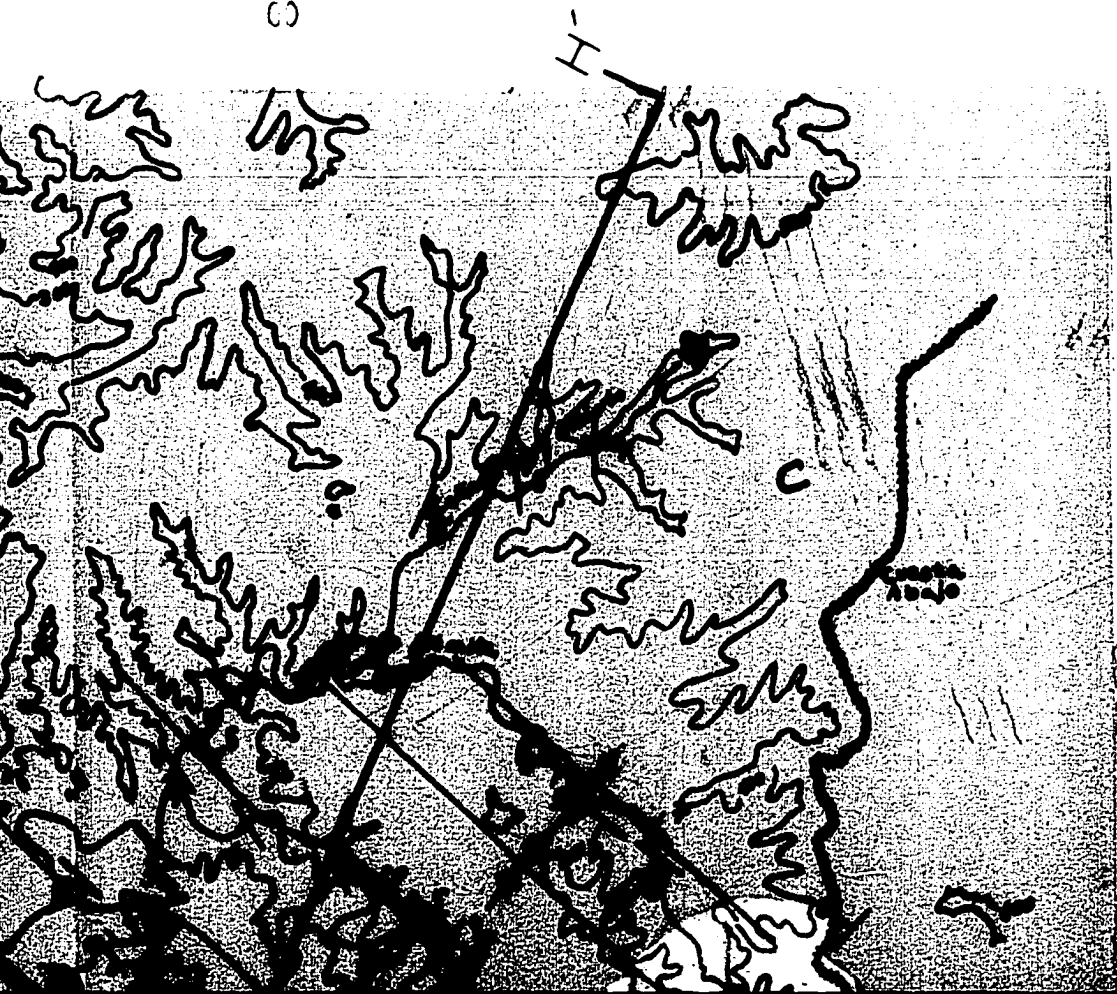
F

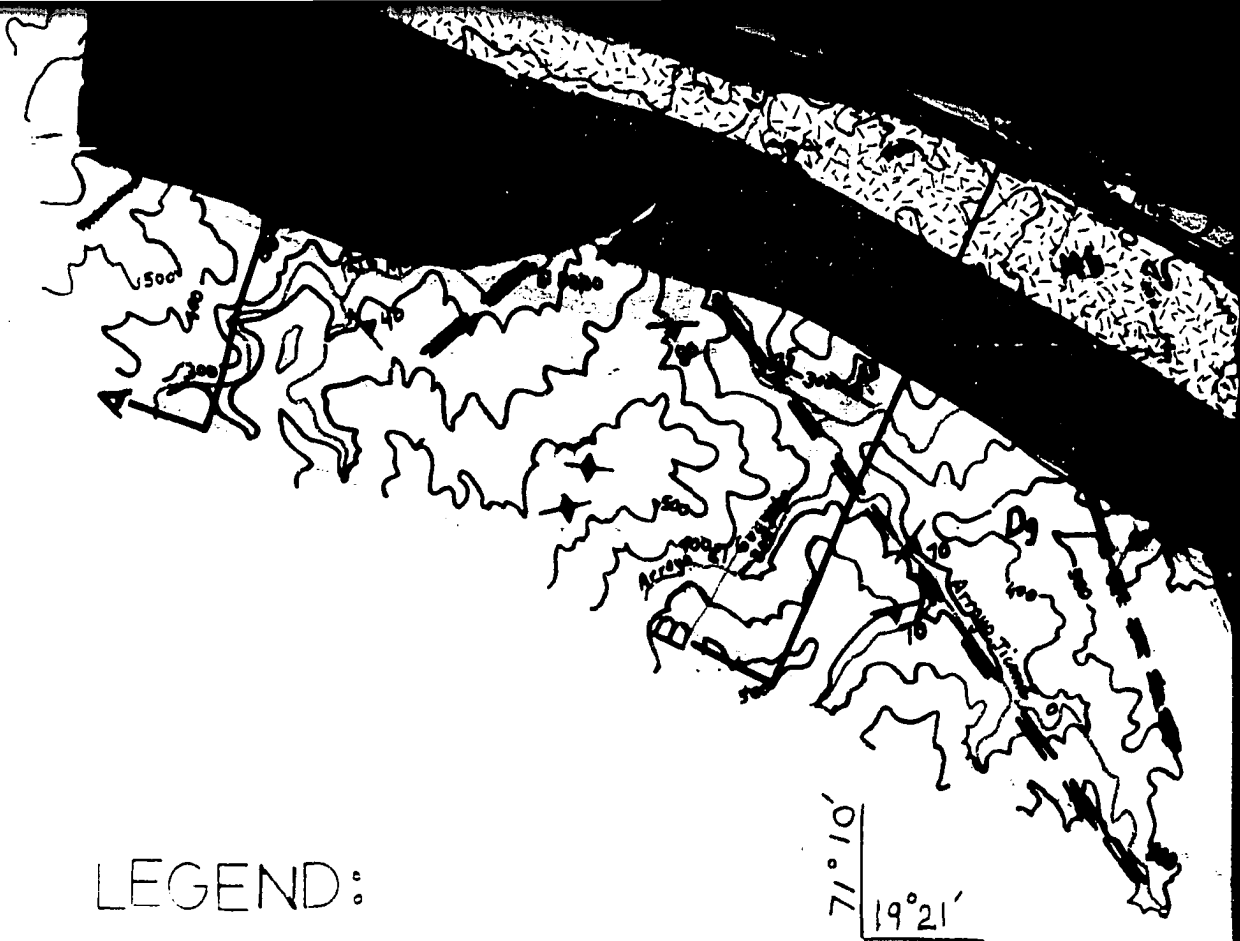
1000  
1000

19°30'  
70°50'

+

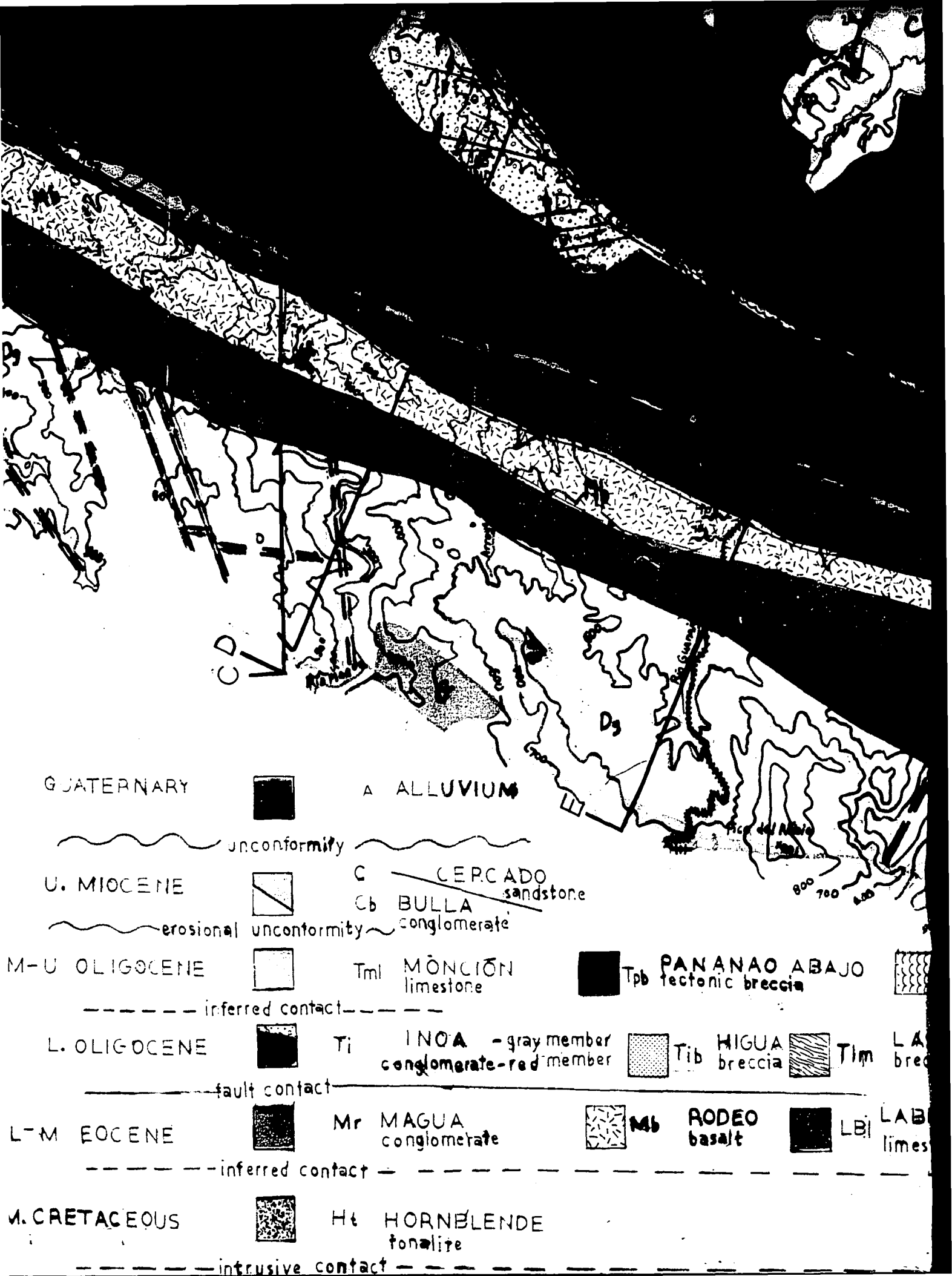
00

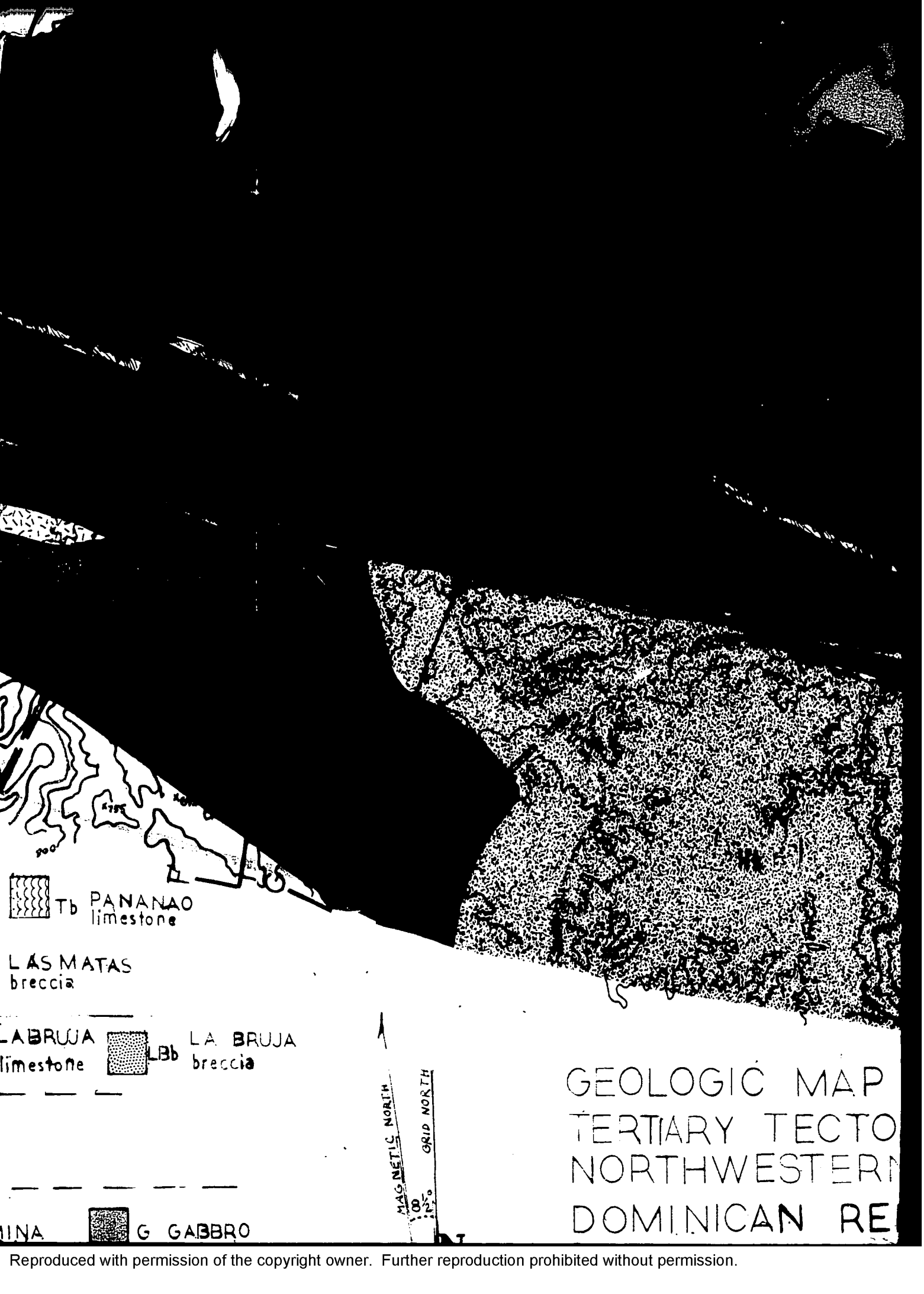




LEGEND:

- |  |  |  |                                    |            |
|--|--|--|------------------------------------|------------|
|  | ANTICLINE  |  | BEARING AND<br>PLUNGE OF FOLD AXIS |            |
|  | SYNCLINE   |  | HORIZONTAL<br>BEDDING              |            |
|  | STRIKE and DIP<br>of BEDS                              |  | VERTICAL<br>BED                    | QUATER     |
|  | STRIKE and DIP<br>of FOLIATION                         |  | VERTICAL<br>FOLIATION              | U. MIOC    |
|  | CRUMPLED<br>FOLIATION                                  |  | ROAD                               |            |
|  | OVERTURNED<br>BEDDING                                  |  | RIVER                              |            |
|  | STRIKE-SLIP<br>DISPLACEMENT                            |  | TOPOGRAPHIC<br>CONTOUR             | M-U OLIG   |
|  | FAULT CONTACT  |  |                                    | L. OLIG    |
|  | SENSE OF SLIP ON<br>STRIKE-SLIP AND<br>DIP-SLIP FAULTS |  |                                    | L-M EOC    |
|  | LESS WELL LOCATED<br>CONTACT                           |  |                                    | M. CRETACE |
|  | COVERED CONTACT  |  |                                    |            |
|  | INFERRED FAULT   |  |                                    |            |





Tb PANANAO limestone

LAS MATAS breccia

LA BRUJA limestone Lb LA BRUJA breccia

G GABBRO

MAGNETIC NORTH  
GRID NORTH

GEOLOGIC MAP  
TERTIARY TECTONIC UNITS  
NORTHWESTERN  
DOMINICAN REPUBLIC



MAP  
TECTONICS OF THE HISPANIOLA FAULT ZONE  
NERN PIEDMONT OF THE CORDILLERA CENTR  
REPUBLIC

2000

SCALE: 1:50,000

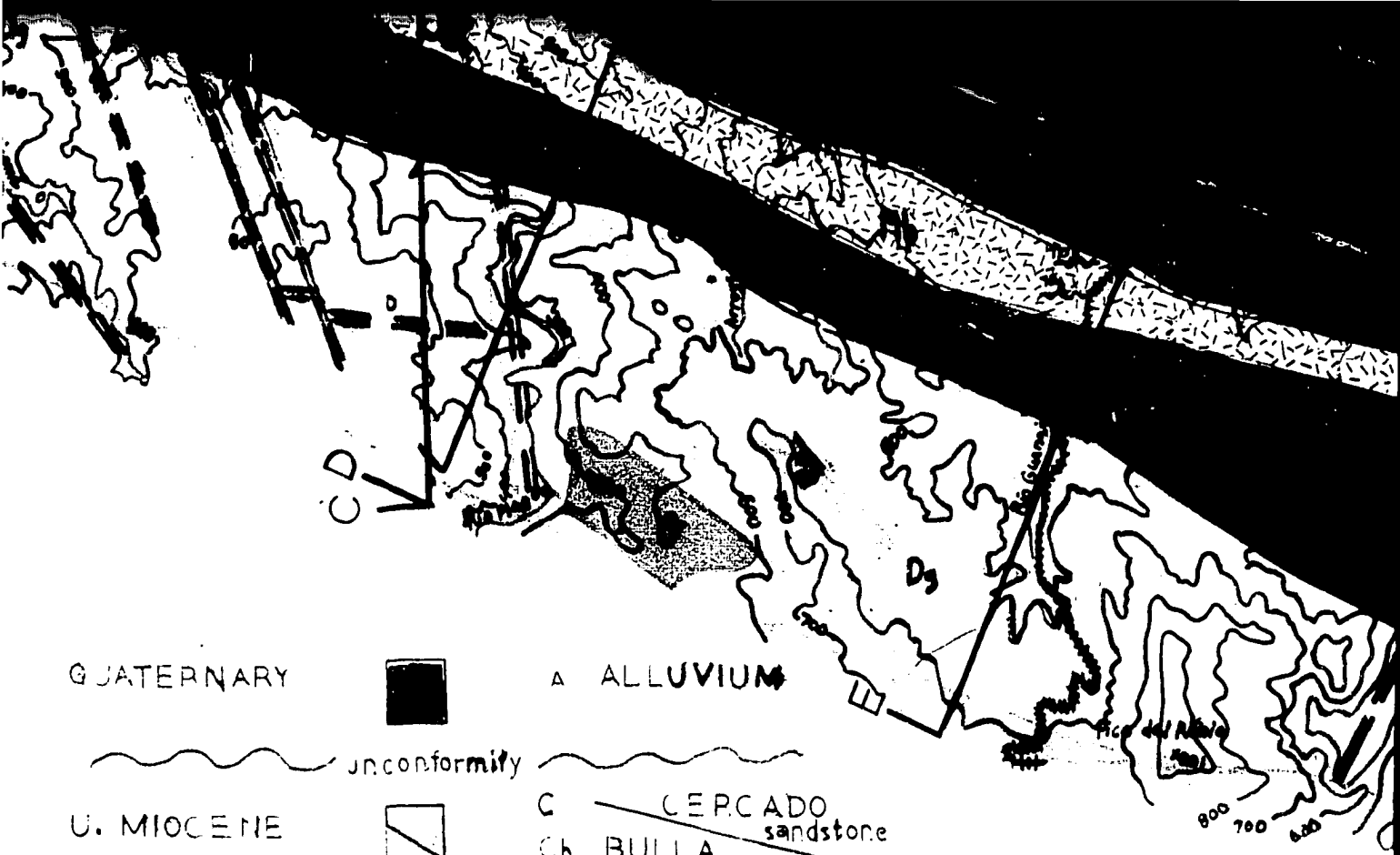


SPANIOLA FAULT ZONE IN THE  
THE CORDILLERA CENTRAL,



# LEGEND:

- |  |  |  |                                 |               |
|--|--|--|---------------------------------|---------------|
|  | ANTICLINE  |  | BEARING AND PLUNGE OF FOLD AXIS |               |
|  | SYNCLINE   |  | HORIZONTAL BEDDING              |               |
|  | STRIKE and DIP of BEDS                           |  | VERTICAL BED                    | QUATERNARY    |
|  | STRIKE and DIP of FOLIATION                      |  | VERTICAL FOLIATION              | U. MIOCENE    |
|  | CRUMPLED FOLIATION                               |  | ROAD                            | M-U OLIGOCENE |
|  | OVERTURNED BEDDING                               |  | RIVER                           | L. OLIGOCENE  |
|  | STRIKE-SLIP DISPLACEMENT                         |  | TOPOGRAPHIC CONTOUR             | L-M EOCENE    |
|  | FAULT CONTACT                                    |  |                                 | M. CRETACEOUS |
|  | SENSE OF SLIP ON STRIKE-SLIP AND DIP-SLIP FAULTS |  |                                 | L. CRETACEOUS |
|  | LESS WELL LOCATED CONTACT                        |  |                                 | L. JURASSIC   |
|  | COVERED CONTACT                                  |  |                                 |               |
|  | INFERRED FAULT                                   |  |                                 |               |
|  | FAULT CONTACT WITH DIP                           |  |                                 |               |
|  | LINE OF CROSS SECTION                            |  |                                 |               |



QUATERNARY



A ALLUVIUM

~ ~ ~ ~ ~ unconformity

U. MIOCENE



C CERCADO sandstone

Cb BULLA conglomerate

~ ~ ~ ~ ~ erosional unconformity

800 700 600

M-U OLIGOCENE



Tml MÓNCIÓN limestone



Tpb PANANAO ABAJO tectonic breccia



- - - - - inferred contact - - - - -

L. OLIGOCENE



Ti INOA - gray member conglomerate-red member



Tib HIGUA breccia



Tim LA bre

— — — — — fault contact — — — — —

L-M EOCENE



Mr MAGUA conglomerate



Mb RODEO basalt



LBj LAE lime

- - - - - inferred contact - - - - -

M. CRETACEOUS



Ht HORNELENDE tonalite

- - - - - intrusive contact - - - - -

L. CRETACEOUS



D DUARTE subgreenschist



Dg DUARTE greenschist



Am AMIN schist

L. JURASSIC



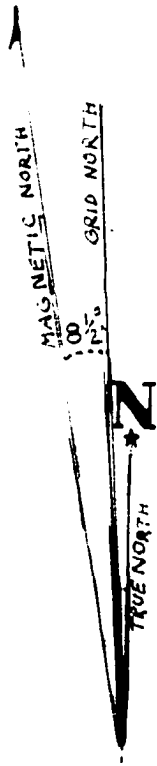


Tb PANANAO limestone

LAS MATAS breccia

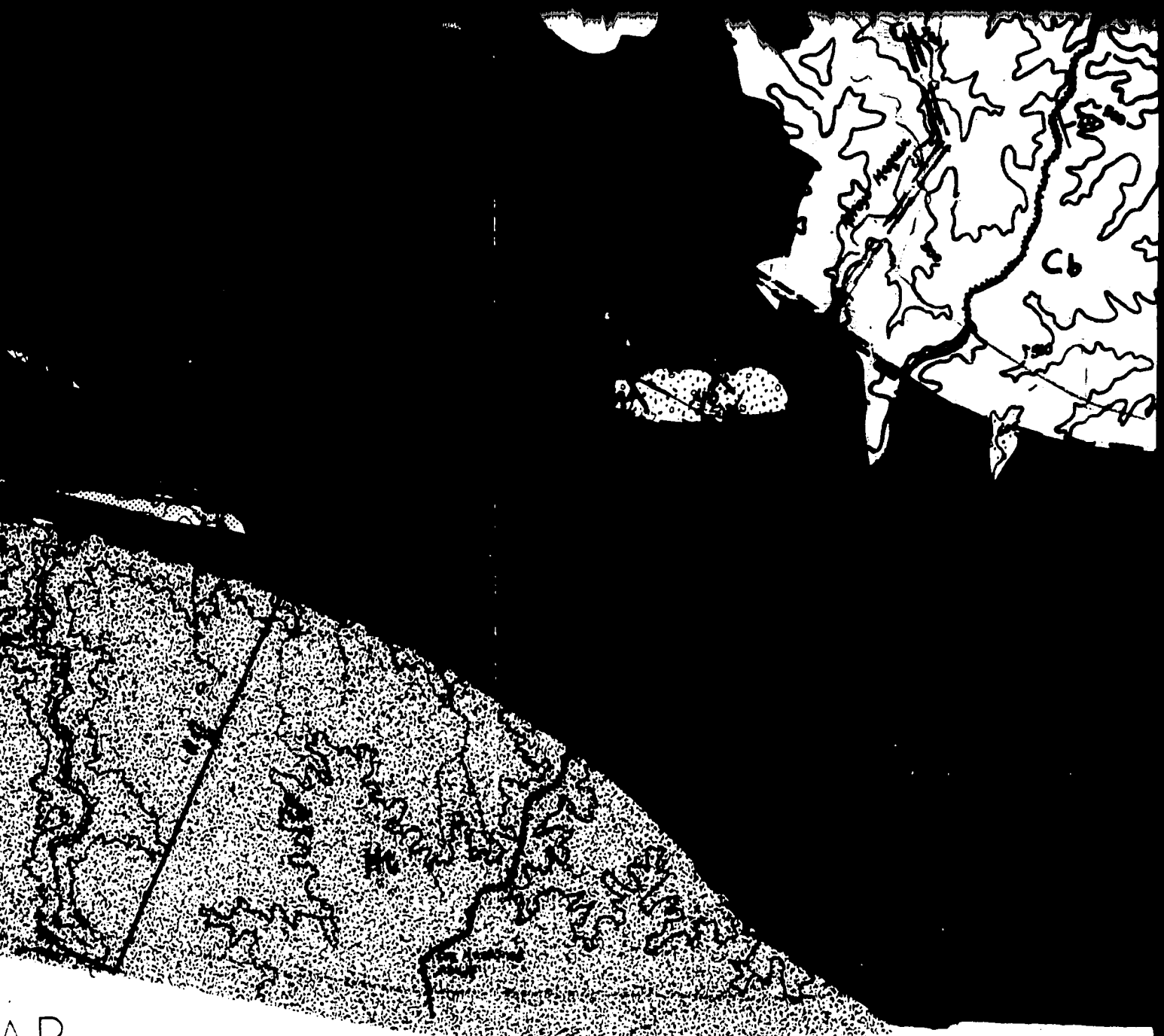
LABRUJA limestone  
 LA BRUJA breccia

MINA list  
 G GABBRO



# GEOLOGIC MAP TERTIARY TECTONIC NORTHWESTERN DOMINICAN REPUBLIC

Geology: Andrew Jay Coleman 2000  
 Cartography:  
 San José de las Matas 1938  
 6074 III E733 Edición 3 ICM D  
 Monción 1986  
 5974 II E733 Edición 3 ICM D  
 Instituto Cartográfico de Militar, R  
 in collaboration with  
 Defense Mapping Agency, USA



MAP  
 TECTONICS OF THE HISPANIOLA FAULT ZONE  
 NORTHERN PIEDMONT OF THE CORDILLERA CENTRAL  
 REPUBLIC

Scale 1:50,000



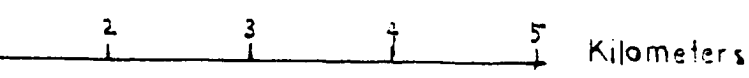
ELEVATIONS IN METERS

CM DMA  
 CM DMA  
 Militar, RD  
 A

THE CITY UNIVERSITY OF NEW YORK  
 NEW YORK, NEW YORK



PANIOLA FAULT ZONE IN THE  
E CORDILLERA CENTRAL,



METERS

SITY OF NEW YORK

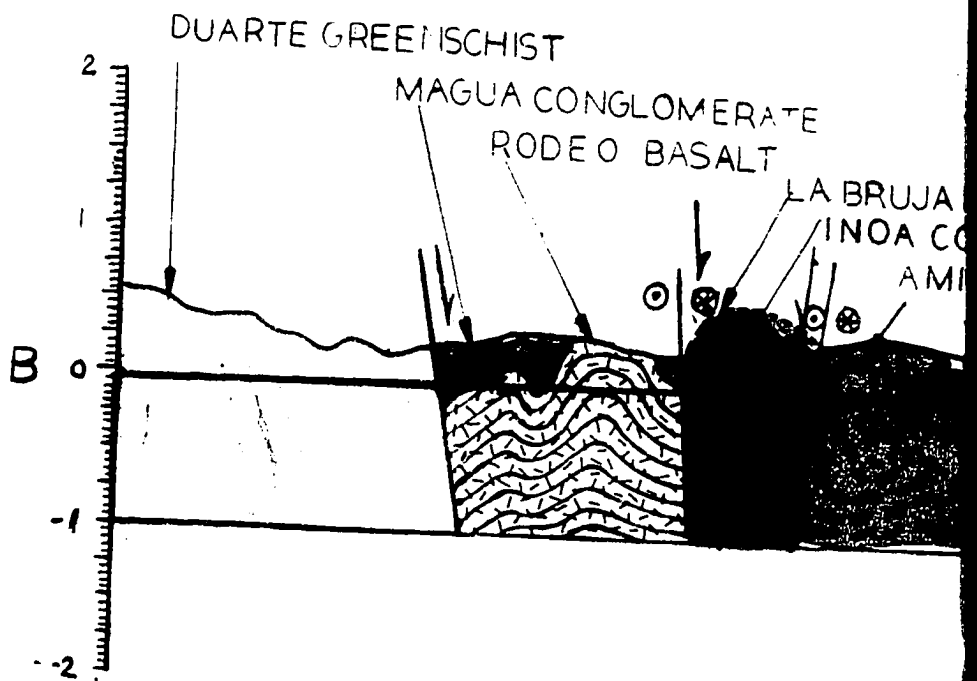
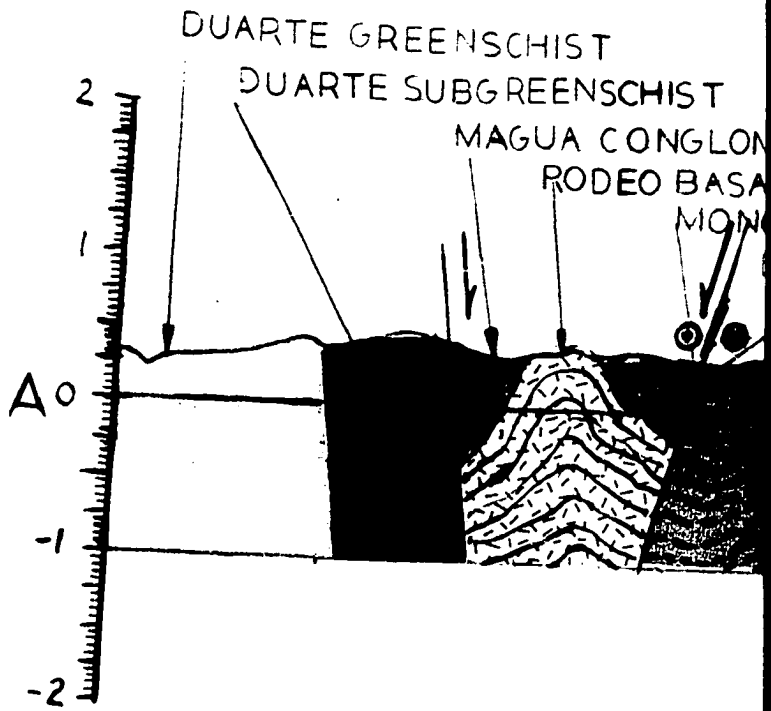
## **NOTE TO USERS**

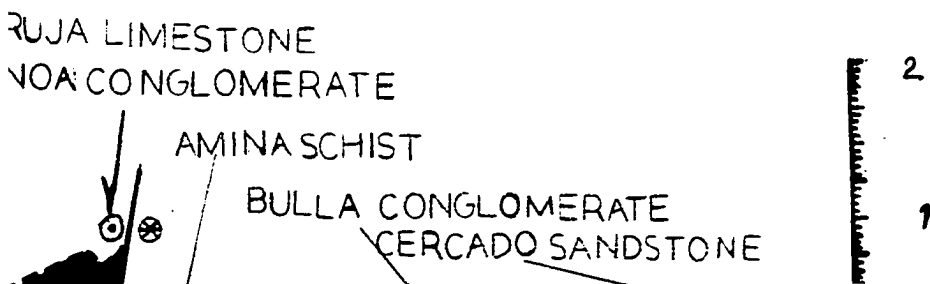
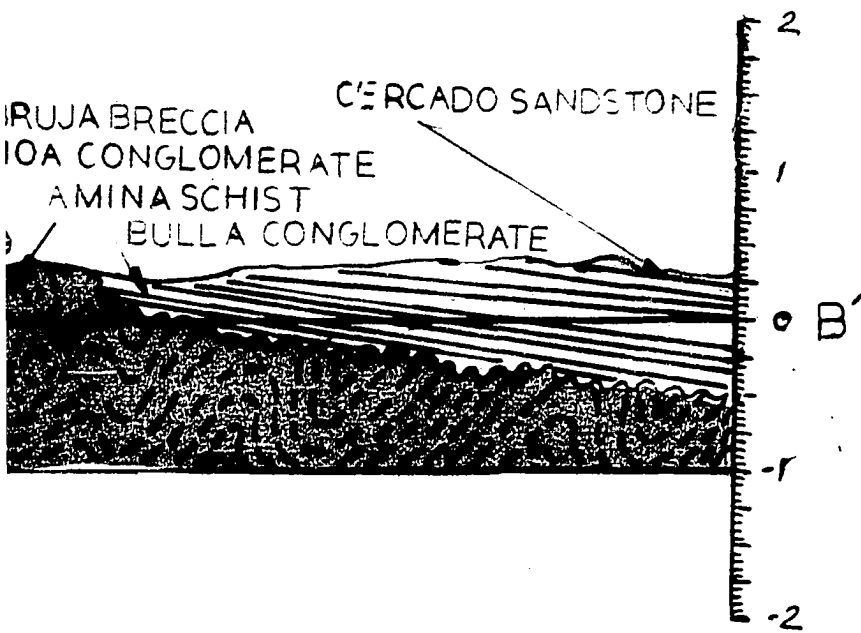
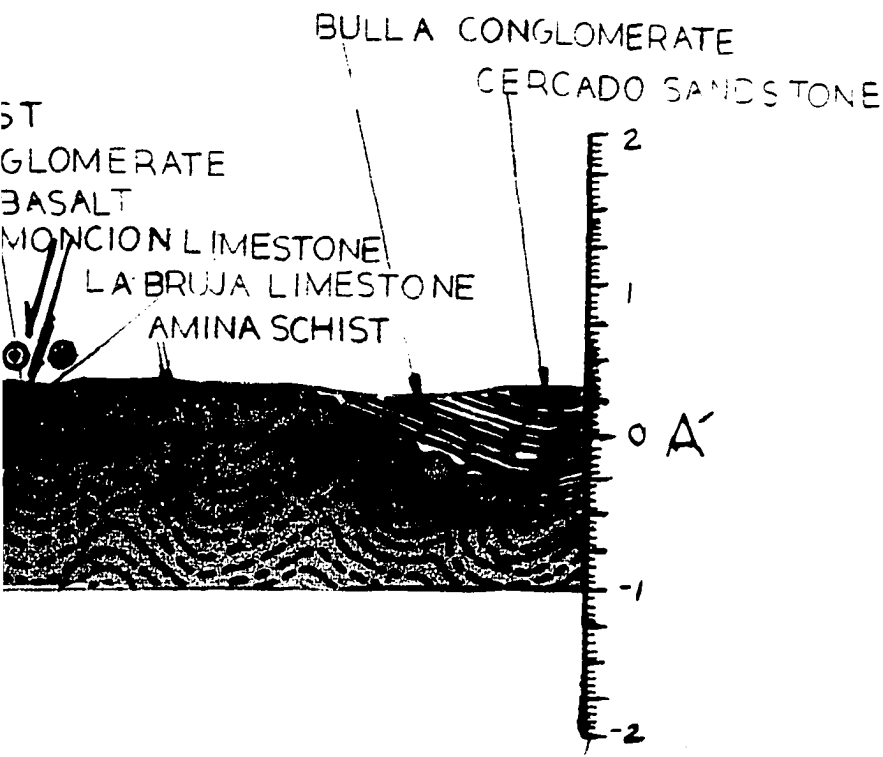
**Oversize maps and charts are microfilmed in sections in the following manner:**

**LEFT TO RIGHT, TOP TO BOTTOM, WITH  
SMALL OVERLAPS**

**UMI**

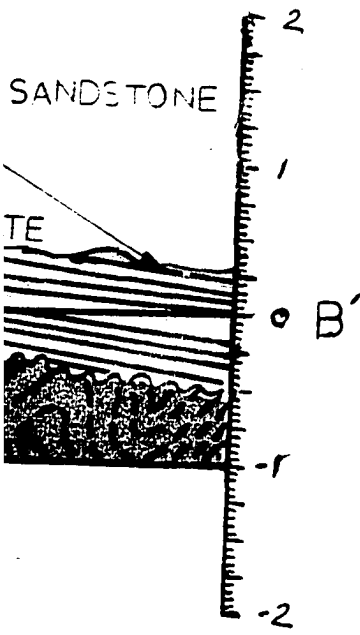
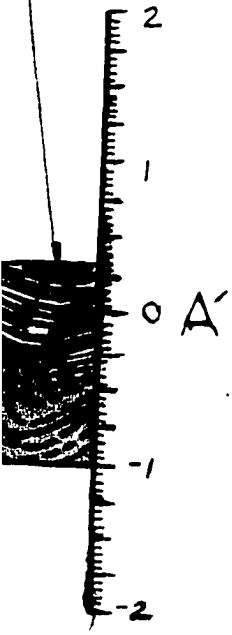




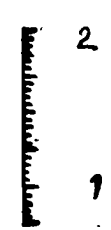


CROSS-SECTIONS  
 TERTIARY TECTONICS OF THE HISPANIOLA  
 PLATEAU IN THE NORTHWESTERN PLATEAU  
 OF THE CORDILLERA CENTRAL, DOMINICAN REPUBLIC

CONGLOMERATE  
CERCADO SANDSTONE

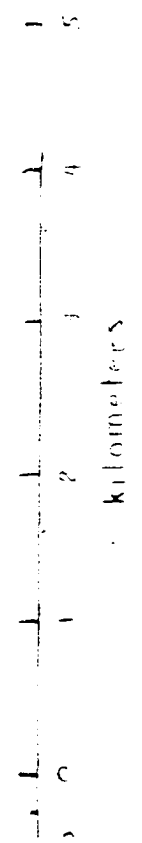


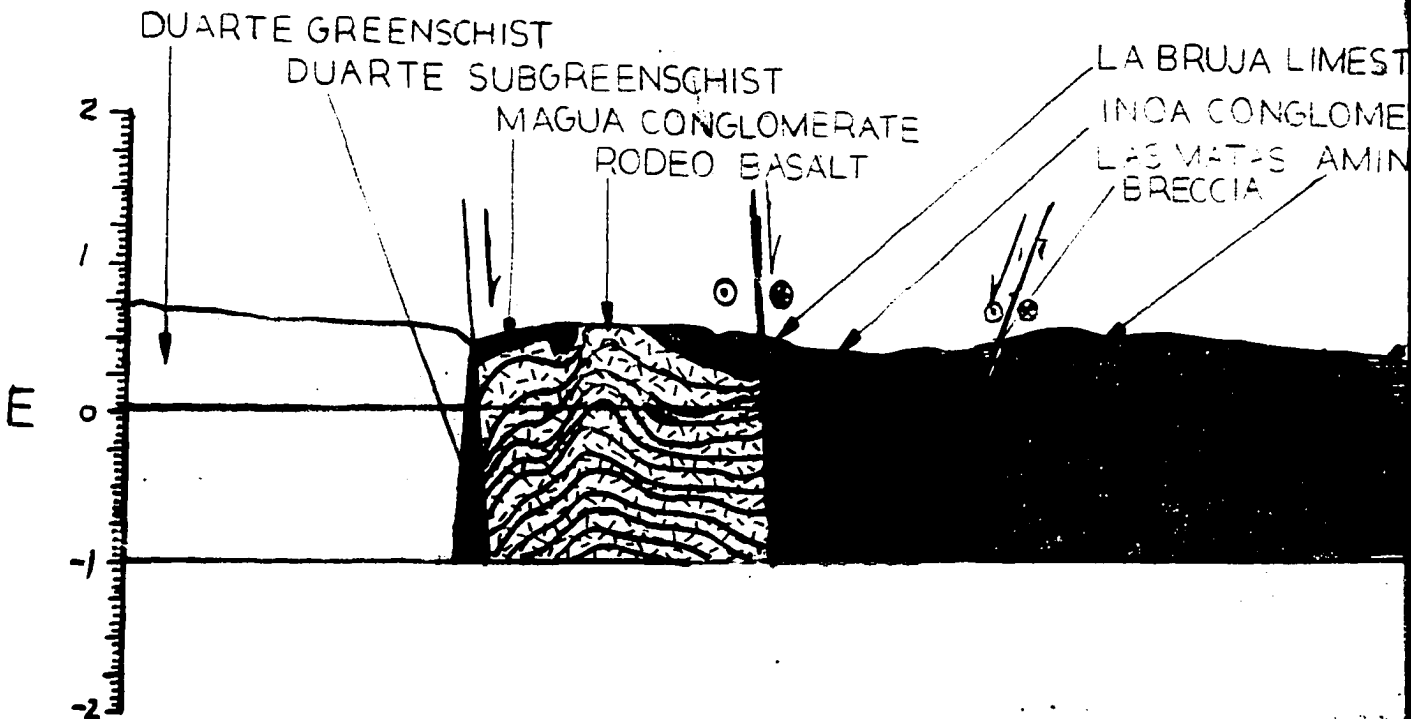
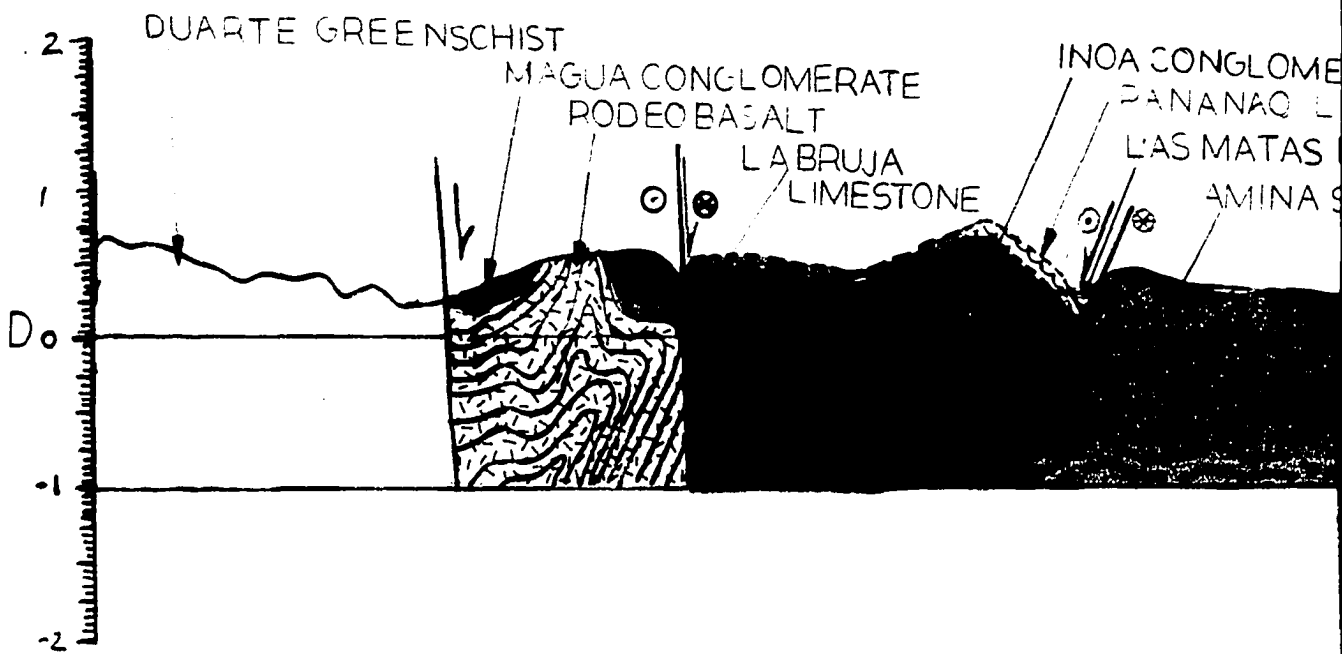
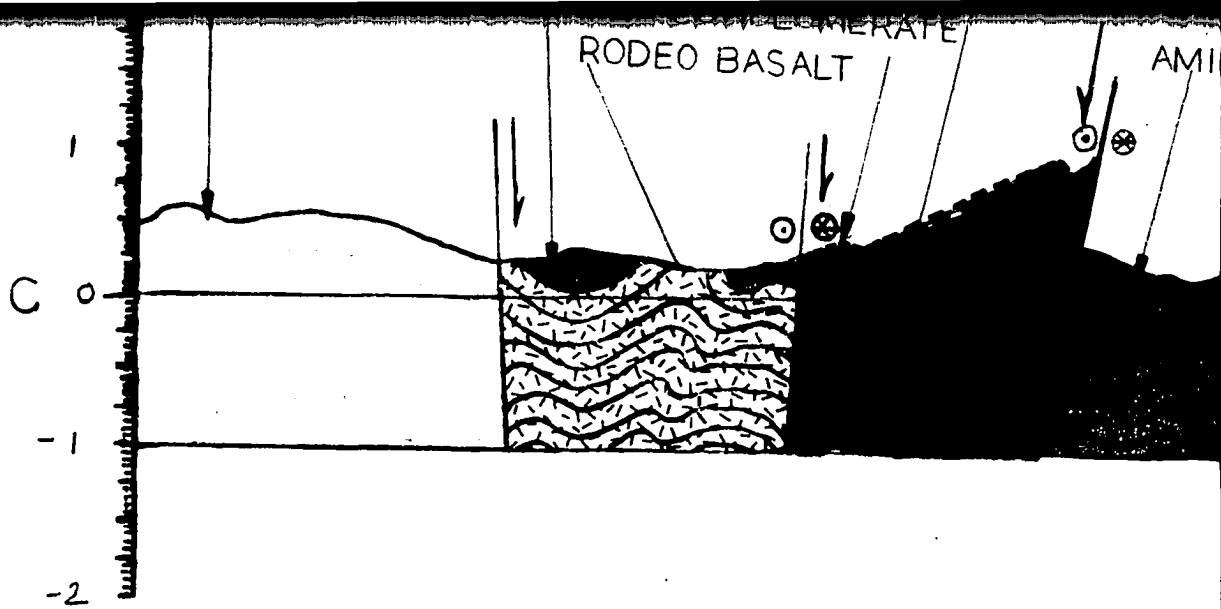
CONGLOMERATE  
CERCADO SANDSTONE

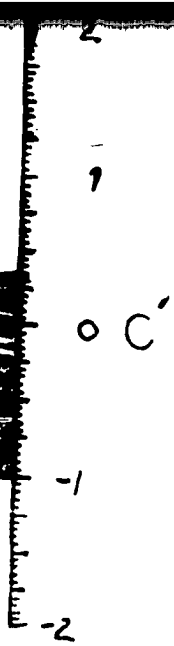
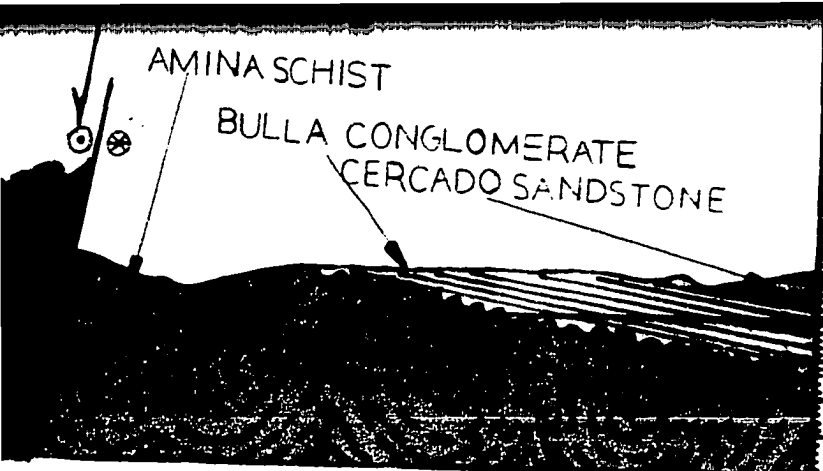


CROSS-SECTIONS OF TERTIARY TECTONICS OF THE HISPANIOLA PLATEAU ZONE IN THE NORTHWESTERN PIEDMONT OF THE CORDILLERA CENTRAL, DOMINICAN REPUBLIC

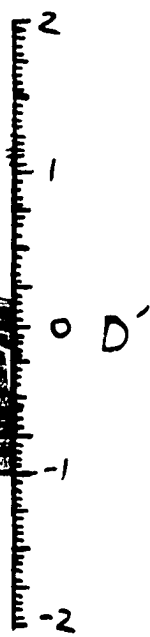
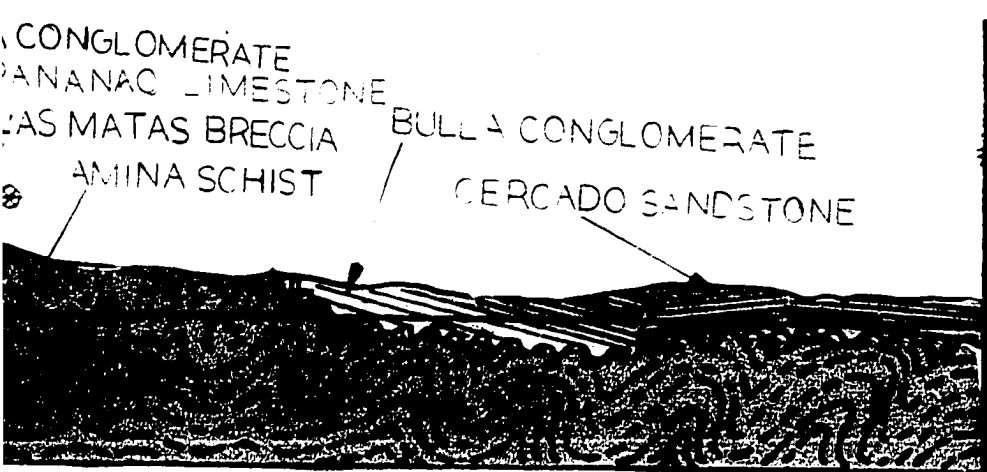
SCALE: 1:50,000







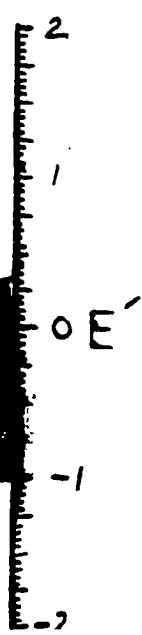
CROSS-SECTION  
 TERTIARY  
 FAULT ZONE  
 OF THE



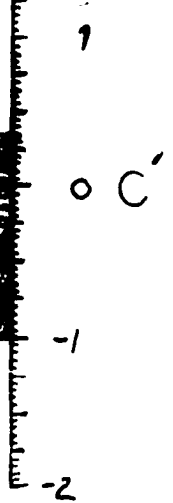
THE CITY UNIVERSITY OF NEW YORK  
 NEW YORK, NEW YORK

ANDREW JAY COLEMAN, 2000

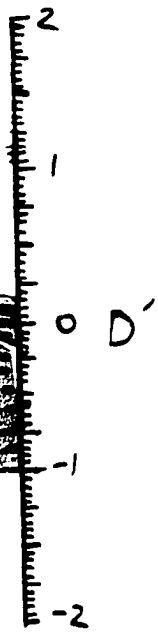
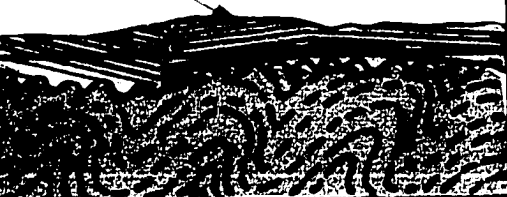
Quadrangles:



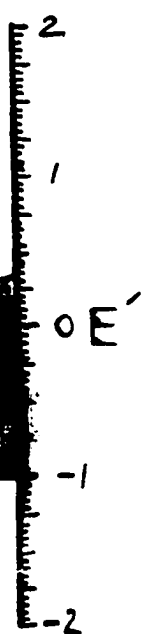
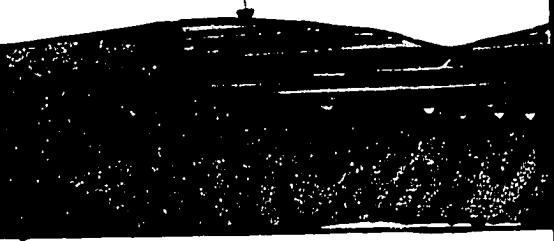
MERATE  
SANDSTONE



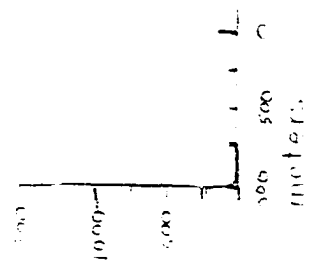
A CONGLOMERATE  
CERCADO SANDSTONE



CONGLOMERATE  
CERCADO SANDSTONE



CROSS  
SECTION  
OF THE  
TERTIARY  
FAULT ZONE



THE CITY UNIVERSITY OF NEW YORK

NEW YORK, NEW YORK

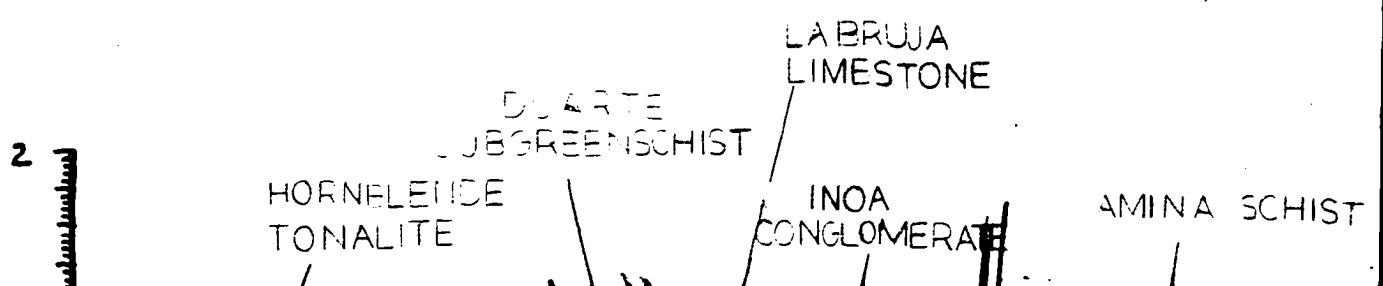
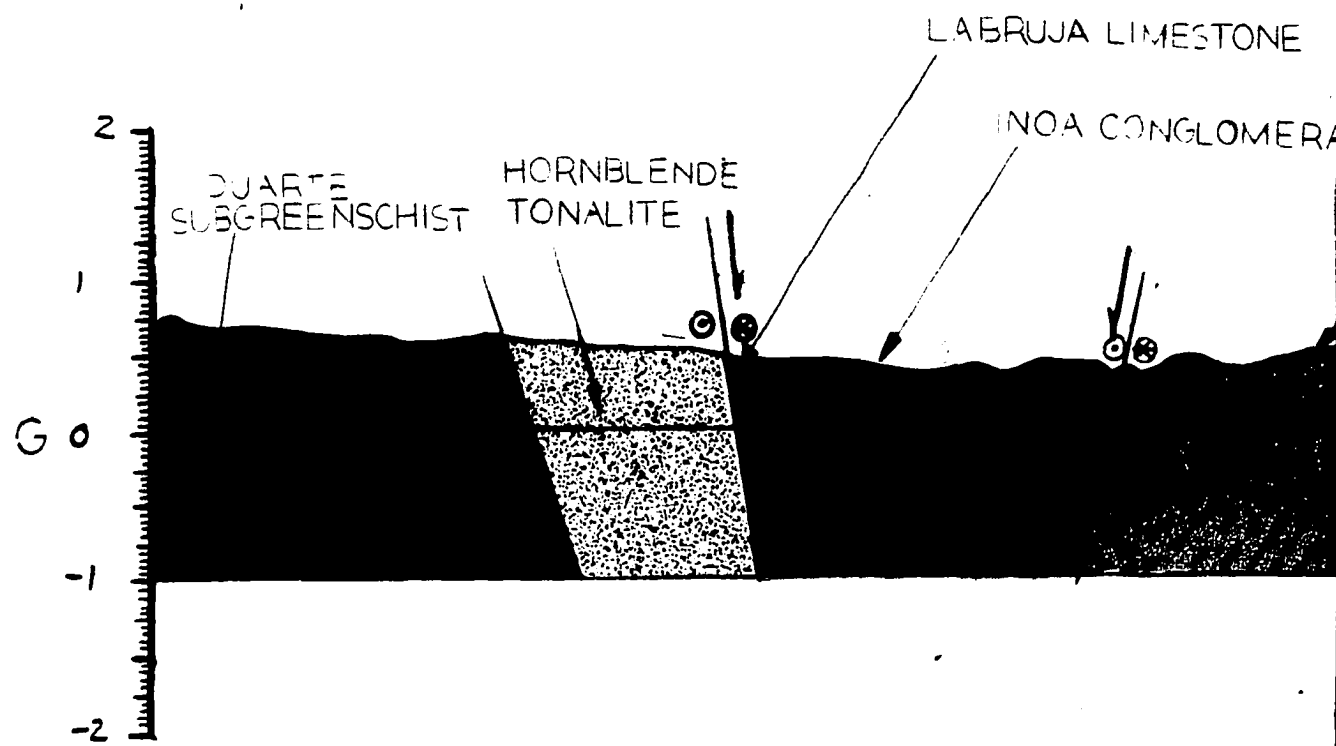
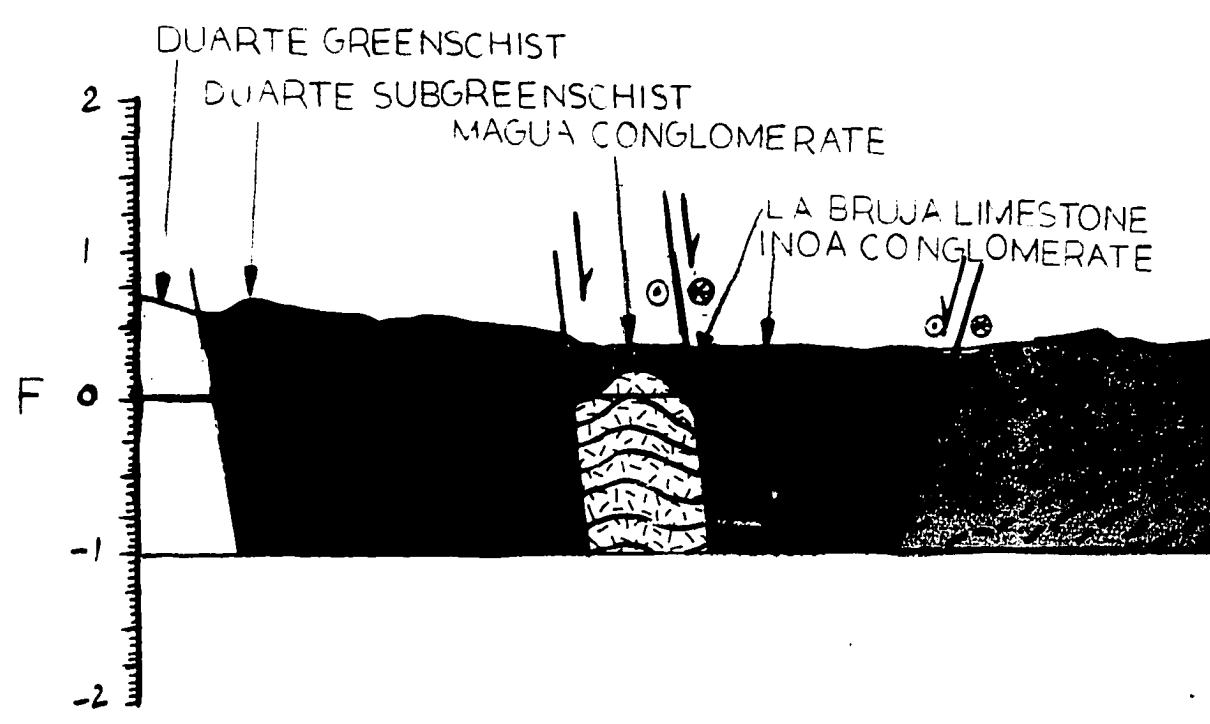
ANDREW JAY COLLEMAN 2000

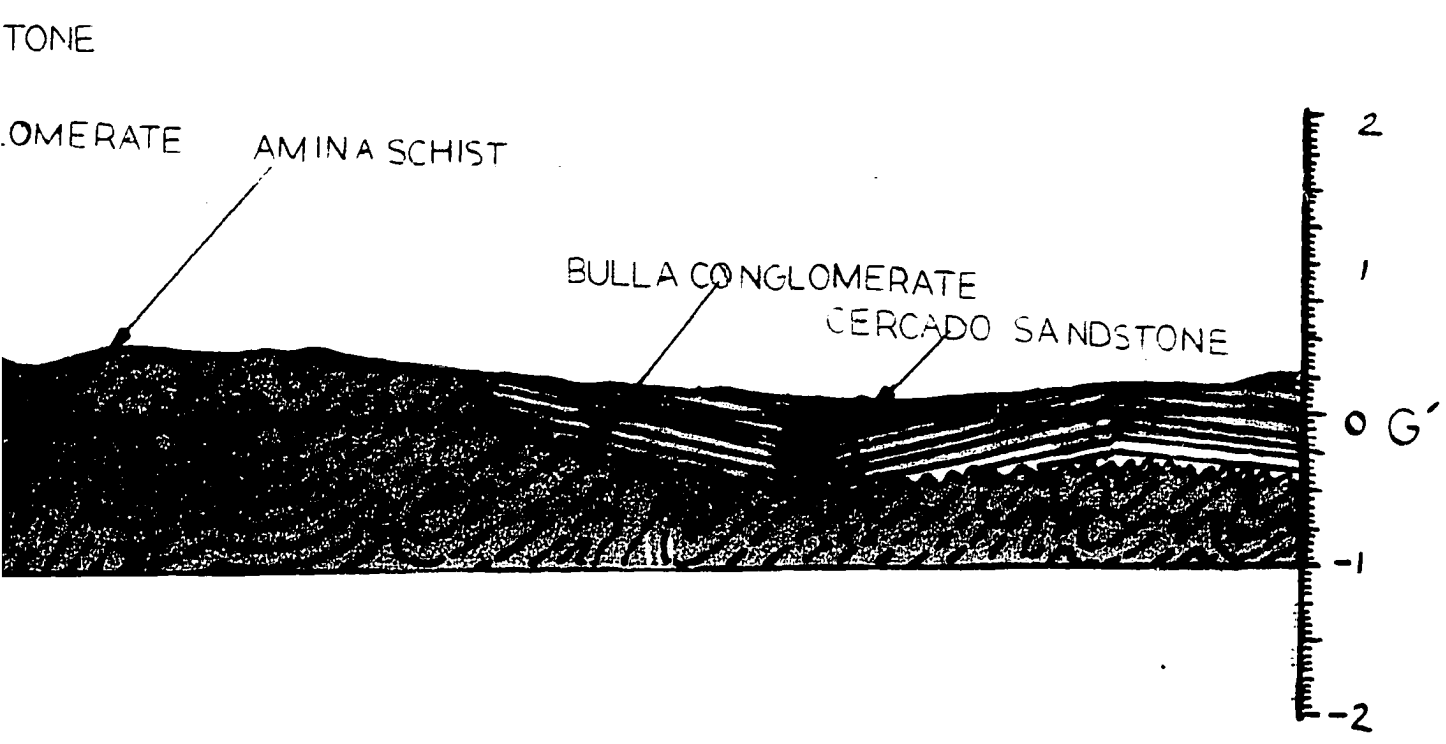
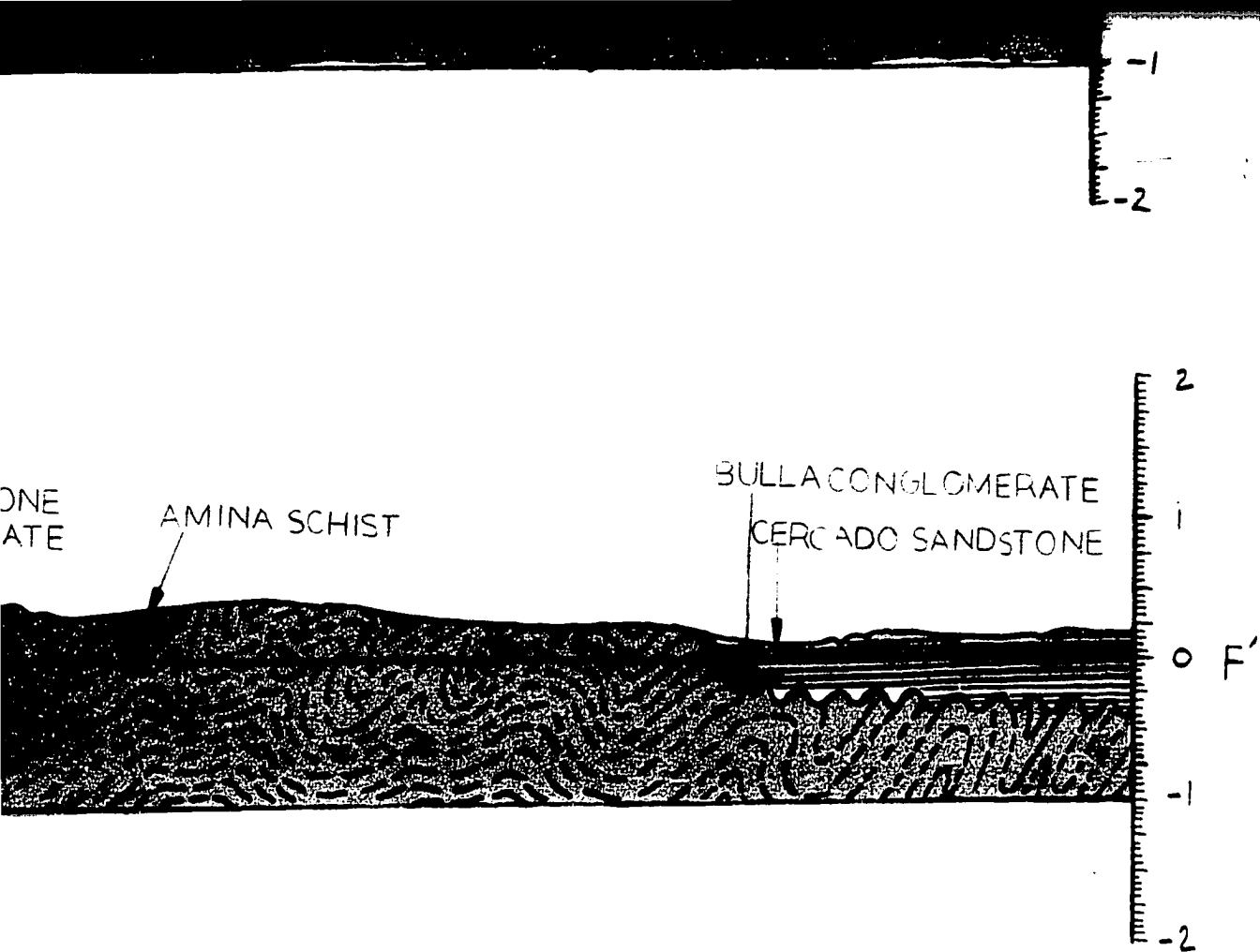
Quadrangles:

San José de las Matas

Monción

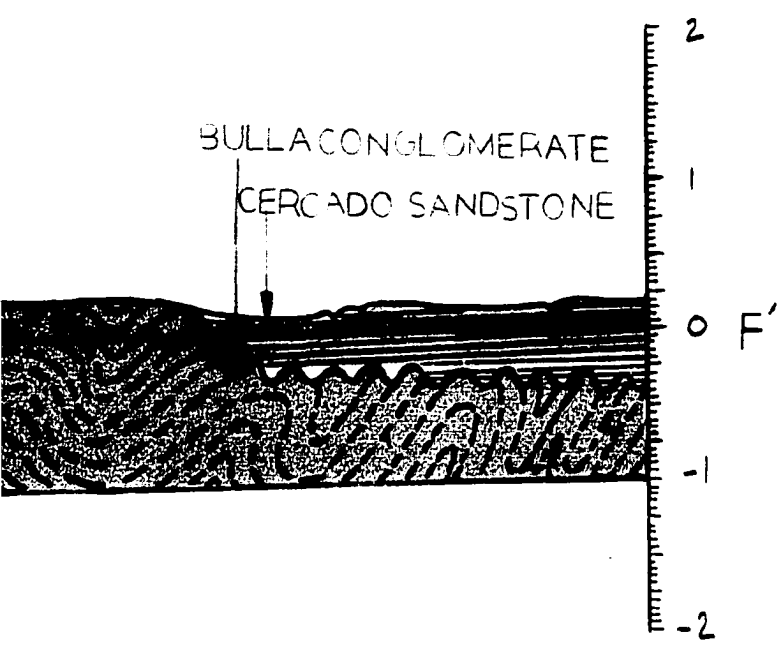
-1  
-2



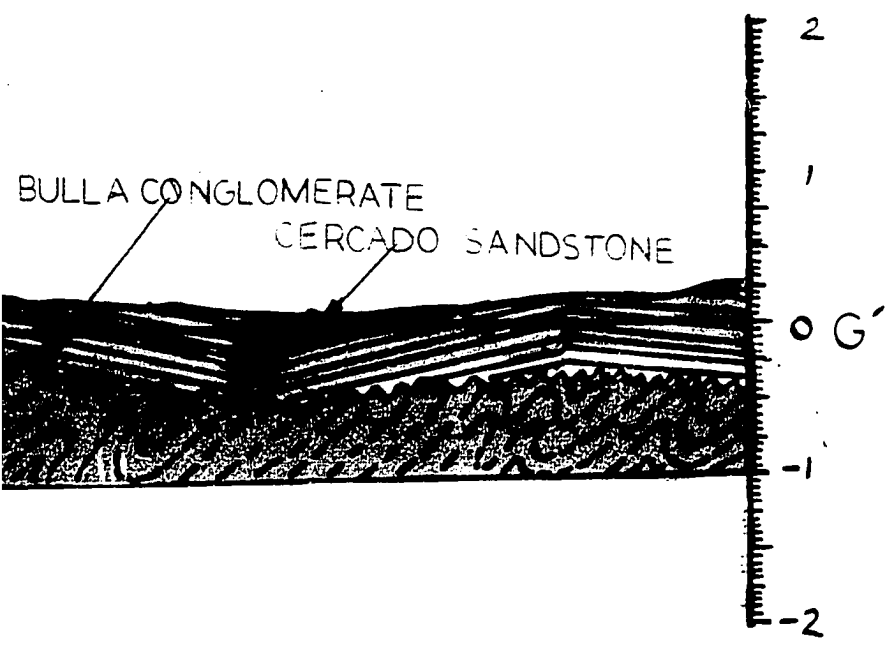


-2

BULLA CONGLOMERATE  
CERCADO SANDSTONE



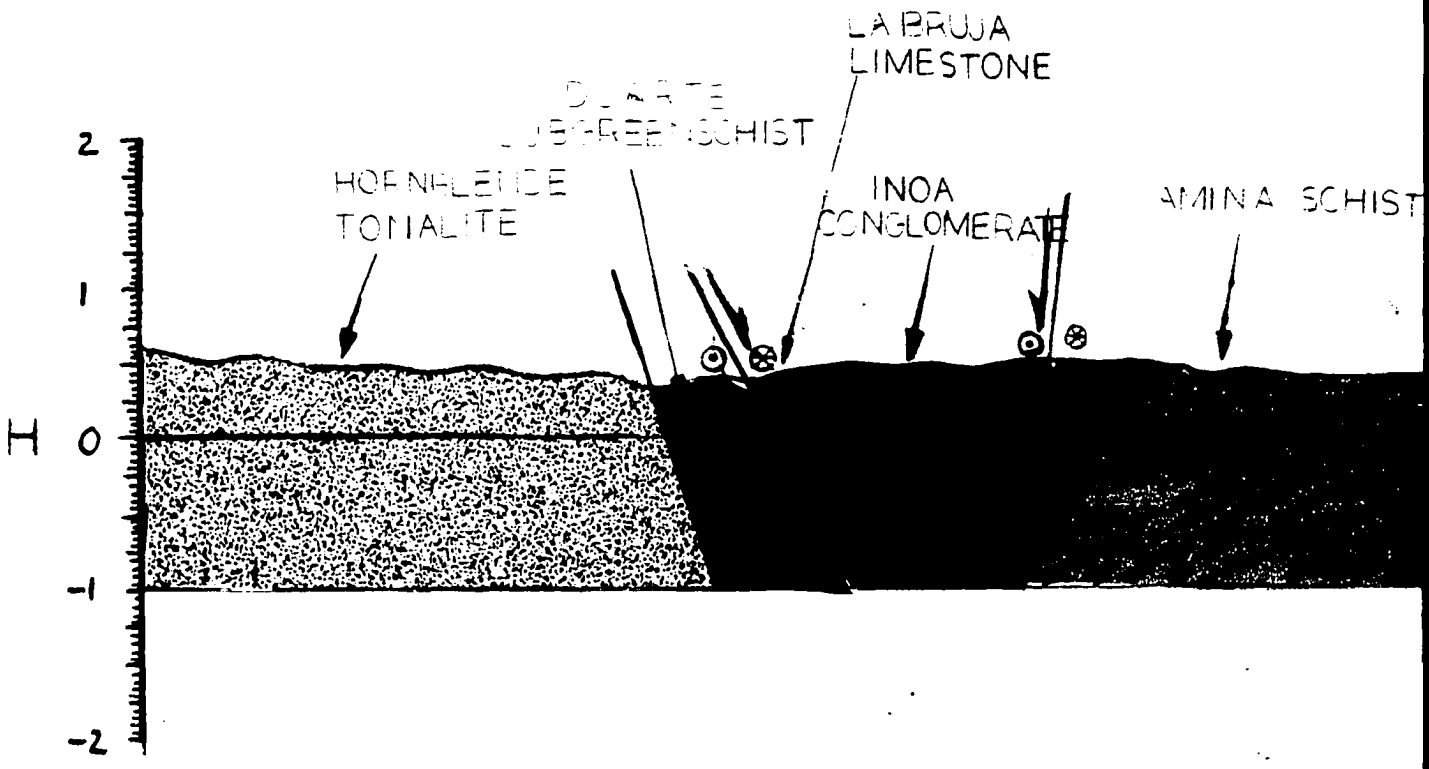
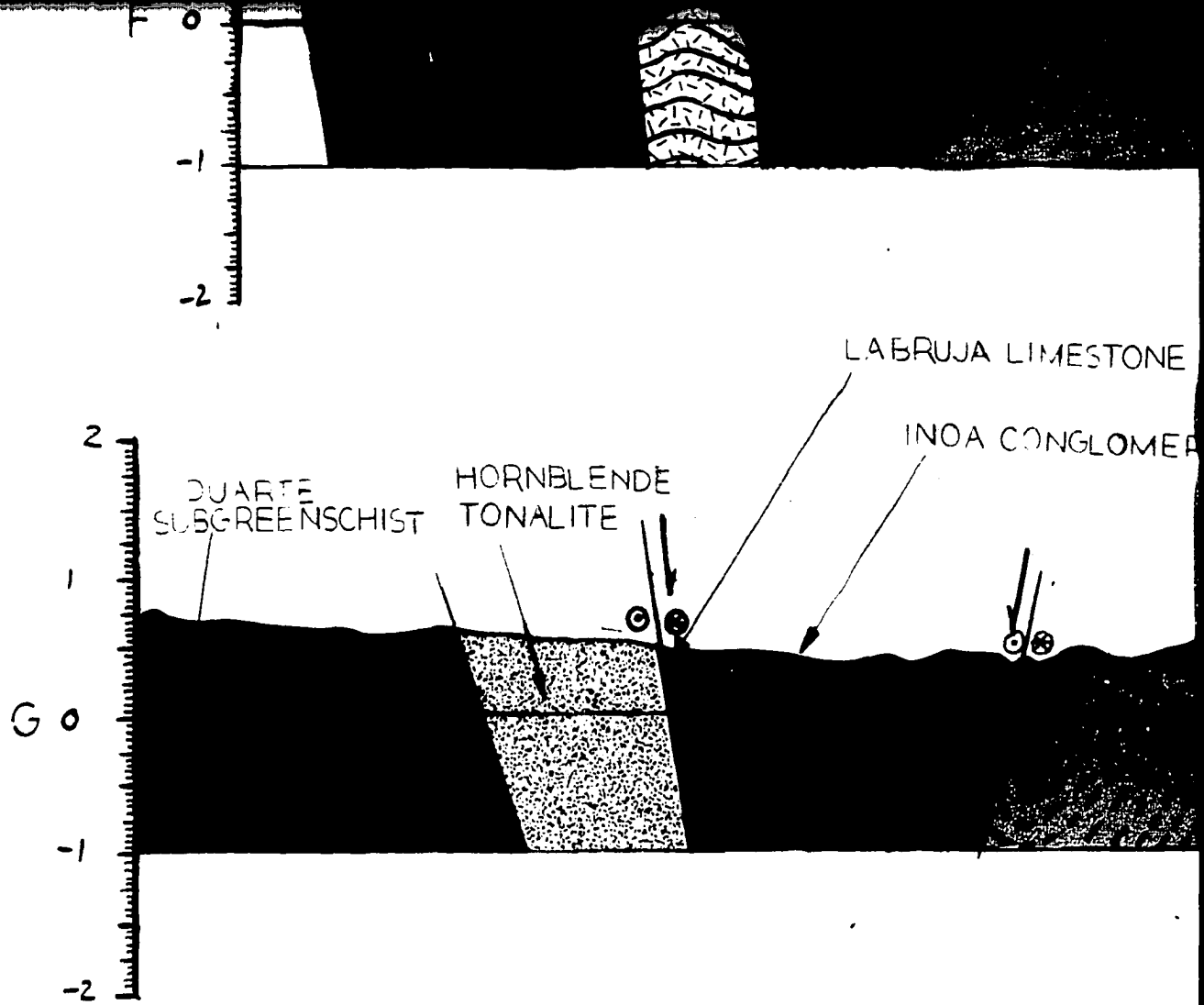
BULLA CONGLOMERATE  
CERCADO SANDSTONE



CERCADO SANDSTONE

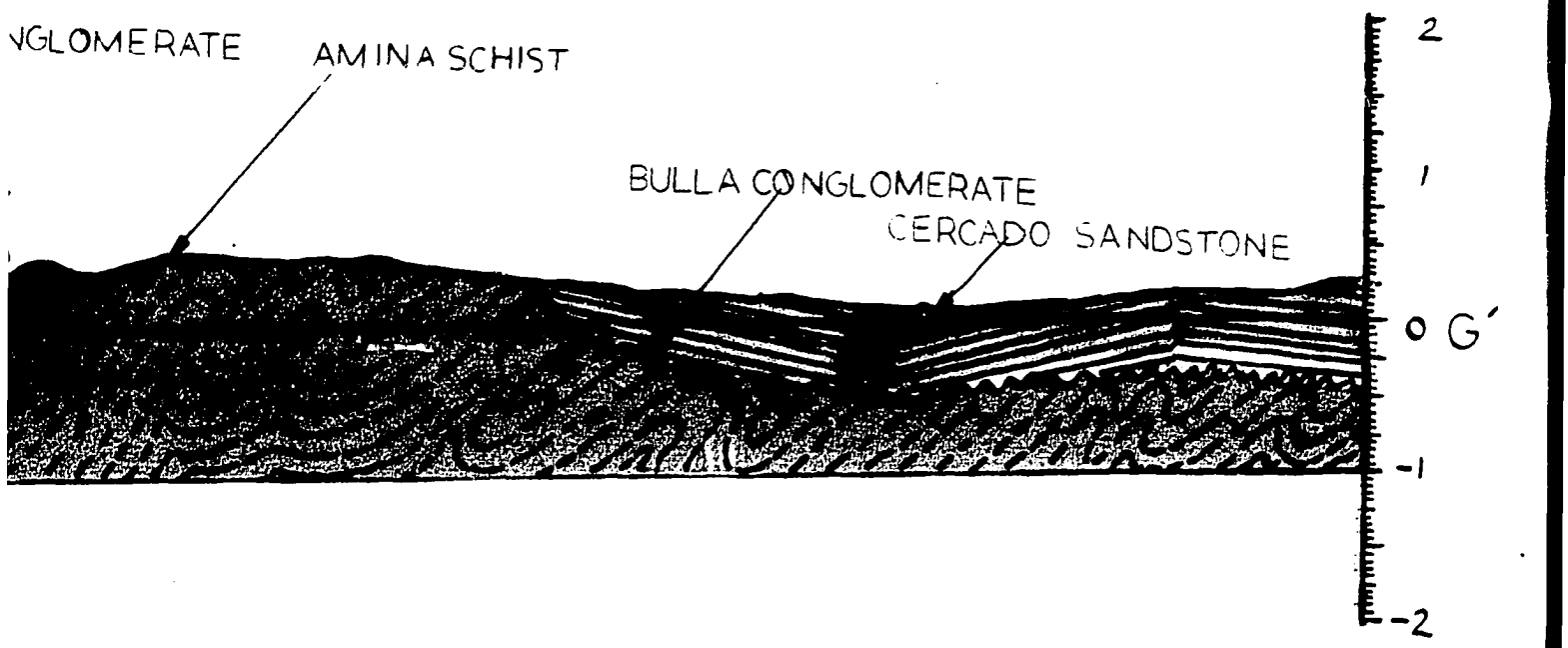
2  
1

CONGLOMERATE

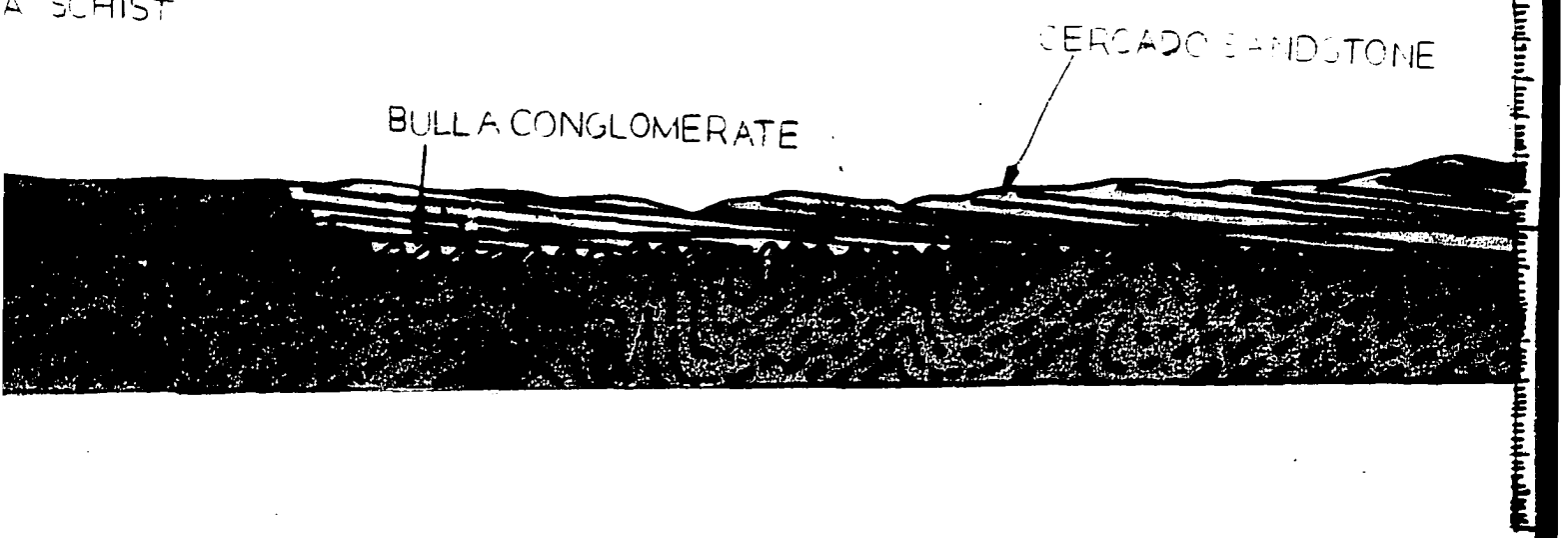


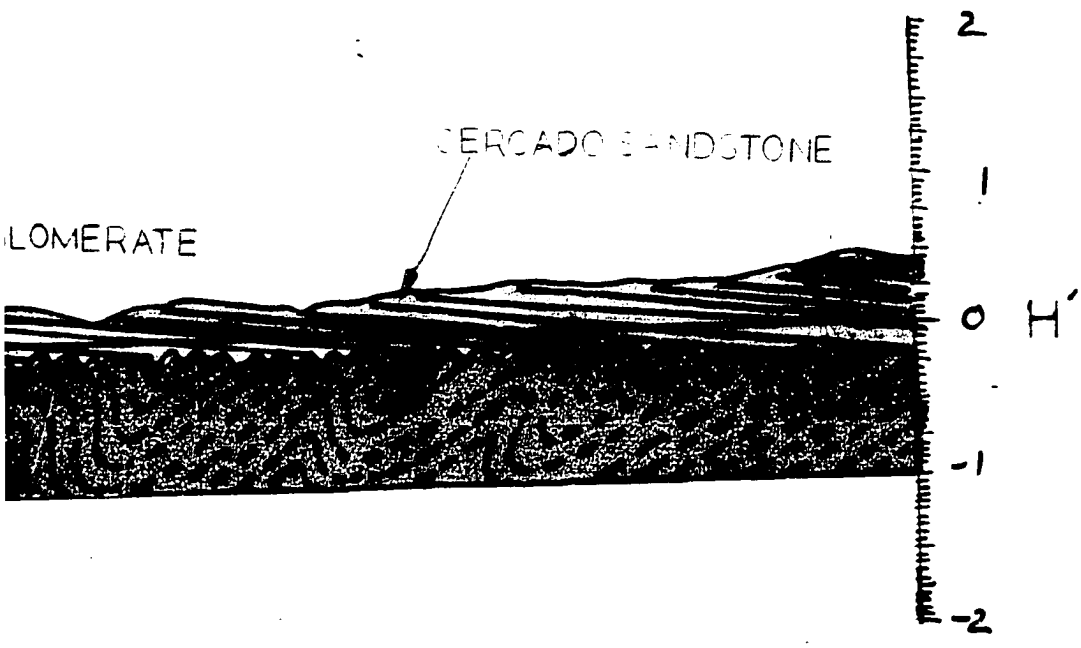
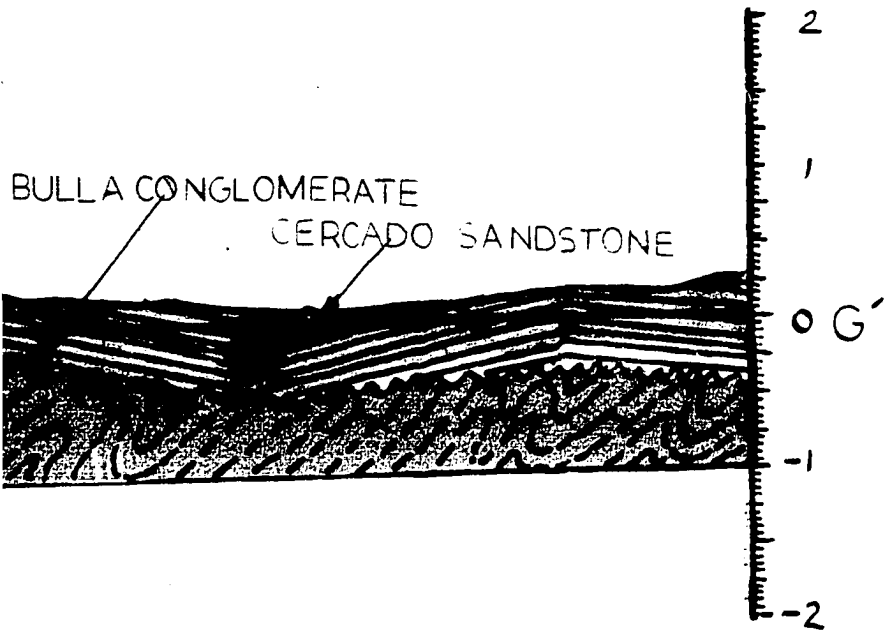
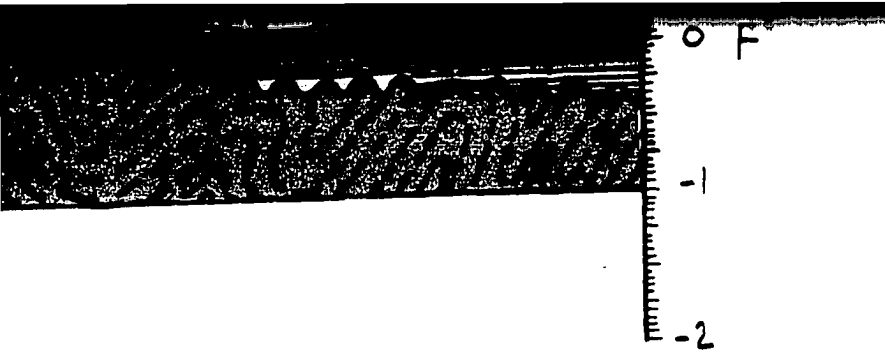


ESTONE



A SCHIST





## **NOTE TO USERS**

**Oversize maps and charts are microfilmed in sections in the following manner:**

**LEFT TO RIGHT, TOP TO BOTTOM, WITH  
SMALL OVERLAPS**

**UMI**

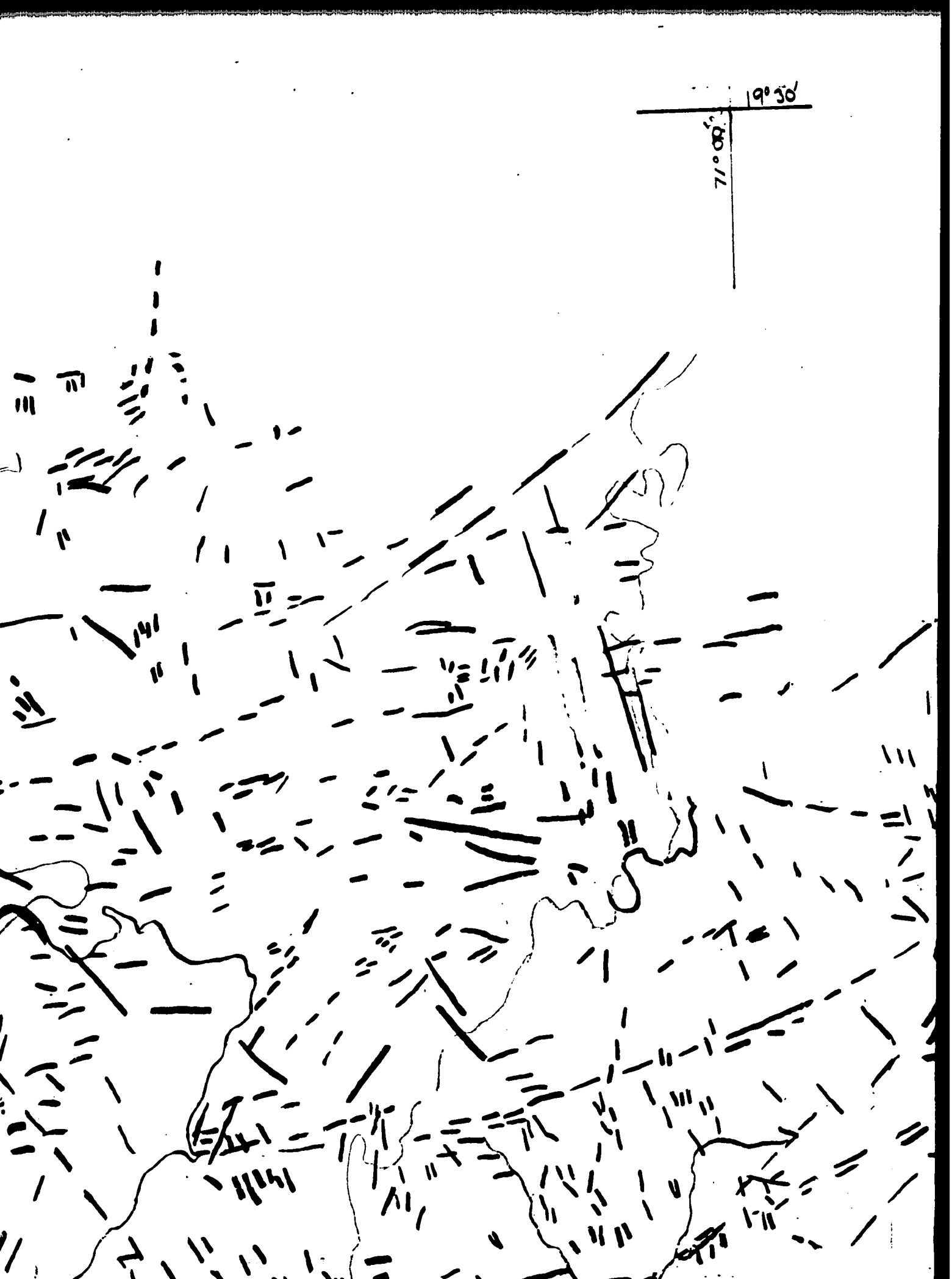


71°15'  
19°30'





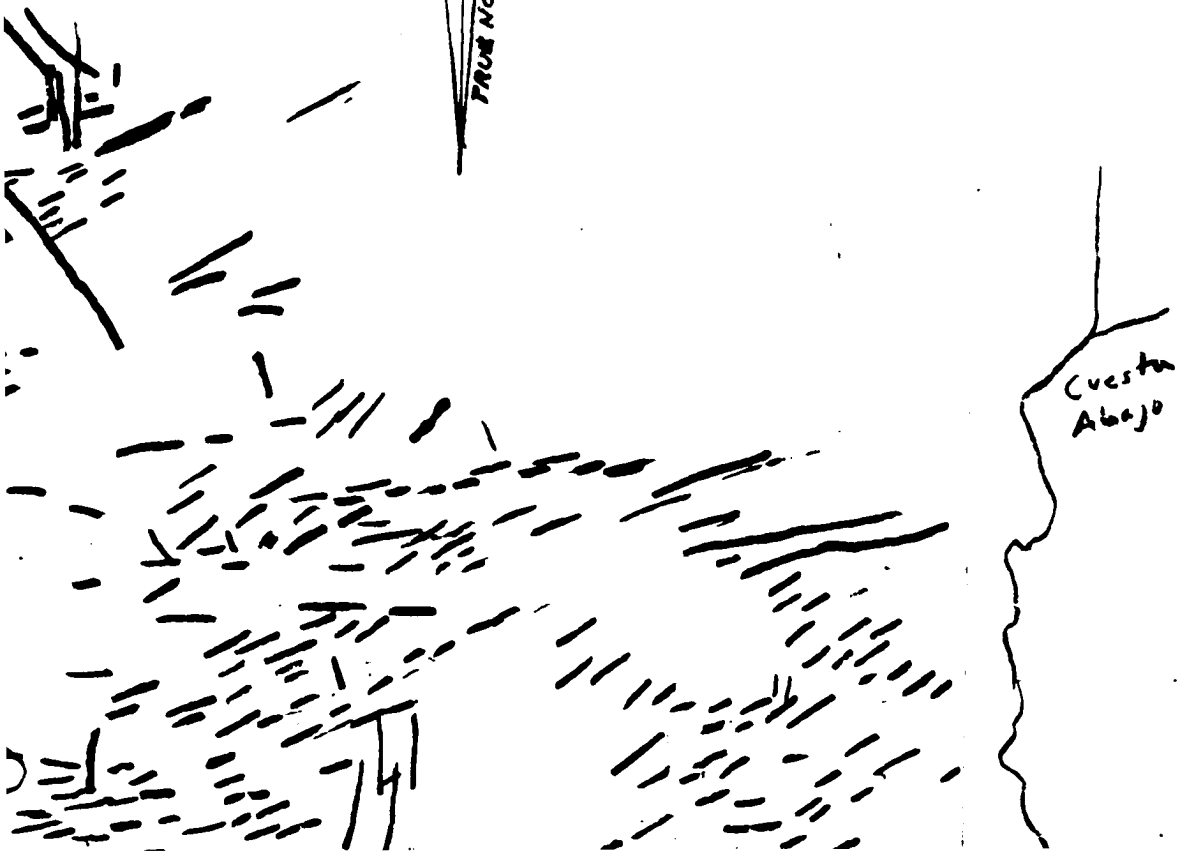
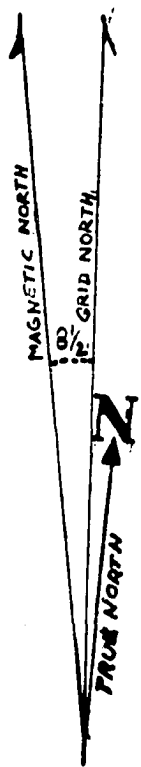
Manción

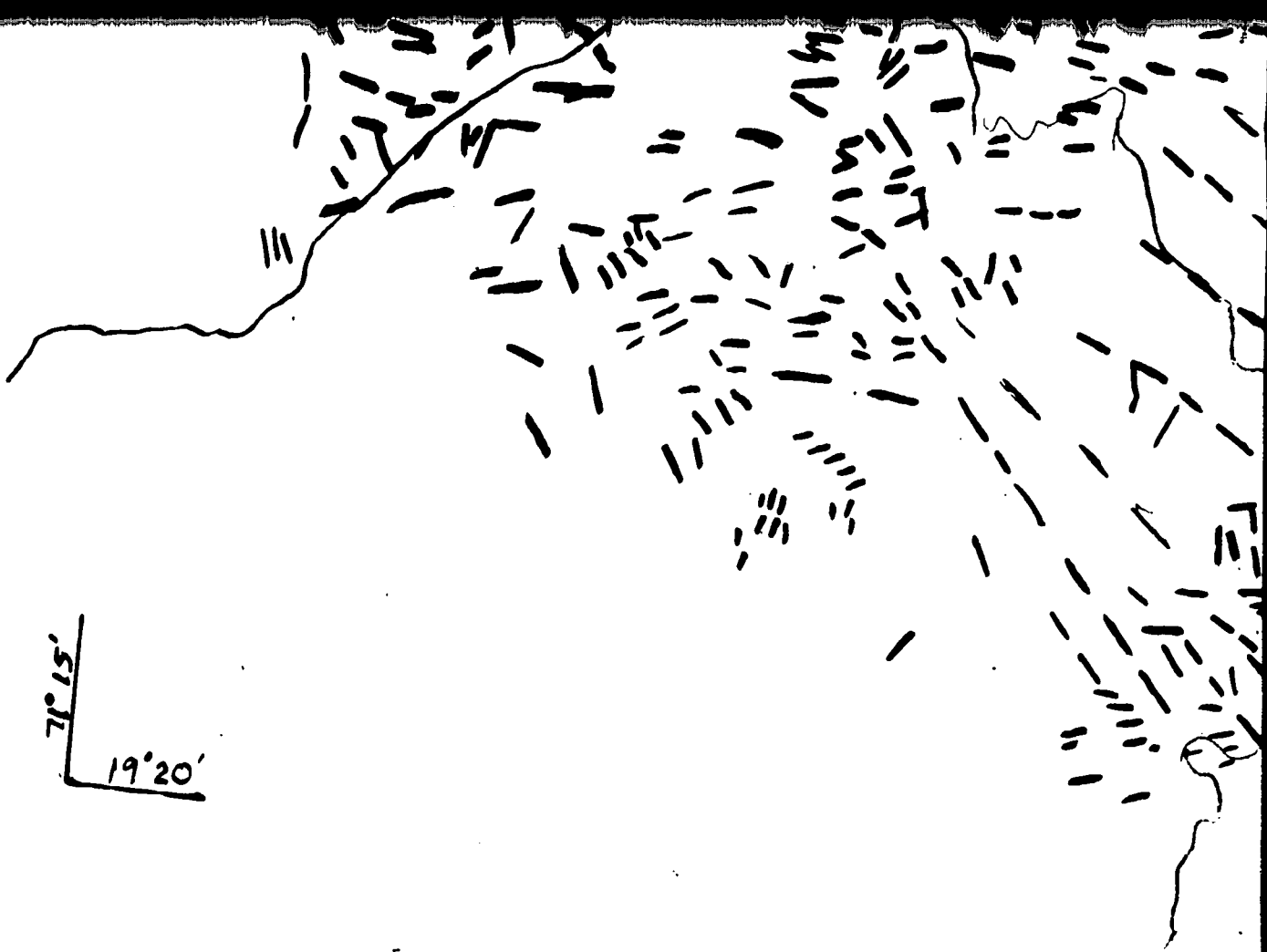


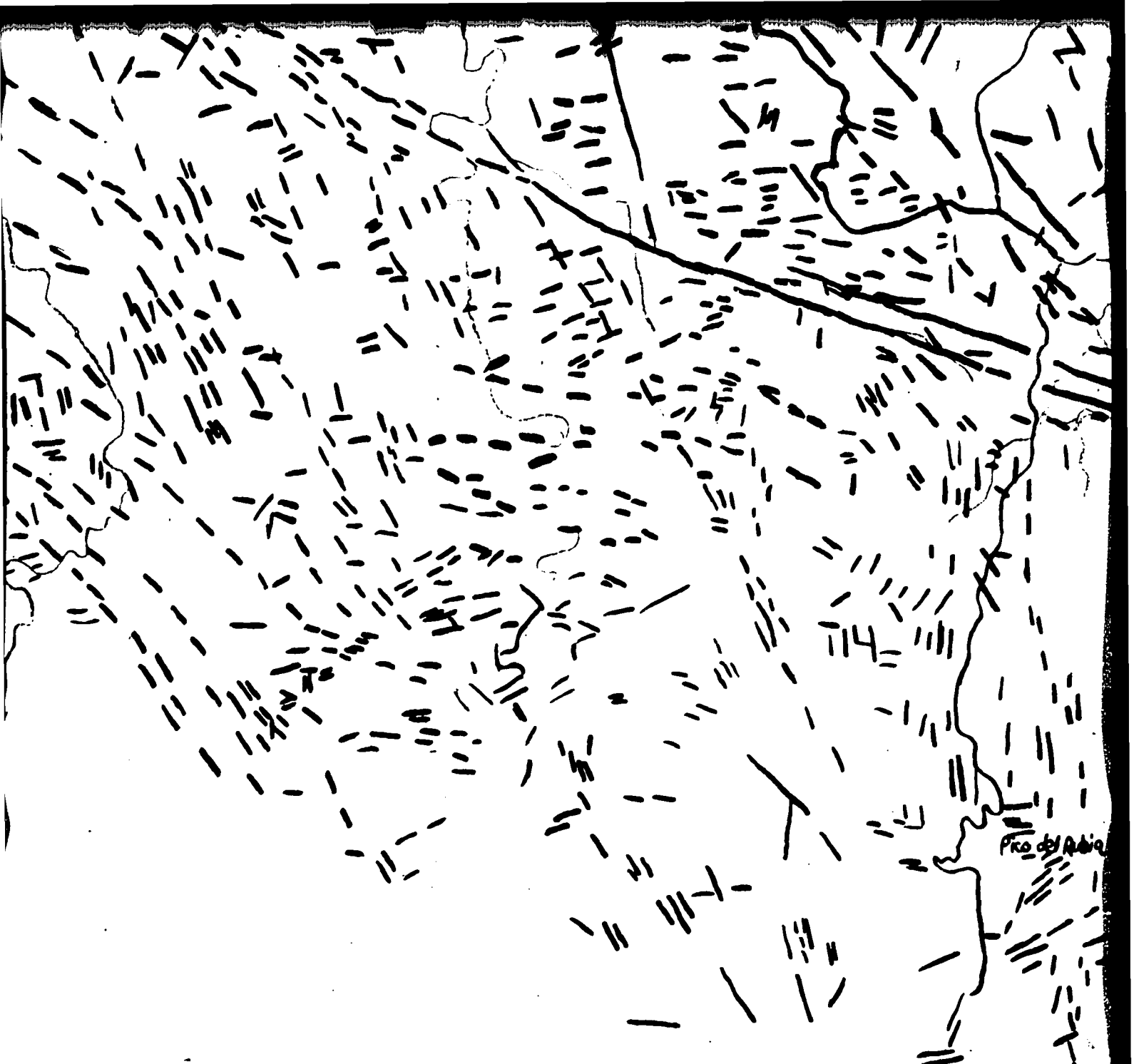


19°30'

70°52'06"





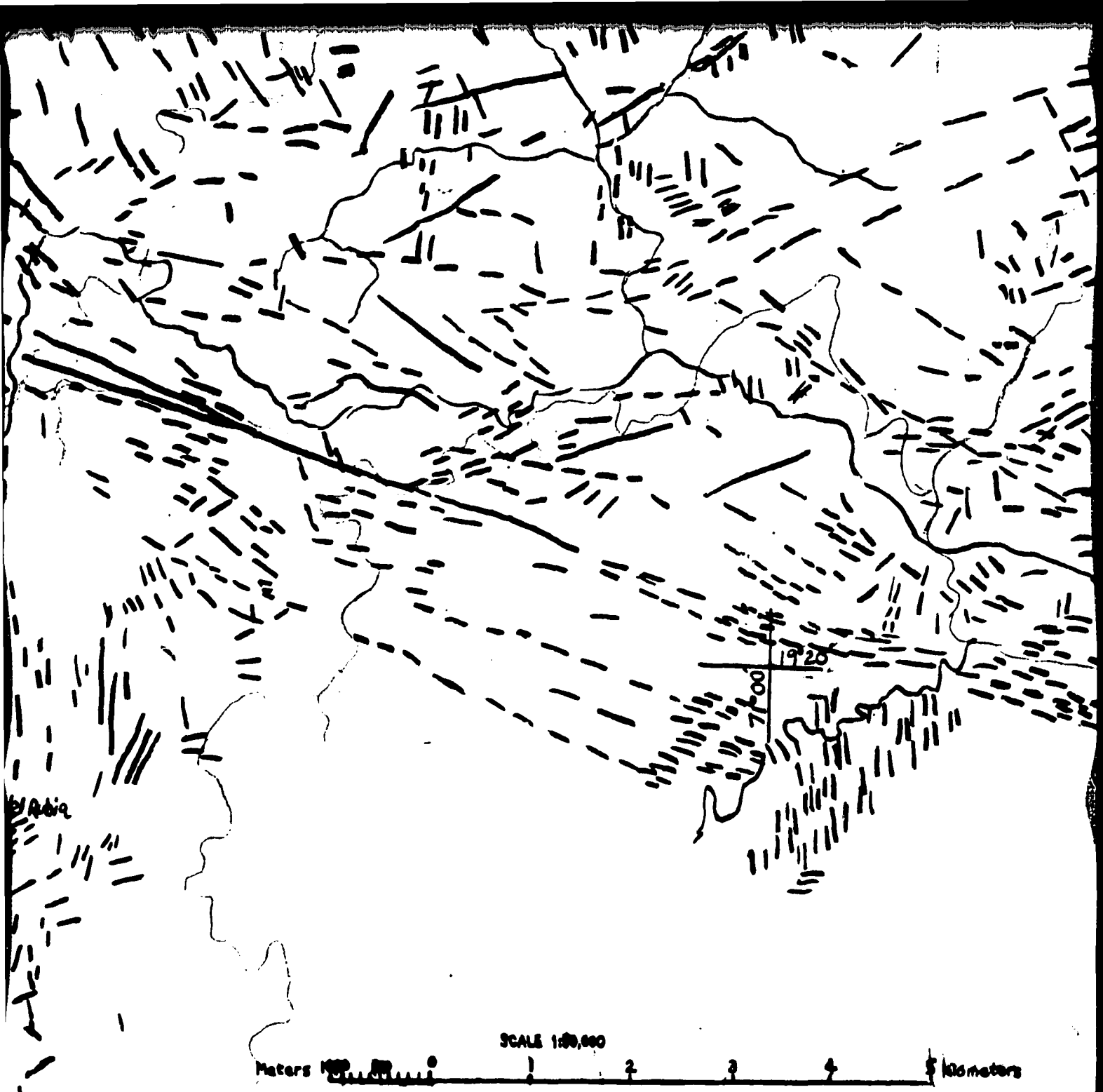


Pro del Abia

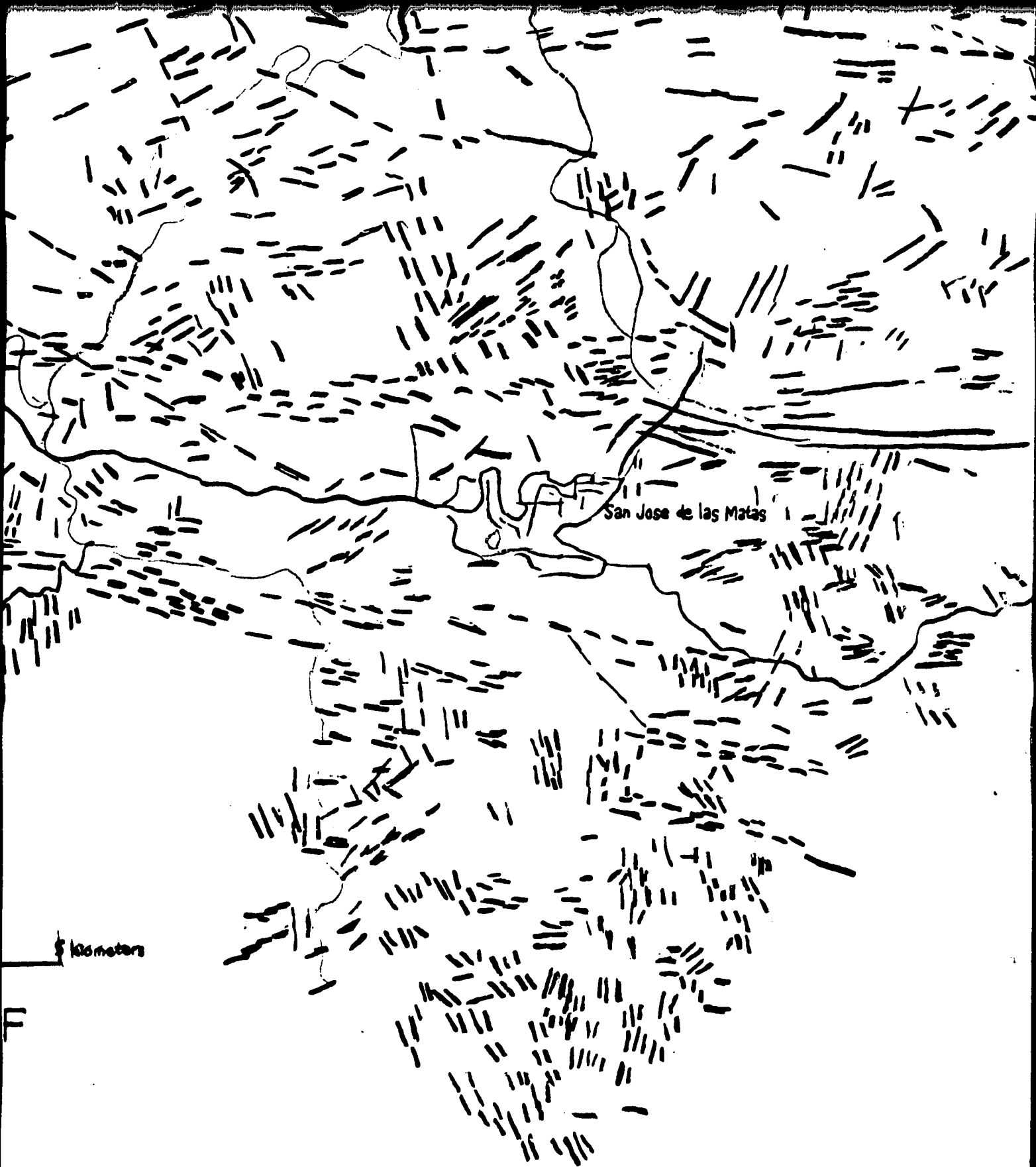
**BASE MAPS:**

**SAN JOSÉ DE LAS MATAS 1988**  
**6074 11 E733 EDICIÓN 3-ICM DMA**  
**MONCIÓN 1988**  
**5974 11 E733 EDICIÓN 3-ICM DMA**

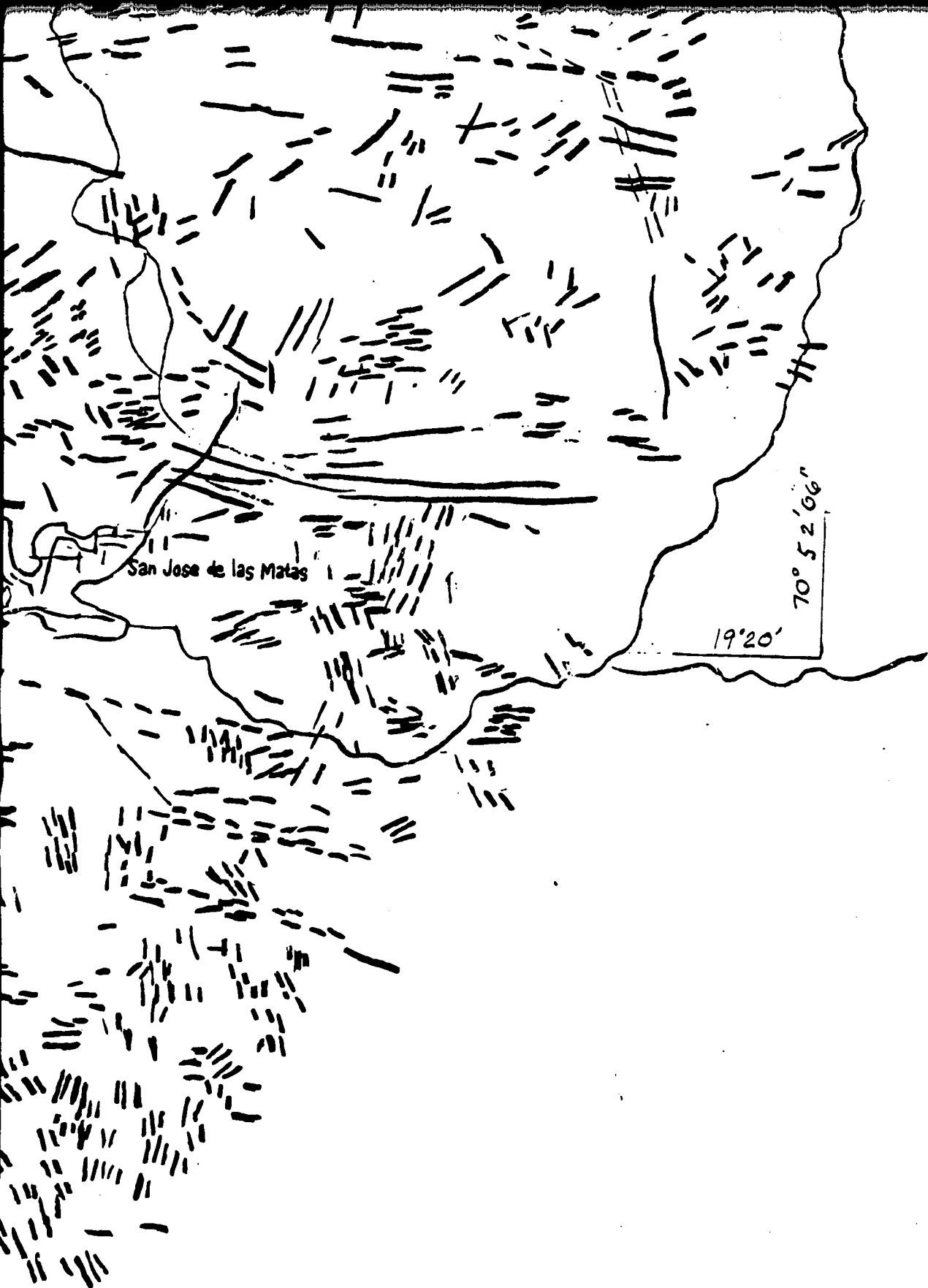
**INSTITUTO CARTIGRAPHICO DE MILITAR, RD**  
**in collaboration with**  
**DEFENSE MAPPING AGENCY, USA**



THE CITY UNIVERSITY OF  
NEW YORK  
NEW YORK, NEW YORK  
LINEAMENT MAP  
TERTIARY TECTONICS OF THE  
PIEDMONT OF THE CORDILLERA CE  
Andrew Jay Coleman 2000



# THE HISPANIOLA FAULT ZONE IN THE NORTHERN CENTRAL, DOMINICAN REPUBLIC



# FULT ZONE IN THE NORTHWESTERN INICAN REPUBLIC